Universidade de Santiago de Compostela

Facultade de Física

Departamento de Física da Materia Condensada

Non-Linear Physics Group

Impact of land-atmosphere fluxes on the spring precipitation regime of the Iberian Peninsula

PhD Thesis

Impacto dos fluxos entre a terra e a atmosfera na pluviometría primaveral da Península Ibérica

Tese de Doutoramento

Impacto de los flujos entre la tierra y la atmósfera en la pluviometría primaveral de la Península Ibérica

Tesis Doctoral

Documento realizado por **Alexandre Rios Entenza**
para optar ao título de Doutor.

Santiago de Compostela, Outubro de 2013.

USC
UNIVERSIDADE
DE SANTIAGO
DE COMPOSTELA

Dr. Gonzalo Miguez Macho, docente e investigador titular da Universidade de Santiago de Compostela, no Departamento de Física da Materia Condensada (*Non-Linear Physics Group*),

CERTIFICA

Que o presente documento, *Impact of land-atmosphere fluxes on the spring precipitation regime of the interior of the Iberian Peninsula*, foi realizado por **Alexandre Rios Entenza** baixo a sua guía, concluíndo desta forma a Tese para optar ao título de Doutor.

Santiago de Compostela, Outubro de 2013

Dr. Gonzalo Miguez Macho

USC
UNIVERSIDADE
DE SANTIAGO
DE COMPOSTELA

Table of Contents

Resume **ix**

Resumo **xvii**

Resumen **xxv**

1 General introduction **1**

1.1 The Iberian precipitation regime 1

1.2 Moisture sources for the Iberian rainfall 9

1.3 Land-atmosphere interactions 11

1.4 The recycling mechanism 19

1.5 The amplification mechanism 30

1.6 Objectives and possible applications 32

2 Data and methods **37**

2.1 The WRF model. Configuration 37

2.2 The IMB Recycling Model 43

2.3 The EBRM Recycling Model 47

2.4 The method of moisture tracers 49

2.5 *No-ET* experiments: relative change in precipitation 50

2.6 The SSM separation method 51

2.7 A new separation method 55
2.8 Data used in this thesis 58

3 Recycling in Iberia: spatio-temporal analysis 61

3.1 Iberian regional recycling ratio 63
3.2 Iberian local recycling ratio 67
3.3 Selected case studies 68
3.4 Conclusions of chapter 3 73

4 Recycling, amplification and spring rainfall 77

4.1 Validation 79
4.2 Water budget and moisture fluxes 80
4.3 Moisture recycling and spring rainfall 87
4.4 Precipitation amplification and spring rainfall 96
4.5 Analysis of May 2004 and May 2008 101
4.6 Conclusions of chapter 4 109

5 WRF simulations with moisture tracers over Iberia 113

5.1 The method of moisture tracers 115
5.2 Recalculation of direct and indirect terms via MMTR 118
5.3 Distribution of moisture tracers in the atmosphere 120
5.4 Conclusions of chapter 5 123

6 General conclusions and outlook 125

Appendices 129

A Computation of the water budget terms 131

B IMB computation details 135

C EBRM computation details **137**

D Configuration of the *No-ET* experiments **141**

E EBRM sensitivity to spatial resolution **143**

References **147**

Acknowledgements **169**

Abbreviations **171**

Symbols **173**

List of Figures **178**

List of Tables **179**

List of Publications **181**

USC UNIVERSIDADE DE SANTIAGO DE COMPOSTELA

USC
UNIVERSIDADE
DE SANTIAGO
DE COMPOSTELA

Heureux le géomètre, en qui une étude consommée des sciences abstraites n'aura point affaibli le goût des beaux-arts ; à qui Horace et Tacite seront aussi familiers que Newton ; qui saura découvrir les propriétés d'une courbe et sentir les beautés d'un poète.

Pensées sur l'interpretation de la Nature
Denis Diderot (1713-1784)

USC UNIVERSIDADE DE SANTIAGO DE COMPOSTELA

USC
UNIVERSIDADE
DE SANTIAGO
DE COMPOSTELA

Resume

Motivation

Water is essential for the Earth's life. The oceans contain 1 338 000 000 km^3 of salt water (Fig. 1). In the continental areas, only 34 921 740 km^3 of fresh water are stored, distributed into glaciers (24 000 000 km^3), groundwater (10 800 000 km^3), lakes and marshes (102 000 km^3), soil moisture (16 500 km^3), rivers (2 120 km^3) and water stored in the biomass (1 120 km^3). Finally, the atmosphere contains 12 900 km^3 (Dingman, 2002 [56]). A simple calculation shows that:

$$\frac{\text{Water stored in land areas}}{\text{Water stored in the oceans}} \approx \frac{\text{Fresh water}}{\text{Salt water}} \approx 2.6\% \tag{1}$$

Over the oceans, there is always water available for evaporation. This implies that oceanic evaporation equals potential evaporation. Over land, in contrast, moisture has to overcome more difficulties to be evapotranspired. For instance, the passage of ice molecules in glaciers towards the atmosphere is very limited, as well as the conversion of liquid water from the groundwater reservoir into atmospheric vapor. This restrictions suggest that the fraction of land evapotranspiration with respect to the oceanic evaporation might represent, globally, much less than the above-calculated 2.6%. Consequently, in terms of precipitation and at a global scale, we might roughly state that rainfall with origin on land evapotranspiration should not exceed 2 or 3% of the rainfall derived from oceanic evaporation.

But does this global water balance hold for a particular land area? And more specifically, is this true for the Iberian Peninsula? Let us examine it in detail. The Iberian Peninsula is located in the southwest corner of the European continent, within an imaginary spherical rectangle defined by latitudes 36°N and 44°N, and longitudes 10°W and 2°E, approximately. Surrounded by two *unlimited* sources of water, the Atlantic Ocean and the Mediterranean Sea, the Iberian Peninsula faces the westerly winds, characteristic at the mid latitudes, which bring humidity from the Atlantic into the Iberian land regions. Under this geographical configuration, it seems clear

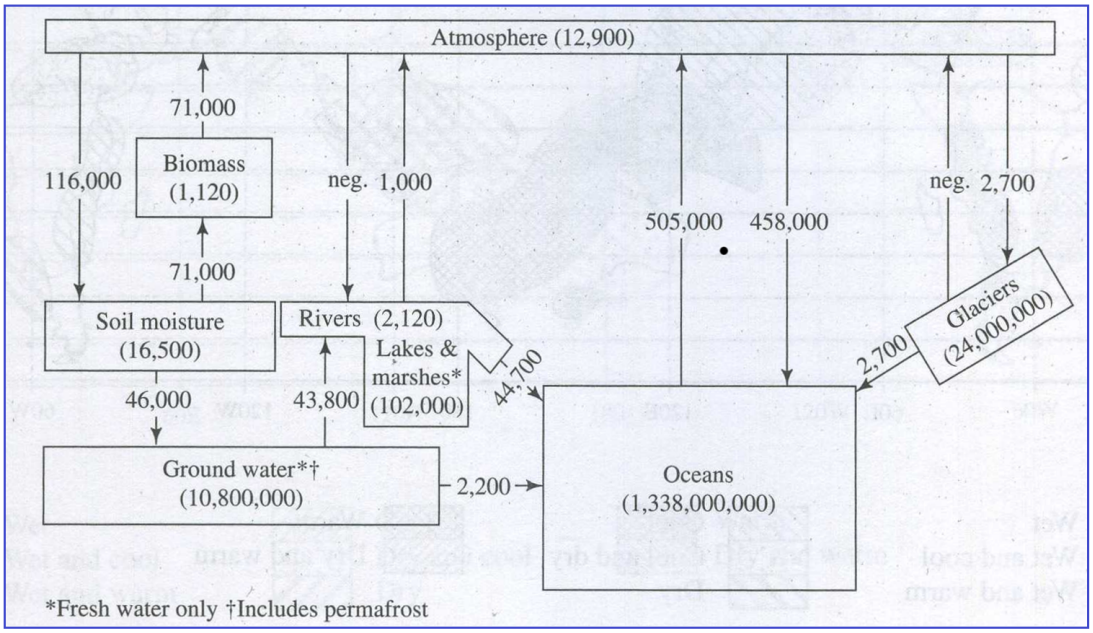

Figure 1: Schematic representation of stocks and water fluxes (km^3) in the global hydrologic cycle. This figure is obtained from Dingman (2002) [56].

that oceanic moisture must be, by large, the main source for the Iberian rainfall. Intuitively, and according to the previous discussion, we could roughly say that the contribution of locally evapotranspired moisture to precipitation, with respect to the oceanic, large-scale contribution, should not be much higher than the global 2 or 3%. But is this always the case?

Actually, it is not. In this thesis, we show that in the arid and semiarid regions of the interior, east and northeast of the Iberian Peninsula, locally evapotranspired moisture can be responsible, directly or indirectly, for over 50% of the total precipitation during spring and early summer. This contrasts with the Atlantic and Cantabrian coastal areas, where this contribution is very reduced. The question is, therefore, why this "unexpected" intensification of the impact of evapotranspiration on the rainfall regime takes place in inland Iberia. Giving a comprehensive answer to this question constitutes, precisely, the main goal of this thesis.

The relevance of spring precipitation

An important part of the interior, eastern and northeastern regions of Iberia, where agriculture has been traditionally the mainstay of the local economy, presents arid or semiarid characteristics, often suffering from water limitations. In the context of a

changing climate, which is expected to affect the Mediterranean area, and in particular the Iberian Peninsula, with higher-than-average intensity, understanding the major sources of moisture and the specific physical processes whereby precipitation falls over these areas becomes crucial for their medium and long term sustainability.

The remarkable impact of evapotranspiration fluxes on precipitation, observed during spring and early summer throughout the interior of Iberia, would not be that relevant if it was associated to low rainfall totals and had a reduced impact on human activities. Nevertheless, this is not the case. Actually, it is precisely during spring and early summer when the absolute maximum of precipitation in the annual cycle takes place in large interior, eastern and northeastern regions. The significant amount of rainfall registered in spring is reflected in a large amount of popular sayings and proverbs throughout the Iberian Peninsula, as it is the case with the spanish saying *en abril, aguas mil* ("in April, lots of rain"), or in its portuguese version, *é próprio do mês de abril as águas serem às mil.* As mentioned, it is impossible to account for this peak of rainfall without considering the contribution of internal evapotranspiration. The convective nature of an important fraction of this rain is also described in several proverbs. In the northeastern sector of Iberia, we find, for instance, *tronades d'abril, fruites mil* ("stormy April, lots of fruits") or *al maig, cada dia un raig* ("in May, one lightning a day"). Similarly, in the western side it is said, with a similar meaning, that *maio que não der trovoada, não dá coisa estimada.*

Furthermore, the spring surplus of precipitation in inland Iberia has a critical impact on human activities, specially on agriculture. This is also reflected in a variety of proverbs, from Portugal to Catalonia and from Andalusia to the Basque Country. A good example is found in the castilian saying *como agua de mayo* (literally "like water of May", with the meaning of "like a breath of fresh air"), widely used in the everyday speech to describe any thing or action that produces a very positive effect. Similarly, in the interior of Portugal, a variety of proverbs highlight the relevance of rainfall in April and May. For instance, *seca de abril, deixa o lavrador a pedir* ("a drought in April makes the farmer poor"); *maio pardo e ventoso faz o ano farto e formoso* ("a humid and windy May turns the year abundant and beautiful"); *água de maio, pão todo o ano* ("rainfall in May, bread for the whole year"); *em maio verás a água com que regarás* ("in May, you will have the rain you need for farming"), also said in the interior of Galicia; or with a similar meaning, *quando chove na Ascensão, até as pedrinhas dão pão.* Similar sayings expressing this idea are found in the Basque Country: *Pazkoa euritsu, urte hura ogitsu* ("rain at Easter, fruitful year"); *maiatz eurite, urtea ogite* ("rain in May, fruitful year"). Also, in the eastern side of Iberia, many popular proverbs state the relevance of the spring precipitation for agriculture. For example, *l'abril mullat, de pa ve carregat* ("a wet April brings a lot of bread"); *a l'abril cada gota en val mil* ("in April, every raindrop is very valuable"); or *maig humit fa al pagès ric* ("a humid May makes the farmer rich").

Contents of this thesis

This thesis is organized in six main chapters and five appendices including supplementary materials. Whereas chapter 1 provides a general introduction to this investigation, in chapter 2 we examine the different methods and datasets used in this work. The main results are presented and discussed in chapters 3, 4 and 5. Chapters 3 and 4 correspond in large parts to the articles *"Precipitation recycling in the Iberian Peninsula: spatial patterns and temporal variability"* and *"Moisture recycling and the maximum of precipitation in spring in the Iberian Peninsula"*, respectively (see the List of Publications for the complete references). Chapter 5 completes these studies by analyzing regional simulations that include an innovative tool of moisture tracers. The material included in this chapter will be part of the article *"Regional climate simulations with moisture tracers to investigate land-atmosphere interactions in the terrestrial water cycle over the Iberian Peninsula"* (see the List of Publications for the complete reference), which is now in preparation. Each of these three chapters is introduced by an initial abstract. In a final section at the end of each of these chapters, the corresponding partial conclusions are briefly summarized. Finally, the general conclusions of the whole investigation are presented in chapter 6.

Chapter 1 provides a general introduction to contextualize the investigation presented in this thesis. In this framework, the experimental motivation, the objectives and the theoretical bases of this study are explained and examined in detail. First, a complete description of the Iberian precipitation regime is given. We pay special attention to the relative maximum of precipitation observed throughout the interior of the Iberian Peninsula, which tends to become the absolute maximum in the annual cycle in the eastern and northeastern regions. The need to fully understand the physical processes responsible for this peak of rainfall constitutes, as mentioned, the main motivation for this thesis. This requires a comprehensive investigation of the major moisture sources contributing to rainfall over the Iberian Peninsula and, in particular, over its interior lands. In practice, this means separating the contribution to the Iberian precipitation of locally evapotranspired moisture from that of moisture advected from outside by the winds. The recycling ratio, defined in chapter 1, is shown to be a crucial magnitude to assess the relative weight of both terms.

Our working hypothesis is that locally evapotranspired moisture is the key to explain the upturn of precipitation amounts during April and May in inland Iberia. This implies that land-atmosphere interactions in general, and recycling and amplification mechanisms in particular, may play a fundamental role on the spring rainfall regime of the interior areas. In this first chapter, a detailed characterization of these land-atmosphere processes is provided, including a discussion on their dependence in different features, as is the case with human activities, soil moisture, groundwater and water table dynamics. The double effect whereby evapotranspiration fluxes enhance precipitation is also discussed: on the one hand, by adding new moisture to

the atmosphere that can be used for further precipitation (direct or recycling effect); on the other hand, by increasing the instability of the atmospheric column and thus favoring the ascend of moisture and the development of convective structures (indirect or amplification effect).

In **chapter 2**, the technical details of the different methods, computational tools and datasets used in this thesis are provided. WRF model simulations constitute the main experimental material for our analysis. In this chapter, we describe the model setups used in our runs, indicating the geographical domains, time periods, horizontal resolution, model options and parameterizations used. Apart from the standard WRF model simulations, it is interesting to note that experimental runs, where the evapotranspiration flux is suppressed over the Iberian Peninsula, were also carried out for the months of January and May of the years 2000 to 2010. This procedure constitutes an optimal way to explore the distinct effect of land evapotranspiration in the winter and spring rainfall regimes of the Iberian Peninsula. This impact is examined in more detail in chapter 5 through additional WRF model simulations including a new option of moisture tracers. This original capability allows tracking the trajectories described by the moisture molecules, since they are evapotranspired until they precipitate or are advected out of the model's domain.

The methods used in this thesis can be classified into two types. On the one hand, three different procedures to compute the recycling ratio are used: 1) the analytical recycling model developed by Schär et al. (1999); 2) the numerical recycling model due to Eltahir and Bras (1994); and 3) the explicit method of moisture tracers. On the other hand, two methods are used to separate the direct (recycling) contribution from the indirect (amplification) contribution of evapotranspiration fluxes to the spring peak of precipitation. The first method is also due to Schär et al. (1999), whereas the second is original, based on the comparison of control simulations, with all land-atmosphere fluxes normally activated, to the above-mentioned experimental runs where those fluxes are eliminated.

In **chapter 3**, the recycling ratio is computed at the monthly scale, over the Iberian Peninsula, along a period of 18 complete annual cycles, from January 1990 to December 2007. The recycling ratio is found to be the highest during late spring and early summer. Interestingly, the highest intensity of recycling is observed to occur in the interior, overlapping those areas where the spring peak of precipitation is observed. In general, two conditions are found to be directly related to high recycling values over the Iberian Peninsula: 1) the availability of sufficient soil moisture, directly linked to the rainfall amounts registered during the previous season; and 2) the occurrence of appropriate synoptic configurations favoring the development of convective regimes. The combination of these two conditions seems to explain the magnitude of recycling ratios at any period of the year in Iberia. We hypothesize that this scheme might also hold for other regions in the world with semi-arid types of climate. Regardless, this preliminary investigation, complemented in chapters 4 and 5, confirms that recycling

processes play a crucial role in spring precipitation over the interior areas of the Iberian Peninsula.

In **chapter 4**, we focus our attention in the months of May along the last decade (2000-2010). The reason for selecting this month is twofold: firstly, because it is precisely in May when the annual maximum of rainfall takes place in large areas of the interior, east and northeast of Iberia; and secondly, because the activity of land-atmosphere interactions is significantly enhanced in this month. In addition, the corresponding months of January along the same period are also simulated, as a manner to assess the essential differences in the Iberian rainfall regime between winter and late spring. From this analysis, we conclude that suppressing land evapotranspiration in May would lead to an average reduction of precipitation by 37%. In addition, recycling and amplification contributions are found to have a similar impact on the extra spring precipitation. In general, the recycling term tends to predominate when the external forcing is weak, principally in the northern half of the Iberian Peninsula. This is expected, since in this case locally evapotranspired water is almost the only source of moisture for precipitation. On the contrary, when the synoptic circulation is more intense and a substantial amount of external moisture is advected into Iberia, the amplification mechanism tends to prevail. This indirect effect of evapotranspiration fluxes is of the greatest relevance, as it helps incorporating external wetness to the Iberian hydrology cycle.

In **chapter 5**, regional WRF model simulations incorporating moisture tracers are performed, along the period May 2000 - May 2010, over the Iberian Peninsula. This tool of moisture tracers allows computing the recycling ratio and presents two major advantages with respect to classical recycling models: 1) the method computes explicitly the fractions of precipitation with internal (locally evapotranspired) and external (advected) origin, without requiring any additional assumption; and 2) the recycling ratio can be computed at any time scale, and not only at monthly or larger scales as the limitations of the traditional recycling models impose. These final simulations with moisture tracers show that both the recycling ratio and the recycling contribution to the extra spring precipitation are more spread throughout the northern half of the interior Iberia, with the highest intensity in the North Plateau, Central and Iberian Systems and the Pyrenees, and no so concentrated to the eastern and northeastern regions as the classical calculations through the method by Eltahir and Bras (1994) suggest. The latter method is found to systematically overestimate the recycling values, whereas the simpler model by Schär et al. (1999) produces regional recycling values much closer to the more accurate ones obtained through this innovative method of moisture tracers.

Finally, the most important conclusions of the whole investigation are summarized in **chapter 6**. In the light of our results, we can state that the spring maximum of precipitation taking place in inland Iberia cannot be explained without considering the crucial role of land-atmosphere interactions, and in particular evapotranspiration

fluxes. We strongly believe that this thesis constitutes a relevant improvement in the description of the precipitation regime of the interior Iberian lands. The main physical mechanisms underlying the upturn of rainfall totals in spring are identified, and the methods used and developed here account satisfactorily for their relative impacts.

At the end of this thesis, complementary material is organized in five appendices. In appendices A, B and C, we include additional details on the computation of the water budget terms and the recycling ratio through the methods of Schär et al. (1999) and Eltahir and Bras (1994). In appendix D, we thoroughly explain the procedure whereby we removed the land evapotranspiration in the WRF simulations analyzed in chapter 4. In appendix E, the sensitivity to horizontal resolution of the classical recycling model developed by Eltahir and Bras (1994) is explored.

Possible applications and future work

The possible practical applications of the investigation presented in this thesis can be classified into two major blocks. On the one hand, our study can contribute to the improvement of seasonal forecasting in the Iberian Peninsula and, related to this, to the improvement of alert systems management. In this thesis, the impact of local evapotranspiration on spring rainfall is found to be crucial in the interior of the Iberian Peninsula. As a result, if the winter of a certain year is very dry, the subsequent water shortage of the soil will result in a decrease of evapotranspiration and, consequently, of precipitation. In this context, the probability of a dry summer is enhanced and flood risks are reduced. On the contrary, the likelihood of extreme rainfall events after a humid winter is significantly increased, even though their occurrence or not will be modulated by the specific synoptic configuration of the subsequent spring and summer. This analysis shows that the assessment of the impact of land-air fluxes on the precipitation regime can be critical to estimate flood and drought risks in the Iberian Peninsula.

We believe that this investigation could be also very valuable in terms of hydrological planning and regional sustainability. This is related to the fact that human activities have a critical impact on the local fraction of precipitation. As a result, in inland Iberia, where this contribution plays a major role in the spring precipitation regime, a correct planning of the use of land and an appropriate management of the limited water resources is essential for the regional sustainability.

In the future, carrying out WRF model simulations including moisture tracers and a fully coupled land-surface scheme representing the groundwater and water table dynamics would probably constitute the best manner to explore the Iberian hydrology cycle and precipitation regime. We suggest that this procedure might be useful not only in the interior areas of the Iberian Peninsula but also in any other semiarid region all over the world.

USC
UNIVERSIDADE
DE SANTIAGO
DE COMPOSTELA

Resumo

Motivação

A água é essencial para a vida na Terra. Os oceanos de todo o planeta contêm 1 338 000 000 km^3 de água salgada (Fig. 2). As regiões continentais, por sua vez, armazenam apenas 34 921 740 km^3 de agua doce, distribuída em glaciares (24 000 000 km^3), águas subterrâneas (10 800 000 km^3), lagos e pântanos (102 000 km^3), humidade do solo (16 500 km^3), rios (2 120 km^3) e água contida na biomasa (1 120 km^3). Finalmente, a atmosfera contém 12 900 km^3 (Dingman, 2002 [56]). Um cálculo simples mostra que:

$$\frac{\text{Água contida nos continentes}}{\text{Água contida nos oceanos}} \approx \frac{\text{Água doce}}{\text{Água salgada}} \approx 2.6\% \tag{2}$$

Nos oceanos há sempre água disponível para a evaporação. Isto quer dizer que a evaporação oceânica é igual à evaporação potencial. Nas regiões continentais, em troca, a humidade tem mais dificuldade para ser evapotranspirada. Por exemplo, a passagem de partículas de água congelada nos glaciares para a atmosfera apresenta enormes limitações, tal como a conversão em vapor atmosférico da água líquida armazenada no reservatório de águas subterrâneas, nas camadas profundas do solo. Estas restrições sugerem que a fração de evapotranspiração nas áreas continentais com respeito à evaporação nos oceanos deveria representar, globalmente, um valor notavelmente abaixo dos 2,6 % calculados anteriormente. Em consequência, em termos de precipitação e à escala planetária, poderíamos afirmar que, aproximadamente, a chuva proveniente de evapotranspiração terrestre não devia constituir mais de 2 ou 3% da chuva com origem na evaporação oceânica.

Mas é correto este balanço hídrico global para qualquer região continental? E mais especificamente, é correto para a Península Ibérica? Analisemos a questão em detalhe. A Península Ibérica ocupa o canto sudoeste do continente Europeu, no interior de um retângulo esférico imaginário definido pelas latitudes 36°N e 44°N e as longitudes 10°W e 2°E, aproximadamente. Rodeada por duas fontes *ilimitadas* de

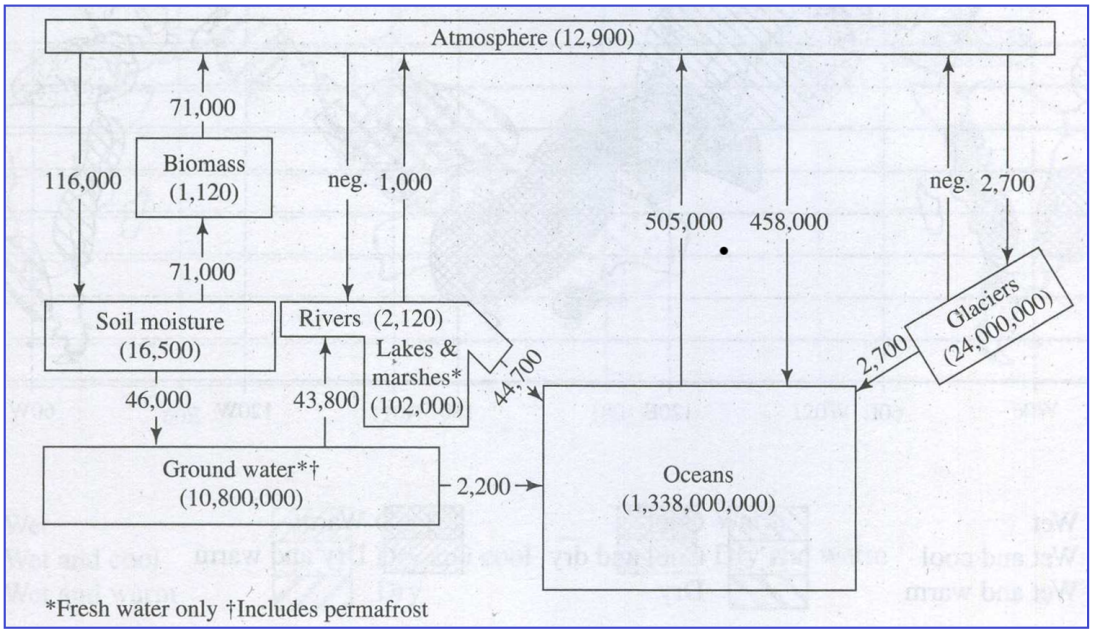

Figura 2: Representação esquemática dos reservatórios e fluxos de água (km^3) no ciclo hidrológico global. Figura obtida de Dingman (2002) [56].

água (o Oceano Atlântico e o Mar Mediterrâneo), a Península Ibérica recebe os ventos de Oeste, próprios das latitudes médias e responsáveis por transportarem a humidade evaporada no Atlântico para o interior da Península. Sob esta configuração geográfica, é claro que a humidade oceânica devia constituir, de longe, a principal fonte de água para a precipitação ibérica. Intuitivamente, e em concordância com a discussão prévia, poderíamos dizer numa primeira aproximação que a contribuição para a precipitação da humidade localmente evapotranspirada, com respeito à contribuição da humidade oceânica ou de grande escala, não devia ser muito maior do que os nossos 2 ou 3% globais. Mas é isto sempre assim?

A resposta é não. Nesta tese de doutoramento demonstramos que nas regiões áridas e semiáridas do interior, do Leste e do Nordeste da Península Ibérica, a humidade evapotranspirada localmente pode se responsável, direta ou indiretamente, por mais de 50% da precipitação durante a primavera e o começo do verão. Nas regiões costeiras do Atlântico e do Cantábrico, em troca, esta contribuição é muito mais baixa. A pergunta é, portanto, por que razão acontece esta "inesperada" intensificação do impacto da evapotranspiração na precipitação em grandes extensões do interior da Península Ibérica. Conhecer uma resposta completa a esta pergunta constitui, precisamente, o objetivo principal desta tese.

A relevância da precipitação primaveral

Grandes extensões do interior, Leste e Nordeste da Península Ibérica, onde a agricultura tem sido tradicionalmente o alicerce principal da economia local, apresentam características de aridez ou semiaridez e frequentes problemas de escassez de água. Num contexto de mudança climática, que muito provavelmente vai afetar a área Mediterrânica, e nomeadamente a Península Ibérica, com uma intensidade superior do que a média, conhecer as principais fontes de humidade e os mecanismos físicos específicos que controlam a precipitação nestas áreas torna-se essencial para a sustentabilidade das mesmas a médio e longo prazo.

O forte impacto da evapotranspiração na precipitação, observado durante a primavera e o início do verão em todo o interior da Ibéria, não seria assim tão relevante se estivesse associado a quantidades pequenas de chuva ou tivesse um impacto reduzido nas atividades humanas. No entanto, a situação é precisamente a contrária, pois é durante a primavera e o começo do verão que acontece o máximo absoluto no ciclo anual de precipitação em grandes extensões do interior, do Leste e do Nordeste peninsular. A elevada quantidade de chuva observada na primavera espelha-se numa grande quantidade de ditados e provérbios populares por toda a Ibéria, como é o caso do ditado castelhano *en abril, aguas mil* ou da versão portuguesa do mesmo, *é próprio do mês de abril as águas serem às mil*. Como já foi assinalado, é mesmo impossível descrever este pico de precipitação sem considerarmos a contribuição do fluxo interno de evapotranspiração. A natureza convectiva de muita desta precipitação reflete-se igualmente em vários provérbios, tanto no setor nordeste da Península, onde encontramos, por exemplo, *tronades d'abril, fruites mil* ("trovoadas de abril, frutas mil") ou *al Maig, cada dia un raig* ("em maio, cada dia um raio"), como na parte occidental, onde se diz que *maio que não der trovoada, não dá coisa estimada*.

Por outro lado, o aumento da precipitação na primavera no interior peninsular tem um forte impacto nas atividades humanas, nomeadamente na agricultura. Isto espelha-se também num grande número de ditados populares, de Portugal à Catalunha e da Andaluzia ao País Basco. Um bom exemplo é o dito castelhano *como agua de mayo*, muito comum na fala quotidiana para descrever qualquer facto ou ação que produz um efeito muito positivo. Igualmente, no interior de Portugal, uma grande quantidade de provérbios salientam a importância das chuvas de abril e maio. Assim, temos por exemplo *seca de abril, deixa o lavrador a pedir*; *maio pardo e ventoso faz o ano farto e formoso*; *água de maio, pão todo o ano*; *em maio verás a água com que regarás*, próprio também do interior da Galiza; ou *quando chove na Ascensão, até as pedrinhas dão pão*. Ditados semelhantes, a exprimirem esta mesma ideia, encontram-se também no País Basco: *Pazkoa euritsu, urte hura ogitsu* ("chuva na Páscoa, ano de abundância"); *maiatz eurite, urtea ogite* ("chuva em maio, ano de abundância"). Também na área oriental da Península são muitos os provérbios populares que confirmam a importância da precipitação primaveril para a agricultura. Por

exemplo, *l'abril mullat, de pa ve carregat* ("abril molhado, de pão vem carregado"); *a l'abril cada gota en val mil* ("em abril, cada pinga vale mil"); ou *maig humit fa al pagès ric* ("maio húmido torna o lavrador rico").

Conteúdos desta Tese

Esta Tese organiza-se em seis capítulos principais e cinco apêndices que incluem os materiais suplementares. Enquanto o capítulo 1 apresenta uma introdução geral a esta investigação, no capítulo 2 os diferentes métodos e conjuntos de dados utilizados neste trabalho são examinados. Os principais resultados são apresentados e discutidos nos capítulos 3, 4 e 5. Os capítulos 3 e 4 correspondem, em grande parte, com os artigos *"Precipitation recycling in the Iberian Peninsula: spatial patterns and temporal variability"* e *"Moisture recycling and the maximum of precipitation in spring in the Iberian Peninsula"*, respectivamente (as referências completas podem consultar-se na Lista de Publicações). O capítulo 5 complementa estes estudos mediante a análise de simulações regionais que incluem a inovadora ferramenta dos traçadores de humidade. O material incluído neste capítulo fará parte do artigo *"Regional climate simulations with moisture tracers to investigate land-atmosphere interactions in the terrestrial water cycle over the Iberian Peninsula"* (Lista de Publicações), que se encontra em preparação. Cada um desses três capítulos é introduzido por um pequeno *abstract* ou resumo inicial. No fim de cada um desses capítulos, as conclusões parciais correspondentes são sintetizadas. Finalmente, as conclusões gerais do conjunto deste estudo apresentam-se no capítulo 6.

O **capítulo 1** consiste numa introdução geral que permite contextualizar a investigação desenvolvida nesta tese de doutoramento. A motivação experimental, os objetivos e as bases teóricas deste estudo são exprimidas e examinadas em detalhe neste capítulo. Em primeiro lugar, inclui-se uma descrição completa do regime de precipitação na Península Ibérica. Em particular, uma especial atenção é dada ao máximo relativo de precipitação observado por todo o interior da Península, que tende a se converter no máximo absoluto do ciclo anual nas regiões do Leste e do Nordeste. A necessidade de compreender de forma completa os processos físicos responsáveis por este pico de precipitação constitui, como já foi assinalado, a principal motivação para esta tese. Isto requer uma investigação completa das principais fontes de humidade que contribuem para a precipitação na Ibéria e, especificamente, nas regiões do interior. Na prática, isto significa separar a contribuição da humidade localmente evapotranspirada da contribuição da humidade advectada do exterior da Península pelos ventos. A taxa de reciclagem, definida no capítulo 1, é uma magnitude crucial para avaliar o peso relativo destes dois termos.

A nossa hipótese de trabalho baseia-se na ideia de que a humidade localmente evapotranspirada constitui a chave para explicar o aumento da precipitação durante os

meses de abril e maio no interior da Península Ibérica. Isto quer dizer que as interações terra-atmosfera em geral, e os mecanismos de reciclagem e amplificação em particular, podem desempenhar um papel fundamental no regime pluviométrico primaveril das regiões do interior. Neste primeiro capítulo, esses processos terra-atmosfera são analisados em detalhe, incluindo-se uma discussão sobre a sua dependência com vários fatores, como é o caso das atividades humanas, da humidade do solo ou da dinâmica das águas subterrâneas e do lençol freático. O duplo efeito através do qual os fluxos de evapotranspiração intensificam a precipitação é também discutido: em primeiro lugar, fornecendo humidade adicional às camadas baixas atmosfera, de modo que essa humidade possa fazer parte de episódios posteriores de precipitação (efeito direto ou de reciclagem); em segundo lugar, favorecendo a instabilidade na coluna atmosférica e, consequentemente, a ascensão de vapor de água e o desenvolvimento de estruturas convectivas (efeito indireto ou de amplificação).

No **capítulo 2** descrevem-se os detalhes técnicos dos diferentes métodos, ferramentas computacionais e bases de dados utilizados nesta tese. As simulações realizadas com o modelo WRF constituem o principal material experimental usado na nossa análise. Neste capítulo descrevemos a configuração das simulações realizadas com o modelo WRF, especificando os domínios geográficos, períodos de tempo, resolução horizontal, opções do modelo e parametrizações utilizadas. Para além das simulações padrão com o modelo WRF, também foram realizadas, durante os meses de janeiro e maio dos anos 2000-2010, onze pares de simulações experimentais em que o fluxo de evapotranspiração sobre a Península Ibérica foi suprimido. Este procedimento representa a melhor maneira para explorar os diferentes efeitos da evapotranspiração terrestre nos regimes pluviométricos de inverno e de primavera na Península Ibérica. Esse impacto é discutido em maior profundidade no capítulo 5 por meio de simulações adicionais, também realizadas com o modelo WRF, nas quais é incluída uma nova ferramenta computacional: o uso de traçadores de humidade. Esta ferramenta inovadora permite seguir as trajetórias descritas pelas moléculas de humidade, desde o momento e lugar da evapotranspiração até precipitarem ou serem advectadas para fora do domínio do modelo.

Os métodos usados neste trabalho podem ser classificados em dois tipos. Por um lado, três métodos diferentes são utilizados para calcular a taxa de reciclagem: 1) o modelo analítico de reciclagem desenvolvido por Schär et al. (1999); 2) o modelo numérico de reciclagem de Eltahir e Bras (1994); e 3) o método explícitos dos traçadores de humidade. Por outro lado, dois métodos são empregues para separar as contribuições direta (reciclagem) e indireta (amplificação) dos fluxos de evapotranspiração ao pico de precipitação primaveril. O primeiro método é também devido a Schär et al. (1999), enquanto que o segundo é original, baseado na comparação de simulações de controlo (com todos os fluxos terra-atmosfera ativados) com as simulações experimentais, indicadas acima, nas quais esse fluxo é eliminado.

No **capítulo 3**, a taxa de reciclagem é calculada à escala mensal, para a Penín-

sula Ibérica, ao longo de um período de 18 anos completos (de janeiro de 1990 até dezembro de 2007). As taxas de reciclagem mais elevadas encontram-se no final da primavera e no início do verão. Curiosamente, os valores mais altos de reciclagem são observados no interior, coincidindo em grande parte com as áreas em que se regista o máximo anual de precipitação na primavera. Em geral, as duas condições especificadas a seguir estão diretamente relacionadas com os valores mais altos de reciclagem sobre a Península Ibérica: 1) a disponibilidade de humidade suficiente no solo, diretamente ligada à quantidade de chuva registada durante a estação prévia; e 2) a existência de configurações sinópticas apropriadas que favoreçam o desenvolvimento de regimes convectivos. A combinação destas duas condições permite explicar corretamente a magnitude das taxas de reciclagem em qualquer período do ano para a Península Ibérica. A nossa hipótese é que este esquema pode também ser válido para outras regiões do mundo com climas semiáridos. De qualquer maneira, esta pesquisa preliminar, complementada nos capítulos 4 e 5, confirma que os processos de reciclagem desempenham um papel crucial na precipitação primaveril do interior da Península Ibérica.

No **capítulo 4** concentramos a nossa atenção nos meses de maio da última década (2000-2010). Escolhemos este mês por duas razões: em primeiro lugar, porque é justamente em maio que ocorre o máximo anual de precipitação em grandes áreas do interior, Leste e Nordeste da Península Ibérica; e em segundo lugar, porque a intensidade das interações solo-atmosfera aumenta significativamente neste mês. Além disso, os correspondentes meses de janeiro ao longo do mesmo período são também simulados, com a finalidade de avaliar as importantes diferenças entre os regimes de precipitação do inverno e da primavera na Península. À luz desta análise, conclui-se que a supressão da evapotranspiração terrestre em maio teria como resultado uma redução média da precipitação total de cerca de 37%. Além disso, podemos concluir que as contribuições da reciclagem e da amplificação têm um impacto semelhante na precipitação extra de primavera associada aos fluxos terra-ar. Em geral, o termo de reciclagem tende a predominar quando o forçamento externo é fraco, nomeadamente na metade norte da Península Ibérica. Isso faz sentido, pois neste caso a água evapotranspirada localmente é praticamente a única fonte de humidade para precipitação. Inversamente, quando a circulação sinóptica é mais intensa e uma quantidade substancial de humidade externa é advectada do exterior da Península, o mecanismo de amplificação tende a predominar. Este efeito indireto dos fluxos de evapotranspiração é de grande importância, ao facilitar a incorporação de água externa adicional ao ciclo hidrológico peninsular.

No **capítulo 5** descrevem-se os resultados das simulações regionais sobre a Península Ibérica realizadas com o modelo WRF, ao longo do período de maio 2000 - maio 2010, incorporando os traçadores de humidade. Esta nova ferramenta computacional permite calcular a taxa de reciclagem e apresenta duas vantagens principais em relação aos métodos clássicos de computação da mesma: 1) O método calcula explicitamente as frações de precipitação com origem interna (evapotranspiração local)

e externa (advecção), sem precisar de qualquer suposição adicional; e 2) a taxa de reciclagem pode ser calculada em qualquer escala temporal, e não apenas às escalas mensais ou superiores, tal como as limitações dos modelos tradicionais de reciclagem impõem. Estas simulações com traçadores de humidade demonstram que tanto a taxa de reciclagem como a contribuição de reciclagem para a precipitação adicional da primavera encontram-se distribuídas de forma bastante uniforme pelo interior da metade norte peninsular, com particular incidência no Planalto Norte, na região Centro, no Sistema Ibérico e nos Pirenéus, e não tão concentradas nas regiões Leste e Nordeste como sugere o cálculo clássico segundo o método de Eltahir e Bras (1994). Este último método tende a subestimar sistematicamente os valores de reciclagem, enquanto o modelo (mais simples) desenvolvido por Schär et al. (1999) produz valores regionais de reciclagem muito mais próximos dos resultados mais precisos e fiáveis obtidos por meio do método dos traçadores de humidade.

Finalmente, as conclusões mais importantes do conjunto da presente investigação são resumidas no **capítulo 6**. À luz dos nossos resultados, podemos dizer que o máximo primaveril de precipitação que ocorre no interior da Península Ibérica não pode ser explicado sem ter em conta o papel crucial das interações terra-atmosfera e, especificamente, dos fluxos de evapotranspiração. Temos a certeza que esta tese constitui uma melhora significativa na descrição do regime de precipitação das regiões interiores da Península. Os principais mecanismos físicos que explicam o aumento da quantidade de chuva na primavera foram identificados e os métodos utilizados e desenvolvidos permitem avaliar satisfatoriamente o seu impacto.

Nos apêndices incluídos no fim desta tese, alguns materiais adicionais são apresentados. Nos apêndices A, B e C certos aspetos complementares relativamente ao cálculo dos termos do balanço hídrico e a taxa de reciclagem por meio dos métodos de Schär et al. (1999) e Eltahir and Bras (1994) são discutidos. No apêndice D explica-se minuciosamente o procedimento a seguir para suprimir a evapotranspiração terrestre nas simulações com o modelo WRF analisadas no capítulo 4. No apêndice E, finalmente, estuda-se a sensibilidade do método clássico de reciclagem de Eltahir e Bras (1994) à resolução horizontal.

Possíveis aplicações e trabalho futuro

As possíveis aplicações práticas da investigação apresentada nesta tese poderão ser classificadas em dois grandes blocos. Por um lado, o nosso estudo pode contribuir para a melhoria dos sistemas de predição sazonal na Península Ibérica e, consequentemente, para o aperfeiçoamento na gestão de sistemas de alerta perante eventos extremos. Nesta tese mostra-se que o efeito da evapotranspiração local na precipitação primaveril é fundamental no interior da Península Ibérica. Deste modo, se o inverno de um determinado ano é extremamente seco, a subsequente escassez de água no solo

resultará numa diminuição da evapotranspiração e, portanto, da precipitação posterior. Nestas condições, a probabilidade de um verão seco é muito maior, reduzindo-se ao mesmo tempo os riscos de enxurradas. Pelo contrário, a probabilidade de eventos extremos de chuva após um inverno húmido aumenta significativamente, embora a sua ocorrência fique sujeita, em grande medida, à configuração sinóptica específica da primavera e verão seguintes. Esta análise mostra que a avaliação do impacto dos fluxos terra-ar no regime de chuvas pode ser essencial para estimar o risco de secas e inundações na Península Ibérica.

Temos a convicção que este estudo pode ser também muito útil em termos de planejamento hidrológico e sustentabilidade regional. Isto tem a ver com o facto de as atividades humanas terem um impacto decisivo na fração local da precipitação. Em consequência, no interior da Península Ibérica, onde esta contribuição desempenha um papel essencial no regime pluviométrico primaveril, uma melhor planificação do uso da terra e uma correta gestão dos limitados recursos hídricos torna-se fundamental para a sustentabilidade da região a médio e longo prazo.

No futuro, a realização de simulações com o modelo regional WRF incluindo os traçadores de humidade, bem como um esquema de superfície totalmente acoplado e que represente a dinâmica completa das águas subterrâneas e do lençol freático, constituirá provavelmente a melhor maneira de investigar o ciclo hidrológico e do regime de precipitação da Península Ibérica. Consideramos que este procedimento pode ser útil não só nas regiões interiores da Península, mas também em qualquer outra região do mundo com características semiáridas.

Resumen

Motivación

El agua es esencial para la vida en la Tierra. Los océanos de todo el planeta contienen 1 338 000 000 km^3 de agua salada (Fig. 3). Las regiones continentales, por su parte, almacenan únicamente 34 921 740 km^3 de agua dulce, distribuida en glaciares (24 000 000 km^3), aguas subterráneas (10 800 000 km^3), lagos y marismas (102 000 km^3), humedad del suelo (16 500 km^3), ríos (2 120 km^3) y agua contenida en la biomasa (1 120 km^3). Por último, la atmósfera contiene 12 900 km^3 (Dingman, 2002 [56]). Un cálculo simple muestra que:

$$\frac{\text{Agua contenida en los continentes}}{\text{Agua contenida en los océanos}} \approx \frac{\text{Agua dulce}}{\text{Agua salada}} \approx 2{,}6\,\% \tag{3}$$

En los océanos hay siempre agua disponible para la evaporación. Esto implica que la evaporación oceánica coincide con la evaporación potencial. En las regiones continentales, en cambio, la humedad tiene más dificultades para ser evapotranspirada. Por ejemplo, el paso de partículas de agua congelada en los glaciares hacia la atmósfera es mínimo, como también lo es la conversión en vapor atmosférico de agua líquida almacenada en el reservorio de aguas subterráneas, en las capas profundas del suelo. Estas restricciones sugieren que la fracción de evapotranspiración en zonas continentales con respecto a la evaporación en los océanos debería representar, globalmente, un valor mucho menor que el 2.6 % calculado arriba. Por lo tanto, en términos de precipitación y a escala planetaria, podríamos afirmar *grosso modo* que la lluvia con origen en evapotranspiración terrestre no debería de suponer más de un 2 ó un 3 % de la lluvia procedente de evaporación oceánica.

Pero, ¿es correcto este balance hídrico global para una región continental concreta? Y más específicamente, ¿es cierto para la Península Ibérica? Examinémoslo en detalle. La Península Ibérica se encuentra en la esquina suroccidental del continente europeo, dentro de un rectángulo esférico imaginario definido por las latitudes 36°N y 44°N y las longitudes 10°W y 2°E, aproximadamente. Rodeada de dos fuentes *ili-*

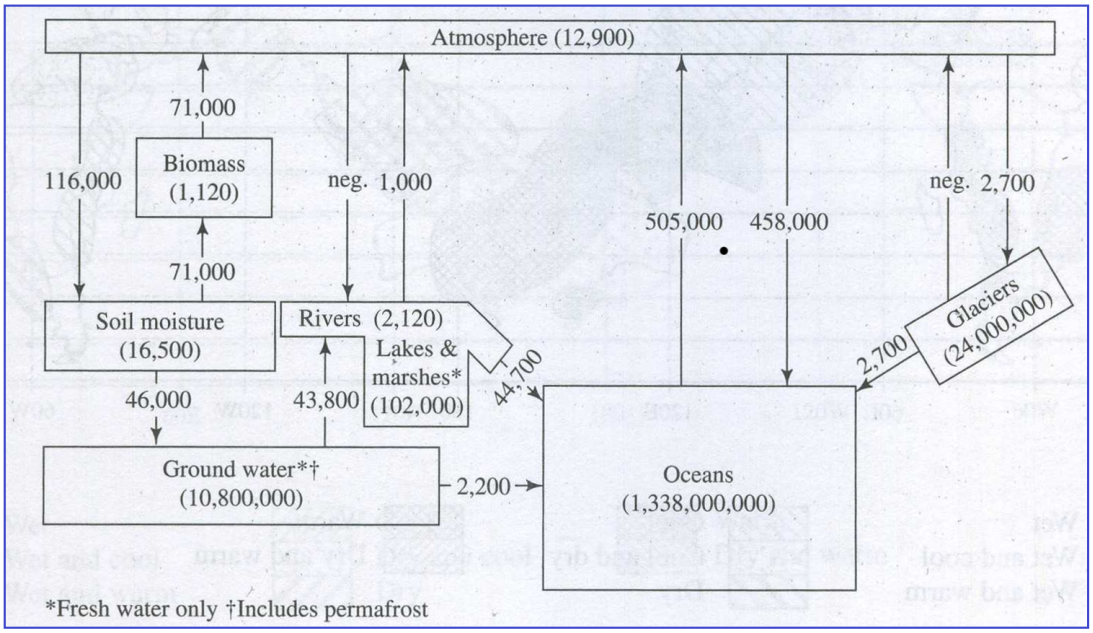

Figura 3: Representación esquemática de los reservorios y flujos de agua (km^3) en el ciclo hidrológico global. Figura obtenida de Dingman (2002) [56].

mitadas de agua como son el Océano Atlántico y el Mar Mediterráneo, la Península Ibérica recibe los vientos del Oeste, característicos de las latitudes medias, que transportan humedad evaporada en el Atlántico hacia el interior de la Península. Con esta configuración geográfica, resulta claro que la humedad oceánica debería constituir, con mucha diferencia, la principal fuente de agua para la precipitación ibérica. Intuitivamente, y de acuerdo con la discusión anterior, podríamos decir en una primera aproximación que la contribución de humedad localmente evapotranspirada a la precipitación, con respecto a la contribución de humedad oceánica o de larga escala, no debería ser mucho mayor que nuestro 2 ó 3 % global. Pero, ¿es esto siempre así?

La respuesta es no. En esta tesis doctoral demostramos que en las regiones áridas y semiáridas del interior, del Este y del Noreste de la Península Ibérica, la humedad evapotranspirada localmente puede ser responsable, directa o indirectamente, de más del 50 % de la precipitación total durante la primavera y el comienzo del verano. En las regiones costeras del Atlántico y del Cantábrico, en cambio, esta contribución es muchísimo más pequeña. La pregunta es, entonces, por qué razón se produce esta "inesperada" intensificación del impacto de la evapotranspiración en la precipitación a lo largo de buena parte del interior de la Península Ibérica. Proporcionar una respuesta integral a esta pregunta constituye, justamente, el objetivo principal de esta tesis.

La importancia de la precipitación primaveral

Muchas de las regiones del interior, Este y Noreste de la Península Ibérica, donde la agricultura ha sido tradicionalmente el principal pilar de la economía, presentan características áridas o semiáridas y frecuentes problemas de escasez de agua. En un contexto de cambio climático, que muy posiblemente afectará al área Mediterránea, y en particular a la Península Ibérica, con una intensidad superior a la media, conocer las principales fuentes de humedad y los mecanismos físicos específicos que controlan la precipitación en estas zonas resulta crucial para su sostenibilidad a medio y largo plazo.

El notable impacto de la evapotranspiración en la precipitación, que se observa durante la primavera y el comienzo del verano a lo largo de la Iberia interor, no sería tan relevante si estuviese asociado a cantidades de lluvia pequeñas o tuviese un impacto reducido en las actividades humanas. Sin embargo, la situación es precisamente la contraria, puesto que es precisamente durante la primavera y el inicio del verano cuando tiene lugar el máximo absoluto en el ciclo anual de precipitación de extensas regiones del interior, del Este y del Noreste peninsular. La notable cantidad de lluvia registrada en primavera se ve reflejada en una gran cantidad de proverbios y refranes populares por toda la Península, como es el caso del dicho castellano *en abril, aguas mil* o, en su versión portuguesa, *é próprio do mês de abril as águas serem às mil.* Como se ha indicado, es imposible describir este pico de precipitación sin tener en cuenta la contribución al mismo del flujo interno de evapotranspiración. La naturaleza convectiva de buena parte de esta lluvia aparece también recogida en diversos proverbios, tanto en el sector nororiental de la Península, donde encontramos, por ejemplo, *tronades d'abril, fruites mil* ("tormentas de abril, frutas mil") o *al maig, cada dia un raig* ("en mayo, cada día un rayo"), como en la zona occidental, donde se dice, con un significado similar, que *maio que não der trovoada, não dá coisa estimada.*

Por otro lado, el aumento de la precipitación en primavera en el interior peninsular tiene un gran impacto en las actividades humanas, y muy especialmente en la agricultura. Ello se traduce también en un enorme número de dichos y proverbios populares, desde Portugal a Cataluña y de Andalucía al País Vasco. Un buen ejempo es el refrán castellano *como agua de mayo*, muy usado en el habla cotidiana para describir cualquier hecho o acción que produce un efecto muy positivo. Igualmente, en el interior de Portugal, una gran cantidad de proverbios destacan la importancia de la lluvia en abril y mayo. Por ejemplo, *seca de abril, deixa o lavrador a pedir* ("sequía de abril, pone al labrador a pedir"); *maio pardo e ventoso faz o ano farto e formoso* ("mayo pardo y ventoso hace al año abundante y hermoso"); *água de maio, pão todo o ano* ("agua de mayo, pan todo el año"); *em maio verás a água com que regarás* ("en mayo verás el agua con que regarás"), propio también del interior de Galicia; o *quando chove na Ascensão, até as pedrinhas dão pão* ("cuando llueve en la Ascensión, hasta las piedras dan pan"). Dichos parecidos, expresando esta misma idea, se pueden

encontrar también en el País Vasco: *Pazkoa euritsu, urte hura ogitsu* ("lluvia en la Pascua, año de bienes"); *maiatz eurite, urtea ogite* ("lluvia en mayo, año de bienes"). Asimismo, en la zona oriental de la Península, muchos proverbios y refranes confirman la importancia de esta precipitación primaveral para la agricultura. Por ejemplo, *l'abril mullat, de pa ve carregat* ("abril mojado, de pan viene cargado"); *a l'abril cada gota en val mil* ("en abril, cada gota vale mil"); o *maig humit fa al pagès ric* ("mayo húmedo hace al labrador rico").

Contenidos de esta Tesis

Esta Tesis se organiza en seis capítulos principales y cinco apéndices que incluyen los materiales suplementarios. Mientras que el capítulo 1 proporciona una introducción general a esta investigación, en el capítulo 2 se examinan los diferentes métodos y conjuntos de datos utilizados en este trabajo. Los principales resultados se presentan y discuten en los capítulos 3, 4 y 5. Los capítulos 3 y 4 se corresponden, en gran medida, con los artículos *"Precipitation recycling in the Iberian Peninsula: spatial patterns and temporal variability"* y *"Moisture recycling and the maximum of precipitation in spring in the Iberian Peninsula"*, respectivamente (las referencias completas pueden verse en la Lista de Publicaciones). El capítulo 5 complementa estos estudios mediante el análisis de simulaciones regionales que incluyen la herramienta de los trazadores de humedad. El material incluido en este capítulo formará parte del artículo *"Regional climate simulations with moisture tracers to investigate land-atmosphere interactions in the terrestrial water cycle over the Iberian Peninsula"* (Lista de Publicaciones), que se encuentra en preparación en el momento de la presentación de esta Tesis. Cada uno de estos tres capítulos incluye un pequeño *abstract* o resumen inicial, así como una breve sección final en la que se recapitulan las conclusiones parciales más relevantes. Finalmente, las conclusiones generales del conjunto de esta investigación se presentan en el capítulo 6.

El **capítulo 1** consiste en una introducción general que permite contextualizar adecuadamente la investigación desarrollada en esta tesis. En este capítulo se explican y examinan detalladamente la motivación experimental, los objetivos y las bases teóricas del presente estudio. En primer lugar, se incluye una descripción completa del régimen de precipitaciones en la Península Ibérica, prestando una atención especial al máximo relativo de lluvia observado a lo largo del interior peninsular, que tiende a convertirse en el máximo absoluto en el ciclo anual en las regiones orientales y nororientales. La necesidad de comprender por completo los procesos físicos responsables de este pico de lluvia constituye, como se ha mencionado, la principal motivación para esta tesis. Ello requiere una investigación integral de las principales fuentes de humedad que contribuyen a la precipitación en la Península y, en particular, en el interior de la misma. En la práctica, esto implica separar la contribución de la humedad localmente evapotranspirada de la contribución de la humedad advectada

desde el exterior de la Península por los vientos. La tasa de reciclaje, cuidadosamente definida en el capítulo 1, es una magnitud crucial para evaluar el peso relativo de ambos términos.

Nuestra hipótesis de trabajo se basa en la idea de que la humedad localmente evapotranspirada puede ser la clave para explicar el repunte de la precipitación durante los meses de Abril y Mayo en el interior de la Península Ibérica. Esto implica que las interacciones tierra-atmósfera en general, y los mecanismos de reciclaje y amplificación en particular, pueden jugar un papel fundamental en el régimen pluviométrico primaveral de las regiones interiores. En este primer capítulo caracterizamos detalladamente estos procesos tierra-atmósfera e incluimos una discusión sobre su dependencia de diferentes factores, como las actividades humanas, la humedad del suelo o la dinámica de las aguas subterráneas y de la capa freática. El doble efecto mediante el cual los flujos de evapotranspiración intensifican la precipitación es asimismo discutido: por un lado, añadiendo más humedad a la atmósfera, de forma que dicha humedad pueda formar parte de episodios posteriores de precipitación (efecto directo o de reciclaje); por otro lado, incrementando la inestabilidad de la columna atmosférica y, por lo tanto, favoreciendo la ascensión de vapor de agua y el desarrollo de estructuras convectivas (efecto indirecto o de amplificación).

En el **capítulo 2** se describen los detalles técnicos de los distintos métodos, herramientas computacionales y bases de datos utilizadas en esta tesis. Las simulaciones realizadas con el modelo WRF constituyen el principal material experimental utilizado en nuestro análisis. En este capítulo describimos la configuración de las simulaciones realizadas con dicho modelo, explicitando los dominios geográficos, períodos de tiempo, resolución horizontal, opciones del modelo y parametrizaciones utilizadas. Además de las simulaciones estándar con el modelo WRF, se han llevado también a cabo, para los meses de enero y mayo de los años 2000 a 2010, once pares de simulaciones experimentales en las que se ha suprimido el flujo de evapotranspiración sobre toda la Península Ibérica. Este procedimiento constituye una forma óptima de explorar el diferente efecto de la evapotranspiración terrestre en los regímenes pluviométricos de invierno y primavera en la Península Ibérica. Dicho impacto se examina con aún más detalle en el capítulo 5 mediante simulaciones adicionales, realizadas también con el modelo WRF, en las que se incluye una nueva herramienta computacional: el uso de trazadores de humedad. Esta herramienta innovadora permite seguir las trayectorias descritas por las moléculas de humedad, desde que se evapotranspiran hasta que precipitan o son advectadas hacia el exterior del dominio del modelo.

Los métodos empleados en esta tesis se pueden clasificar en dos tipos. Por un lado, se utilizan tres procedimientos diferentes para calcular la tasa de reciclaje: 1) el modelo analítico de reciclaje desarrollado por Schär et al. (1999); 2) el modelo numérico de reciclaje de Eltahir y Bras (1994); y 3) el método explícito de trazadores de humedad. Por otro lado, se utilizan dos métodos para separar las contribuciones directa (reciclaje) e indirecta (amplificación) de los flujos de evapotranspiración al

pico de precipitación primaveral. El primer método es también debido a Schär et al. (1999), mientras que el segundo es original, basado en la comparación de simulaciones de control, con todos los flujos tierra-atmósfera activados, con las simulaciones experimentales antes mencionadas, en las cuales dichos flujos son eliminados.

En el **capítulo 3** calculamos la tasa de reciclaje a escala mensual, sobre la Península Ibérica, a lo largo de un período de 18 años completos (desde enero de 1990 hasta diciembre de 2007). Las tasas de reciclaje más elevadas aparecen a finales de la primavera y principios del verano. Curiosamente, los valores más altos de reciclaje se observan en el interior, coicidiendo en buena medida con aquellas áreas en las que se observa el máximo anual de precipitación primaveral. En general, las dos siguientes condiciones están directamente relacionadas con los valores más elevados de reciclaje sobre la Península Ibérica: 1) la disponibilidad de suficiente humedad en el suelo, directamente ligada a la cantidad de lluvia caída durante la estación anterior; y 2) la existencia de configuraciones sinópticas adecuadas que favorezcan el desarrollo de regímenes convectivos. La combinación de estas dos condiciones parece explicar correctamente la magnitud de las tasas de reciclaje en cualquier período del año para la Península Ibérica. Nuestra hipótesis es que este esquema también podría ser válido para otras regiones del mundo con climas semiáridos. En cualquier caso, esta investigación preliminar, que se complementa en los capítulos 4 y 5, confirma que los procesos de reciclaje juegan un papel crucial en la precipitación primaveral del interior de la Península Ibérica.

En el **capítulo 4** centramos nuestra atención en los meses de mayo de la última década (2000-2010). La razón para seleccionar este mes es doble: en primer lugar, porque es justamente en mayo cuando tiene lugar el máximo anual de precipitación en grandes extensiones del interior, Este y Nordeste de la Península Ibérica; y en segundo lugar, porque la actividad de las interacciones tierra-atmósfera aumenta significativamente en este mes. Además, se simulan también los correspondientes meses de enero del mismo período, como el fin de evaluar las importantes diferencias entre los regímenes de precipitación de invierno y primavera (tardía) en la Península. A la luz de este análisis se concluye que la supresión de la evapotranspiración terrestre en mayo implicaría una reducción media de la precipitación total de un 37 %. Además, se concluye que las contribuciones del reciclaje y de la amplificación tienen un impacto similar en la precipitación extra de primavera asociada a los flujos tierra-aire. En general, el término de reciclaje tiende a predominar cuando el forzamiento externo es débil, sobre todo en la mitad norte de la Península Ibérica. Esto es esperable, puesto que en este caso el agua evapotranspirada localmente es prácticamente la única fuente de humedad para la precipitación. Por el contrario, cuando la circulación sinóptica es intensa y una cantidad sustancial de humedad externa es advectada hacia la Península, el mecanismo de amplificación tiende a prevalecer. Este efecto indirecto de los flujos de evapotranspiración es de la mayor importancia, al permitir la incorporación de agua externa adicional al ciclo hidrológico peninsular.

En el **capítulo 5** se describen los resultados de las simulaciones regionales sobre la Península Ibérica realizadas con el modelo WRF, a lo largo del período mayo 2000 a mayo 2010, incorporando los trazadores de humedad. Esta nueva herramienta computacional permite calcular la tasa de reciclaje y presenta dos ventajas principales con respecto a los métodos clásicos de estimación de la misma: 1) el método calcula explícitamente las fracciones de precipitación con origen interno (evapotranspiración local) y externo (advección), sin necesidad de ninguna suposición adicional; y 2) la tasa de reciclaje puede calcularse a cualquier escala temporal, y no sólo a escalas mensuales o superiores, tal como las limitaciones de los modelos tradicionales de reciclaje imponen. Estas simulaciones con trazadores de humedad demuestran que tanto la tasa de reciclaje como la contribución del término de reciclaje a la precipitación adicional de primavera están distribuidas de forma bastante uniforme por el interior de la mitad norte peninsular, con especial intensidad en la Meseta Norte, la zona Centro, el Sistema Ibérico y los Pirineos, y no tan concentradas en las regiones Este y Nordeste como sugiere el cálculo clásico mediante el método de Eltahir y Bras (1994). Este último método tiende a sobreestimar sistemáticamente los valores de reciclaje, mientras que el modelo (más sencillo) desarrollado por Schär et al. (1999) produce valores regionales de reciclaje mucho más próximos a los más exactos y fiables resultados obtenidos a través del método de trazadores de humedad.

Por último, las conclusiones más importantes de la presente investigación en su conjunto se resumen en el **capítulo 6**. A la luz de nuestros resultados, podemos afirmar que el máximo primaveral de precipitación que tiene lugar en el interior de la Península Ibérica no puede explicarse sin tener en cuenta el papel crucial de las interacciones tierra-atmósfera y, en particular, de los flujos de evapotranspiración. Creemos firmemente que esta tesis constituye una mejora importante en la descripción del régimen de precipitación de las regiones interiores de la Península. Los principales mecanismos físicos que explican el repunte de la cantidad de lluvia en primavera han sido identificados, y los métodos aquí utilizados y desarrollados dan cuenta, satisfactoriamente, del impacto relativo de los mismos.

En los apéndices que aparecen al final de esta tesis se incluyen algunos materiales adicionales. En los apéndices A, B y C se proporcionan ciertos detalles complementarios sobre el cálculo de los términos del balance hídrico y la tasa de reciclaje a través de los métodos de Schär et al. (1999) y Eltahir and Bras (1994). En el apéndice D se explicar con detenimiento el procedimiento seguido para eliminar la evapotranspiración terrestre en las simulaciones con WRF analizadas en el capítulo 4. En el apéndice E, por último, se explora la sensibilidad del método clásico de reciclaje de Eltahir y Bras (1994) a la resolución horizontal de los cálculos.

Posibles aplicaciones y trabajo futuro

Las posibles aplicaciones prácticas de la investigación presentada en esta tesis podrían clasificarse en dos grandes bloques. Por un lado, nuestro estudio puede contribuir a la mejora de los sistemas de predicción estacional en la Península Ibérica y, en relación con esto, a la mejora en la gestión de los sistemas de alerta ante eventos extremos. En esta tesis hemos demostrado que el efecto de la evapotranspiración local en la precipitación primaveral es crucial en el interior de la Península Ibérica. Así, si el invierno de un cierto año es muy seco, la consiguiente escasez de agua en el suelo dará lugar a una disminución de la evapotranspiración y, en consecuencia, de la precipitación posterior. En esta situación, la probabilidad de un verano seco es mucho mayor, reduciéndose al mismo tiempo los riesgos de inundaciones. Por el contrario, la probabilidad de eventos extremos de precipitación después de un invierno húmedo se incrementa de manera significativa, a pesar de que su ocurrencia o no depende en gran medida de la configuración sinóptica específica de la primavera y verano posteriores. Este análisis muestra que la evaluación del impacto de los flujos tierra-aire en el régimen de precipitaciones puede ser fundamental para estimar los riesgos de sequías e inundaciones en la Península Ibérica.

Creemos que esta investigación puede ser también muy útil en términos de planificación hidrológica y sostenibilidad regional, como consecuencia del impacto decisivo de las actividades humanas sobre la fracción local de la precipitación. En consecuencia, en el interior de la Península Ibérica, donde esta contribución juega un papel fundamental en el régimen pluviométrico primaveral, una adecuada planificación del uso de la tierra y una correcta gestión de los limitados recursos hídricos resulta esencial para la sostenibilidad de estas áreas a medio y largo plazo.

En el futuro, la realización de simulaciones con el modelo regional WRF incluyendo los trazadores de humedad, así como un esquema de superficie totalmente acoplado y que represente la dinámica completa de las aguas subterráneas y de la capa freática, constituirá probablemente la mejor forma de investigar el ciclo hidrológico y el régimen pluviométrico de la Península Ibérica. Creemos que este procedimiento puede ser útil no sólo en las zonas interiores de la Península sino también en cualquier otra región del mundo con características semiáridas.

1

General introduction

1.1 The Iberian precipitation regime

It is widely known that the water cycle plays a prominent role on the Earth's climate (e.g. Eltahir and Bras, 1996 [77]). As a result, exploring the precipitation regime of a certain region becomes a central feature for describing its specific climate. In our study area, the Iberian Peninsula (IP), both the European Atlantic and the Mediterranean climates converge. Located in the extreme southwest of the European continent, and surrounded by the Atlantic Ocean and the Mediterranean Sea, the Iberian Peninsula presents a complex orography that is often compared to a castle, with high plateaus in the interior bounded by mountain ranges that sometimes are close to the coast (Millán et al., 2005 [183]). This configuration of the relief facilitates the delimitation of climatic sub-regions, with specific characteristics resulting from the topographic insulation from the surrounding seas (Capel-Molina, 2000 [42]; Estrela et al., 2000 [83]; González-Hidalgo et al., 2001 [117]).

The Iberian Peninsula is located at mid latitudes, where precipitation falls approximately during ten per cent of the time (Trenberth, 1998 [246]). In general, and also for the IP, the intensity and spatio-temporal distribution of rainfall is controlled by four basic aspects (Chen and Avissar, 1994 [45]): 1) synoptic-scale wind patterns; 2) atmospheric moisture availability; 3) intensity of humidity fluxes from the land surface; and 4) atmospheric instability favoring moisture to rise.

Roughly, the Iberian precipitation regime is controlled by the westerly circulation during the winter half of the year and by the subtropical Azores anticyclone during summer (e.g. Lana and Burgueño, 2000 [160]). As mentioned, the IP presents an intricate orography that is largely responsible for the geographical hetereogeneity of the rainfall patterns (Rodríguez-Puebla et al., 1998 [210]; Sumner et al., 2001 [240]; Castro et al., 2005 [44]; Millán et al., 2005 [183]; Martín-Vide and López-Bustins, 2006

[174]; González-Hidalgo et al., 2009 [118]; De Luis et al., 2010 [52]), which show essential differences from the northwestern areas to the Mediterranean coast and have a critical impact on climate. Following the Cantabrian Mountains along the northern coast, the contour of 700 mm of precipitation per year (Font-Tullot, 2000 [97]) separates the most northern and northwestern regions (*humid Iberia*) from the rest of the Peninsula (*Mediterranean Iberia* with dry summers). South of this boundary, the valleys of the great rivers draining into the Atlantic (Douro, Tagus, Guadiana and Guadalquivir) facilitate the penetration inland of southwest winds bringing humidity from the ocean, mainly from October to March (Capel-Molina, 2000 [42]). In contrast, the Iberian System and the Baetic Mountains obstruct the penetration of humid Mediterranean winds, only facilitated through the Ebro and Júcar river basins (Font-Tullot, 2000 [97]). The predominance of the western circulation over the IP, in accordance to the global dynamics of the atmosphere at mid-latitudes (Martín-Vide, 1991 [170]; Sendiña and Muñuzuri, 2006 [222]; Wallace and Hobbs, 2006 [260]), turns the effect of this *Levante* wind in the interior of the Ebro catchment much less relevant than that of the Atlantic southwestern winds over the great basins of the Atlantic Watershed. In the areas to the north, the Galician Massif, the Cantabrian Mountains and the Pyrenees become a natural obstacle which attenuates the advection of the cold north, northwest and northeast winds into the North Plateau. The Mediterranean shore, located in the rain shadow of Iberia, sees much less of the above-mentioned oceanic moisture. The driest areas are placed in the southeast (Rodríguez-Puebla et al., 1998 [210]; Romero et al., 1998 [212]), with less than 200 mm of precipitation per year. Cabo de Gata, with 130 mm per year, reaches the absolute minimum of precipitation in Europe (Font-Tullot, 2000 [97]). In contrast, over 2500 mm of precipitation per year are measured in the northwestern mountainous areas (Romero et al., 1998 [212]; Trigo et al., 2004 [252]).

The Iberian precipitation regime is also characterized by a strong seasonal and interannual variability (Raso-Nadal, 1996 [208]; Esteban-Parra et al., 1998 [82]; Serrano et al., 1999 [226]; Lana and Burgueño, 2000 [160]; Trigo and DaCamara, 2000 [250]; Sáenz et al., 2001 [214]; Trigo and Palutikof, 2001 [251]; García et al., 2002 [102]; Trigo et al., 2004 [252]; Gallego et al., 2006 [101]; López-Moreno et al., 2010 [166]; Vicente-Serrano et al., 2011 [259]; Cardoso et al., 2012 [43]). Only in the humid mountainous areas in the north and northwest, that interannual variability is significantly reduced (Rodríguez-Puebla et al., 1998 [210]). For Iberia as a whole, the spatio-temporal rainfall variability is expected to be significantly intensified during the next decades as a result of climate change (Galán et al., 1999 [99]; Giorgi and Lionello, 2008 [115]).

A complete classification and analysis of the different Iberian climates and subclimates can be found in Capel-Molina (2000) [42] and Martín-Vide and Olcina-Cantos (2001) [172]. A more detailed study of the different geographical and dynamical features affecting the Iberian climate is provided in the classic study by Capel-Molina (1981) [41]. Finally, a review on the evolution of the Iberian climate and a brief

summary of the history of meteorological and climatological research in Portugal and Spain can be found in Font-Tullot (1988) [96] and Capel-Molina (2000) [42], respectively.

The maximum of precipitation in late autumn and winter over central and western Iberia

The Iberian Peninsula receives the largest amounts of precipitation from October to March (Trigo et al., 2000 [249]; Paredes et al., 2006 [198]). This winter precipitation, which mainly affects western and central Iberia, is originated by synoptic low pressure systems, with their associated fronts, approaching from the Atlantic Ocean (Esteban-Parra et al., 1998 [82]; Serrano et al., 1999 [226]; Andrés et al., 2000 [3]; Trigo et al., 2000 [249]; Goodess and Jones, 2002 [119]; García-Herrera et al., 2005 [105]; Paredes et al., 2006 [198]). Fig. 1.1 shows on a map the monthly mean annual evolution of precipitation for 28 representative Iberian locations over the period 1950-2007, illustrating the spatial variability of the Iberian precipitation regime. At the monthly and seasonal scales, the precipitation regime is strongly modulated by just a few large scale modes of atmospheric circulation such as the North Atlantic Oscillation (NAO) and, to a lesser extent, the Eastern Atlantic (EA), the Scandinavian (SCAN) pattern (Rodríguez-Puebla et al., 2001 [211]; Goodess and Jones, 2002 [119]; Trigo et al., 2008 [254]), the Mediterranean Oscillation (MO) and the Western Mediterranean Oscillation (WeMO) (Martín-Vide and López-Bustins, 2006 [174]; González-Hidalgo et al., 2009 [118]). Some relevant linkages between the Iberian rainfall and El Niño-Southern Oscillation (ENSO) have also been found (Rocha, 1999 [209]; Pozo-Vázquez et al., 2005 [205]). Over the western half of Iberia, the NAO index is strongly connected with rainfall amounts (Martín-Vide and Fernández-Belmonte, 2001 [171]; Trigo et al., 2004 [252]; Gallego et al., 2005 [100]; García et al., 2005 [103]; López-Moreno et al., 2007 [165]), largely determined by the main position of the storm track. At these latitudes, this results in high seasonality, with a maximum of precipitation in winter and a dry period in the summer, more pronounced and long lasting in the southern areas and less so in the north, still marginally impacted by frontal systems. As shown in Fig. 1.1, this gradual variation from the winter maximum to the summer minimum, directly related to the meridional displacement of the westerlies through the year, dominates along the Atlantic coast (e.g. Corunna (8), Vigo (26), Lisbon (14) Cádiz (6) and Málaga (18) in Fig. 1.1), but is also visible in all those areas under the Atlantic influence, as is the case of Seville (22 in Fig. 1.1), located in the wide valley of the Guadalquivir river, which facilitates the advection of oceanic humidity inland by southwest winds. The description of the precipitation dataset used in Fig. 1.1 and also in Figs. 1.2, 1.3 and 1.4 is provided in section 2.8.

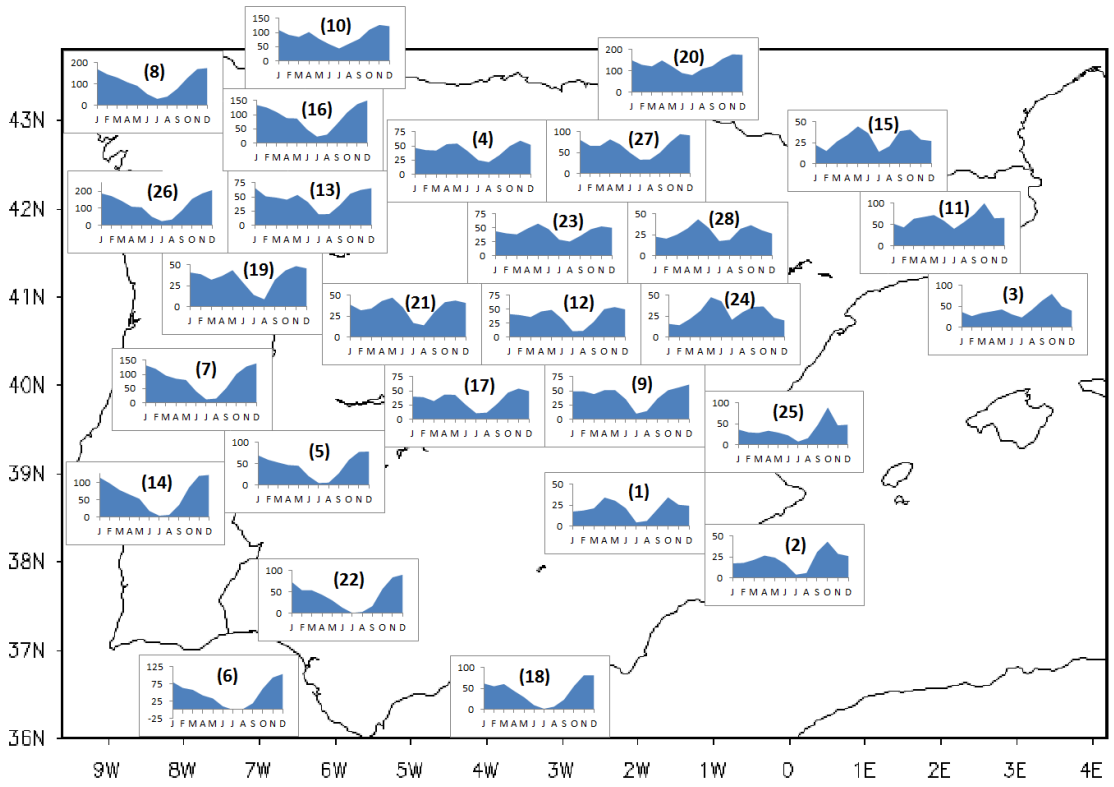

Figure 1.1: Monthly mean precipitation (mm/month) over the period 1950-2007 for 28 representative Iberian locations: (1) Albacete; (2) Alacant; (3) Barcelona; (4) Burgos; (5) Cáceres; (6) Cádiz; (7) Coimbra; (8) Coruña, A; (9) Cuenca; (10) Gijón; (11) Girona; (12) Guadalajara; (13) León; (14) Lisboa; (15) Lleida; (16) Lugo; (17) Madrid; (18) Málaga; (19) Salamanca; (20) San Sebastián/Donostia; (21) Segovia; (22) Sevilla; (23) Soria; (24) Teruel; (25) València; (26) Vigo; (27) Vitoria/Gasteiz; (28) Zaragoza. Source: Herrera et al. 2010 [123], Belo-Pereira et al. 2011 [13].

The early autumn maximum of precipitation in the Mediterranean

As mentioned above, the areas facing the Mediterranean Sea are shielded from the humid westerlies by the Iberian mountain ranges and are in general much drier. Along the Mediterranean shore, the maximum of rainfall takes place in early autumn (e.g. Romero et al., 1998 [212]; Martín-Vide and Olcina-Cantos, 2001 [172]; Millán et al., 2005 [183]; Muñoz-Díaz and Rodrigo, 2005 [186]; Martín et al., 2007 [169]), as shown for Girona (11), Barcelona(3), València (25) and Alacant (2) in Fig. 1.1, being related to deep convective systems strengthened by the overheated surface of the Mediterranean Sea after the long summer. The Mediterranean region is also characterized by the high intensity of the precipitation events there, with over 70% of total annual rainfall corresponding to only 25% of the rainy days (Martín-Vide, 2004 [173]). This constitutes a relevant feature of the Mediterranean rainfall regime,

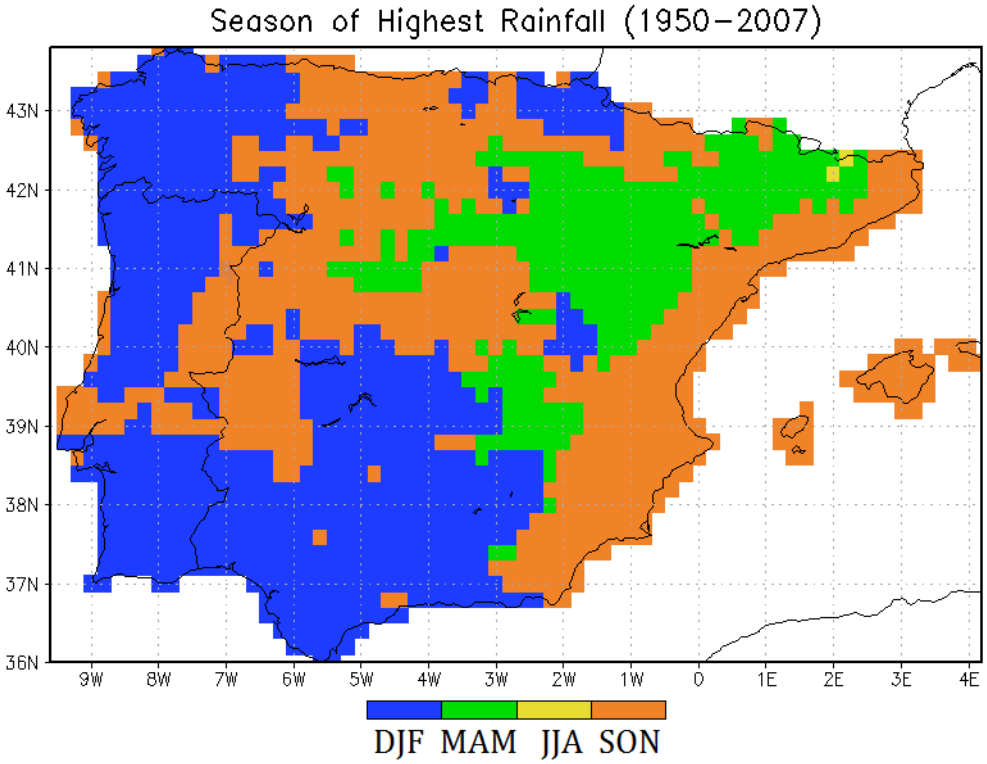

Figure 1.2: Season of highest rainfall (winter, DJF; spring, MAM; summer, JJA; autumn, SON) over the Iberian Peninsula for the period 1950-2007. Source: Herrera et al., 2010 [123]; Belo-Pereira et al., 2011 [13].

particularly intense in the Gulf of València, that distinguishes it from that of the rest of the IP.

The spring peak of rainfall in inland Iberia

In contrast with the western Iberia, dominated by a single winter peak, precipitation regimes for central and eastern Iberian regions are more spread out through the year and often characterized by two maxima occurring in spring and autumn. The spring relative maximum of precipitation can be observed in Fig. 1.1 throughout all the interior of the IP (e.g. León (13), Burgos (4), Vitoria/Gasteiz (27), Salamanca (19) and Guadalajara (12)). Interestingly, it tends to become the absolute maximum of rainfall in the annual cycle towards the interior eastern and northeastern regions (e.g. Segovia (21), Soria (23), Teruel (24), Zaragoza (28), Lleida (15) and Albacete (1) in the same figure). In these areas, the amplitude of the annual cycle typical of coastal areas is attenuated and, as a result, the spring peak becomes the dominant feature (Rodríguez-Puebla et al., 1998 [210]; Font-Tullot, 2000 [97]; Marín-Vide and Olcina-

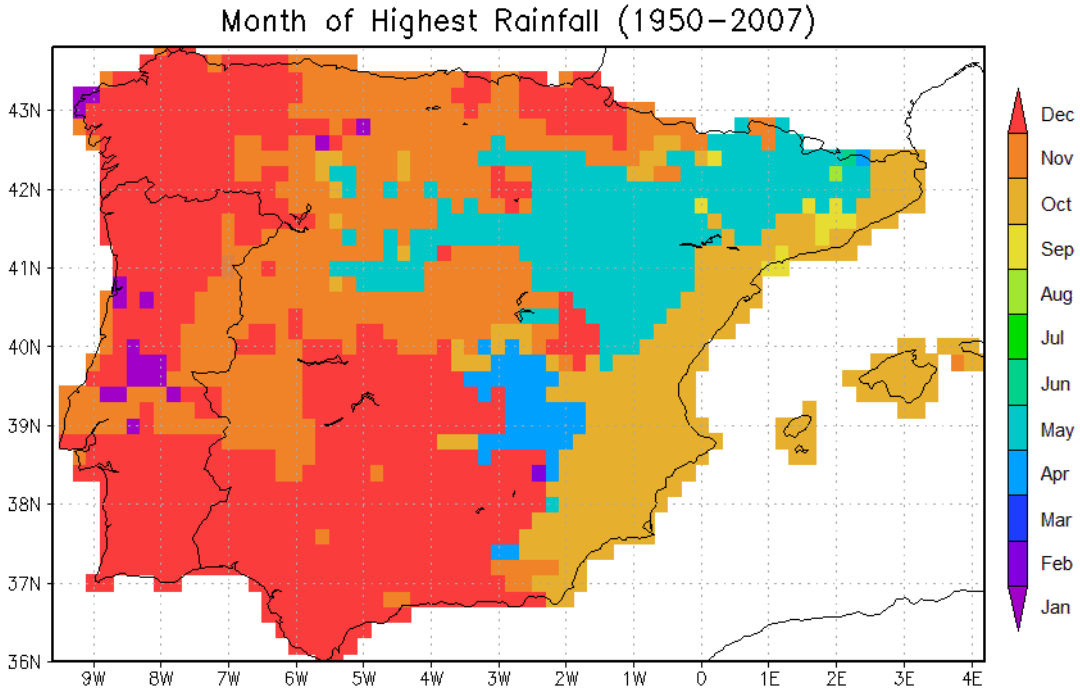

Figure 1.3: Month of highest rainfall over the IP for the period 1950-2007. Source: Herrera et al., 2010 [123]; Belo-Pereira et al., 2011 [13].

Cantos (2001) [172]; De Luis et al., 2010 [52]). The presence of an absolute maximum of precipitation in spring can be also observed in the green area of Fig. 1.2, where the season of maximum precipitation for the period 1950-2007 is depicted with a color code. More specifically, Fig. 1.3 represents the month of highest rainfall over the IP, with all the interior northeast showing the maximum occurring in May. Interestingly, a shift in the maximum of rainfall is observed from the interior southeast in April (blue region) to the interior northeast in May (region in cyan). In both Figs. 1.2 and 1.3, one can also see that the maximum of precipitation occurs in summer in a very small sector confined to the eastern Pyrenees. On the other hand, Autumn registers the absolute maximum of seasonal rainfall over the large Iberian areas depicted in orange in Fig. 1.2. Nevertheless, this maximum takes place in early autumn (October) along the Mediterranean Coast and in late autumn (November) within the Atlantic basins (Fig. 1.3), and is related to disparate physical processes, as discussed above. Finally, Fig. 1.4 ranks the position of the month of May during the year in terms of precipitation, highlighting again the relative importance of spring rainfall over most of central and eastern Iberia.

We remark that Figs. 1.1, 1.2, 1.3 and 1.4 represent average values along the period 1950-2007. Nevertheless, relevant variations in the Iberian annual cycle of precipitation have been found in previous works, namely a remarkable reduction of

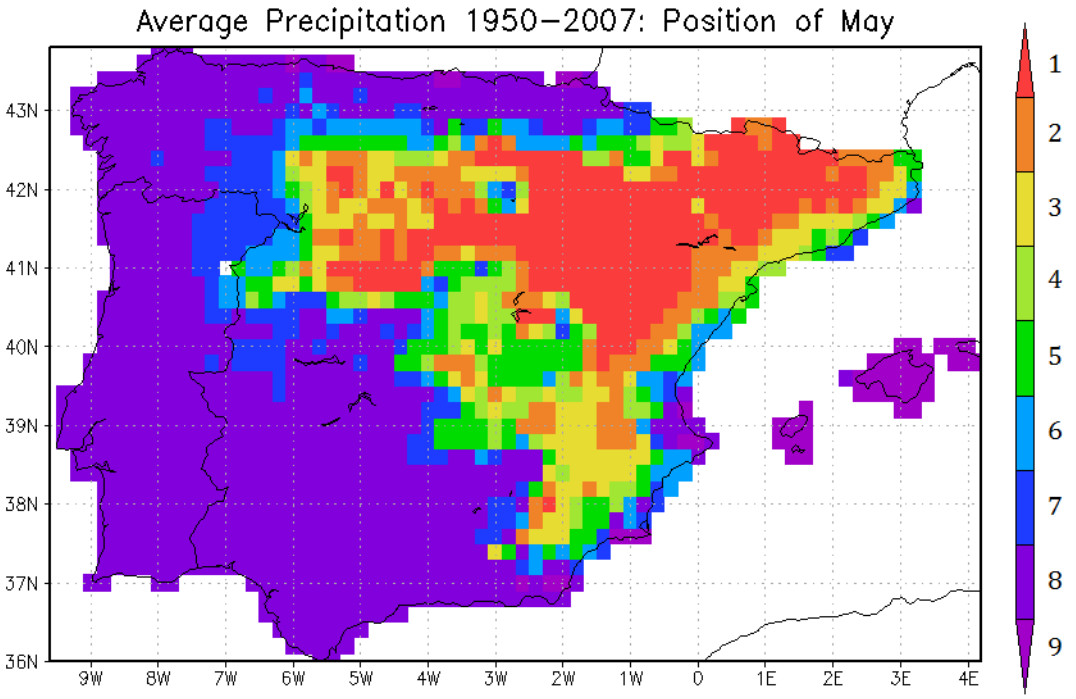

Figure 1.4: Climatology (1950-2007) position of May in the monthly ranking of precipitation. Source: Herrera et al., 2010 [123]; Belo-Pereira et al., 2011 [13].

the areas where spring is the main precipitation season between 1946-1975 and 1976-2005 (Paredes et al., 2006 [198]; De Luis et al., 2010 [52]). The confirmation of this trend in the context of climate change is a matter of the greatest relevance for Iberia, even though it is not addressed here as it is out of the scope of this thesis.

Arid and semiarid areas in the interior: the humidity index

Those land areas where water deficits are permanent or frequent are referred to as arid or semiarid regions (Martín-Vide and Olcina-Cantos, 2001 [172]). The great extension of these water-limited zones, periodically affected by drought episodes (García-Herrera et al., 2007 [106]; Gouveia et al., 2009 [121]), is a relevant characteristic of the Iberian climate. The North Plateau, topographically insulated from the surrounding humid and sub-humid areas, and with precipitation amounts that do not exceed 400 mm per year, is probably the paradigm of the continental, semiarid Iberia. This topographic insulation is less marked in the South Plateau, where the valleys of the Tagus, Guadiana and Guadalquivir rivers favor a higher climatic variability. Fig. 1.5, obtained from Font-Tullot (2000) [97], classifies the different Iberian areas according to their humidity index (HI), defined as (Font-Tullot, 2000 [97]):

$$HI = \frac{P}{ET} \tag{1.1}$$

where P stands for the mean annual precipitation and ET represents the mean annual evapotranspiration, computed in this case through the Thornthwaite formula (see the appendix I of Thornthwaite, 1948 [244]). In those areas where $HI \geq 1.00$, rainfall totals exceed the amounts of moisture lost by the land surface through ET. As a result, these areas are consistently referred to as *humid*. In contrast, wherever $HI < 1.00$, rainfall is not enough to balance ET and thus some hydric stress might appear. This is not always the case, as also groundwater fluxes (and not only precipitation), contribute to compensate local evapotranspiration (Fan et al., 2007 [84]; Fan and Miguez-Macho, 2010 [85]). More specifically, and according to Font-Tullot (2000) [97], if $0.70 < HI \leq 1.00$ the corresponding area is designed as *sub-humid*, if $0.30 < HI \leq 0.70$ the region is *semiarid* and finally, if $HI \leq 0.30$, the area is labeled as *arid*. The representation of the humidity index for the IP (Fig. 1.5) confirms that arid and semiarid regions, where changes in soil moisture can potentially control ET and precipitation regimes, cover large areas to the center, east and south (Font-Tullot, 2000 [97]; Castro et al., 2005 [44]).

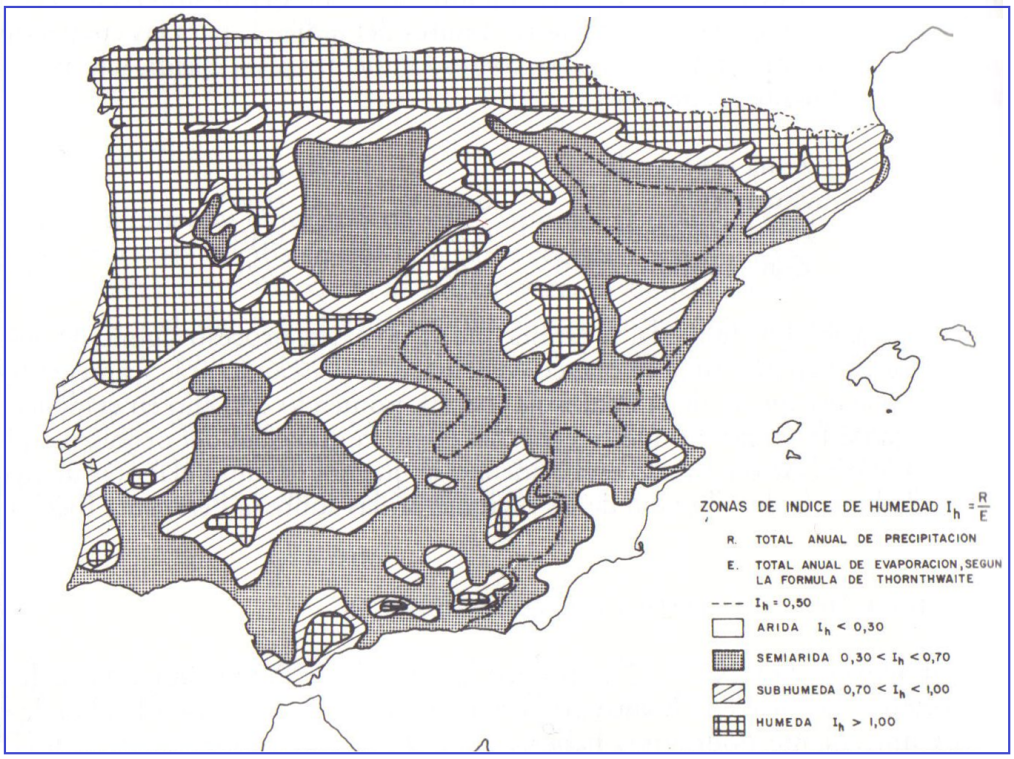

Figure 1.5: Spatial distribution of the humidity index [-] over Iberia. Figure obtained from Font-Tullot (2000) [97].

Experimental motivation for this study

We showed in this section that the yearly absolute maximum of precipitation occurs in spring over large areas to the east and northeast of Iberia. In addition, this spring peak becomes a relevant secondary maximum of rainfall over most of the North Plateau, South Plateau and center region. Even though the existence of this major feature of the Iberian precipitation regime has been described in different studies, as reported above, the physical processes responsible for it have not been explored in detail and still remain unclear. This contrasts with the rainfall peaks of late Autumn and Winter over the Atlantic Iberia and of early Autumn along the Mediterranean shore, which have been widely explored in the literature. The comprehensive analysis and understanding of the physical mechanisms underlying the Iberian spring peak of precipitation constitutes, hence, the main experimental motivation for this thesis. In addition, we want to assess the relevance of the spring rainfall for human activities (in particular, for agriculture), as well as its connections with extreme precipitation events (floods and droughts) in inland Iberia. A detailed analysis of the intensity and distribution over the IP of such extreme rainfall events along the second half of the Twentieth Century can be found in the studies of García et al. (2007) [104] and Acero et al. (2011) [1]. In the framework of a changing climate, this is of the greatest relevance for the medium and long-term sustainability and hydrological planning of the large water-limited areas in the interior of the Iberian Peninsula.

1.2 Moisture sources for the Iberian rainfall

As stated in section 1.1, in this thesis we aim to investigate the physical processes leading to the spring maximum of precipitation in inland Iberia. For this purpose, we need to thoroughly explore the moisture sources for the Iberian rainfall.

Precipitation falling over a certain region results from moisture with three different origins (Trenberth, 1999 [247]; Burde and Zangvil, 2001a [37]; Gimeno et al., 2012 [113]):

1. Moisture already present in the atmosphere;
2. Evapotranspiration (ET) from the considered region itself (usually referred to as *recycling*); and
3. Moisture advected into the region by the winds.

This can be mathematically expressed through the following equation:

$$P = P_s + P_m + P_a \tag{1.2}$$

where subindex s refers to water stored within the atmospheric volume under study, subindex m refers to water of local origin (ET) and subindex a to water of advected origin. Over sufficiently long periods, the contribution from the first source is widely assumed to be negligible. This approximation is supported by the fact of the average residence time of a water molecule in the atmosphere being close to 8 days (Trenberth, 1998 [246]; Numaguti, 1999 [192]; Dingman, 2002 [56]; Van der Ent and Savenije, 2011 [257]). Consequently, as the time period under consideration increases, the probability that a molecule of rainfall had been already stored within the same region since the beginning of the analyzed period becomes progressively reduced. As a result, we assume that the precipitation over our region is given by the sum of water molecules from the two major sources: evaporation and advection. For the Iberian Peninsula, these terms essentially correspond to local (recycled) and large-scale (oceanic) precipitation, respectively:

$$P \approx P_m + P_a \approx P_{\text{local}} + P_{\text{oceanic}} \tag{1.3}$$

Gimeno et al. (2010a) [110] and Gimeno et al. (2011) [112] studied the sources of moisture for precipitation in the IP using a back trajectory lagrangian model on ECMWF analysis data. These studies confirm that long distance transport is largely dominant in the winter and autumn Iberian precipitation, but in contrast, during spring and summer, an internal source of moisture (i.e. a recycling component) provides most of the humidity for further precipitation. This is coherent with the observed weakening of the intense zonal, winter-like circulation during spring and summer, giving rise to a more active role of local and mesoscale convective mechanisms (Llasat and Puigcerver, 1997 [164]; Serrano et al., 1999 [226]; Mosmann et al., 2004 [185]; García-Herrera et al., 2005 [105]; Bisselink and Dolman, 2008 [21]; Gimeno et al., 2010a [110]). This also agrees with the general conclusions of e.g. Brown and Arnold (1998) [31] or Schär et al. (1999) [221], who confirmed that the highest ET-precipitation coupling is related to convective processes in absence of strong synoptic forcings. In terms of extreme precipitation events, as pointed out by Trenberth and Guillemot (1996) [245], these mesoscale convective systems, usually modulated by the landscape structure (Chen and Avissar, 1994 [45]; Avissar and Liu, 1996 [8]), are not generally sufficient to trigger extreme rainfall periods, but they can be critical to intensify and modulate them.

To sum up, exploring the physical processes behind the spring peak of rainfall requires a comprehensive investigation of the major moisture sources affecting the Iberian Peninsula and, in particular, its interior lands. In practice, the latter means separating the two fractions of the total rainfall (locally recycled and advected from the Atlantic Ocean) in order to assess their relative weight. According to our analysis, P_a is expected to constitute, by far, the main contribution to the Iberian winter precipitation, whereas P_m might play a more relevant role as spring and summer progress. The separation of both contributions can be done by estimating a crucial

variable: the recycling ratio. This magnitude, of the greatest relevance to investigate the water cycle of land areas, is introduced and carefully defined in section 1.4. The estimation of the recycling ratio over the Iberian Peninsula constitutes a key step (although not the only one, as it will be shown) to give a comprehensive answer to our scientific question: *why does the Iberian spring peak of precipitation take place?*

1.3 Land-atmosphere interactions

As stated in the previous section, the fraction of the total precipitation with internal origin derives from evapotranspiration (ET) within the study region (in our case, the Iberian Peninsula). The evapotranspirative water and heat flux, including plant transpiration and direct evaporation from the land surface to the atmosphere (e.g. Seneviratne et al., 2010 [225]) is mostly modulated by the following factors (Shukla and Mintz, 1982 [228]):

1. Sufficient moisture availability in the upper, unsaturated layer of the soil, accessible for the roots of plants and trees;
2. Vegetation to transport humidity from the soil to the atmosphere;
3. Heat energy to evaporate the liquid water into vapor; and
4. Atmospheric demand (a warmer atmosphere may store a higher amount of water vapor).

This implies that the ET flux is simultaneously controlled by the physical characteristics of both the land surface and the atmosphere, thus constituting an example (actually, a very important example) of a land-atmosphere interaction. The intensest ET flux is observed when a positive coupling of these four conditions occurs. Over most of the Iberian Peninsula, the soil is significantly humid during the winter half of the year, but in contrast the atmospheric demand is reduced during that period. On the contrary, in summer, when the atmosphere has the higher availability to store water vapor, the amount of moisture in the soil is limited all over the large interior, southern and Mediterranean regions. As a result, the more intense evapotranspiratopm flux might take place in late spring and early summer, thus providing extra humidity that might have a critical impact on the observed surplus of rainfall. In this section, we examine the main properties of land-atmosphere interactions, such as ET, which are directly connected to the local contribution to precipitation, as it has been discussed, and also to a variety of physical processes as shortwave and longwave radiation, cloud formation or water vapor convergence (Betts and Viterbo, 2005 [18]; Betts, 2007 [19]).

In general, it is assumed that the feedbacks between the land surface and the lower atmosphere can have a relevant impact on climate (Pielke et al., 1998 [201]; Pielke, 2001 [202]; Hohenegger et al., 2009 [125]; Jaeger et al., 2009 [135]) and are expected to be critical to understand its evolution as a consequence of climate change (Seneviratne et al., 2006a [223]). The investigation of land-atmopshere interactions is a wide and complex scientific task that involves several major scientific disciplines, as is the case of hydrology, meteorology, atmospheric sciences or soil physics (Seneviratne et al. (2010) [225]).

Land-atmosphere interactions refer to any connection among the soil, the vegetation cover and the atmosphere (Wei et al., 2006 [262]). In practice, this concept is directly related to the physical linkages among soil moisture, ET and precipitation. As shown in Fig. 1.6, these interactions are often represented as a *diminishing cascade* (Dirmeyer, 2006 [61]; Dirmeyer et al., 2009a [64]). Thereby, precipitation usually exerts an intense influence on soil moisture, whereas soil moisture has a more moderate impact on ET (modulated by vegetation dynamics) and ET presents a much more reduced influence on precipitation. Nevertheless, even at mid latitudes, the latter connection is intensified over certain regions and periods of the year, and thus ET may play a critical role on the regional precipitation regime.

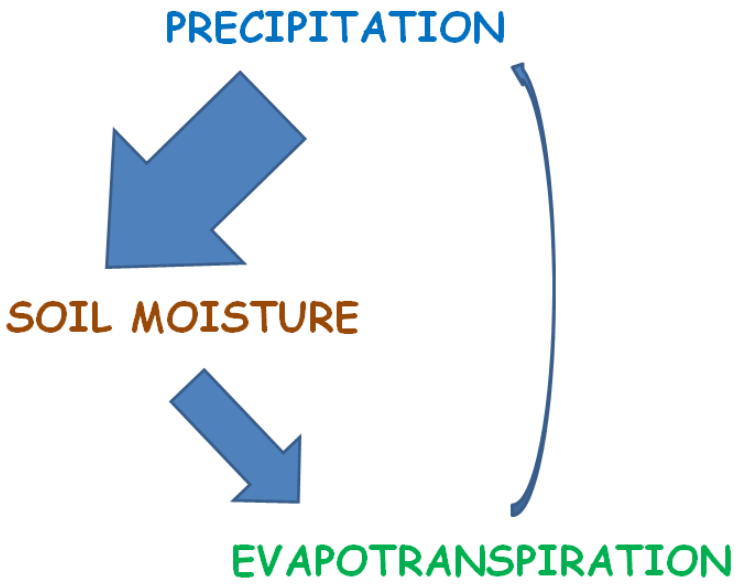

Figure 1.6: Feedback loop in the terrestrial branch of the water cycle.

The generalization of what has been discussed above for the Iberian Peninsula implies that in wet climates, where soils have no shortage of water, ET is mostly controlled by atmospheric demand. In dry climates, in contrast, the amounts of ET and precipitation are reduced and are strongly dependent on moisture availability

(Koster et al., 2004 [156]). As a consequence, land-atmosphere interactions are the strongest in the transition zones from wet to dry climates, where the amount of ET is suitably high but still sensitive to soil moisture (Koster et al., 2004 [156]). Our area of interest, the Iberian Peninsula (IP), is one of such transition zones (Giorgi and Lionello, 2008 [115]).

As discussed in the previous section, the semiarid interior of the IP presents a distinct precipitation regime, with a peak of rainfall in late spring that is not observed in the Atlantic or Mediterranean coastal areas, where the annual cycle of precipitation follows large scale forcing and moisture supply (Rodríguez-Puebla et al., 1998 [210]; Castro et al., 2005 [44]). It is important to remark that this clear difference in the seasonality of precipitation with respect to the coastal areas is an indication of the prominent role of land-atmosphere fluxes, and in particular ET fluxes, on rainfall dynamics there.

The synthesis of the process is the following. As spring progresses, the increase of solar radiation and plant activity accelerate the evapotranspiration of moisture accumulated in the soil during the previous winter. In this period of the year, the subtropical anticyclone does not control the upper Iberian atmosphere yet (Martín-Vide and Olcina-Cantos, 2001 [172]), and thus the synoptic configuration enhances the development of local convective regimes throughout the interior lands of the IP. It must be stated that for some specific years the intense zonal, winter-like circulation is maintained during spring, resulting in a severe reduction of the frequency and intensity of those mesoscale convective processes (Chen and Avissar, 1994 [45]). In general, however, the ET flux is suitably high in the large water-stressed interior areas of the IP, providing "extra" humidity to the lower atmospheric levels which might favor unstable conditions to enhance the triggering of the soil moisture - precipitation feedback, thus increasing rainfall amounts through direct or indirect processes (Schär et al., 1999 [221]; Jódar et al., 2010 [138]). The intensity of this ET flux, mostly limited by soil moisture availability in this period of the year, strengthens the hypothesis that inland Iberia may be an area where land-air feedbacks could play an important role on climate (Koster et al., 2004 [156]), particularly in spring and early summer, when an important fraction of the precipitation does not derive from oceanic sources but results from terrestrial moisture (water recycling).

Before examining other important aspects of land-atmosphere interactions, such their sensitivity to human impacts or the role of soil moisture, we are now ready to establish our working hypothesis, which naturally follows from the analysis above: we suggest that the maximum of precipitation in spring is directly related to the enhancement of the hydrological cycle through local convective mechanisms in inland Iberia. The most general objective of this thesis is thus assessing and eventually confirming this scientific hypothesis.

Apart from the scientific interest itself, the comprehensive exploration of the spring surplus of precipitation becomes critical for plant ecology and for a variety of

human activities (among which agriculture is probably the most relevant) in the large arid and semiarid areas in the center, east and northeast of Iberia. Consequently, a deeper analysis of the physical mechanisms underlying this spring rainfall is of the greatest relevance for regional hydrological planning (Gallego et al., 2006 [101]) and for the medium and long-term sustainability of those broad water-limited regions.

The role of soil moisture and the water table

The relevant impact of land surface processes, and soil moisture in particular, on the regional precipitation regime has been widely explored during the last decades (e.g. Entekhabi et al., 1996 [81]; De Ridder, 1997 [54]; Findell and Eltahir, 1997 [88]; Eltahir, 1998 [79]; Zheng and Eltahir, 1998 [272]; Findell and Eltahir, 1999 [89]; Douville and Chauvin, 2000 [71]; Dirmeyer, 2001 [59]; Salvucci et al., 2002 [216]; Georgescu et al., 2003 [107]; D'Odorico and Porporato, 2004 [66]; Kochendorfer and Ramírez, 2005 [146]; Ferranti and Viterbo, 2006 [87]; Kanae et al., 2006 [144]; Fan et al., 2007 [84]; Lam et al., 2007 [159]; Dirmeyer et al., 2009b [65]), even though some examples of negative soil moisture - rainfall correlation have been also reported (Cook et al., 2006 [48]; Wei et al., 2008 [263]). In particular, soil moisture variability seems to play a relevant role in arid and semiarid climates where convective processes are largely responsible for precipitation (Finder and Eltahir, 2003a [90]; Finder and Eltahir, 2003b [91]).

Soil moisture is commonly referred to as the humidity stored in the unsaturated column of the soil, limited by the land surface at the top and by the water table (or phreatic level) at the bottom (Seneviratne et al., 2010 [225]). In the upper soil layer, accessible to the roots of the plant cover, the pores (that is, the spaces between the solid particles) are filled partially with water and partially with air. Below the water table, in contrast, all the pores are fully saturated with liquid water, usually referred to as groundwater (Dingman, 2002 [56]; Fitts, 2002 [94]). A simplified representation of the soil structure can be observed in Fig. 1.7, which shows the above-mentioned soil layers and the corresponding water fluxes connecting them.

The distribution of the water content into the soil is essentially driven by gravity, which is responsible for the percolation of moisture into deeper layers of the soil, thus recharging the groundwater reservoir. Reversely, the hydric demand of the vegetation roots may lead to the ascend of groundwater via capillary rise and plant uptake (York et al., 2002 [266]; Brolsma et al., 2010 [30]; Fan and Miguez-Macho, 2010 [85]), attenuating soil moisture and ET deficits during the dry season. It is relevant to mention that capillarity processes are highly sensitive to the soil type (Fan et al., 2007 [84]; Miguez-Macho et al., 2008 [182]). For instance, capillarity effects are very intense in a clay soil, where the roots can absorb groundwater even with a water table located at around 10 m depth. In a sandy soil, in contrast, the roots are only able to absorb groundwater if the water table is located approximately at the roots level

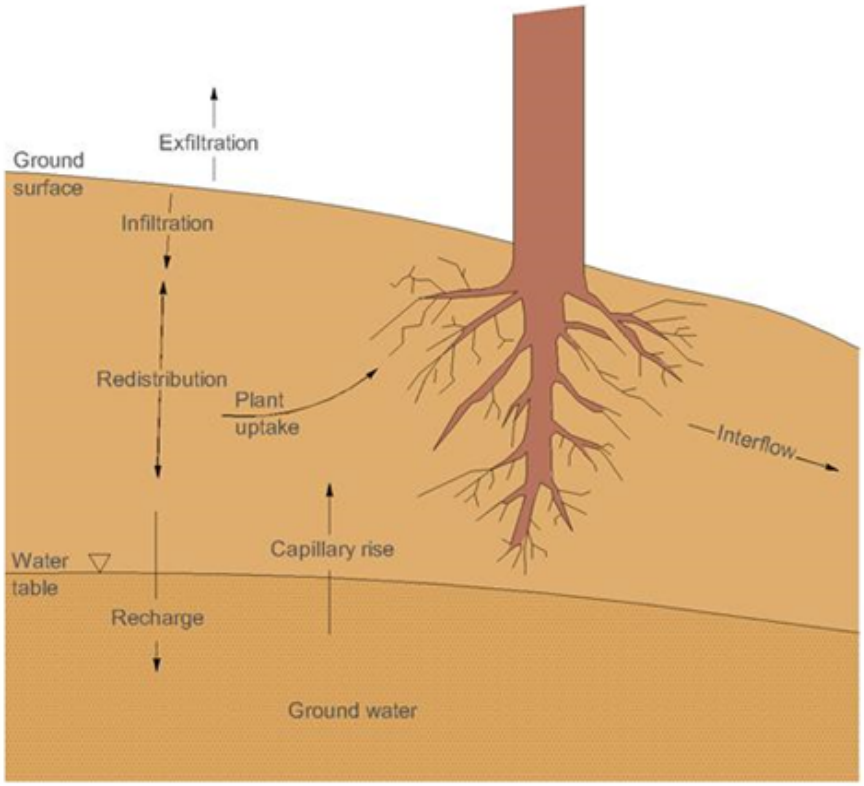

Figure 1.7: Simplified representation of the soil structure. Image obtained from Gestal-Souto et al., 2010 [109].

(Fan et al., 2007 [84]; Miguez-Macho et al., 2008 [182]).

On the other hand, the water table depth is also modulated by the lateral groundwater flux, directly related to the orography and physically described through Darcy's Law (Fitts, 2002 [94]). This groundwater flux is responsible for the spatial redistribution of the water resources of the soil, being connected with the rivers and thus closing the terrestrial water cycle. An interesting example of the effects of lateral froundwater flux is groundwater convergence, taking place in the green and fertile valleys and plateaus surrounded by mountain ranges, where the water table is found to be generally shallow (Fan et al., 2007 [84]). Arid and semiarid regions with this kind of hydrological configurations are typically characterized for a strong coupling between soil moisture and groundwater, which acts as a reservoir of the water excess during the humid season and feeds the unsaturated soil through capillarity during the long summer, thus sustaining the subsequent land-atmosphere fluxes and precipitation (York et al., 2002 [266]; Fan et al., 2007 [84]).

In Iberian Peninsula, a shallow water table is found to take place in large areas of the interior (Gestal-Souto et al., 2010 [109]), as it is shown in Fig. 1.8. Interestingly,

most of these regions are arid or semiarid, presenting relevant water limitations. In the North Plateau, which constitutes a clear example of the hydrological configuration described in the paragraph above, the water table is less than 5 m depth in large areas (Fig. 1.8). The degree of soil moisture - water table coupling is also expected to be similarly intense in the eastern areas of the South Plateau (Fig. 1.8). In general, this suggests that in the interior areas of the Iberian Peninsula, the water table depth, the dynamics of the soil moisture and the groundwater supply in the dry season are expected to play a crucial role on land-atmosphere interactions and, therefore, in the regional rainfall regime. In contrast, in the humid northern and northwestern areas, where precipitation is essentially controlled by large-scale circulation and favored by orography, the potential impacts of the water table and soil moisture are expected to be significantly reduced (Anyah et al., 2008 [5]; Miguez-Macho et al., 2008 [182]).

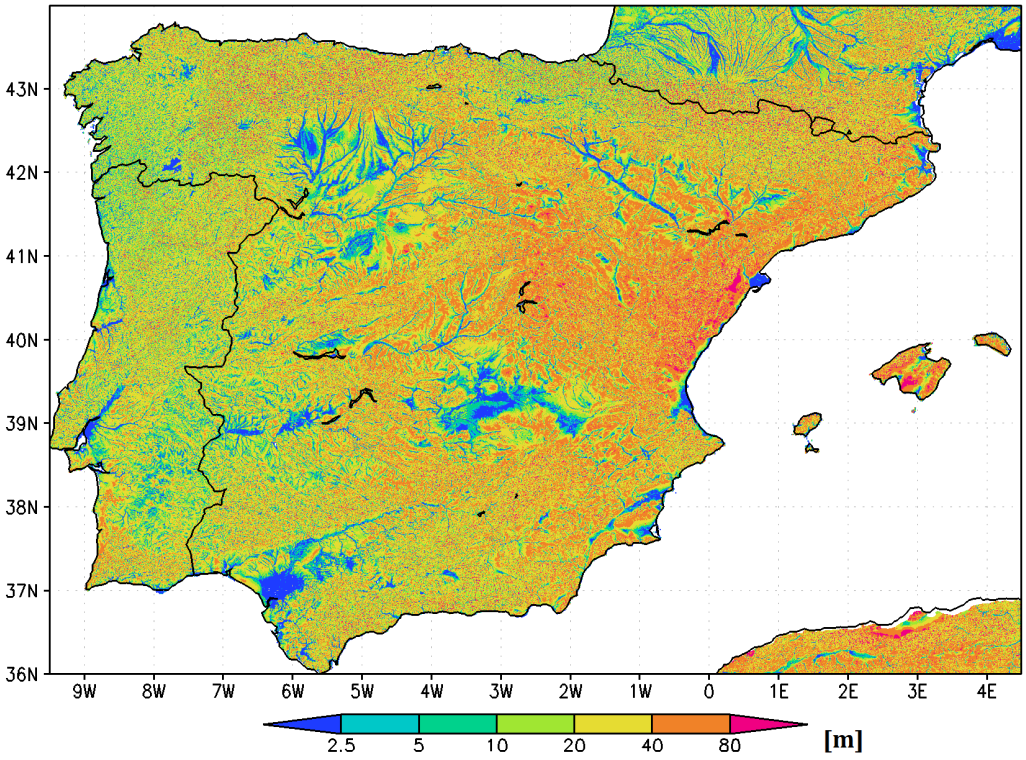

Figure 1.8: Equilibrium water table depth, EWTD (m), for the Iberian Peninsula. Image obtained from Gestal-Souto et al., 2010 [109].

Soil moisture and climate memory

It is well known that the atmosphere is intrinsically a non-linear and chaotic system (e.g. Koster and Suarez, 2003 [153]). As a consequence, small variations in the initial

conditions may lead to significantly distinct evolutions of the system. This has a direct impact on weather predictability, whose reliability decreases to an important extent beyond the fourth or fifth day. Extending the forecasting capability of our meteorological and climate models is hence a priority for researchers in these disciplines. Interestingly, unlike the atmosphere, there are some other elements of the climatic system that are able to *keep the memory* of what happened during the previous months and seasons. Koster et al. (2004) [156] identifies the three main reservoirs of memory to be: 1) the oceans; 2) the soil moisture; and 3) the vegetation cover. Long-term predictability depends to a large extent on a better understanding of the interactions among these elements (Liu and Avissar, 1999 [162]; Fennessy and Shukla, 1999 [86]; Dirmeyer, 2003 [60]; Koster and Suarez, 2003 [153]; Wu and Dickinson, 2004 [265]; Dirmeyer et al., 2009a [64]). In general, however, soil moisture and vegetation impacts on precipitation are much more relevant than ocean-atmosphere feedbacks (Koster and Suarez, 1995 [150]; Koster et al., 2000 [151]; Koster et al., 2004 [156]). As a result, investigating soil-atmosphere interactions over a certain region (in our case, the Iberian Peninsula) is not only a way to assess the effects of local and mesoscale processes on the regional climate and precipitation regime, but additionally provides valuable information that may contribute to the improvement of seasonal forecasting and longer-term climatic research (Dirmeyer, 2000 [58];Douville and Chauvin, 2000 [71]; Betts, 2004 [17]).

The persistence that soil moisture induces on climate has been explored in different works (e.g. Entekhabi et al., 1992 [80]; Brubaker and Entekhabi, 1996 [33]; Eltahir and Bras, 1996 [77]; Trenberth and Guillemot, 1996 [245]; Liu and Avissar, 1999 [162]; Pal and Eltahir, 2001 [196]; Koster et al., 2003 [154]; Pal and Eltahir, 2003 [197]; Koster and Suarez, 2004 [155]; Bierkens and Van der Hurk, 2007 [20]; Domínguez et al., 2008 [69]; Seneviratne et al., 2010 [225]). For instance, Eltahir and Bras, 1996 [77] concluded that a wet (dry) year favors that the following years keep on being wet (dry): this implies that wet (dry) cycles show a tendency to perpetuate. Similarly, soil moisture memory and land-atmosphere interactions may have a relevant impact on droughts, such as the well-known 2003 European summer heat wave (Trigo et al., 2005 [253]; Ferranti and Viterbo, 2006 [87]; Zaitchik et al., 2006 [270]; Fischer et al., 2007a [92]; Fischer et al., 2007b [93]; Vautard et al., 2007 [258]; Quesada et al., 2012 [207]). In the North Plateau of the Iberian Peninsula, as over many other arid and semi-arid regions, the soil has a tendency to keep dry during the summer. Nevertheless, the groundwater convergence from the surrounding mountains, which sustains a shallow water table and the subsequent connections between land and air, may avoid the complete drying of the soil and reset of its memory (Bierkens and Van der Hurk, 2007 [20]). As a result, even over water-stressed areas as the Iberian North Plateau, groundwater may keep the memory of the system from year to year.

Human impacts on land-atmosphere interactions

The land surface is the element of the climate system that is more sensitive to the human activities. Nowadays, changes in land use take place incessantly all over the world. Deforestation is probably the most aggressive among such processes, and its effects on climate have been a matter of research for the last decades, particularly in the Amazon (e.g. Nobre et al., 1991 [191]; Bastable et al., 1993 [10]; Eltahir and Pal, 1996 [78]; Gordon et al., 2005 [120]).

Land-atmosphere water and heat fluxes, principally evapotranspiration (ET), are largely modulated by the land cover (Eltahir and Pal, 1996 [78]; Van der Ent et al., 2010 [256]), and their intensity is intuitively different over urban, forest, grassland or farmland areas. In a recent work, Pielke et al. (2007) [203] analyze several examples of how human changes in land cover may affect the regional climate. Similarly, a detailed assessments of the impact of changes in the vegetation cover on further convective precipitation can be found in the works by Anthes (1984) [4], Arora (2002) [7]; Dekker et al. (2007) [51] or Jiang et al. (2009) [136].

In general, ET can be enhanced via reducing runoff (e.g. building dams) and, reversely, can be reduced by facilitating the drainage of water into the soil (e.g. reducing the extension of urban areas) (Van der Ent et al., 2010 [256]). The effects of concrete human actions, as is the case with irrigation, on further convective precipitation have been explored in classical studies (McDonald, 1962 [176]; Stidd et al., 1975 [235]) and also in more recent works (Eltahir and Pal, 1996 [78]; De Ridder and Gallée, 1998 [55]; Boucher et al., 2004 [29]; DeAngelis et al., 2010 [49]; Jódar et al., 2010 [138]). Nevertheless, it is also widely assumed that local changes in the land use do not necessarily lead to alterations of the precipitation regime in the same area. This erroneous interpretation is known in the literature as the "evaporation-precipitation fallacy" (McDonald, 1962 [176]; Stidd et al., 1975 [235]). The reason is essentially that the water cycle typically operates at a greater scale, with water molecules traveling hundreds and even thousands of kilometers (Trenberth, 1998 [246]), during time periods ranging from 3 to 20 days (Van der Ent and Savenije, 2011 [257]). To refute the above-referred fallacy, McDonald (1962) [176] provides the clear example of the Caspian Sea, a large natural body of water that, being surrounded by arid regions, is unable to relief their water scarcity.

Another anthropogenic activity which has an effect on land-air fluxes is groundwater abstraction. In large areas of the Iberian South Plateau, for instance, massive groundwater pumping for agriculture and other economical activities has led to a remarkable depletion of the phreatic level for the last decades (Gestal-Souto et al., 2010 [109]). This evidences that the consumption of groundwater resources has taken place at a faster rate than its natural replenishment. The alteration of these vulnerable hydric equilibriums may modify land-air feedbacks at the regional scale (Sutanudjaja et al., 2011 [241]) and even affect the future sustainability of these areas. Over the arid

and semiarid Iberia, therefore, human perturbations in land-use may have an important impact on the precipitation of local, convective origin (Millán et al., 2005 [183]) and, in general, may play a role in local-scale climate change (Brown and Arnold, 1998 [31]). As a result, the anthropogenic impact must be taken into account for an appropriate management of the water resources in such water-stressed areas.

1.4 The recycling mechanism

In the previous section, we examined the different factors controlling land-air interactions and, as a result, the fraction of precipitation with a local origin. In this section, we explore some of the procedures to effectively quantify this fraction, separating its contribution from that of advective origin. This is essentially the aim of any regional recycling study.

Let us revisit and clarify the rough estimations on the planetary water cycle presented in the initial resume. At the global scale, about 90% of the atmospheric vapor originates from oceanic evaporation (Quante and Matthias, 2006 [206]; Gimeno et al., 2010a [110]), and only 10% of the water evaporated from the oceans precipitates over land (Oki, 2005 [193]; Gimeno et al., 2010b [111]). The latter water molecules, transported by the winds from the ocean to the continents, where they precipitate, may then evaporate and precipitate several times over land areas before going back to the oceans, mainly as river flow (Numaguti, 1999 [192]). This process is known as *water recycling* and plays a critical role in the water cycle of the continental areas. In fact, estimates show that 40% of the terrestrial precipitation originates from evapotranspiration over land, and 57% of all terrestrial evapotranspiration reverts as land precipitation (Van der Ent et al., 2010 [256]). For a complete representation of the terrestrial hydrology cycle and quantification of the moisture fluxes involved, see Fig. 1 of Oki and Kanae (2006) [194].

As evapotranspiration, recycling is another relevant example of a physical process controlled by both the soil and the atmosphere. Nevertheless, recycling is a peculiar land-atmosphere interaction, since it can be regarded as a measure of the degree of control that soil moisture and local ET dynamics exert on the regional climate (Eltahir and Bras, 1994 [76]; Burde and Zangvil, 2001a [37]). The intensity of the recycling mechanism is quantified through the recycling ratio (Burde and Zangvil, 2001b [38]). The computation of this variable provides the above-mentioned assessment of the potential impact of land-atmosphere interactions on the regional precipitation regime (Eltahir and Bras, 1994 [76]; Burde and Zangvil, 2001a [37]). In other words, recycling can be seen as a measure of the connections between hydrological and meteorological processes at the regional scale (Bosilovich and Schubert, 2001 [23]).

Even though the recycling ratio provides information about the current state

of the climatic system (Eltahir and Bras, 1996 [77]), the analysis of this parameter might be of great relevance to explore the possible effects of climate change at the regional scale. Nowadays, it is widely accepted that human-induced global warming associated with higher concentrations of greenhouse gases will amplify the water cycle, thus increasing the global mean precipitation and evaporation rates (IPCC, 1990 [131]; IPCC, 1996 [132]; IPCC, 2001 [133]; IPCC, 2007 [134]). However, these changes will be highly asymmetric, with semi-arid regions, such as the Mediterranean, suffering some of the heaviest burden when compared to other areas of the world (Giorgi, 2006 [114]; IPCC, 2007 [134]). According to Seneviratne et al. (2006a) [223], the European climates are expected to shift northwards during the next decades as a result of climate change, and this may critically affect transition regions such as the Iberian Peninsula. In fact, most modeling studies using global and regional circulation models (GCMs and RCMs) do suggest that the Mediterranean area, including the Iberian Peninsula, will register a general trend towards less precipitation and increase precipitation variability and evapotranspiration during the 21st century (Giorgi, 2006 [114]; Giorgi and Lionello, 2008 [115]; Mariotti et al., 2008 [168]). In this regard, a recent thorough study using the CMIP3 multi-model ensemble indicates a decrease in land surface water availability resulting from precipitation reduction and warming-enhanced evaporation (Mariotti et al., 2008 [168]). The reduction in the available moisture to precipitate will affect the rainfall averages over land (reduction of the recycling component) and equally over the Mediterranean Sea. Interestingly, recent studies show that there has been a tendency towards more frequent drought events in the Mediterranean region (Sousa et al., 2011 [232]) and towards desertification in southern Iberia (Balabanis et al., 1999 [9]), with such trends being already partially driven by climate change (Hoerling et al., 2012 [124]). As a result, apart for being a relevant variable for the investigatation of climate change scenarios, the Iberian recycling ratio itself is expected to suffer important variations during the next decades.

Recycling studies have focused on many different regions of the world. Among them, three areas have been historically given special attention:

1. *The European part of the Russian Federation*, where recycling studies have been carried out by e.g. Budyko (1974) [35], Shiklomanov (1989) [227] or Brubaker et al. (1993) [32].

2. *North America* and, in particular, the *Mississippi river basin*, studied by e.g. Benton et al. (1950) [14], Koster et al. (1986) [147], Brubaker et al. (1993) [32] or Trenberth (1999) [247].

3. *The Amazon river basin*, analyzed by e.g. Lettau et al. (1979) [161], Eltahir and Bras (1994) [76], Trenberth (1999) [247] or Marengo (2006) [167].

Additionally, other regions have been also explored, to a relevant extent, in terms of moisture recycling. This is the case of the Mackenzie river basin (e.g. Szeto, 2002

[242], who estimated a mean annual recycling ratio of around 25% for that catchment) or the Sahel region (e.g. Savenije, 1995a [218]; Nieto et al., 2006 [188]). In the latter area, Savenije (1995a) [218] estimates that 90% of the (scarce) rainfall is recycled; that is, almost all the precipitation comes from ET within the Sahel itself.

A classification of recycling models

The analysis of the moisture sources for precipitation over a certain region and the subsequent assessment of the recycling ratio has been a matter of research for decades. The first studies on precipitation recycling date from the 19th century (Van der Ent et al., 2010 [256]). However, it has not been until the 20th century when more systematic investigations have explored this mechanism. In particular, the classical works by Holzman (1937) [127], Benton et al. (1950) [14] and McDonald (1962) [176] has been taken as a reference for further investigations, as well as those by Horton (1933) [129] or McNish (1936) [177]. A complete review on these first recycling studies can be found in Brubaker et al. (1993) [32] and Eltahir and Bras (1996) [77].

In the 1950s, Budyko developed an analytical model to mathematically compute the recycling ratio (Budyko, 1974 [35]) that represented a key step for recycling research. In fact, most of the recent recycling models are shown to be generalizations and modifications of Budyko's model (Burde and Zangvil, 2001a [37]). Budyko's model is classified as a one-dimensional recycling model, since although it can be applied to a real, two-dimensional region, the moisture flux is assumed to be always parallel to the boundaries of the region. In addition, evapotranspiration and precipitation are assumed to be constant, both in space and time. This assumption, relatively acceptable for ET, does not represent the reality of the precipitation process, which is known to be highly non-homogeneous. As a result, the method biases towards an underestimation of the recycling ratio (Dirmeyer and Brubaker, 1999 [57]; Bosilovich and Schubert, 2001 [23]; Bosilovich and Chern, 2006 [28]). This underestimation may reach 10 or even 15% with respect to more refined models (Dirmeyer and Brubaker, 1999 [57]).

As is the case with Budyko's model, any other analytical recycling model is based on two equations of conservation of vapor mass for the two different fractions of moisture available in the atmosphere (advected and evapotranspired), and a third equation assuming that these two fractions are well mixed (Burde and Zangvil, 2001a [37]). The latter equation is referred to as the *well-mixed atmosphere hypothesis* and underlies all analytical recycling models. The well-mixed atmosphere assumption is based on the fact that most of the moisture in the air is contained within the planetary boundary layer (PBL), where turbulent and convective processes, driven by sensible heat fluxes (Bosilovich and Chern, 2006 [28]), efficiently mix the dry air with water vapor coming from different sources (Eltahir and Bras 1996 [77]; Stull, 1988 [238]; Schär et al., 1999 [221]; Domínguez and Kumar, 2008 [68]; Domínguez et al.,

2009 [70]). Eltahir and Bras (1994) [76] provide a detailed justification of this critical assumption and conclude that the mixing process is significantly quick, taking only 15 minutes, on average, for the evapotranspired water molecules to completely mix up with the surrounding vapor. Nevertheless, the well-mixing through the column is not always satisfied. For instance, locally evapotranspired humidity has a tendency to remain in the lower layers of the atmosphere (Gimeno et al., 2010a [110]) and a part of it gives rise to "fast recycling" - precipitation coming from ET that did not mix with advected moisture from further above (Stidd, 1967 [234]; Lettau et al., 1979 [161]; Burde, 2006 [39]). Similarly, in a global study using passive tracers, Bosilovich (2002) [24] concluded that the fraction of locally evapotranspirated moisture in the precipitable water can be significantly different from the fraction of locally evapotranspirated moisture in precipitation, which might have an impact on recycling calculations (Bosilovich, 2002 [24]). Moreover, precipitation can also originate from condensate coming from somewhere else and have very little contribution from local ET. These and some other limitations of the well-mixed hypothesis were discussed by Burde (2006) [39], Fitzmaurice (2007) [95] and Domínguez and Kumar (2008) [68].

In 1965, Drozdov and Grigor'eva (1965) [72] extended Budyko's model by allowing ET and precipitation to vary along the streamline, so that $ET = ET(x)$ and $P = P(x)$, with x standing for the flow direction, still parallel to the boundaries. Lettau et al. (1979) [161] incorporate the consideration of the *fast recycling* mechanism in their algorithm. The two-dimensional extension of these models was carried out by Brubaker et al. (1993) [32], where the flux is now allowed not to be parallel to the region boundaries. Nevertheless, this model provides good estimates only if the flow is essentially parallel and does not meander to a significant extent. A complete representation of the two-dimensional structure of the flow is incorporated to Burde et al.'s (1996) [36] recycling model. This approach is improved in Burde and Zangvil (2001b) [38], yielding much better recycling estimations under complex, non-parallel moisture fluxes. Finally, in Burde (2006) [39] and Burde et al. (2006) [40], a more sophisticated bulk recycling model is presented. This model accounts for fast recycling and incomplete vertical mixing, by introducing a new parameter that quantifies the accuracy of the well-mixed assumption in every concrete situation.

Eltahir and Bras (1994) [76] developed a numerical procedure to compute the recycling ratio by subdividing the study region into multiple small grid cells and applying the two equations of conservation of water mass and the well-atmosphere condition to each of them. This model represents an important improvement on recycling studies, as it provides not only an average regional value of recycling but also the spatial distribution of this magnitude over the considered region. Among the model limitations, the most relevant is the fact that calculations are performed by using time averaged ET and horizontal moisture fluxes, which leads to highly smooth spatial patterns that are excessively related to the prevailing wind direction. Nevertheless, the Eltahir and Bras's (1994) [76] recycling model, hereafter referred to as EBRM, is still widely used for recycling analysis. Generally, this numerical model

computes higher recycling ratios than Budyko-type models (Domínguez et al., 2006 [67]), although it still seems to underestimate the intensity of the recycling mechanism (Van der Ent et al., 2010 [256]). Our recent results with moisture tracers, presented in chapter 5, contradict however the latter statement for the Iberian Peninsula.

A particular type of analytical recycling models are the so-called integral moisture budget (IMB) recycling models, also designated as bulk recycling models. Among them, in this thesis we make use of the model by Schär et al. (1999) [221], hereafter referred to as IMB. Interestingly, the IMB model converges technically with the EBRM when the latter is applied in the limit case of the whole region corresponding to one grid cell. On the other hand, Savenije developed in the mid nineties an analytical procedure to compute the recycling ratio in terms of the runoff coefficient (Savenije, 1995b [219] and Savenije, 1996 [220]). A variant of Brubaker et al.'s (1993) [32] and Schär et al.'s (1999) [221] bulk recycling formulae has been developed by Zangvil et al. (2004) [271]. In all these bulk recycling models, precipitation and ET are assumed to be uniformly distributed in space and time (Eltahir and Bras, 1994 [76]

; Dirmeyer and Brubaker, 1999 [57]). In addition, these models do not make any hypothesis about the direction and structure of the flow, as they only account for the total amounts of moisture that enter or leave the region through ET, precipitation and moisture convergence. These makes integral moisture budget models very easy to be applied, although their results are consequently affected by a remarkable degree of uncertainty. Rather than an accurate estimation of the regional recycling ratio, bulk recycling models are thus assumed to provide a qualitative diagnostic of the intensity of land-atmosphere interactions (e.g. Bosilovich and Schubert, 2001 [23]). A complete analysis of the atmospheric water budget, underlying these bulk recycling models, can be found in Peixoto (1973) [199] and Peixoto and Oort (1992) [200].

In addition to the classical analytical recycling models, several different procedures have been explored to compute the recycling ratio over many areas all over the world. The underlying idea of all these methods is to *track* the trajectories described by the water molecules, in order to directly quantify the contribution of both internal and external sources of moisture to the regional precipitation. This purpose has been implemented throught three different techniques, that we briefly discuss below: 1) studies based on isotope data; 2) lagrangian or back-trajectory methods; and 3) numerical experiments with moisture tracers.

The first technique is based on the fact that water of different origins has a distinct content of certain isotopes (Domínguez et al., 2006 [67]). Several studies have taken advantage of this property to estimate the recycling ratio, as is the case with the works by Salati et al. (1979) [215], Rozanski et al. (1982) [213], Jouzel and Merlivat (1984) [141], Koster et al. (1992) [148], Koster et al. (1993) [149], Kurita et al. (2004) [158], Yu et al. (2007) [268], Froehlich et al. (2008) [98] or Liu et al. (2008) [163]). The most relevant drawback of this approach lies in the large uncertainty associated to the variability in the isotopic content of the water vapor

(Kurita et al., 2004 [158]).

On the other hand, lagrangian or back-trajectory methods simulate the paths whereby individual water molecules are transported by the equations of the atmospheric dynamics. The quantification of the fraction of the precipitated water molecules with their origin in regional ET allows to directly compute the recycling ratio. A theoretical introduction to this technique can be found in Merrill et al. (1986) [178]. The lagrangian method has been applied to different regions and periods of the year in a variety of studies, as e.g. those by Joussaume et al. (1984) [139], Dirmeyer and Brubaker (1999) [57], Brubaker et al. (2001) [34], Stohl and James (2004) [236], Stohl and James (2005) [237], Domínguez et al. (2006) [67], Nieto et al. (2006) [188], Dirmeyer and Brubaker (2007) [63], Domínguez et al. (2009) [70], Gimeno et al. (2010a) [110], Drumond et al. (2011) [73] or Gimeno et al. (2011) [112]. The three last studies are focused on the Iberian Peninsula. In general, lagrangian techniques are assumed to be a good alternative to the traditional recycling methods. The comparison of the recycling values obtained through both procedures provides useful information to characterize the regional precipitation regime.

Similarly, numerical tracer experiments have been also carried out for the last decades. In such experiments, water molecules are tagged at the time of their evapotranspiration and followed until they precipitate. Koster et al. (1986) [147] implemented this kind of passive tracers in a GCM to explore the sources and sinks of moisture at the golbal scale. Similar methodologies have been used by Joussaume et al. (1986) [140], Numaguti (1999) [192] Bosilovich (2002) [24], Bosilovich and Schubert (2002) [25]), Bosilovich et al. (2003) [26] and Bosilovich et al. (2005) [27]. Recently, at the University of Santiago de Compostela, professor Gonzalo Miguez-Macho has implemented passive tracers in a regional numerical model (more specifically, in the WRF model). The latter technique allows calculating the recycling ratio explicitly and at high-resolution, becoming the best tool, by far, that we have nowadays to quantify the recycling ratio at the regional scale. The main features of this innovative tool, experimentally applied in chapter 5 over Iberia, are described in chapter 2 (sections 2.1 and 2.4).

In this thesis, we make use of two of the classical recycling models described above to calculate the recycling ratio over the IP: on the one hand, the numerical, two-dimensional model developed by Eltahir and Bras (1994) [76]; on the other, the analytical bulk recycling model developed by Schär et al. (1999) [221]. As mentioned, we refer to both of them as EBRM and IMB, respectively. The theoretical bases, analytical formulae and ranges of applicability are discussed in detail in chapter 2. Additionally, as mentioned in the paragraph above, the new technique based on moisture tracers introduced in the WRF model is experimentally used in chapter 5 to compute the Iberian recycling ratio. Moisture tracers label the water molecules evapotranspired within our study region, which essentially corresponds to the land area of the Iberian Peninsula, allowing to compute the recycling ratio in a direct way,

unlike the IMB and EBRM classical models that rely on assumptions that sometimes do not represent the reality accurately. The comparison of these results becomes very useful to assess the ability of IMB and EBRM recycling methods to reproduce the actual recycling patterns.

Local and regional recycling ratio

Over a certain region of area size A and shape ξ, and during a given period of time Δt, the recycling ratio can be defined either locally or regionally. Considering an area element, ΔA, inside the study region (Fig. 1.9), the local recycling ratio quantifies the fraction of the precipitation falling within this infinitesimal area with its origin in ET within the region (Burde and Zangvil, 2001a [37]). Mathematically, this can be expressed through the equation below (Burde and Zangvil, 2001a [37]; Van der Ent et al., 2010 [256]):

$$\rho(x, y, \Delta t|A, \xi) = \lim_{\Delta A \to 0} \frac{\iint_{\Delta A} P_m(x, y, \Delta t|A, \xi) dxdy}{\iint_{\Delta A} P(x, y, \Delta t|A, \xi) dxdy} \tag{1.4}$$

where $P_m(x, y, \Delta t|A, \xi)$ represents the fraction of precipitation falling at the area element ΔA within the study area, centered at (x, y), with the origin in moisture evapotranspirated at any location within the same region. Similarly, $P(x, y, \Delta t|A, \xi)$ stands for the total amount of rainfall observed at ΔA, centered at (x, y), during a period of time Δt. The corresponding discrete definition of the local recycling ratio can be found in Domínguez et al. (2006) [67]. According to this practical approach, the local recycling ratio for a given grid cell, centered at point (i, j) and with an area size $\Delta A(i, j)$, is given by:

$$\rho(i, j, \Delta t|A, \xi) = \frac{P_m(i, j, \Delta t|A, \xi)}{P(i, j, \Delta t|A, \xi)} \tag{1.5}$$

At the regional scale, the recycling ratio is defined as the total fraction of rainfall within the study area originated from ET inside it (Brubaker et al., 1993 [32]; Trenberth, 1999 [247]). This is expressed as:

$$r(\Delta t|A, \xi) = \frac{\langle P_m \rangle}{\langle P \rangle} = \frac{\iint_A \rho(x, y, \Delta t|A, \xi) P(x, y, \Delta t|A, \xi) dxdy}{\iint_A P(x, y, \Delta t|A, \xi) dxdy} \tag{1.6}$$

where $\langle P_m \rangle$ and $\langle P \rangle$ represent the spatial average of locally evapotranspired and total precipitation, respectively. According to the grid-based approach (Eltahir and Bras, 1994 [76]; Domínguez et al., 2006 [67]), the regional recycling ratio for a study region of area size A and shape ξ is alternatively given by:

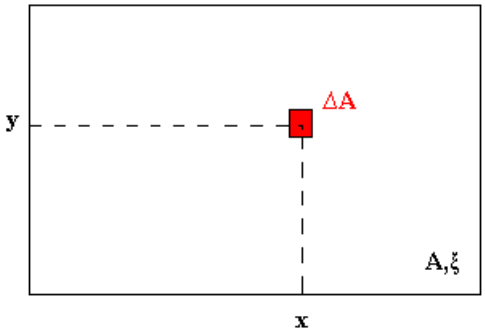

Figure 1.9: Illustration of the concept of local recycling ratio.

$$r(\Delta t|A,\xi) = \frac{\sum_{i,j} \rho(i,j,\Delta t|A,\xi) P(i,j,\Delta t|A,\xi) \Delta A(i,j)}{\sum_{i,j} P(i,j,\Delta t|A,\xi) \Delta A(i,j)} \tag{1.7}$$

where the sums are extended to all the grid cells of the region.

The information provided by regional recycling ratios can be complemented through the calculation of the regional evaporation recycling ratio, $\epsilon(\Delta t|A,\xi)$. This new variable, which arises naturally from this analysis, is defined by Van der Ent et al. (2010) [256] as:

$$\epsilon(\Delta t|A,\xi) = \lim_{\Delta A \to 0} \frac{\iint_{\Delta A} ET^*(x,y,\Delta t|A,\xi) dxdy}{\iint_{\Delta A} ET(x,y,\Delta t|A,\xi) dxdy} \tag{1.8}$$

In this equation, $ET^*(x,y,\Delta t|A,\xi)$ stands for the fraction of moisture evapotranspired from an area element ΔA, centered at the point (x,y), which precipitates at any location within the study region, A. Similarly, $ET(x,y,\Delta t|A,\xi)$ represents the total amount of moisture evapotranspired from that infinitesinal area, regardless the location where it precipitates. Specifically, the fraction of ET that blows out of the region and precipitates beyond its borders is referred to as *moisture export* (e.g. Domínguez et al., 2009 [70]).

Limitations of classical recycling definitions

The definition of the recycling ratio through equations (1.4) and (1.6), widely used in the literature, presents however some relevant shortcomings. The most important one is related to the dependence of the recycling ratio on the size and shape of the study region (Trenberth, 1999 [247]; Van der Ent et al., 2010 [256]). Of course, the recycling ratio tends to increase with the size of the region. Theoretically, it reaches

the maximum value of *1* in the limit case when the study region coincides with the whole globe. Similarly, the minimum value of *0* would be invariantly obtained if the region was reduced to a point. The nature of the function linking the recycling value and the region size has been a matter of intense discussion. For instance, a logarithmic relationship was suggested by Domínguez et al. (2006) [67] and Bisselink and Dolman (2008) [21], whereas Eltahir and Bras (1996) [77] and Dirmeyer and Brubaker (2007) [63] propose this correlation to follow a power law. On the other hand, the shape of the study region, and more specifically its orientation with respect to the predominant direction of the atmospheric flow, also affects recycling values to a significant extent (Burde and Zangvil, 2001a [37]; Van der Ent et al., 2010 [256]; Van der Ent and Savenije, 2011 [257]). This fact is illustrated in Fig. 1.10, where an ideal zonal flow passes over two imaginary rectangular regions with approximately the same area size, A. If the region is too *wide* (that is, the perpendicular dimension to the main flow direction is much greater than the parallel dimension), then most of the moisture evapotranspired within the region will be exported out of its boundaries, thus leading to very low recycling values. On the contrary, if the region is too *long* (the parallel dimension to the main flow direction is much greater than the perpendicular dimension), a relevant fraction of the humidity evapotranspired within the region will precipitate inside it, and thus the local recycling ratio will be significantly high on the *right* side of the study area. As a result, and in order to attenuate the strong dependence of the recycling ratio with the shape of the region, illustrated with this simple example, most of the recycling studies at the regional scale have been carried out over regular domains, not very far from squared shapes. This analysis confirms that recycling ratios alone might not be sufficient to evaluate the impact of the local component of rainfall in the regional precipitation regime.

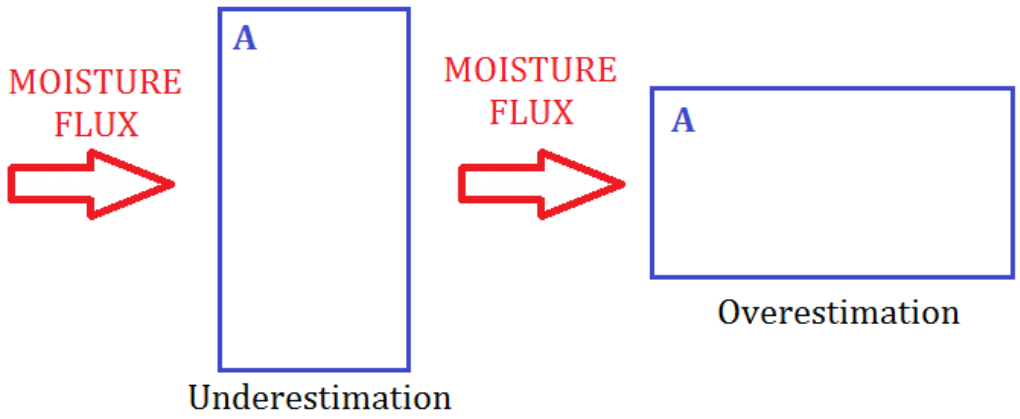

Figure 1.10: Illustration of the impact of the area shape of the study region on recycling calculations.

Continental recycling ratio

As mentioned in the previous subsection, the recycling ratio depends on the shape and size of the region where it is calculated. In order to overcome this limitation, an alternative magnitude has been proposed by Van der Ent et al. (2010) [256]. In the latter study, local and regional *continental* recycling ratios are defined, respectively, as

$$\rho_c(x,y,\Delta t) = \lim_{\Delta A \to 0} \frac{\iint_{\Delta A} P_c(x,y,\Delta t|A,\xi)dxdy}{\iint_{\Delta A} P(x,y,\Delta t|A,\xi)dxdy} \tag{1.9}$$

and

$$r_c(\Delta t) = \frac{\langle P_c \rangle}{\langle P \rangle} = \frac{\iint_A P_c(x,y)dxdy}{\iint_A P(x,y)dxdy} = \frac{\iint_A \rho_c(x,y)P(x,y)dxdy}{\iint_A P(x,y)dxdy} \tag{1.10}$$

In equations (1.9) and (1.10), $P_c(x,y,\Delta t|A,\xi)$ stands for the fraction of precipitation falling within an area element ΔA, centered at the point (x,y), originated from moisture evapotranspirated at *any continental area* over the world. Similarly, $P(x,y,\Delta t|A,\xi)$ represents the total amount of rainfall observed at ΔA, centered at (x,y), during a period of time Δt. $\langle P_c \rangle$ and $\langle P \rangle$ represent the corresponding area-averaged quantities over the study region, A. Unlike standard regional recycling ratios, continental recycling ratios are scale- and shape-independent (Van der Ent et al., 2010 [256]; Van der Ent and Savenije, 2011 [257]).

Nevertheless, over the Iberian Peninsula, mainly affected by the westerly circulation, the computation of the classical regional recycling ratio is expected not to differ significantly from the continental recycling estimations, since the fraction of the Iberian precipitation originated in ET over the Americas can be negligible (Van der Ent et al., 2010 [256]). Similarly, the moisture supply from western Europe or northern Africa is very reduced. On the other hand, unlike continental recycling ratios, which need global simulations to be obtained, the standard local and regional recycling ratios present the advantage that they can be computed from regional climate simulations. As a result, the higher resolution of the regional runs may facilitate a more detailed assessment of the specific characteristics of the Iberian hydrological cycle.

The role of topography on recycling patterns

As it naturally follows from the analysis above, recycling patterns are expected to present a strong connection with the prevailing direction of the wind and moisture

flux. Moreover, they are also very sensible to topography. In fact, mountain ranges are natural obstacles that may sometimes retain the advected moisture, thus modulating the local intensity of recycling (Van der Ent et al., 2010 [256]). An interesting illustration of this mechanism is analyzed, for the Amazon river basin, by Eltahir and Bras (1994) [76]. Surrounded by mountain chains to the north, west and south, the Amazon basin is predominantly influenced by the prevailing easterly winds that transport humidity from the Atlantic Ocean. To a great extent, this orographic configuration blocks the exit of the water vapor advected into the region by the easterly flux. Ideally, that moisture can only leave the region after precipitating within the river basin, through surface and groundwater runoff. Similarly, nearly all the moisture evapotranspired within the basin is unable to flow out, being forced to precipitate as recycled water. According to this rough approximation, one can consider that $P_m \approx ET$ and therefore the regional recycling ratio can be simply estimated as $r = ET/P$. More refined calculations showed that the Amazon river basin is not such a close system, and therefore the actual recycling ratio at the basin scale is significantly reduced with respect to the initial approach discussed above. Regardless, the topography of the region plays in this case a crucial role, enhancing the recycling of internal moisture.

Previous recycling estimates over the Iberian Peninsula

As described at the begining of this section, recycling studies have essentially focused on a few regions of the world. For the Iberian Peninsula, only a limited number of previous works has evaluated the sources of moisture and the recycling ratio at the regional scale. For an area including most of the IP, Schär et al. (1999) [221] estimated a monthly, regional recycling value close to 0.06 for both July of 1990 and July of 1993, providing an analysis of the sensitivity of the summer recycling ratio to different initializations of soil moisture over Iberia. This study concludes that a wet (dry) initialization of soil conditions leads to a significant increase (decrease) of both recycling ratio and precipitation efficiency in the Iberian summer. Bisselink and Dolman (2008) [21] estimated, for a similar region, the average summer (June-July-August, JJA) regional recycling ratio over the period 1979-2001, with results ranging from 0.1 to 0.2. In a recent work, Dirmeyer et al. (2009b) [65] provide absolute values of mean recycling ratio over the period 1979-2003 for Spain (0.13) and Portugal (0.04). The corresponding area-scaled recycling ratios (for a reference area of $10^5 km^2$) were found to be 0.06 for Spain and 0.04 for Portugal. In a global study including the IP, Trenberth (1999) [247] found an average annual recycling ratio ranging from 0.05 to 0.10, for a 500 km length scale, for the period 1979-1995, by using the Climate Prediction Center Merged Analysis of Precipitation (CMAP) and the National Centers for Environmental Prediction (NCEP) reanalysis data (see Trenberth, 1999 [247] for details). These values vary from 0.04 to 0.08 in winter and from 0.10 to 0.12 in spring, when the highest recycling values are obtaind (in summer, recycling ratios remain below 0.10). For a 1000 km length scale, the mean annual recycling

ratio ranged from 0.14 to 0.16 throughout Iberia. Also in a global context, Van der Ent et al. (2010) [256] obtained annual continental recycling ratios (measuring the fraction of the Iberian precipitation originated in ET from any continental area in the world), between nearly 0 and 0.2 over the IP. Additionally, other authors have examined the sources of moisture affecting Iberia, assessing the relevance of oceanic moisture sources vs. recycling. The most relevant contribution is that of Gimeno et al. (2010a) [110], who studied the sources of moisture for precipitation in the IP using a back trajectory lagrangian model on ECMWF analysis data, concluding that long distance transport is largely dominant in winter and autumn, but that in spring and particularly in summer, an internal source of moisture, i.e. a recycling component, is more relevant (Gimeno et al., 2010a [110]; Gimeno et al., 2011 [112]). Gimeno et al., (2010a) [110] also confirmed that atlantic baroclinic systems and convective processes have a similar impact on the mean annual totals of precipitation in the interior and eastern regions, where recycling mechanisms are of high relevance, in contrast to the northern and Atlantic sides of the IP. Finally, Jódar et al. (2010) [138] provide an assessment of the impact of irrigation on further precipitation in southern Spain during summer, showing that for two semiarid areas of study, a significant increase in rainfall occurs in the mountains downwind from the irrigated zones. Altogether, these studies suffer from different caveats, related to several key factors: a) low resolution data available, b) short period of data available, c) often concentrated in annual or seasonal values, thus lacking a complete assessment of the recycling at the monthly scale, and d) reliance on just one method to compute the recycling ratio. In this thesis we intend to overcome these shortcomings and provide a more comprehensive evaluation of the recycling ratio over Iberia at high resolution, at the monthly scale, covering a longer period of time and relying on three different methods, which are explained in detailed in chapter 2, appendix B and appendix C.

1.5 The amplification mechanism: impact on the Iberian precipitation

As stated in the previous section, assessing the intensity of the recycling mechanism, through the computation of the recycling ratio, may not be sufficient to completely investigate the impact of the locally evapotranspired moisture on the regional precipitation regime. Interestingly, this is not only due to the above-discussed dependence of the recycling ratio with the size and shape of the study region. On the contrary, the main reason lies in the following critical fact: apart from moistening the lower atmosphere, the evapotranspired humidity increases its thermodynamic instability (e.g. Stidd, 1967 [234]), thus favoring the development of convective cells and the subsequent precipitation of convective nature. This indirect effect of the ET fluxes is known in the literature as the *amplification* mechanism (Schär et al., 1999 [221]). In this section, we revise and discuss the physical features underlying this process,

whose effects on the Iberian spring peak of precipitation are analyzed in chapter 4.

The soil moisture - precipitation feedback refers, in the words of Seneviratne et al. (2010) [225], to the "retroaction of soil moisture on itself through the combination of its impact on precipitation". This soil moisture-precipitation feedback is implemented via two main physical mechanisms: recycling and amplification (Schär et al., 1999 [221]). Their simplified representation is illustrated in Fig. 1.11.

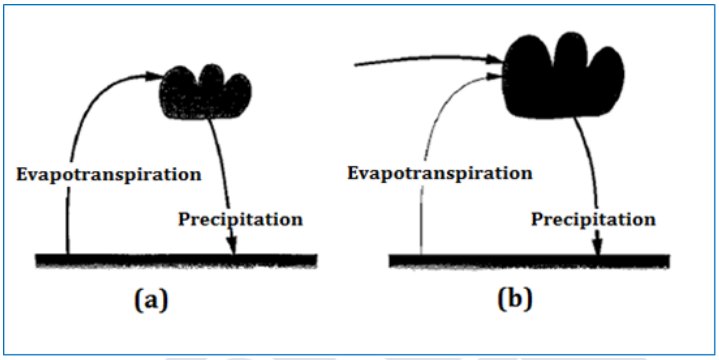

Figure 1.11: Illustration of the two mechanisms for the soil-precipitation feedback: (*a*) recycling and (*b*) amplification. Adapted from Schär et al. (1999) [221].

As mentioned, ET fluxes are not only a source of water for more precipitation. In addition, they also affect the thermodynamic structure of the lower atmosphere, enhancing convection and potentially altering the regional circulation to produce more rainfall (Beljaars et al., 1996 [11]; Paegle et al., 1996 [195]; Dirmeyer and Brubaker, 1999 [57]; Schär et al., 1999 [221]; Goessling and Reick, 2011 [116]). In contrast to the direct or recycled contribution, the latter intensification of the precipitation amounts is said to occur via indirect or amplification processes.

The main consequence of the indirect effect of ET is that a fraction of the advected moisture, which otherwise would be simply blown across the region, can be retained and added to the precipitation totals (Schär et al., 1999 [221]), thus becoming a source of extra precipitation induced by land-atmosphere interactions, in addition to local ET. Actually, the higher extraction of moisture from the large-scale flow attributable to the effect of ET fluxes can be as relevant as the direct impact of ET fluxes alone as mere suppliers of water (Betts et al., 1996 [16]; Eltahir, 1998 [79]; Schär et al., 1999 [221]; Findell and Eltahir, 2003a [90]; Findell and Eltahir, 2003b [91]; Ek and Holtslag, 2004 [75]; Alfieri et al., 2008 [2]; Seneviratne et al., 2010 [225]). This is somehow expected, since vertical motions in the atmosphere constitute a necessary condition to trigger precipitation. In other words, an increase in the amount of water vapor in the lower levels is not always sufficient to enhance rainfall (Brubaker et al., 1993 [32]), and the ascend of water vapor favored by the atmospheric instability is also required. ET fluxes can critically modulate the large-scale environment, locally or at a regional scale (Koster and Suarez, 2001 [152]; Goessling and Reick, 2011 [116]),

to trigger precipitation that otherwise would not have occurred at all.

Separating the pure recycling (direct) contribution from the indirect effect of ET fluxes on precipitation is not straightforward, since both processes occur simultaneously and affect one another. As it is known, recycling ratios can be obtained from a data set of atmospheric analysis or a single model simulation. Similarly, from any of these sources, the relative contribution of both direct and indirect mechanisms in increasing rainfall can be also assessed through an analytical method developed by Schär et al. (1999) [221]. This procedure is described in detail in section 2.6. Furthermore, in this thesis we introduce a new procedure to separate both contributions, based on the comparison between control model simulations (with all land-air fluxes normally set up) and experiments where water vapor from terrestrial ET is removed. This procedure, fully explained in section 2.7, is inspired in the numerous examples in the literature where ET is modified (either directly or by changing soil moisture in the model) to study the potential impact of land-surface interactions on precipitation (see the review by Seneviratne et al. 2010 [225] for an extensive list of references). Results may vary with season and place, and even if convection is parameterized or resolved by the model, depending on the horizontal resolution of the computations (Hohenegger et al., 2009 [125]). Nevertheless, it is generally accepted that there are potent land surface-precipitation feedbacks that can alter significantly the regional atmospheric circulation and the associated precipitation patterns.

1.6 Objectives and possible applications of this thesis

As discussed in section 1.1, the need to understand why a maximum of precipitation occurs in spring over the broad interior of Iberia constitutes the main experimental motivation for this thesis. Consequently, a comprehensive analysis of the physical mechanisms underlying this relevant feature of the Iberian rainfall regime becomes our principal objective. More in detail, the questions that we want to address along the next chapters are: first, to what extent and through which mechanisms land surface fluxes, in particular ET, might control the rainfall amounts in the spring in the vast semiarid plateaus in the core of the IP; and second, how much of this precipitation is new moisture added into the region and not recycled water. This requires a deep investigation of the sources of moisture for the Iberian precipitation. As discussed, the humidity that precipitates over the Iberian Peninsula is originated either within (through land surface ET) or derives from outside (mostly from the Atlantic Ocean). The latter contribution is largely responsible for the October-to-March precipitation, whereas the internal source plays a more relevant in spring and summer. Investigating the above-mentioned spring peak of precipitation implies quantifying the relative contribution of those main moisture sources to the Iberian rainfall (local and oceanic). For this purpose, the impact of recycling and amplification mechanisms over the interior lands of the IP must be assessed over a long enough period of time. Results

have important implications to understand the potential influence of anthropogenic changes in land surface conditions and hydrology on the region's climate.

Possible applications

As mentioned, apart from the scientific interest of the present investigation, it might have some relevant practical applications, which may be classified into two major blocks:

1. *Improvement of seasonal forecasting and alert management.* As discussed in this section, the soil keeps the memory of the precipitation falling over a region during the previous season. This fact has a critical impact on arid and semiarid regions where the recycling contribution is relevant, as is the case of most interior lands of the Iberian Peninsula in spring. After a dry winter, for instance, the scarcity of soil moisture to fuel the ET fluxes will enhance the probability of a dry summer, with flood risks being simultaneously reduced. On the contrary, the availability of soil moisture after a humid winter increases the probability of the following summer being more humid than average, even though that probability is strongly modulated by the synoptic configuration. In this case, the likelihood of extreme rainfall events is also increased, mostly in those areas where convective precipitation contributes critically to spring and early summer rainfall. As a result, the comprehensive knowledge of the spatio-temporal patterns of recycling over the Iberia, combined with the analysis of the dry or wet nature of a given period, may lead to a significant improvement of the forecasts for the subsequent seasons, also modulating the probability of extreme events to take place.

2. *Hydrological planning and regional sustainability.* As mentioned, human activities have a critical impact on the local fraction of precipitation. Therefore, in those areas where this contribution plays a relevant role in the regional rainfall regime, an appropriate plannig of the land use and a responsible management of the water resources (very limited e.g. in large interior Iberian lands), becomes essential for a sustainable preservation of the local sources for precipitation. Processes like an uncontrolled abstraction of groundwater or the transformation of forest areas into farmlands or urban areas may have an impact on this locally originated precipitation that must be comprehensively assessed, as a way to preserve the hydrological equilibrium. In a context of climate change, with precipitation amounts over Iberia being expected to decrease during the next decades (Giorgi and Lionello, 2008 [115]; Mariotti et al., 2008 [168]), the investigation of soil moisture - atmopshere feedbaks requires particular attention, since apart from being a key player for climate change, land-atmosphere connections are expected to be significantly affected by this global process (Seneviratne et

al., 2006a [223]), with especial emphasis in all the Mediterranean region, including the Iberian Peninsula.

Structure of this thesis

Along this introductory section, and according to the working hypothesis formulated in section 1.3, we essentially focused on the physical mechanisms that modulate the local fraction of precipitation: soil moisture and groundwater dynamics, land-atmosphere interactions, including ET fluxes, as well as recycling and amplification processes.

In chapter 2, the different methods used in this work are carefully described. First, we provide a brief introduction to the WRF model, presenting the configuration used to perform our numerical simulations. Then, we analyze the procedures to compute the recycling ratio and to separate the recycling contribution from that related to amplification processes. At this point, we present a new approach, based on model experiments where the land ET is suppressed over the Iberian Peninsula, to more accurately carry out this calculation. Finally, we describe an innovative computational tool, consisting in the implementation of moisture tracers in the WRF model, which is used to explore the moisture sources of the Iberian precipitation and compute the local recycling ratio in a direct and more realistic way.

We develope our analysis by computing monthly recycling ratios over the Iberian Peninsula, along a period of 18 complete annual cycles, from January 1990 to December 2007. In this work, based on WRF model simulations, we find the Iberian recycling ratio to be the highest during late spring and early summer and precisely over those areas where the spring maximum of precipitation corresponds to the actual absolute maximum along the yearly cycle. This preliminary investigation, suggesting a critical role of recycling processes in the spring precipitation over the interior areas of the IP, is presented in chapter 3. In large parts, it corresponds to the article *Precipitation recycling in the Iberian Peninsula: spatial patterns and temporal variability* (see the List of Publications for the complete reference), submitted to the *International Journal of Climatology* on August 2nd 2013 and under review at the moment of the presentation of this thesis.

In chapter 4, we focus our attention on the months of May along the last decade (2000-2010). As mentioned, it is in May when the annual maximum of rainfall takes place in large areas of the interior, east and northeast of Iberia. In addition, the activity of land-atmosphere interactions is enhanced in this month, as we learn from the analysis developed in chapter 3. In this study, which mostly corresponds to the article *Moisture recycling and the maximum of precipitation in spring in the Iberian Peninsula*, accepted for publication in *Climate Dynamics* on October 9 th 2013 (DOI: 10.1007/s00382-013-1971-x), we explore the relative contributions of recycling and

amplification mechanisms to the observed surplus of precipitation in May. For this purpose, high-resolution WRF model simulations (with all land-air interactions normally activated) are compared to experimental runs where ET is suppressed over the land areas of the Iberian Peninsula. In addition, the months of January along the same period are simulated, as a manner to assess the essential differences in the Iberian recycling regime between winter and late spring.

Finally, in chapter 5, regional WRF model simulations incorporating moisture tracers are carried out over the Iberian Peninsula along the period May 2000 - May 2010. The use of numerical moisture tracers is of the greatest interest, as it constitutes a mean to directly compute the recycling ratio, avoiding the assumptions imposed by the classical recycling models that sometimes do not represent the reality with accuracy. This method provides useful information to complete the characterization of the spring peak of precipitation and, at the same time, constitutes a way to assess the accuracy of the classical procedures to estimate recycling. The material included in this chapter will be part of the article *"Regional climate simulations with moisture tracers to investigate land-atmosphere interactions in the terrestrial water cycle over the Iberian Peninsula"*, which is now in preparation. A final outlook, together with the critical review of the most relevant conclusions of this research is provided in chapter 6.

USC
UNIVERSIDADE
DE SANTIAGO
DE COMPOSTELA

2

Data and methods

In this chapter, we provide a detailed description of the different methods, datasets and computational tools used in this thesis. Among them, we highlight the development of a new method to separate the recycling and amplification contributions, based on WRF model experiments where the evapotranspitation flux is not incorporated to the atmosphere. This procedure is presented in section 2.7. On the other hand, an innovative computational tool, consisting in the implementation of numerical moisture tracers in the WRF model, allows a realistic identification of the Iberian humidity sources and an accurate calculation of the recycling ratio. Both aspects are critical to correctly identify the physical processes that modulate the Iberian precipitation regime, with the focus in the springtime and in the interior regions.

2.1 The Weather Research and Forecasting Model (WRF). Configuration

The Weather Research and Forecasting (WRF) model is used to carry out the simulations for this thesis. Apart from being a regional, numerical tool for weather forecasting, analysis of real and ideal meteorological events and climatic research, the WRF model constitutes an open platform for the development of more accurate codes and algorithms that better serve these objectives. Consequently, the WRF model is periodically updated with new options, tools and parameterizations that expand its applicability and improve the accuracy and reliability of its results.

The mathematical analysis of the atmospheric dynamics is essentially based on the application of classical mechanics and thermodynamics to the atmosphere (Sendiña and Muñuzuri, 2006 [222]) through three fundamental conservation laws (Holton, 1972 [126]): 1) the continuity equation (conservation of mass); 2) the equa-

tion of conservation of momentum (Navier-Stokes equation); and 3) the equation of conservation of energy. Numerical meteorological models solve these basic equations in a discrete number of points, homogeneously distributed over a three-dimensional grid whose base is projected over the spheroidal surface of the Earth. In addition, these basic equations are solved at discrete time steps in order to track the evolution of the system. Such spatio-temporal discretization of the equations of the atmosphere is intrinsically required by their non-linear nature.

Numerical models can either simulate the atmospheric dynamics at the global scale (in this case they are referred to as Global Circulation Models or GCMs) or focus on a certain region of the planet. In the latter type of models (referred to as Regional Climate Model or RCMs), the lateral boundaries that limitate the study region receive information from GCMs to drive the atmospheric dynamics at the regional scale according to the global circulation. RCMs such as the WRF model were initially used only for numerical prediction, taking advantadge of their higher horizontal resolution (tipically in the range from 10 to 1 km) with respect to GCMs. Nowadays, however, regional models, which are able to better reproduce the specific climatic details of a concrete region, are widely used for meteorological and climate studies all over the world (Jiménez, 2010 [137]). Further technical information about the WRF model can be found in Skamarock et al. (2005) [229] and Skamarock et al. (2008) [230]). Additionally, a very interesting overview on the WRF model is provided in the Ph.D. thesis by Jiménez (2010) [137].

WRF simulation 1 (WRFS-1)

The recycling computations described in chapter 3 were performed by using a climate simulation of 18 years, from January 1990 to December 2007, developed at the *Instituto Dom Luiz* (CGUL, Universidade de Lisboa) by professor Dr. Pedro M. M. Soares, professor Dr. Rita M. Cardoso and other coauthors, who gently provided us with that material and colaborated in the developement of this study. The simulation was carried out with the WRF (Weather Research and Forecasting) model, version 3.1.1 (Skamarock et al., 2008 [230]), using a 27 km horizontal resolution outer domain with a nested 9 km domain, both centered in the Iberian Peninsula (Figs. 2.1a and 2.1b). Initial and lateral boundary conditions were obtained from the ERA-Interim pressure-level reanalysis and updated every 6 h. Further technical specifications about the WRF runs tuned for the Iberian Peninsula region can be found in Cardoso et al. (2012) [43] and Soares et al. (2012) [231]. Hereafter, this simulation is referred to as WRFS-1.

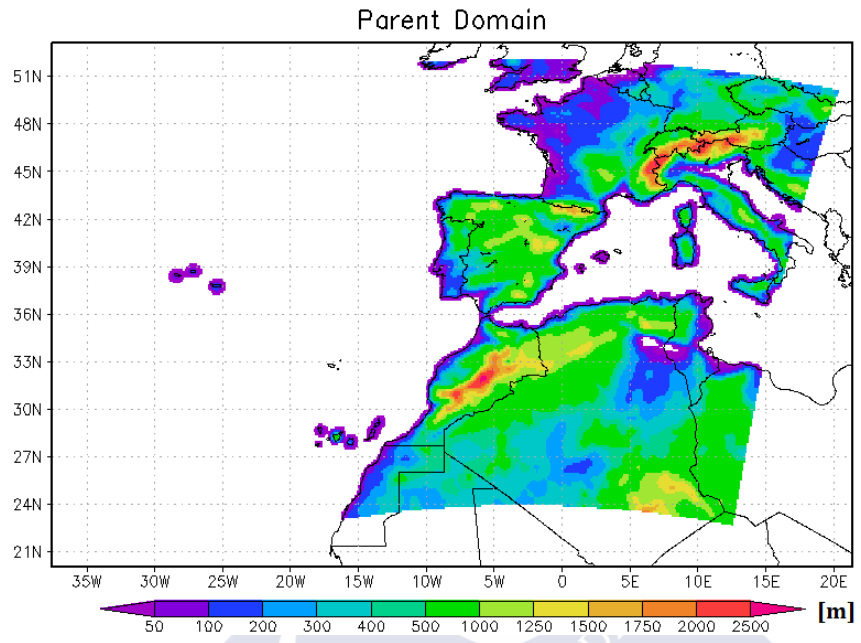

(a)

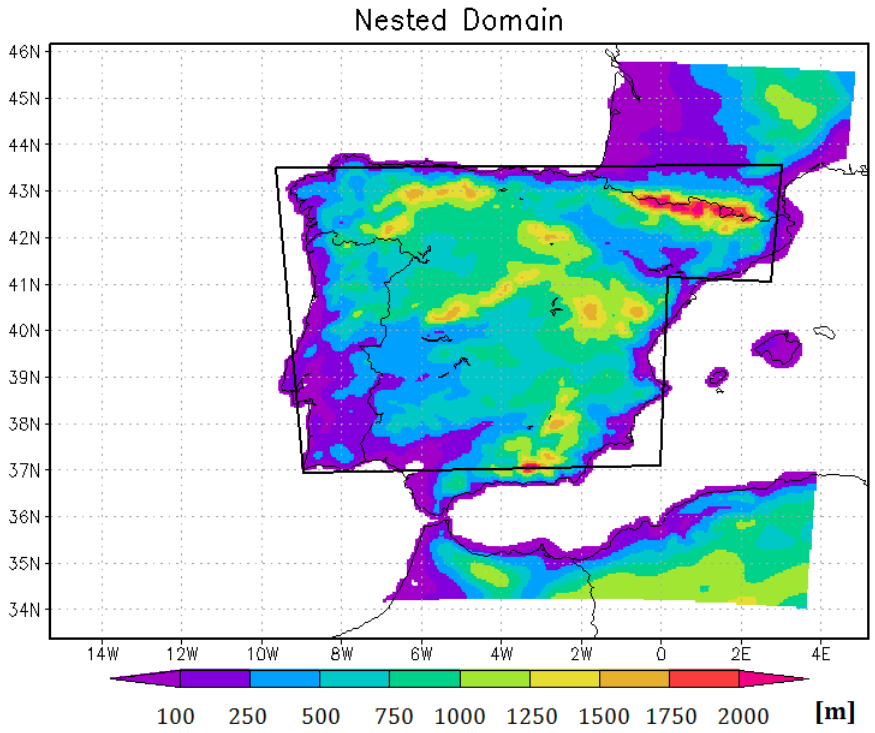

(b)

Figure 2.1: Parent (*a*) and nested (*b*) domains used in WRF simulation 1 (WRFS-1), analyzed in chapter 3. In panel (*b*), the region selected for the computation of the recycling ratio is also shown. The terrain height above the sea level is expressed in (m).

Set of WRF simulations 2 (WRFS-2)

To carry out the analysis described in chapter 4, we perform simulations for eleven months of May (from May 2000 to May 2010) with version 3.0.1.1 of the WRF model (Skamarock et al., 2005 [229]). For comparison, eleven months of January (from January 2000 to January 2010) were also run. For each of these months, we perform two simulations: on the one hand, a control run with all land-atmosphere fluxes normally set up; on the other, an experimental run where ET over land is suppressed. We conducted the above-mentioned 22 pairs of simulations by using a parent grid of 225 x 225 points at 20 km resolution (Fig. 2.2a) and a 1500 x 1500 km^2 nested grid that covers the IP at 5 km horizontal resolution (Fig. 2.2b). Hereafter, this whole set of WRF runs is referred to as WRFS-2.

It is important to remark that, in the *no-ET* runs, the evapotranspiration flux is only removed from the land areas within the nested domain, as a way to bring out the effect of the Iberian ET and more explicitly assess the impact of local water fluxes on precipitation dynamics. In these sensitivity experiments, the energy absorbed at the surface is still converted into latent heat flux, although the corresponding water vapor flux is not incorporated into the atmospheric boundary layer, being simply removed from the system. With this procedure, the surface is still cooled by evapotranspiration and therefore the thermal effects on atmospheric stability of a significantly warmer soil are prevented, allowing us to focus on the effect of the moisture flux. Hence, our experiments partially uncouple the land surface from the atmosphere, exploring the subsequent effects on the regional climate with respect to the *control* runs. The procedure to modify the WRF model code in order to remove land ET from the model simulations is described in detail in appendix D.

This technique of altering the ET fluxes has been used by several authors, either directly or via changes in soil moisture configurations, as a way to assess their impact on the regional water cycle. For instance, Shukla and Mintz (1982) [228] investigated the role of ET by comparing a model experiment in which ET had been suppressed to a control run where ET was set equal to the potential evapotranspiration calculated by the model. Similarly, Delworth and Manabe (1989) [53] compared global control simulations to sensitivity experiments where land-atmosphere interactions were inhibited. A similar experiment, in this case through regional climate simulations, was carried out by Fischer et al. (2007a) [92] to assess the impact of land-air connections on the four major recent European summer heat weaves (1976, 1994, 2003 and 2005). Schär et al. (1999) [221] explored the effects of different initializations of the soil moisture content on fundamental climatic variables as precipitation, precipitation efficiency, ET and recycling ratio. Cook et al. (2006) [48] compared control model simulations with experimental runs where the availability of soil moisture for further ET is set to be unlimited. In this work, a surprising negative ET-precipitation feedback is found over South Africa. In a more systematic study (the GLACE project: see Koster et al., 2004 [156]; Koster et al., 2006 [157], Dirmeyer et al., 2006 [62];

Guo et al., 2006 [122]; Seneviratne et al., 2006b [224]), an ensemble of Atmospheric General Circulation Models (AGCMs) was run under different soil moisture initializations to asses the degree of control of surface water and heat fluxes on further atmospheric processes and determine the *hot spots* of land-atmosphere coupling in the world, which are found to be located in the Great Plains of the USA, the Sahel region and equatorial Africa, India, central Asia and China (Koster et al., 2004 [156]; Wang et al., 2007 [261]). Recently, Seneviratne et al. (2006a) [223] investigated the effects of climate change over Europe by comparing regional simulations with and without land-atmosphere feedbacks. In our case, the actual ET is routinely calculated by the model in the control runs, according to atmospheric demand and soil moisture availability.

The parameterizations used include spectral nudging for the parent grid, in order to avoid the distortion of the large-scale circulation caused by the interaction of the modeled flow with the lateral boundaries (Miguez-Macho et al., 2004 [179]; Miguez-Macho et al., 2005 [180]) and the Kain-Fritsch convection scheme (Kain and Fritsch, 1990 [142]; Kain and Fritsch, 1993 [143]). For the nested grid, we assume convection is resolved and hence the convective parameterization is turned off, and so is spectral nudging. This decision is widely supported by previous literature (e.g. Weisman et al., 1997 [264]; Arakawa, 2004 [6]; Gerard, 2007 [108]; Yu and Lee, 2010 [267]), even though the use of convective parameterizations in the *grey-zone* resolution (2 to 10 km), where convective processes are partly resolved and partly subgrid (Yu and Lee, 2010 [267]) is still a matter of debate. Both parent and nested grids use the WSM6 cloud microphysics scheme (Hong and Lim, 2006 [128]), the RRTM scheme for long wave radiation (Mlawer et al., 1997 [184]) and Dudhia scheme (Dudhia, 1989 [74]) for short wave radiation; the Monin-Obukhov surface layer parameterization, the YSU scheme for turbulence in the PBL and the Noah land-surface model (Chen and Dudhia, 2001a [46]; Chen and Dudhia, 2001b [47]). A detailed explanation of the above-mentioned parameterizations can be found in Stensrud (2007) [233]. In addition, a thorough assessment of the effects of horizontal resolution and cloud and convective parameterizations on simulating precipitation can be found in Iorio et al. (2004) [130]. Control and *no-ET* experiments are driven by the same initial and lateral boundary conditions, taken from the National Centers for Environmental Prediction (NCEP) Global Forecast System (GFS) and available at the resolution of 1°x 1°(http://rda.ucar.edu/datasets/ds083.2). The nesting is one-way interacting.

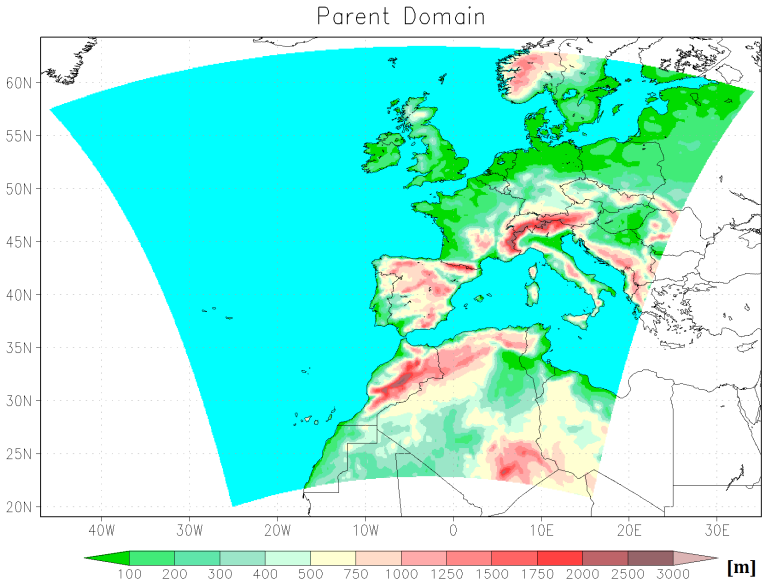

(a)

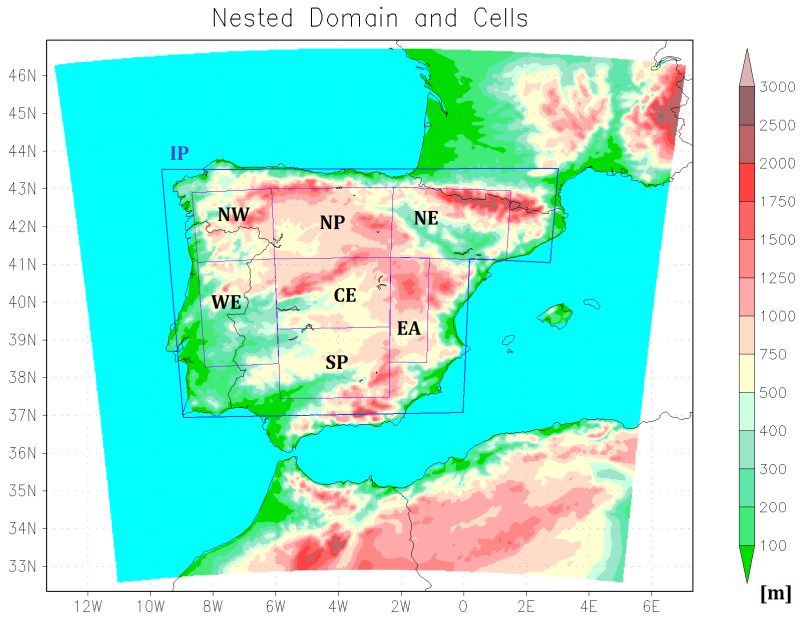

(b)

Figure 2.2: Terrain height above the sea level (m) for (*a*) parent and (*b*) nested domains used in the WRFS-2 simulations, together with the boxes considered within (IP, Iberian Peninsula; NW, Northwest; WE, West; NP, North Plateau; CE, Center; SP, South Plateau; NE, Northeast; and EA, East).

Set of WRF simulations 3 (WRFS-3)

For the work described in chapter 5, the WRF model (version 3.4.1) is used to simulate eleven months of May, from May 2000 to May 2010. In order to carry out these simulations, hereafter referred to as WRFS-3, a new capability of moisture tracers was experimentally incorporated to the WRF model by professor Dr. Gonzalo Miguez-Macho. This tool allows to explicitly investigate the sources, pathways and sinks of humidity in the terrestrial water cycle and thus explicitly calculate the recycling ratio. Six new prognostic variables are added in the WRF model, corresponding to tracers for water vapor and other moisture species (cloud water, ice, snow, rain and graupel) originating from moisture evapotranspired in a selected region (in our case, this region essentially corresponds with the land mass of the Iberian Peninsula). The new moisture variables are advected, diffused, and convectively and turbulently mixed identically to the full moisture species including all humidity sources (terrestrial, maritime and lateral boundaries). In addition, the convective scheme (Kain-Fritsch) and the microphysics scheme (WSM6) need to be modified, in order to account for generation and depletion among the different tracer species. It is important to remark the assumption that, within one model layer and in a grid cell, moisture of all origins is assumed to be well mixed. With these modifications, the terrestrial hydrology cycle can be explicitly tracked and thus the contribution of locally evapotranspired moisture to rainfall can be exactly measured with high resolution within our region of interest. To facilitate the comparison of results, the parent and nested domains used in WRFS-3 simulations including moisture tracers correspond exactly with those defined for the above-mentioned WRFS-2 simulations (Figs. 2.2a and 2.2b). Furthermore, horizontal resolution, initial and lateral boundary conditions and all the selected model options and parameterizations are the same as those used in WRFS-2 simulations, so that results can be compared. Note that, even though these model domains are not identical to the ones used in WRFS-1, the region where the recycling ratio is computed is always the same along this thesis, corresponding to the area bounded in black in Fig. 2.1b and the corresponding area bounded in blue in Fig. 2.2b.

2.2 The Schär et al.'s (1999) Integral Moisture Budget Recycling Model

In section 1.4, we briefly discussed the most relevant characteristics and limitations of a variety of recycling models developed during the last decades. Among them, analytic Integral Moisture Budget (IMB) models are probably the easiest manner to compute the regional recycling ratio over a certain area (Goessling and Reick, 2011 [116]). In this thesis, we make use of the formula due to Schär et al. (1999) [221], whose derivation is presented next.

As in all bulk recycling models, the equation of conservation of water over a certain region,

$$\frac{\partial N}{\partial t} = IN + ET - OUT - P \tag{2.1}$$

constitutes the base of the method. In this equation, N stands for the amount of water stored in the atmosphere (also referred to as *precipitable water*), IN represents the input of moisture into the region, ET is the evapotranspiration, OUT stands for the moisture blown outside the region and P is the precipitation per unit time. Usually, the difference between IN and OUT is called *moisture convergence* ($MC \equiv IN - OUT$). Fig. 2.3 illustrates the above-mentioned water budget terms. The explicit procedure to calculate them is described in detail in appendix A.

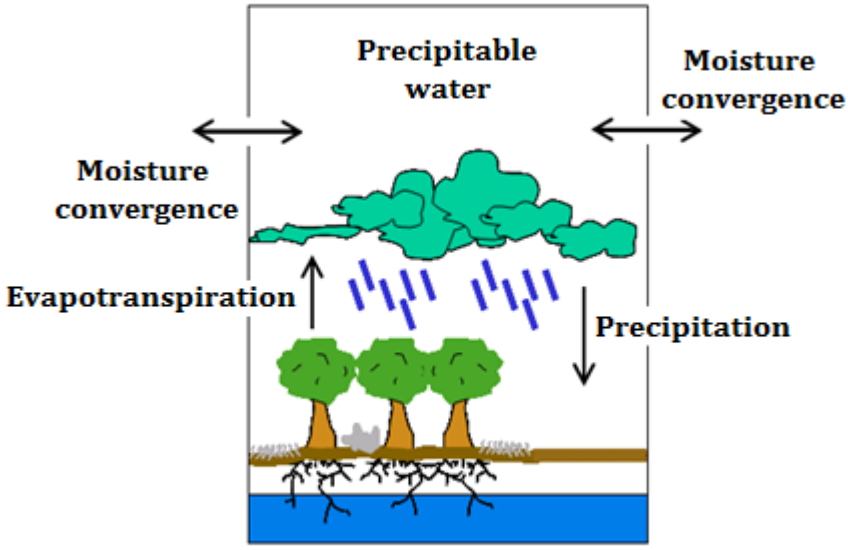

Figure 2.3: Representation of the water budget terms: precipitation, evapotranspiration, moisture convergence and precipitable water.

Water molecules contained within the considered atmospheric volume may have been evapotranspirated either inside or outside it. According to this, the equation of conservation (2.1) can be split in two for each of these components:

$$\frac{\partial N_m}{\partial t} = ET - OUT_m - P_m \tag{2.2a}$$

$$\frac{\partial N_a}{\partial t} = IN - OUT_a - P_a \tag{2.2b}$$

where subindex m refers to water molecules evapotranspirated within the study region and subindex a refers to molecules advected from outside. Assuming that the atmosphere is well-mixed (a discussion on the accuracy of this hypothesis is given in section 1.4) and that the recycling ratio keeps constant over the region, one can say that

$$r \equiv \frac{P_m}{P} = \frac{OUT_m}{OUT} = \frac{N_m}{N} = \frac{\frac{\partial N_m}{\partial t}}{\frac{\partial N}{\partial t}} \tag{2.3}$$

As it can be observed, the complete mixing of the atmospheric water vapor becomes a major assumption for the IMB (and in general for all traditional recycling models), as it allows writing the recycling ratio as a ratio of moisture fluxes, instead of as a precipitation fraction. From equations (2.2a) and (2.3) we obtain:

$$ET = r(OUT + P + \frac{\partial N}{\partial t}) \tag{2.4}$$

Similarly, from (2.2b) and (2.3):

$$IN = (1 - r)(OUT + P + \frac{\partial N}{\partial t}) \tag{2.5}$$

By dividing (2.4) over (2.5) and rearranging, we deduce an analytical formula to compute the regional recycling ratio (Schär et al., 1999 [221]):

$$r = \frac{ET}{IN + ET} \tag{2.6}$$

In equation (2.6), ET and IN represent the accumulated evapotranspiration and the total input of moisture entering the boundaries of the region during the considered period (in all the cases considered within this thesis, this period corresponds to one month). Both ET and IN are obtained from WRF model output. This means that, in reality, equation (2.1) results from the rearrangement of the *empirical* equation of conservation of water,

$$\frac{\partial N}{\partial t} = IN_0 + ET - OUT_0 - P + \alpha \tag{2.7}$$

where α stands for the experimental residual. This term is commonly added to the water budget equation in order to account for different sources of error, as is the case with biases derived from model parameterizations (Domínguez et al., 2006 [67]). Although α can be of the same order of magnitude as the other terms in equation (2.7) (Kanamitsu and Saha, 1996 [145]; Domínguez et al., 2006 [67]), it has been shown not to affect the recycling patterns strongly (Domínguez et al., 2006 [67]; Bisselink and Dolman, 2009 [22]). In accordance with Schär et al. (1999) [221], the connection between equations (2.1) and (2.7) is given by

$$IN = IN_0 + \frac{\alpha}{2} \tag{2.8a}$$

$$OUT = OUT_0 - \frac{\alpha}{2} \tag{2.8b}$$

As mentioned in section 1.4, a relevant limitation of analytical recycling methods, such as the IMB, is related to its strong dependence on the dimensions and shape of the selected region. In the recycling literature, analytical recycling ratios like the one presented here are computed for areas with length scales over 500 km. This can be easily justified by considering equation (2.6). For very small regions, the recycling ratio diminishes rapidly, given that the base area of the selected box is reduced but not its height, which is the top of the atmosphere and remains always the same, and therefore the ET term (water influx from the base) diminishes much quicker than the IN term (water influx from the sides). Additionally, the IMB has the drawback that it does not consider the spatial distribution of moisture within the region, since the terms used for calculations are area-averaged quantities (Burde et al., 1996 [36]; Burde and Zangvil, 2001a [37]). As a result of this, the IMB recycling model shows a tendency to underestimate the recycling ratio, as all Budyko-type models, mostly under complex, non-parallel flow configurations (Burde et al., 1996 [36]; Burde and Zangvil, 2001a [37]), as it does not consider the direction of the moisture flux with respect to the geometry of the region (van der Ent et al. 2010 [256]). Nevertheless, as mentioned in section 1.4, this method becomes a very simple way to get a qualitative diagnose of precipitation recycling over our region.

On the other hand, the region inside the nested domain where the IMB was applied is shown in Fig. 2.2b. To facilitate comparison between recycling methods, the EBRM model (explained in section 2.3) and the tracers method (section 2.4) are also applied over the same area. The interested reader can find further details on the IMB computation method in appendix B.

2.3 The Eltahir and Bras's (1994) Recycling Model

A more detailed procedure to compute the recycling ratio was developed by Eltahir and Bras (1994) [76]. According to this procedure, the region is subdivided into multiple cells, providing not only a regional value, as is the case with the IMB recycling model, but also a spatial pattern of recycling, thus allowing to account for the spatial variability of recycling over the study area. Similarly, the base of this method (referred to as EBRM) is the equation of conservation of water, which must be satisfied now for each grid cell:

$$\frac{\partial N(x,y)}{\partial t} = IN^*(x,y) + ET(x,y) - OUT^*(x,y) - P(x,y) \tag{2.9}$$

In (2.9), $N(x,y)$ stands for amount of water stored in an atmospheric column limited by the grid cell centered at (x,y), IN^* (OUT^*) represents the average inward (outward) moisture fluxes into (from) the considered atmospheric column, which equals the outward (inward) fluxes from (to) the neighboring cell. $ET(x,y)$ stands for the evapotranspiration and $P(x,y)$ is the precipitation over the considered grid cell per unit time. It is important to note the need to use different symbols to represent the moisture input and output terms in both recycling methods, EBRM and IMB, since the computation procedure is not exactly the same in both cases (see appendix B for a detailed explanation of this question).

In a similar way as it was described for the IMB, equation (2.9) is split into two, thus expressing the simultaneous conservation of water from internal and external origin. These two new conservation laws must hold for every grid cell in the EBRM; as a result of this, they are slightly different to equations (2.2a) and (2.2b):

$$\frac{\partial N_m(x,y)}{\partial t} = IN_m^*(x,y) + ET(x,y) - OUT_m^*(x,y) - P_m(x,y) \tag{2.10a}$$

$$\frac{\partial N_a(x,y)}{\partial t} = IN_a^*(x,y) - OUT_a^*(x,y) - P_a(x,y) \tag{2.10b}$$

The EBRM requires the time frame to be sufficiently large (e.g. one month, as is the case along this thesis), so that the variation of the storage term for each cell is much smaller than all of the other contributions and thus can be neglected (Eltahir and Bras, 1994 [76]). By introducing this approximation, equations (2.10a) and (2.10b) can be expressed as:

$$IN_m^*(x,y) + ET(x,y) \approx OUT_m^*(x,y) + P_m(x,y) \tag{2.11a}$$

$$IN_a^*(x,y) \approx OUT_a^*(x,y) + P_a(x,y) \tag{2.11b}$$

The well-mixed atmosphere assumption, (see section 1.4 for a discussion of its validity) must hold now for every atmospheric column over the corresponding grid cell. This can be expressed as:

$$\rho(x,y) \equiv \frac{P_m(x,y)}{P(x,y)} = \frac{IN_m^*(x,y)}{IN^*(x,y)} = \frac{OUT_m^*(x,y)}{OUT^*(x,y)} \tag{2.12}$$

The combination of equations (2.11a) and (2.12) leads to:

$$IN_m^*(x,y) + ET(x,y) = \rho(x,y)\,(OUT^*(x,y) + P(x,y)) \tag{2.13}$$

and similarly, from (2.11b) and (2.12):

$$IN_a^*(x,y) = (1-\rho(x,y))\,(OUT^*(x,y) + P(x,y)) \tag{2.14}$$

By dividing (2.13) over (2.14) and rearranging, we finally obtain an expression for the local recycling ratio (Eltahir and Bras, 1994 [76]):

$$\rho(x,y) = \frac{IN_m^*(x,y) + ET(x,y)}{IN_m^*(x,y) + IN_a^*(x,y) + ET(x,y)} \tag{2.15}$$

An initial guess for $\rho(x,y) = \rho_0(x,y)$ is required to split $IN^*(x,y)$ into $IN_m^*(x,y)$ plus $IN_a^*(x,y)$. Then, an iterative procedure is used to find $\rho(x,y)$ satisfying both equation (2.15) and the well-mixed atmosphere assumption, expressed in equation (2.12). This numerical computation is found to converge quickly (Eltahir and Bras, 1994 [76]). In appendix C, the interested reader can find a detailed explanation of the computation method. Note that equation (2.15) yields the local recycling ratio at any cell in the region as the fraction of precipitation coming from ET from anywhere within the same region, and not just in the small subdivision considered. For the calculations, we used as subdivisions the cells of the model themselves, so that the horizontal resolution is 9k for the WRFS-1 simulation, analyzed in chapter 3, and 5 km for the WRFS-2 runs, used in chapter 4.

Burde and Zangvil (2001a) [37] and Fitzmaurice (2007) [95] sum up the three major issues of this method: 1) Moisture fluxes are time-averaged quantities; 2) Changes in atmospheric storage are neglected; and 3) The well-mixed atmosphere assumption is invoked. Limitations 1 and 3 also hold for the IMB, whereas assumption 2 is not required in that method. A detailed discussion on the impact of the above-mentioned assumptions on recycling calculations is provided in Fitzmaurice (2007)

[95]. In particular, the role of the storage term on precipitation recycling computations is assessed by Domínguez et al. (2006) [67]. In this study, this impact is shown to be small at the monthly or larger time scales, even though it might not be negligible at daily or lower time scales.

From the local recycling ratio, the corresponding regional value is given by

$$r = \frac{\iint_A \rho(x,y)P(x,y)dxdy}{\iint_A P(x,y)dxdy} \tag{2.16}$$

where A stands for the area size of the study region.

2.4 The method of moisture tracers to compute the recycling ratio

During the last decades, many studies have explored the sources and sinks of moisture contributing to precipitation over land (Trenberth et al., 2003 [248]). As it has been discussed, the fundamental goal of any regional recycling calculation is separating the precipitation due to advected moisture from that precipitation related to evapotranspiration within the study region. As a result, the ideal method to carry out an accurate computation of the recycling ratio would consist on "labeling" one of these two moisture species and count its relative contribution to the regional precipitation. Of course, the drawback of this strategy is that we are not able to tag the water molecules in Nature. Nevertheless, tracers labeling the water molecules can be implemented on numerical meteorological models, which are nowadays the best tool that we have for describing the climatic system and for predicting its evolution. As stated in section 1.4, passive tracers have been implemented on GCMs in recent studies. However, GCMs are not able to reproduce the climate system at high resolution, which becomes critical to explore the specific features of the hydrological cycle at the regional scale. This suggests that the implementation of this capability on regional models (RCMs) is of the greatest scientific interest. In this thesis, we perform experimental simulations including moisture tracers in a widely used regional model: the Weather Research and Forecasting (WRF) model. The technical details about this innovative simulations have been stated in section 2.1.

As mentioned, the implementation of moisture tracers in a regional meteorological model allows tracking the pathways followed by the water molecules, from their sources as ET to their sinks as precipitation. This means that, if our numerical model was able to accurately describe the climate system, then the recycling ratio computed through the tracers technique would correspond exactly to reality. As a result, the capability of moisture tracers on the WRF model constitutes, nowadays, the more precise procedure to estimate the recycling ratio. Of course, numerical climate mod-

els still have relevant limitations (namely in some concrete but crucial issues as it is the case of the representation of cloud microphysics), and thus the reliability of the information provided by the moisture tracers is directly linked to the evolution and improvement of the climate models.

From this argumentation, it naturally follows that the recycling ratio computed through moisture tracers represents the *truth* in the framework of regional numerical models (which does not mean that it corresponds to the *actual truth*, as discussed). As a result, the comparison of these results to those provided by the classical recycling models becomes a manner to assess the validity of the latter and the impact of their assumptions on an accurate representation of the recycling mechanisms.

In the WRFS-3 set of simulations, all the water molecules evapotranspired within our study region (corresponding to the area bounded in black in Fig. 2.1b and to the area bounded in blue in Fig. 2.2b) are *tagged* and *followed* until the moment they precipitate or are transported out of the model's domain. Hence, at every grid cell precipitation of internal origin, $P_m(i,j)$, is explicitly distinguished from precipitation derived from moisture advected into the region, $P_a(i,j)$. Therefore, the method of moisture tracers (hereafter, MMTR) allows computing the local and regional recycling ratios by directly applying equations (1.5) and (1.7). That is,

$$\rho(i,j,\Delta t|A,\xi) = \frac{P_m(i,j,\Delta t|A,\xi)}{P(i,j,\Delta t|A,\xi)} = \frac{P_{tr}(i,j,\Delta t|A,\xi)}{P(i,j,\Delta t|A,\xi)} \tag{2.17a}$$

$$r(\Delta t|A,\xi) = \frac{\sum_{i,j} P_{tr}(i,j,\Delta t|A,\xi)\Delta A(i,j)}{\sum_{i,j} P(i,j,\Delta t|A,\xi)\Delta A(i,j)} \tag{2.17b}$$

where subindex *tr* refers to rainfall molecules that have been tagged with moisture tracers.

2.5 *No-ET* experiments: the experimental relative change in precipitation

In addition to the recycling ratios calculated through IMB and EBRM from equations (2.6) and (2.15), which can be obtained from just a single model simulation, in chapter 4 we also compute a relative change in precipitation by comparison of control simulations, with all the land-atmosphere fluxes normally activated, to model experiments where ET is disabled over the land areas of the nested domain (*no-ET* experiments). The most relevant characteristics of these experiments are described in section 2.1. This new magnitude provides further information to characterize the regional (in this case, the Iberian) rainfall regime.

For each of the cells within our domain, which we assume to be centered at a point (x, y), we define:

$$\Delta P(x,y) = P_{\text{control}}(x,y) - P_{\text{no-ET}}(x,y) \tag{2.18}$$

In this equation, P_{control} stands for the total precipitation in the control runs, whereas $P_{\text{no-ET}}$ represents the precipitation simulated in the *no-ET* experiments. The definition of a local, experimental relative change in precipitation attributable to evapotranspired water follows naturally from this analysis and is defined as:

$$\rho^*(x,y) = \frac{\Delta P(x,y)}{P_{\text{control}}(x,y)} \tag{2.19}$$

This parameter, $\rho^*(x,y)$ is computed for each grid point from both control and experimental model outputs. The corresponding regional magnitude, referred to as the regional relative change in precipitation, is given by:

$$r^* = \frac{\iint_A \Delta P(x,y)dxdy}{\iint_A P_{\text{control}}(x,y)dxdy} \tag{2.20}$$

The calculations presented in chapter 4 are performed over the whole IP and also over the smaller boxes defined within (Fig. 2.2b). In all the cases, we used the same experiment setting with ET suppressed over the whole land area of the IP, and not just over each examined box. Thus, it is possible that the divergence in precipitation values between the control and the experiment in a particular box arise not from the difference in ET within that same box but from differences elsewhere within Iberia. These experimental rate can be directly compared to the recycling ratio calculated through the EBRM, since this method also provides values for each grid cell, representing the fraction of precipitation with origin in ET from anywhere within the land area of all of the Iberian Peninsula.

2.6 Separation of the recycling and amplification contributions: the Schär et al.'s (1999) method

As indicated in section 1.5, the ET fluxes, apart from moistening the lower layers of the atmosphere, contribute to increase its instability, thus favoring the ascend and subsequent condensation and precipitation of atmospheric moisture. The latter indirect effect of the ET fluxes on precipitation is commonly referred to as *amplification*, as discussed in section 1.5. As a result of their critical contribution, amplification

mechanisms must be taken into account to describe the regional hydrology cycle (Schär et al., 1999 [221]).

In chapter 4, we assess the increase of precipitation occurring in monthly WRF simulations with respect to the corresponding experiments where evapotranspiration is suppressed. In addition, the relative contribution of direct and indirect processes to the observed increase of precipitation is estimated. For this purpose, two methods are used. One of them is original (see section 2.7 for a complete description), whereas the second is due to Schär et al. (1999) [221]. The latter procedure, that we name Schär et al.'s (1999) Separation Method and refer to as SSM, is based on the concept of precipitation efficiency (χ), which essentially represents the ratio of the accumulated precipitation over the sum of moisture entering a study region (Trenberth, 1998 [246]; Schär et al. (1999) [221]; Sui et al., 2007 [239]) over a certain period of time. The precipitation efficiency is a measure of the capability of the atmospheric system to transform the moisture available in the region into precipitation. In our case, it can be easily computed for both the control simulation and the *no-ET* experiments as:

$$\chi_{\text{control}} = \frac{P_{\text{control}}}{IN_{\text{control}} + ET_{\text{control}}} \tag{2.21a}$$

$$\chi_{\text{no-ET}} = \frac{P_{\text{no-ET}}}{IN_{\text{no-ET}} + ET_{\text{no-ET}}} = \frac{P_{\text{no-ET}}}{IN_{\text{no-ET}}} \tag{2.21b}$$

where subscripts *control* and *no-ET* refer to control runs and experiments, respectively, P stands for precipitation, ET for evapotranspiration and IN represents the inward moisture flux through the lateral boundaries of the region. By construction of the experiments, $ET_{\text{no-ET}} = 0$. Note that all the variables in this method represent area-averaged quantities. Moreover, note that according to equation (2.6), $r_{\text{IMB}} = ET/(IN + ET)$, and thus the IMB regional recycling ratio and the precipitation efficiency are linked by the following equation (Schär et al. (1999) [221]):

$$\frac{\chi}{r_{\text{IMB}}} = \frac{P}{ET} \tag{2.22}$$

Let us now define the following differences between *control* and *no-ET* simulations:

$$\Delta P = P_{\text{control}} - P_{\text{no-ET}} \tag{2.23a}$$

$$\Delta\chi = \chi_{\text{control}} - \chi_{\text{no-ET}} \tag{2.23b}$$

$$\Delta IN = IN_{\text{control}} - IN_{\text{no-ET}} \tag{2.23c}$$

$$\Delta ET = ET_{\text{control}} - ET_{\text{no-ET}} = ET_{\text{control}} \tag{2.23d}$$

Substitution of (2.21a) and (2.21b) into (2.23a) leads to:

$$\Delta P = \chi_{\text{control}}(IN_{\text{control}} + ET_{\text{control}}) - \chi_{\text{no-ET}} IN_{\text{no-ET}} \tag{2.24}$$

By adding and substracting $\chi_{\text{control}} \cdot IN_{\text{no-ET}}$ and rearranging according to (2.23b), (2.23c) and (2.23d), we obtain the following expression:

$$\Delta P = \underbrace{\chi_{\text{control}}(\Delta IN + \Delta ET)}_{(1)} + \underbrace{\Delta\chi IN_{\text{no-ET}}}_{(2)} \tag{2.25}$$

As stated by Schär et al. (1999) [221], the first term of equation (2.25) depends only on changes in the fluxes entering the considered atmospheric box, and not in variations in the precipitation efficiency. As a result, this term quantifies to what extent changes in the moisture fluxes modify precipitation, but assuming that these variations do not alter the efficiency of the system in transforming moisture into rainfall. Therefore, the first term of ΔP, represents the direct contribution to the increased precipitation. On the contrary, the second term of (2.25) measures the complementary effect that a variation in the moisture fluxes exerts on the precipitation efficiency of the system; whereby it represents the indirect contribution to ΔP. Schär et al. (1999) [221] identify the direct contribution with the *recycling* term, and the indirect contribution with the *amplification* term:

$$\Delta P_{\text{rec}} \equiv \Delta P_{\text{dir}} = \chi_{\text{control}}(\Delta IN + \Delta ET) \tag{2.26a}$$

$$\Delta P_{\text{amp}} \equiv \Delta P_{\text{ind}} = \Delta\chi IN_{\text{no-ET}} \tag{2.26b}$$

where subscripts *dir*, *ind*, *rec* and *amp* stand for *direct*, *indirect*, *recycling* and *amplification*. As a result, equation(2.25) can be written as:

$$\Delta P = \Delta P_{\text{rec}} + \Delta P_{\text{amp}} \tag{2.27}$$

This equation constitutes the mathematical expression of the qualitative argumentation above, related to the double mechanism (direct and indirect) whereby ET

fluxes can intensify precipitation. Note that equation (2.25) is only meaningful if the following double condition is verified:

$$\Delta IN + \Delta ET \geq 0 \tag{2.28a}$$

$$\Delta\chi \geq 0 \tag{2.28b}$$

since both ΔP_{rec} and ΔP_{amp} have to be greater (or at least equal) than zero.

Discussion of the method

The above-described method constitutes a useful analytic tool to easily separate both direct and indirect contributions to the increased precipitation, ΔP (the surplus of rainfall observed in the control simulations with respect to the *no-ET* runs). Nevertheless, this procedure presents an important limitation, which is directly related to the identification of the direct contribution with a recycling term. This identification (expressed in equation 2.26a) remains unclear, and this is somehow admitted by the authors themselves, when they affirm that the first summand in (2.25) *essentially* corresponds to the recycling contribution (Schär et al., 1999 [221]). Let us analyze this assumption.

We say that an alteration in ET has an *indirect* (*direct)* effect on rainfall if it does (does not) modify the precipitation efficiency of the system; that is, if it does (does not) alter the thermodynamical structure of the atmospheric column. According to this, let us rewrite equation (2.25) as:

$$\Delta P = \underbrace{\chi_{\text{control}}\Delta IN}_{(1)} + \underbrace{\chi_{\text{control}}\Delta ET}_{(2)} + \underbrace{\Delta\chi IN_{\text{no-ET}}}_{(3)} \tag{2.29}$$

According to Schär et al. (1999) [221], the two first summands of (2.29) correspond to the direct contribution, while the third summand represents the indirect contribution to ΔP. This is exactly true and we completely agree with that interpretation. Nevertheless, we note the first term in (2.29) is clearly not related to recycling processes at all, as it depends on ΔIN. Actually, it quantifies a direct impact (χ remains constant) on precipitation due to the variation of moisture input values. Hence, this term must not be associated with a recycling contribution; on the contrary, we rather suggest its identification with a change in precipitation related to *direct advection*:

$$\Delta P_{\text{da}} \equiv \chi_{\text{control}}\Delta IN \tag{2.30}$$

where subscript *da* stands for *direct advection*. As far as the second term in (2.29) is concerned, we do agree with the analysis by Schär et al. (1999) [221], since this term quantifies the direct effect of a variation in the ET fluxes on precipitation, thus corresponding clearly to a recycling contribution:

$$\Delta P_{\text{rec}} \equiv \chi_{\text{control}} \Delta ET \tag{2.31}$$

Finally, the third term in equation (2.29), depending on $\Delta\chi$, corresponds to the amplification contribution, as stated by Schär et al. (1999) [221]. This means that equation (2.26b) is correct:

$$\Delta P_{\text{amp}} \equiv \Delta\chi IN_{\text{no-ET}} \tag{2.32}$$

As a result, equation (2.27) should be more accurately written as:

$$\Delta P = \Delta P_{\text{rec}} + \Delta P_{\text{amp}} + \Delta P_{\text{da}} \tag{2.33}$$

From the analysis of the SSM method, we conclude that a third term, apart from the recycling and amplification contributions, must be taken into account in order to accurately represent the increased precipitation in the control runs. Only if we assume that the direct advection term is much lower than the recycling and amplification contributions to ΔP, equation (2.27) can be rewritten as:

$$\Delta P \approx \Delta P_{\text{rec}} + \Delta P_{\text{amp}} \tag{2.34}$$

2.7 A new method to separate recycling and amplification terms

In this thesis, we propose a different approach to estimate both recycling and amplification contributions to the upturn of rainfall totals observed in the interior areas of Iberia in spring. Results obtained through this new procedure can be compared to those given by the Schär et al.'s (1999) Separation Method (SSM), described in the previous section.

As discussed in section 1.2 and as expressed in equation (1.2), precipitation falling in a region results from moisture with three different origins. However, over sufficiently long periods, the contribution from moisture already present in the atmosphere at the beginning of the calculation period is negligible. This leads to the widely

used approximation expressed in equation (1.3). Further splitting the advection term in (1.3) into two components leads to

$$P_a = \tilde{P}_{\mathrm{da}} + \tilde{P}_{\mathrm{ia}} \tag{2.35}$$

where $\tilde{P}_{\mathrm{da}}$ stands for the fraction of precipitation coming directly from advection and, in contrast, $\tilde{P}_{ia}$ represents the fraction of the advected moisture that is indirectly retained and transformed into rainfall as a result of the effect of land-air interactions on the thermodynamic structure of the atmosphere.

In the experiments included in the WRFS-2 set of simulations, we disable the ET fluxes ($P_m = 0$) and subsequently their indirect capacity to modify the atmospheric profile favoring precipitation-generating processes (hence, $\tilde{P}_{ia} = 0$). This implies that, whereas in the control runs we measure all the contributions to the total precipitation:

$$P_{\mathrm{control}} = P_m + \tilde{P}_{da} + \tilde{P}_{ia} \tag{2.36}$$

in the *no-ET* experiments we only register the contribution from direct advection:

$$P_{\mathrm{no\text{-}ET}} = \tilde{P}'_{da} \tag{2.37}$$

In general, this term must be allowed to differ in the experiments with respect to that of the control runs. This makes sense, since the mere presence of the ET flux may have an impact on the advective component. The difference in precipitation between control and experiments can thus be expressed as:

$$\Delta P = P_{\mathrm{control}} - P_{\mathrm{no\text{-}ET}} = P_m + P_{ia} + \left(\tilde{P}_{da} - \tilde{P}'_{da}\right) \tag{2.38}$$

Let us carry out the following identifications:

$$\Delta P_{\mathrm{rec}} \equiv P_m \tag{2.39a}$$

$$\Delta P_{\mathrm{amp}} \equiv P_{ia} \tag{2.39b}$$

$$\Delta P_{\mathrm{da}} \equiv \tilde{P}_{da} - \tilde{P}'_{da} \tag{2.39c}$$

By considering these equations (2.39a, 2.39b and 2.39c) we can rewrite the change in precipitation in terms of three components: recycling (subindex *rec*), amplification (subindex *amp*) and direct advection (subindex *da*):

$$\Delta P = \Delta P_{\text{rec}} + \Delta P_{\text{amp}} + \Delta P_{\text{da}} \tag{2.40}$$

This equation is identical to (2.33), showing that the correction proposed on the SSM turns it compatible with our separation method. According to our results, however, the direct advection contribution tends to be much smaller than the recycling and amplification terms, so that equation (2.40) can be approximated by equation (2.34).

If we consider the definitions of the local recycling ratio and the local relative change in precipitation, that can be expressed as:

$$\rho(x,y) = \frac{P_m(x,y)}{P(x,y)} = \frac{\Delta P_{rec}(x,y)}{P_{control}(x,y)} \tag{2.41}$$

and

$$\rho^*(x,y) = \frac{P_{control}(x,y) - P_{no-ET}(x,y)}{P_{control}(x,y)} = \frac{\Delta P(x,y)}{P_{control}(x,y)} \tag{2.42}$$

we find out that the rate $\frac{\rho(x,y)}{\rho^*(x,y)}$, which can be computed for each grid cell of our domain, equals the fraction of recycled precipitation in ΔP; that is:

$$\frac{\rho(x,y)}{\rho^*(x,y)} = \frac{\Delta P_{rec}(x,y)}{\Delta P(x,y)} = \frac{\Delta P_{rec}(x,y)}{\Delta P_{rec}(x,y) + \Delta P_{amp}(x,y)} \tag{2.43}$$

As a result,

$$\Delta P_{rec}(x,y) = \frac{\rho(x,y)}{\rho^*(x,y)} \cdot \Delta P(x,y) \tag{2.44}$$

Similarly, the fraction of the extra precipitation due to amplification processes will be given by:

$$\Delta P_{amp}(x,y) = \left[1 - \frac{\rho(x,y)}{\rho^*(x,y)}\right] \cdot \Delta P(x,y) \tag{2.45}$$

For the whole region, we similarly have

$$\frac{r}{r^*} = \frac{\iint_A P_m(x,y)dxdy}{\iint_A \left[P_{control}(x,y) - P_{no-ET}(x,y)\right]dxdy} = \frac{\langle P_m \rangle}{\langle P_{control} \rangle - \langle P_{no-ET} \rangle} = \frac{\langle \Delta P_{rec} \rangle}{\langle \Delta P \rangle} \tag{2.46}$$

And therefore,

$$\langle \Delta P_{rec} \rangle = \frac{r}{r^*} \cdot \langle \Delta P \rangle \tag{2.47}$$

and

$$\langle \Delta P_{amp} \rangle = \left(1 - \frac{r}{r^*}\right) \cdot \langle \Delta P \rangle \tag{2.48}$$

The computation of the local relative change in precipitation from the comparison of *control* and *no-ET* simulations, together with the calculation of the recycling ratio, allows estimating the relative contribution of recycling and amplification terms, thus satisfying our goal.

2.8 Data used in this thesis

Observational precipitation data used in Figs. 1.1, 1.2, 1.3 and 1.4 were obtained from a 0.2°-resolution daily precipitation analysis produced by the Universidad de Cantabria (UC), the Agencia Estatal de Meteorología (Spanish Meteorological Office, AEMET) and the Instituto Português do Mar e da Atmosfera (Portuguese Meteorological Institute, IPMA), originally available for the period 1950-2002 (Herrera et al., 2010 [123]; Belo-Pereira et al., 2011 [13]), and recently updated until March of 2008 (Spain02 dataset, http://www.meteo.unican.es/datasets/spain02; PT02 gridded precipitation dataset). This dataset is used, in section 4.1, to validate the precipitation obtained from the WRF model. For this purpose, grid point mean absolute errors (MAE) and mean normalized errors (MAPE) are computed, at the daily, 5-days and monthly scales, according to the standard definitions (e.g. Cardoso et al., 2012 [43]):

$$MAE(i,j) = \frac{1}{n}\sum_{k=1}^{n} |P_k(i,j) - O_k(i,j)| \tag{2.49a}$$

$$MAPE(i,j)(\%) = \frac{\sum_{k=1}^{n} |P_k(i,j) - O_k(i,j)|}{\sum_{k=1}^{n} O_k(i,j)} \cdot 100 = \frac{MAE}{\frac{1}{n}\sum_{k=1}^{n} O_k(i,j)} \cdot 100 \tag{2.49b}$$

where n corresponds to the number of days, periods of 5 days or months while the comparison is performed, $P_k(i,j)$ represents the model precipitation at the grid point (i,j) and $O_k(i,j)$ stands for the corresponding UC-AEMET/IPMA analysis value. Note that an interpolation of the analysis data from the original grid, at 0.2°resolution, to the same grid used in the WRF simulations is required for the grid point validation to be carried out.

In section 3.3, we make use of monthly NAO index data, downloadable from the following site:

http://www.cpc.ncep.noaa.gov/products/precip/CWlink/pna/nao.shtml

USC UNIVERSIDADE DE SANTIAGO DE COMPOSTELA

USC
UNIVERSIDADE
DE SANTIAGO
DE COMPOSTELA

3

Precipitation recycling in the Iberian Peninsula: spatial patterns and temporal variability

Abstract. In this chapter, we explore the spatio-temporal links between the recycling mechanism and the Iberian rainfall regime. We use a 9-km resolution WRF simulation of 18 years (1990-2007) to compute local and regional recycling ratios over Iberia, at the monthly scale, through both an analytical and a numerical recycling model. In contrast to coastal areas, it is known that the interior of Iberia experiences a relative maximum of precipitation in spring. This suggests a prominent role of land-atmosphere interactions on the inland precipitation regime during this period of the year. Local recycling ratios are found to be the highest in spring and early summer, coinciding with those areas where this non-winter peak of rainfall represents the absolute maximum in the annual cycle. This results confirm that recycling processes are crucial to explain the Iberian spring precipitation, particularly over the eastern and northeastern sectors. On average, Iberian monthly recycling values range from 0.04 (0.03) in December to 0.14 (0.07) in June (May), according to the numerical (analytical) model. Our analysis shows that the highest values of recycling are limited by the coexistence of two necessary mechanisms: 1) the availability of sufficient soil moisture resulting from previous months and 2) the occurrence of appropriate synoptic configurations favoring the development of convective regimes. The analyzed surplus of rainfall in spring has a critical impact on agriculture over large semiarid interior areas, and thus a comprehensive assessment of the physical mechanisms behind it is of the greatest relevance in the context of a changing climate. Finally, we evaluate the strong intra and interannual variability of recycling considering three case studies associated with extreme climatic events (1997, 2001 and 2005), confirming that early spring recycling values for these extreme events depend crucially on the observed

precipitation during winter but also on the regional circulation patterns during early spring itself. This chapter corresponds in large parts to the article *Precipitation recycling in the Iberian Peninsula: spatial patterns and temporal variability* (see the List of Publications for the complete reference).

*****

The spatial variability of the Iberian precipitation regime (described in section 1.1) and the different physical processes responsible for it suggest an examination of the relationship between the annual cycles of recycling ratio and precipitation over the Iberian Peninsula (IP) (Gimeno et al., 2010a [110]). As discussed in section 1.3, the working hypothesis for this thesis is that this connection can be critical to understand the spring peak of rainfall observed in inland Iberia. The study described in this chapter focuses on a detailed analysis of the spatial and temporal relations between precipitation and the local recycling ratio, as well as on the analysis of its interannual variability. The aim is, therefore, exploring to what extent land-atmosphere interactions may play a key role on the Iberian climate. The evaluation of the entire annual cycle of recycling during nearly a climatological period (18 annual cycles), including several extreme years, allows a comprehensive assessment of the main physical mechanisms driving recycling in the IP, as well as a deep investigation of the importance of these interactions on the present Iberian climate in a context of climate change.

Along this chapter, two methods are used to compute the recycling ratio every month along the period January 1990 - December 2007:

1. The Integral Moisture Budget analytical model due to Schär et al. (1999) [221] (IMB), thoroughly described in section 2.2 and appendix B.
2. The numerical recycling model due to Eltahir and Bras (1994) [76] (EBRM), examined in detail in section 2.3 and appendix C.

Both recycling methods are applied over the region shown in Fig. 2.1b, from WRF precipitation, evapotranspiration and moisture input values. A complementary description of the procedure to compute this water budget terms is given in appendix A.

The model configuration and setup of simulations is described in section 2.1. As mentioned, an explanation of the methods used to compute the recycling ratio (IMB and EBRM) and the connections between them is provided in sections 2.2 and 2.3. Results of this study are discussed in sections 3.1 and 3.2 of the present chapter. In addition, section 3.3 explores three case studies selected to complement the general discussion. Finally, a summary of the main conclusions of this work are presented in section 3.4.

3.1 Iberian regional recycling ratio

The monthly averaged values of the regional recycling ratio, following both IMB and EBRM methods, are shown in Fig. 3.1, providing a representation of the mean annual cycle (and interannual variability) of recycling over the considered period (1990-2007). In the winter half of the year, which spans from October to February and when the zonal circulation is more intense over Iberia, recycling values are coherently low, suggesting a very limited impact of land-atmosphere interactions on the rainfall regime, as expected. During this period, IMB and EBRM present the lowest values and similar magnitudes. The minima values of recycling ($r_{\mathrm{EBRM}} = 3.9\%$ and $r_{\mathrm{IMB}} = 2.9\%$) are reached in December for both methods. In contrast, recycling ratios are significantly higher in spring and summer, although results provided by both methods show significant differences. According to the EBRM, the yearly maximum of recycling occurs in June ($r_{\mathrm{EBRM}} = 13.9\%$), whereas according to the IMB the peak takes place in May, reaching a value that does not exceed half of that of EBRM ($r_{\mathrm{IMB}} = 6.5\%$). It is important to emphasize the larger interannual variability of the results provided by EBRM. Even though the regional EBRM recycling ratio is computed as an area average via equation (2.16), the latter method takes into account the heterogeneity of the orography and the moisture fluxes, thus capturing the natural variability of the physical processes. On the contrary, this is not reflected in IMB, probably as a consequence of its simplicity; however from a qualitatively perspective, the IMB is also capable to describe the mean annual profile of recycling. (For a detailed discussion on the limitations of both IMB and EBRM, see section 1.4 and appendices B and C). These results are in agreement with the discussion about the spatiotemporal patterns of circulation over Iberia and the physical mechanisms involved (section 1.1), with recycling reaching the highest values during spring and summer, when local convective processes play a more relevant role in the Iberian precipitation regime (Llasat and Puigcerver, 1997 [164]; Serrano et al., 1999 [226]; García-Herrera et al., 2005 [105]; Bisselink and Dolman, 2008 [21]; Gimeno et al., 2010a [110]).

The complete monthly series, for the period 1990-2007, is displayed in Fig. 3.2. Once again the remarkable differences in amplitude obtained by the two methods are apparent. As discussed above, EBRM values tend to converge to those computed via IMB in autumn and winter. On the contrary, in spring and early summer, even though EBRM ratios are significantly higher than those of IMB, the latter method still captures the qualitative evolution of the monthly series. As a result, a significant level of monthly correlation between IMB and EBRM recycling ratios is observed, varying seasonally from 0.65 to 0.70 (Table 3.1). The corresponding dispersion plot and regression lines are shown in Fig. 3.3, with data classified according to seasons: Winter (DJF), Spring (MAM), Summer (JJA) and Autumn (SON). We observe the lowest values of recycling and the highest degree of correlation between both methods taking place in autumn, with a linear correlation coefficient of $R_{SON} = 0.70$ (Table 3.1). In winter, this configuration of low recycling values and high correlation coef-

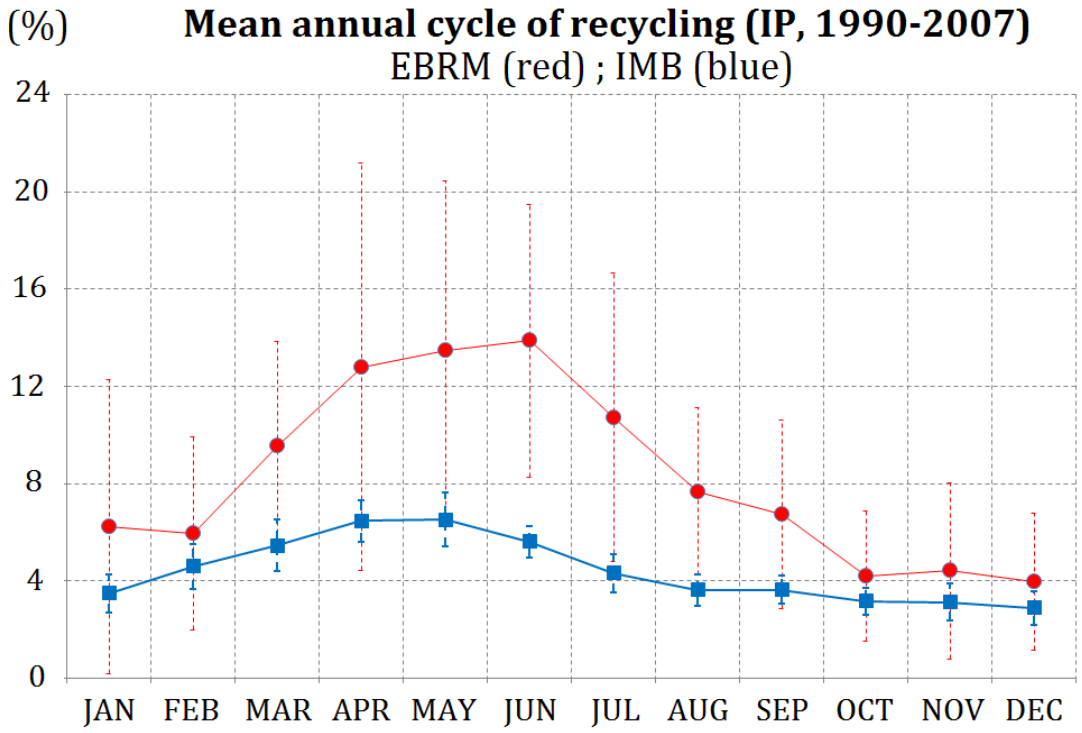

Figure 3.1: Mean annual cycle and interannual variability of the regional recycling ratio (%), according to EBRM (red) and IMB (blue).

ficients between IMB and EBRM is affected by the higher intraseasonal variability, mostly as a consequence of some anomalously high values of recycling in January, which will be discussed below. This month-to-month variability, reflected in the uncertainty bars of Fig. 3.1, is maintained in spring and reduced in late summer, when the correlation coefficient shows a similar value to that of autumn. Despite the relatively good temporal correlation between both methods, we must note again the much higher values obtained with the EBRM method and the reduced interannual variability shown by the IMB method. This suggests that the EBRM provides a more accurate representation of the recycling mechanism and thus it is preferably considered for the remaining of the analysis presented in this chapter. As expected, recycling values obtained for July 1990 and July 1993 through IMB (0.05 in both cases) are very close to those obtained with the same method by Schär et al. (1999) [221] (0.06 for both months, as referred in section 1.4). In general, however, EBRM recycling values appear to be in better agreement with those obtained previously in more refined studies, as e.g. Bisselink and Dolman (2008) [21] and Dirmeyer et al. (2009b) [65].

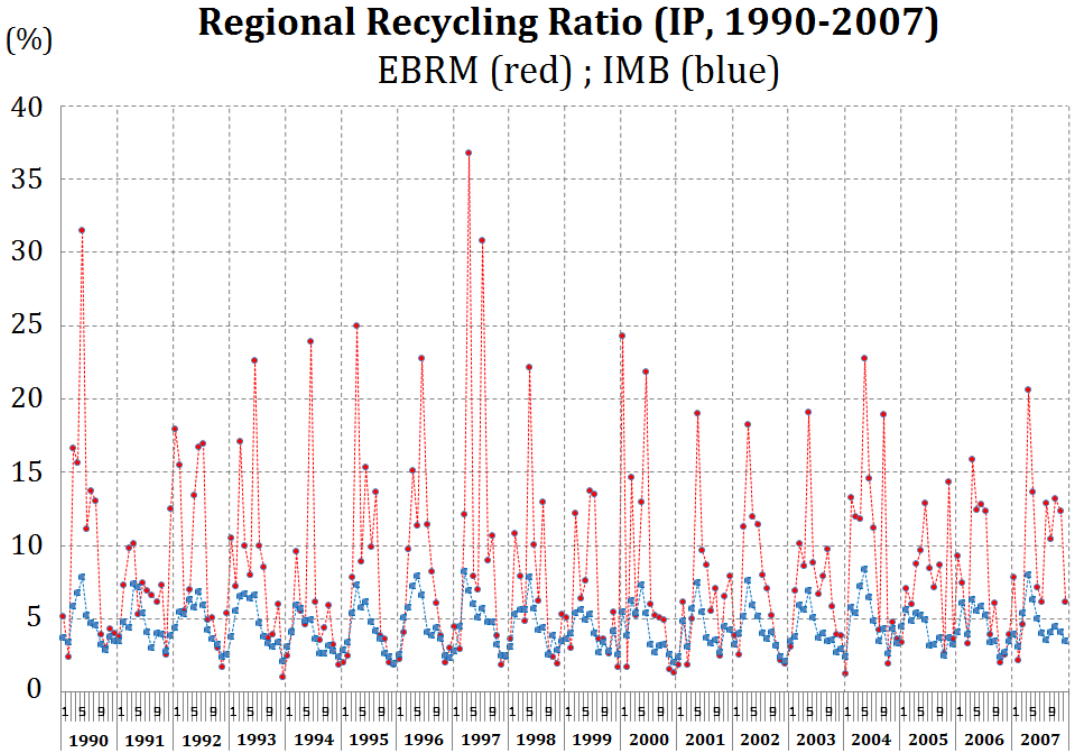

Figure 3.2: Monthly series of regional recycling ratio (%) for the period 1990-2007, computed via EBRM (red) and IMB (blue).

Season	Winter (DJF)	Spring (MAM)	Summer (JJA)	Autumn (SON)
R [-]	0.65	0.65	0.69	0.70

Table 3.1: Seasonal correlation coefficients [-] (EBRM vs IMB).

Regarding the EBRM time series (Fig. 3.2), we observe that the absolute maximum of recycling occurs predominantly during spring and early summer months. More in detail, that maximum takes place in April (1991, 1995, 1997, 2002, 2006 and 2007), May (1990, 1998, 2001, 2003, 2004), or June (1993, 1994, 1996, 1999 and 2005), reflecting the above-mentioned large interannual but also intraseasonal variability. For the remaining years, the annual maximum of recycling occurs in November (2005), December (1991) and January (1992, 2000). Interestingly, these years coincide or are temporally adjacent to the driest years (1991, 1999 and 2005) over the IP within the studied period (García-Herrera et al., 2007 [106]). Among the complete EBRM time series, only for the latter three years regional recycling ratios remain below 15% during the whole annual cycle. This link between the driest conditions over the IP with the lowest recycling ratios and anomalous recycling annual cycles is expected for two reasons. Firstly, the lack of soil moisture inhibits the triggering of the land-

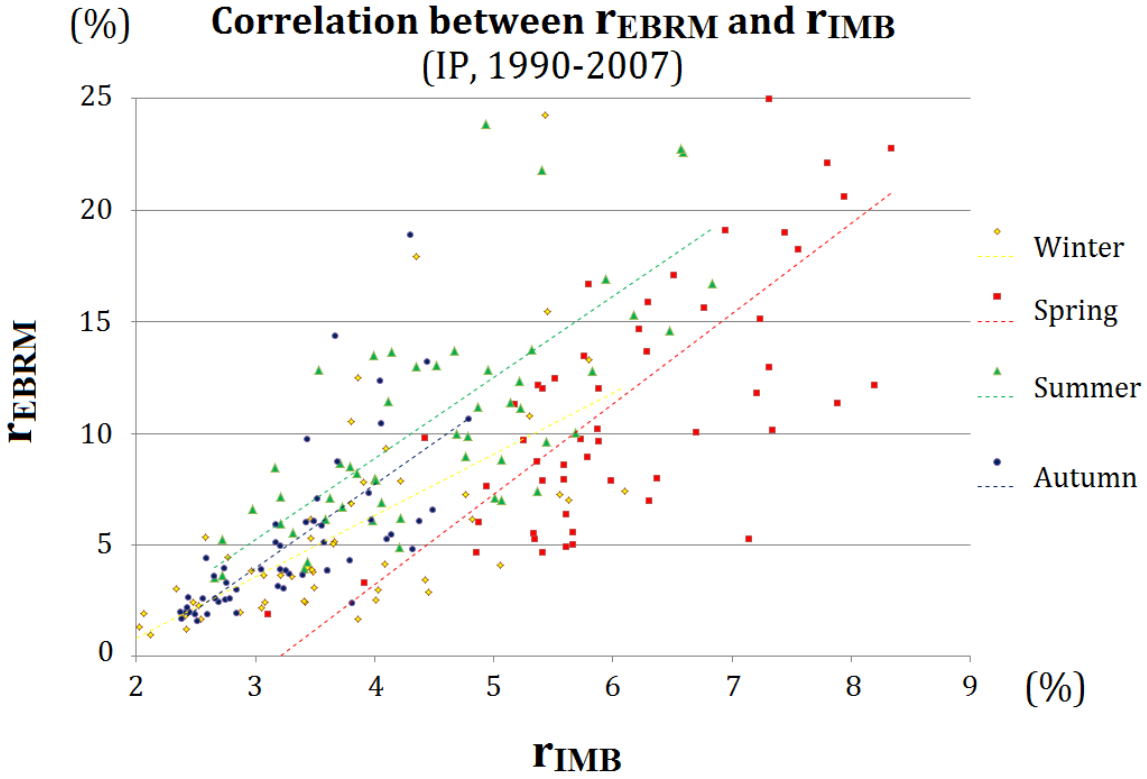

Figure 3.3: Monthly correlation between EBRM and IMB regional recycling ratios (%) for the period 1990-2007. Results are classified according to the corresponding season: Winter (DJF), Spring (MAM), Summer (JJA) and Autumn (SON).

atmosphere interactions (there is limited fuel available for recycling). Secondly, these atypical precipitation and soil moisture patterns are related to exceptional synoptic configurations, which might facilitate the activation of land-air feedbacks in unusual periods. This is the case of the peak of recycling of January 1992, when a high pressure located in the surroundings of the British Islands and Western Europe blocked the zonal circulation during most of the month. This peak took place after a normal previous autumn in terms of precipitation, thus ensuring a certain availability of soil moisture to support ET.

Finally, a secondary peak of recycling can be also observed, in the EBRM series, in September-October for several years (1991, 1994, 1997, 2001, 2003, 2004, 2005, 2006 and 2007). This is not so evident in the mean annual cycle of IMB (Fig. 3.1) and might be related to the enhancement of convective regimes in the specific area of the Mediterranean coast in late summer and early autumn.

3.2 Iberian local recycling ratio

Monthly mean recycling patterns for the Iberian Peninsula (obtained with EBRM), over the period 1990-2007, are represented in Fig. 3.4a, along with the average vertically integrated moisture flux. Fig. 3.4b shows the maps of the corresponding monthly standard deviation of recycling. Because the monthly evolution of the recycling patterns depends to a large extent on the availability of water in the soil, which is in turn conditioned by the rainfall amounts during the previous months (as discussed in section 1.3), we present in Fig. 3.4c the corresponding monthly average rainfall patterns, also computed from WRF model output over the same period. It should be stressed that the overall capacity of the WRF model to reproduce the temporal and spatial characteristics of the Iberian precipitation regime has been attained in the previous works by Cardoso et al., 2012 [43] and Soares et al., 2012 [231], where the simulations used for this study are described in detail. This guarantees the suitability of using WRF precipitation fields for other diagnostic calculations.

From October to February, low recycling values overlap with the highest amounts of precipitation, mainly in the northwest quadrant of the IP. During this period of the year, recycling patterns over Iberia are closely connected to the dominant zonal flow, with recycling tending to increase from western to eastern Iberia. This is expected, since the atmosphere over the eastern area has a higher load of moisture originating from terrestrial ET in the western and central sectors. This process is also responsible for the persistence of a local recycling minimum in the southwest area of the IP throughout the year (Fig. 3.4a). From March onwards, and linked to the weakening of the winter circulation, recycling patterns show a greater heterogeneity and, what is more important within the context of this work, a greater connection with precipitation patterns. The maximum strength in this connection takes place in April and May (Figs. 3.4a and 3.4c), even though small patches with similar high values of recycling are found in March and June. In particular, a recycling maximum shift is observed from the southeast, in April, to the northeast region, in May. This is likely related to the change in the prevailing direction of the moisture flux, from west-northwest to west-southwest (Fig. 3.4a), and presents a clear connection with the analogous shift in the monthly maximum of rainfall described in section 1.1 (Fig. 1.3b). In general, a large variability can be found locally throughout the annual cycle of recycling (Fig. 3.4b). This can be observed, e.g., in the high standard deviation values found over the northwest quadrant in January, March, September and December, but especially in April when a large extent of Iberia is affected by a remarkable variability (Fig. 3.4b), mostly related to the high recycling values observed in 1995, 1997 and 2007. As it is well known, in April there is a secondary maximum in the monthly precipitation in the western Iberia (e.g. Soares et al., 2012 [231]). This feature is related to the low amounts of rainfall persistently recorded in March in the recent decades, associated to a more northern mean trajectory of the Atlantic fronts in March (Paredes et al., 2006 [198]; Soares et al., 2012 [231]). Similarly, the large

variability observed for January (when the average recycling value is relatively low) is influenced by some extreme events such as those mentioned in the previous section relative to the years of 1992 and 2000. In March, May and June, in contrast, the areas where the recycling ratio is the highest (Fig. 3.4a) are affected by a relatively reduced variability (Fig. 3.4b), thus revealing the stability of the spring recycling patterns in eastern and northeastern Iberia.

Overall, most of the IP experiences recycling ratios above 10% from March to June, which confirms that, not only in the east and northeast but also throughout the interior of Iberia, an important fraction of the total amount of rainfall is related to land-atmosphere feedbacks. As mentioned in section 1.1, large interior extensions present arid or semiarid characteristics and attain the maximum of precipitation in spring, turning the recycling contribution essential to describe the precipitation regime locally. On the contrary, the lack of a clear link between recycling and precipitation from October to February confirms that land-atmosphere mechanisms do not play a relevant role on rainfall in the winter half of the year.

USC UNIVERSIDADE DE SANTIAGO DE COMPOSTELA

3.3 Selected case studies

As discussed previously, high values of the recycling ratio only occur when the synoptic, westerly circulation weakens allowing local processes to gain relevance, thus playing an important role on inland Iberia rainfall. The absence of strong zonal winds constitutes therefore a required condition for high values of recycling to happen over the IP, although such pre-requisite is often not sufficient. The availability of moisture in the soil is also a critical issue, as it represents the *fuel* for the recycling mechanisms. In this regard, the amount of precipitation that falls during the previous season becomes a significant variable to better understand the effects of land-air feedbacks. This was addressed in section 1.3 and more precisely in section 3.1, when an explanation including this limiting factor was proposed to account for the anomalously low recycling ratios obtained in 1991, 1999 and 2005. In this section here, our goal is to evaluate this hypothesis more systematically, exploring in what extent the recycling ratios are dependent on the recent (previous months) historical water balance in the area under study.

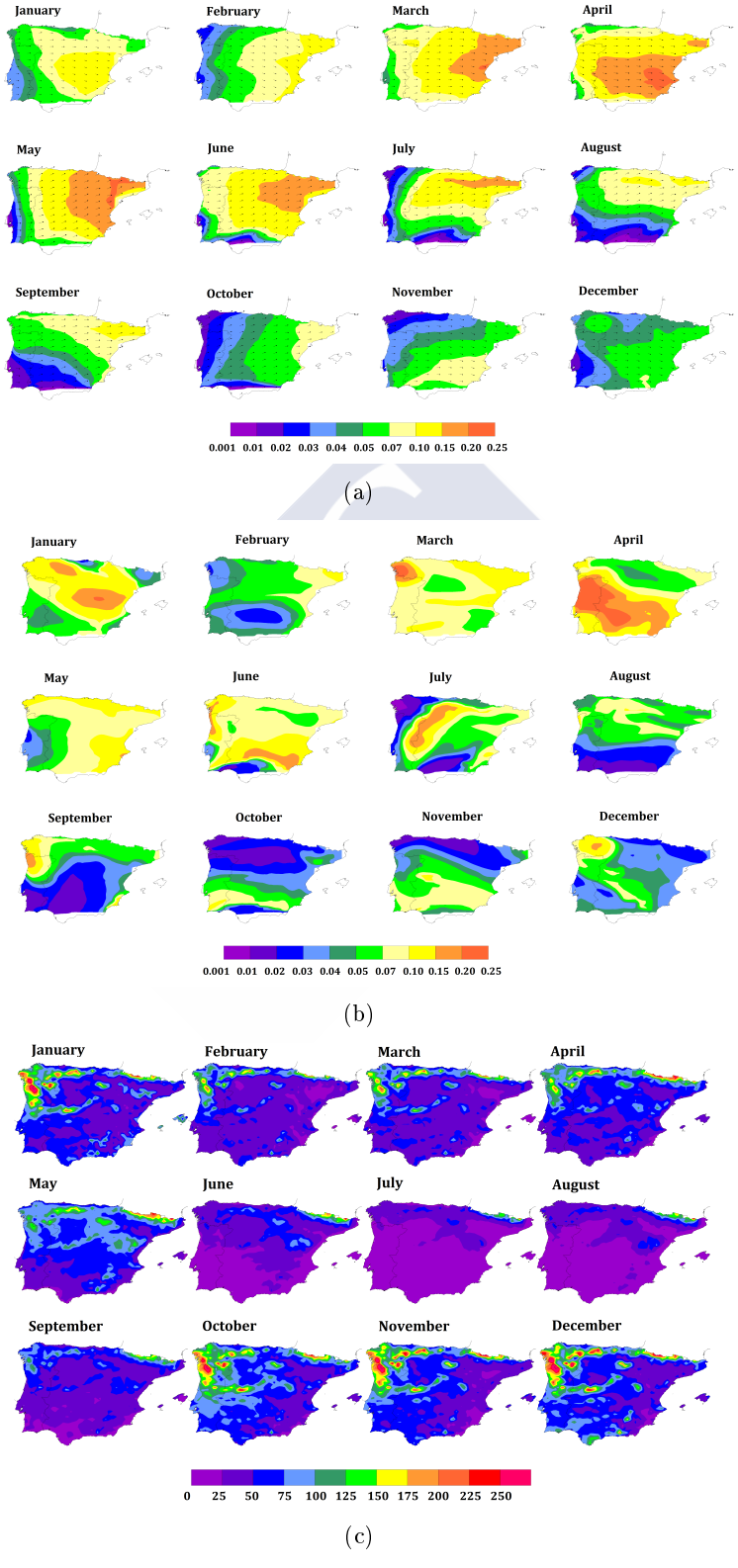

Figure 3.4: (*a*) Mean annual cycle of recycling ratio [-] and vertically integrated moisture flux; (*b*) Monthly standard deviation of recycling ratio [-] with respect to the average maps represented in (*a*); and (*c*) average precipitation (mm/month) over the period 1990-2007.

Early spring is the most appropriate period to focus this analysis, since it presents a higher variability with respect to the previous months. This feature, already corroborated by Paredes et al. (2006) [198], can be as well observed in Fig. 3.1). In this sense, March can be seen as a transition month, presenting a winter-like behavior for some years and clearly spring-like characteristics for others. Furthermore, the previous months (December, January and February; DJF) represent the standard definition of winter in climatological studies and correspond to the period of highest precipitation over large sectors of the IP, as described in section 1.1. The impact of a very humid or dry previous winter season can be assessed in a simplified way by looking at the recycling and precipitation patterns in March. Therefore, we focus on three representative case studies (1997, 2001 and 2005), where the recycling patterns in March are analyzed and connected to the spatial distributions of precipitation for that specific month but also relative to the previous season (DJF). All the results obtained for the three case studies are shown in Table 3.2, including the winter and March precipitation, the recycling values obtained with both methods and the value of the large scale pattern index that controls winter precipitation over the IP, the North Atlantic Oscillation (NAO). March of 2006 is also considered, to complete the possible combinations between dry and humid DJF and March in Table 3.2.

	Precipitation		NAO index	Recycling (March)			
Year	DJF	March	(March)	r_{EBRM} [-]	r_{IMB} [-]	$RD_{\mathrm{EBRM}}(\%)$	$RD_{\mathrm{IMB}}(\%)$
1997	*H*	*D*	1.46	12.33	8.19	+26.8	+50.0
2001	*H*	*H*	-1.26	1.87	3.11	-80.5	-43.0
2005	*D*	*D*	-1.83	6.02	4.87	-37.1	-10.8
2006	*D*	*H*	-1.28	3.28	3.92	-65.7	-28.2

Table 3.2: Precipitation (humid, H, or dry, D), NAO index, regional recycling ratio and relative deviation (RD) of recycling (see equation 3.1) for the period DJF-M during the years of 1997, 2001, 2005 and 2006.

March of 2005 can be qualitatively classified as a *dry* (*D*) month (Fig. 3.5). It occurred after an especially dry winter (Fig. 3.5, right column), when the IP suffered one of the most intense droughts ever recorded (García-Herrera et al., 2007 [106]; Gouveia et al., 2009 [121]). March of 1997 was even drier, but in contrast the previous winter may be qualitatively labeled as *humid* (*H*). November of 1996 (not shown), December of 1996 and January of 1997 (Fig. 3.5, left column) registered above-average amounts of rainfall, whereas this trend reversed in February, showing a dry character which was intensified in March. A very different situation took place in 2001, when the whole winter (with the exception of a *normal* February) and the following month of March were significantly humid (Fig. 3.5, mid column).

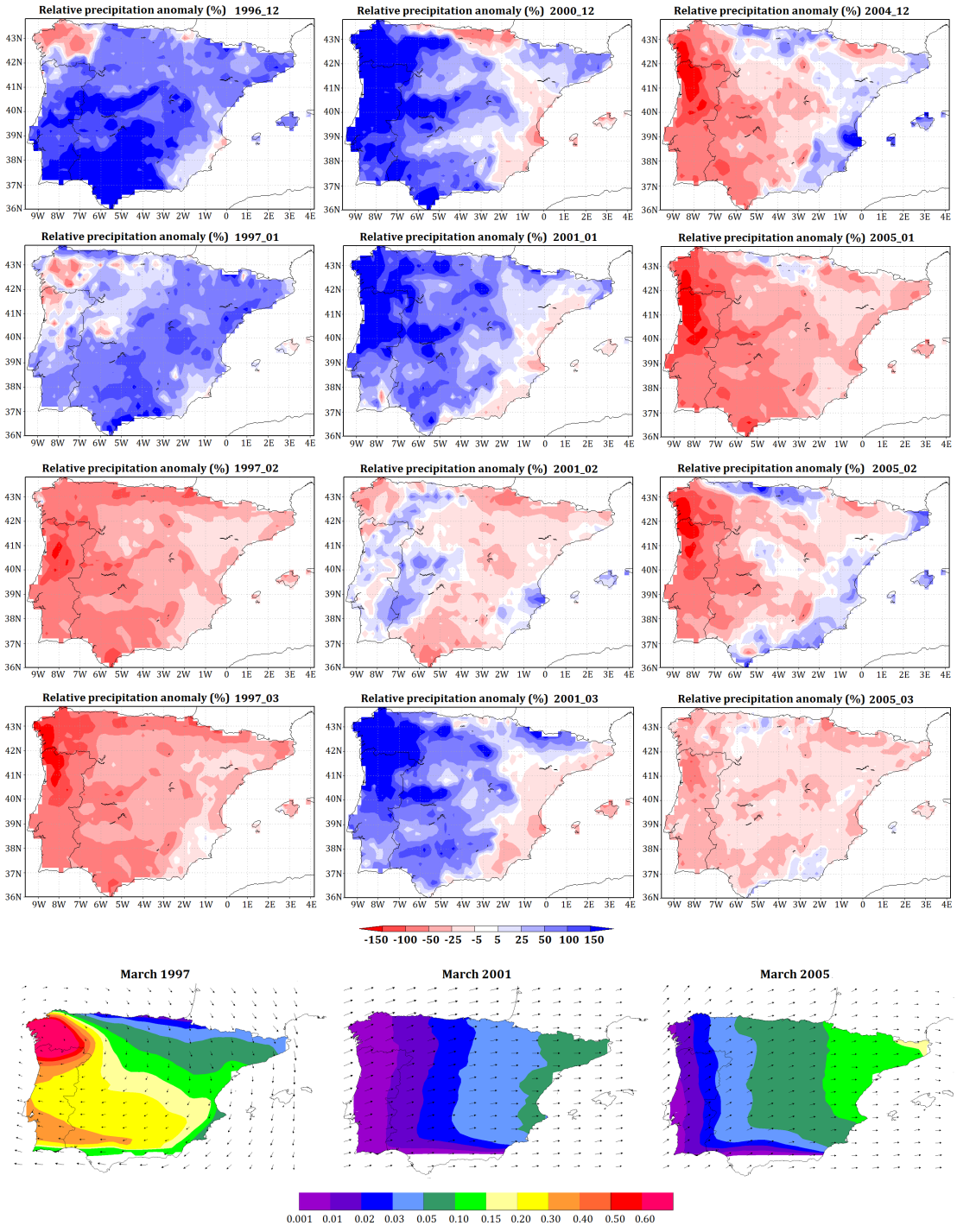

Figure 3.5: Relative precipitation anomalies (%) and EBRM recycling maps [-], together with the vertically integrated moisture flux, for the selected case studies (1997, 2001 and 2005).

The analysis of the 1990-2007 time series of recycling (Fig. 3.2) and the comparison with the 1950-2007 monthly anomalies of precipitation (computed through the AEMET/UC-IPMA dataset described in section 2.8) shows that humid months of March generally present low values of recycling. This is the case with 2001 and 2006, as shown in Table 3.2, where the relative deviations with respect to the mean regional recycling ratio in March along the 1990-2007 time series are computed according to:

$$RD = \frac{r - \langle r \rangle}{\langle r \rangle}(\%) \tag{3.1}$$

The NAO index is found to be consistently negative for these months, and this confirms that recycling is very limited under this large scale atmospheric circulation configuration that steers storms from the Atlantic towards the IP (Trigo et al., 2004 [252]). March of 2001 is preceded by a humid winter, whereas the three previous months to March of 2006 were in general dry (not shown). Despite this relevant differences, the observed recycling ratios were similar and significantly below average in both cases (-80.5% in 2001 and -65.7% in 2006 according to the EBRM), suggesting that the impact of a dry or wet previous winter on March recycling patterns is very limited when the wet winter-like circulation is predominant during this month (negative NAO). This is illustrated in Fig. 3.5 for March of 2001, when a clear west-to-east pattern with low values of recycling can be observed.

In contrast, dry months of March present a much higher variability in terms of recycling, with the amount of rainfall accumulated during the previous months playing a critical role on its recycling patterns. To illustrate this, we next compare the dry March of 2005 preceded by a very dry winter, with the dry March of 1997 preceded by a humid winter.

Generally, below-average rainfall totals in March are connected to positive values of the NAO index (Trigo et al., 2004 [252]), as it was the case in 1990 (1.46), 1993 (0.67), 1994 (1.26), 1995 (1.25), 1997 (1.46), 1998 (0.87) or 2000 (0.77). In this regard, the strong anomalous negative NAO index observed in March of 2005 (-1.83) corresponds to an outlier event since that month was dry over Iberia, and not wet as the consideration of the NAO index alone would suggest. This example emphasizes the need to look beyond the state of the NAO in order to explain the precipitation regime in Iberia (Trigo et al., 2008 [254]). In this case there was an unusual incapacity for the large number of mid-latitude systems passing over the Azores to reach the IP, which was related to the persistence of a stationary blocking anticyclonic structure, especially during the first fortnight of the month, leading to positive pressure anomalies in the surroundings of Iceland and very dry conditions over the IP (see García-Herrera et al., 2007 [106] for a detailed discussion).

In March of 1997, a high pressure center was located in the vicinity of the IP during most of the month, enhancing easterly and northeasterly wind flows (Fig. 3.5).

This synoptic configuration, cumulatively with the availability of moisture in the soil after the wet winter, is responsible for the high values of recycling observed in the IP (+26.8% and +50.0% above average, according to EBRM and IMB, respectively). This is most relevant in the western and northwestern areas, as shown in Fig. 3.5. In this sense, March of 1997 was an unusual and thus interesting example of anomalous moisture transport inside Iberia, in contrast with the predominant zonal circulation, represented in Fig. 3.1a. In March of 2005, the synoptic configuration was also suitable to trigger land-atmosphere interactions; however, the lack of moisture in the soil, as a result of one of the driest winters ever observed over Iberia, explains the below-average recycling values (−37.1% and −10.8% according to EBRM and IMB, respectively), as shown in Table 3.2.

This analysis confirms our preliminary hypothesis, i.e. that two conditions are necessary for recycling to play a relevant role on precipitation over the IP: first, the synoptic configuration must favor the development of local and mesoscale convective regimes; and second, there must be sufficient availability of moisture in the soil to trigger the recycling mechanism. The coupling of these conditions can be easily assessed in early spring, reaching the highest degree of intensity in the period that extends from April to June. We suggest that this scheme might be useful for understanding any other period of the year. In particular, the limited availability of soil moisture in inland Iberia during summer, precisely when convective processes are more intense, may explain the attenuation of recycling values in this period of the year with respect to the spring maximum.

3.4 Conclusions of this chapter

The work presented in this chapter investigates the spatial and temporal links between the recycling processes and the precipitation regime over Iberia. From a 9-km resolution WRF model simulation, carried out for a period of 18 years (from January 1990 to December 2007), local and regional recycling ratios are computed, at the monthly scale, with two different methods: 1) the numerical recycling model due to Eltahir and Bras (1994) [76], referred to as EBRM, and 2) the integral moisture budget (IMB) procedure developed by Schär et al. (1999) [221]. Both recycling models, EBRM and IMB, rely on hypotheses that allow calculating the recycling ratio in terms of moisture fluxes. This is the case of the well-mixed atmosphere assumption, whereby turbulence processes are supposed to effectively mix the water vapor of two different origins (advected and evapotranspired) along the atmospheric column. This hypothesis plays a major role in the classical analytical and numerical recycling models, and its limitations have been a matter of discussion in the recycling literature (see section 1.4 for a more detailed analysis of the limitations of this assumption).

Previous studies, described in section 1.1, highlight the noticeable seasonal and

interannual variability of the Iberian precipitation regime. Interestingly, a relative maximum of precipitation is observed in spring all over the interior of Iberia. This peak of rainfall, coexisting in central Iberia with the one of late autumn and winter, and with that of early autumn along the Mediterranean coast, corresponds to the yearly maximum of precipitation for large areas in the east and northeast. Most of these areas, where agriculture has been traditionally the mainstay of the local economy, present arid or semiarid characteristics, often suffering from water shortage. Therefore, in the context of a changing climate, whose impacts are believed to involve less mean precipitation and more extreme rainfall events in the Mediterranean region, and specifically in Iberia (IPCC, 2001 [133]; Tapiador et al., 2007 [243]; Hoerling et al., 2012 [124]), a comprehensive assessment of the relative contribution of the major moisture sources (oceanic and recycled) affecting these areas is crucial for their medium and long term sustainability.

Over a certain study region, the recycling ratio measures the fraction of the total precipitation originated in moisture evapotranspired within the same region. This parameter is commonly used to quantify the impact of land-atmosphere feedbacks on the regional rainfall regime. Monthly mean recycling values for the Iberian Peninsula are found to range from 0.04 (0.03), in December, to 0.14 (0.07) in June (May), according to EBRM (IMB). Both methods, EBRM and IMB, show the lowest recycling ratios, with similar magnitudes, from October to February, coinciding with the highest amounts of rainfall over the Atlantic basin. From March to June, in contrast, EBRM recycling ratios are significantly higher, presenting also a larger interannual variability with respect to those obtained with the IMB method. This is expected, since the EBRM explores the spatial heterogeneity of the moisture fluxes, thus providing a more realistic description of the recycling process. According to the latter method, average local recycling ratios exceed 10% in most central and eastern Iberia, reaching values above 20% in some specific areas in the east and northeast. During spring and early summer, and in contrast with the winter half of the year, local recycling maximums overlap with the areas where the highest amount of rainfall is registered. This connection, reaching its peak of intensity in April and May, confirms that the recycling contribution is critical to describe the spring peak of precipitation observed throughout most of the continental Iberia.

The above-mentioned intensification of land-atmosphere interactions in spring is related to the debilitation of the winter-like circulation. The subsequent enhancement of local and mesoscale convective regimes in the interior regions represents a necessary (but not sufficient) condition for high recycling values to take place. The availability of soil moisture constitutes the second requirement, since it is the fuel to trigger the recycling mechanism. As a result, the amount of precipitation accumulated during the previous season must be also taken into account for a complete analysis. In Iberia, both conditions (that is, a synoptic configuration favoring convection and sufficient soil moisture availability) reach their maximum coupling in spring and early summer, and can be effectively assessed in early spring (March).

Three representative case studies (1997, 2001 and 2005) were selected to explore the intensity of recycling in March and the associated spatial patterns of precipitation for March and previous season. This analysis shows that humid months of March, generally occurring under an intense westerly circulation, present consistently low recycling values. Under this configuration, the impact of a dry or wet previous winter on March recycling is reduced, suggesting a limited role of land-atmosphere feedbacks on precipitation. In contrast, for dry months of March, a previous wet (dry) winter enhances (attenuates) significantly the magnitude of recycling and its impact on early spring precipitation. This analysis confirms that recycling patterns depend not only in the present synoptic configuration but also in the memory of the precipitation falling during the previous season within the study region. We suggest that this double mechanism hypothesis, here assessed in detail for early spring, might be useful to understand the relevance of the recycling contribution for any other period of the year in Iberia and other regions of the world with semi-arid types of climate.

The computation of the recycling ratio through two different methods, at the monthly scale, at high resolution and covering a period of 18 annual cycles provides a detailed spatio-temporal assessment of the potential impact of land-atmosphere interactions on the Iberian precipitation regime. This study is complemented, in chapter 4, with a more detailed analysis of land-atmosphere connections in May. For this purpose, experimental simulations where land ET is suppresed are carried out for eleven months of May (2000-2010). It is relevant to note that, among the spring and early summer months, when recycling values are found the be the highest along the yearly cycle, the month of May is selected because it coincides with the annual maximum of rainfall in large areas in the interior, east and northeast of the Iberian Peninsula, and thus the effects of land-air interactions on precipitation can be better assessed. This study is also complemented with simulations incorporating moisture tracers (chapter 5), as a way to analyze the regional sources of moisture with more accuracy and compute the recycling patterns in a direct way, thus overcoming the limitations of the classical recycling models. The method of tracers, however, would not be applicable to a variety of simulations and analyses already available. This constitutes a relevant advantage of the methodology proposed in this chapter.

USC
UNIVERSIDADE
DE SANTIAGO
DE COMPOSTELA

4

The maximum of precipitation in spring in the Iberian Peninsula: recycling and amplification contributions

Abstract. In the semiarid interior of the Iberian Peninsula, the topographic insulation from the surrounding seas promotes the role of internal sources of moisture and water recycling in the rainfall regime. In inland Iberia, the annual cycle of precipitation often has a distinctive peak in the springtime, when evapotranspiration (ET) is the highest, in contrast to the coastal areas, where it follows more external moisture availability and synoptic forcing, with a maximum in winter-autumn and a pronounced minimum in the summer. In this chapter we investigate the role of land surface water fluxes in the intensification of the hydrological cycle in the Iberian Peninsula, focusing our attention in spring. We use data from 5 km resolution WRF-ARW model simulations over the Iberian Peninsula for eleven months of May (from May 2000 to May 2010). To bring out the effect of ET fluxes, we conduct experiments where ET water over land is removed from the system. Our findings indicate that the impact of ET on precipitation is on average very large (37% increase), particularly in the interior north and northeast areas where the observed annual rainfall cycle has a peak in May, suggesting that the role of surface water fluxes is substantial to explain it. To investigate whether this role is as a water source or to amplify precipitation dynamics, we compute the recycling ratio analytically from the model data and, in addition, we use an original procedure to quantify the amplification impact by comparing the recycling ratio and the relative change in precipitation between control and experiments with ET removed. Results show that the role of surface water fluxes on precipitation depends on large-scale forcing and moisture advection. When the syn-

optic forcing and moisture advection is strong, such as in fronts associated to Atlantic storms, the impact of ET fluxes is small. On the contrary, when there is potential for convection, as is commonly the case of late spring in the Iberian Peninsula, ET fluxes have a higher impact. Surface moisture fluxes moisten the boundary layer and increase moist static energy, strengthening convective processes, and their role goes from being a primary water source for precipitation (recycling) to have mostly an amplification effect, as external moisture availability increases. Our findings show that for the eleven simulated May cases over the Iberian Peninsula, the role of ET fluxes in activating recycling is very relevant and goes from explaining 27% to 58% of their total impact on precipitation, depending on the method used to calculate the recycling ratio. This indicates that the complementary effect on amplifying rainfall from external sources of moisture is comparable in magnitude to the recycling mechanism and important as well. This chapter corresponds in large parts to the article *Moisture recycling and the maximum of precipitation in spring in the Iberian Peninsula* (see the List of Publications for the complete reference).

*****

In the previous chapter, the analysis of EBRM and IMB recycling ratios confirmed that an intensification of land-atmosphere interactions takes places in spring and early summer over Iberia. In that period of the year, the land surface becomes a relevant source of moisture to the atmosphere, modifying the winter-like equilibrium between locally evapotranspired and advected precipitation and therefore the recycling ratio (Brubaker et al., 1993 [32]). In this chapter, high-resolution (5 km) WRF model simulations for the period 2000-2010 are used to compute recycling ratios using both the IMB and EBRM recycling models. We compare control simulations to experiments with ET disabled, in order to quantify the experimental relative change in precipitation defined in section 2.5 and the relative contributions of recycling and amplification mechanisms to the spring peak of precipitation. The latter is carried out by using the analytical method by Schär et al. (1999) [221], as well as a new formulation proposed in section 2.7.

Significantly high average recycling values have been obtained in the previous chapter during spring and early summer months, mostly in eastern and northeastern Iberia. In addition to this, as discussed in section 1.1, a relative maximum of precipitation is observed in spring over most of inland Iberia (Fig. 1.1). This peak may correspond to the absolute maximum of precipitation (eastern and northeastern areas) or to a secondary peak in the annual cycle (e.g. North Plateau and central Iberia), tending to occur in May for a vast majority of inland locations (Fig. 1.3). This suggest that it is precisely in May when the impact of recycling processes on the annual rainfall regime is maximized and thus it is the most appropriate month to explore in more detail the role of land-atmosphere feedbacks over the Iberian Peninsula (IP). For comparison, we consider winter situations as well, represented by January, a

typical winter month, in order to test the model response and sensitivity to different synoptic forcing. The simulated decade (January 2000 to January 2010, May 2000 to May 2010) includes the driest hydrological year (2004-2005) on record for the Iberian Peninsula (García-Herrera et al. 2007 [106], Santos et al. 2007 [217]) and also the wettest spring ever registered in many locations inland (2008). The main goal of the study presented in this chapter is thus assessing the intensity of land-atmosphere coupling over the IP, and in particular the direct and indirect impact of local ET on precipitation dynamics through both precipitation recycling and amplification mechanisms.

The model configuration and setup of simulations, as well as the different procedures to compute the recycling ratio and to separate the recycling and the amplification contributions to the extra rainfall attributable to land-air interactions are described in sections 2.1, 2.2, 2.3, 2.6 and 2.7. A validation of precipitation results is given in section 4.1. The central results of this study are presented and discussed in sections 4.2, 4.3 and 4.4. Special attention is given to the ET - precipitation coupling mechanisms during May of 2008, one of the wettest Mays ever registered in the IP, and also during May of 2004, in the second position in terms of total precipitation along the simulated decade (section 4.5). A brief summary of the main conclusions of this chapter is provided in section 4.6.

4.1 Validation of precipitation

The comparison of the results obtained from numerical simulations with observational or analysis data is usually referred to as *validation* (Jiménez, 2010 [137]). We next describe the process of validation of the precipitation obtained from the WRFS-2 set of simulations.

As described in section 2.8, an analysis of precipitation over the IP was performed by the Universidad de Cantabria (UC), the Agencia Estatal de Meteorología (Spanish Meteorological Office, AEMET) and the Instituto Português do Mar e da Atmosfera (Portuguese Meteorological Institute, IPMA) by using all stations from the climatic monitoring network of both AEMET and IPMA (Herrera et al., 2010 [123]; Belo-Pereira et al., 2011 [13]) for a period ending in March of 2008. Fig. 4.1 shows the mean precipitation for the period January 2000 to January 2008 from (a) WRF model simulations and (b) UC/AEMET-IPMA analysis. Panels (c) and (d) show the corresponding results for the period May 2000 to May 2007. For both January and May, the observed patterns are well captured by the WRF simulations, which show more fine scale structure associated with their horizontal resolution of 5 km (versus 20 km in the UC/AEMET-IPMA analysis). Amounts are somewhat higher in the WRF results, particularly in January in the mountains directly facing the Atlantic in the northwest of Iberia, but this discrepancy can be attributed, at least

partially, to the lack of density of observations in those mountainous areas. In fact, stations from the independent network of MeteoGalicia in the Galician mountains, just behind the northwestern Iberian coast, indicate that average precipitation totals for January of the period 2000-2008 do exceed 300 mm/month as in the model simulations (*http://www.meteogalicia.es/observacion/informesclima /informesIndex.action?request_ locale=gl*), thus providing observational evidence that these high values are indeed realistic.

On the other hand, we further compare WRF model precipitation values with the UC/AEMET-IPMA analysis by examining grid point statistics. Figs. 4.2a and 4.2g show the daily mean absolute error (MAE) and the daily mean normalized error (MAPE) for the period January 2000 to January 2008, computed via the standard definitions expressed in equations (2.49a) and (2.49b). Figs. 4.2d and 4.2j represent the corresponding results for the period May 2000 to May 2007. In accordance with the previous discussion, daily MAE values are the highest in the mountainous areas of the northwest, corresponding to MAPE results that do not exceed 150% for most of the IP. The corresponding 5-day and monthly MAE and MAPE values, shown in panels b, c, e, f, h, i, k and l, are progressively lower. This is expected, since daily differences tend to compensate when a longer period of time is considered.

Analyzed precipitation observations for validating model results are not readily available for the most recent years of the experiments. From March of 2008 onwards, the UC/AEMET-IPMA analysis is not available yet, and only area averaged monthly precipitation values for Spain are provided by AEMET. Fig. 4.3 shows the time series (2002-2010) for (a) January and (b) May of those AEMET estimations (red) together with model results (blue). The agreement among observations and model results is very good for May of all years for overall precipitation amounts over Spain. In January, values are higher in the model for some years, but as discussed above, this is likely due to the lack of observations in mountain ranges, where orographically enhanced precipitation can reach very large amounts. Since spatial patterns of the simulated precipitation are close to the observation analysis of UC/AEMET-IPMA for years 2000-2007/08 (Figs. 4.1a, 4.1b, 4.1e, 4.1f), we assume that they likely are as well for the more recent period 2008-2010. If the WRF model simulates the precipitation fields with accuracy, we also assume that it may represent the other variables properly. Note that the validation of other relevant magnitudes, as soil moisture or ET, is not strainghtforward, since observations of such land surface variables are, nowadays, still very limited (Dominguez et al., 2009 [70]).

4.2 Water budget and moisture fluxes

Figs. 4.4 and 4.5 show the four terms of the water budget (P, ET, $MC = IN - OUT$ and change in storage ΔN; see equation 2.1), together with the experimental relative

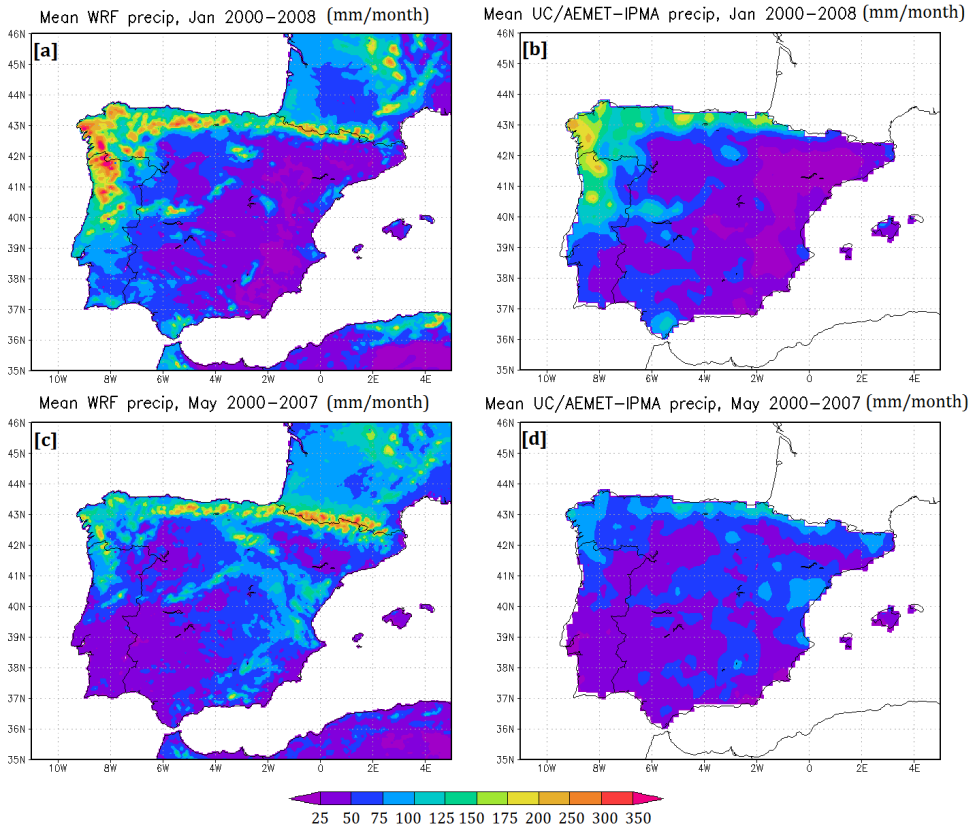

Figure 4.1: Average precipitation (mm/month) for January 2000-2008 according to: (*a*) WRF model; (*b*) UC/AEMET-IPMA analysis. Panels (*c*) and (*d*) show the analogous results in May for the period 2000-2007.

change in precipitation (r^*, defined through equation 2.20) in May and January for the whole IP (Figs. 4.4a and 4.4b) and for the sub-domains defined within (NE, NP and CE in Fig. 4.4 and EA, NW, WE and SP in Fig. 4.5). These small boxes are represented in Fig. 2.2b.

As it can be observed, average precipitation is higher in January than in May only in the west and northwest boxes, directly facing the fronts coming from the Atlantic, which bring moisture from the ocean and dominate the winter circulation at these mid-latitudes. Nevertheless, on average for the whole IP, January is only marginally wetter than May (2.7 vs 2.3 mm/day) and this is mostly due to the high winter precipitation values in the northwest, which more than double those of the springtime (4.4 mm/day vs 2.0 mm/day). For most of the interior, particularly in the North Plateau and in the areas to the east and northeast, May has on average significantly more precipitation than January. Similarly, the experimental relative change in precipitation is significantly higher in May, in accordance with the discussion below.

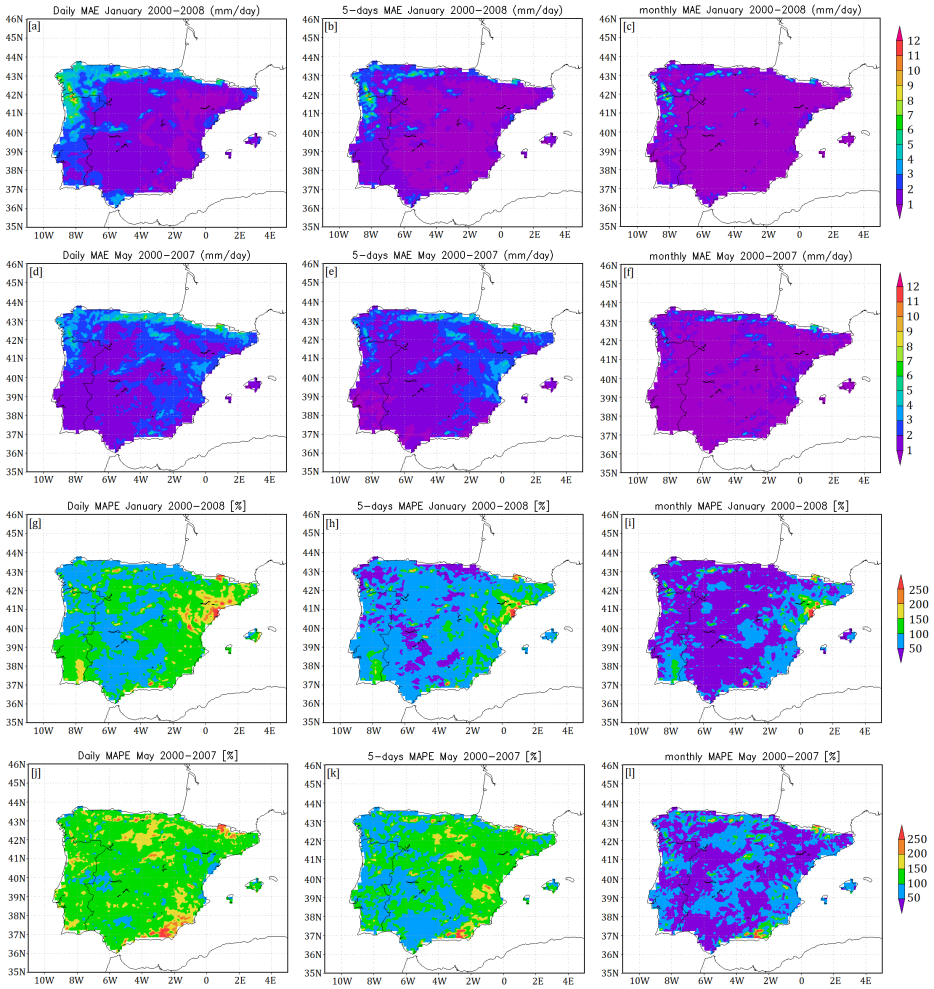

Figure 4.2: Daily, 5-days and monthly MAE (mm/day) and MAPE (%) values (see equations 2.49a and 2.49b) for the periods January 2000-2008 and May 2000-2007.

On the other hand, over the IP and in all the sub-domains considered within, there is a net inflow of moisture from adjacent areas in January (the moisture convergence term is positive). In contrast, in May, for 7 out of the 11 years simulated (Table 4.1) and also for the multiannual average (Table 4.1 and Fig. 4.6a) the monthly moisture convergence is negative, meaning that there is a net export of moisture to the surroundings. Thus, despite May being climatologically the period of highest rainfall in many locations inland, the precipitated water cannot compensate ET, and therefore some of the moisture stored into the soil during the winter is lost and transported elsewhere by the atmospheric flow. The examination of the moisture convergence values for the different subareas indicates that the regions to the south and particularly to the west tend to be net water vapor exporters in this springtime period, while the regions to the east and northeast are net importers. The North Plateau and

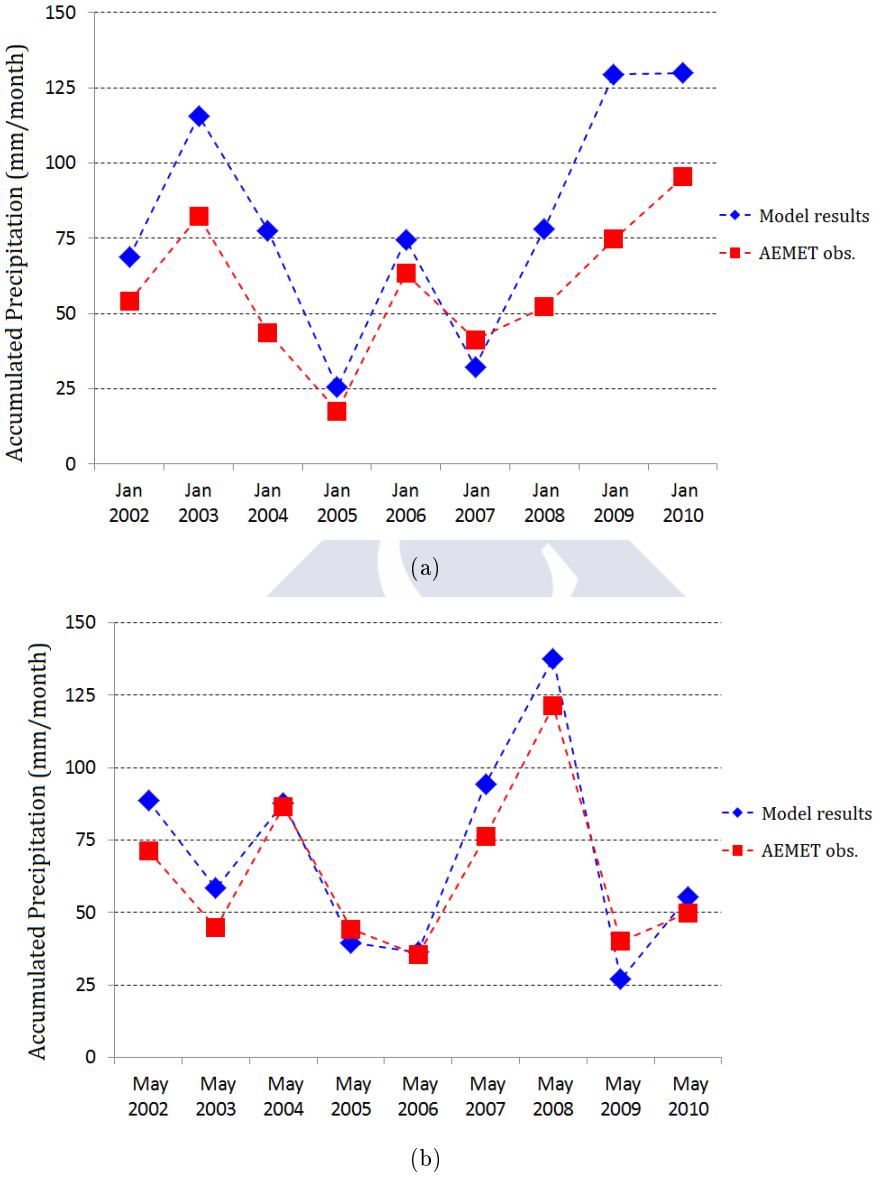

Figure 4.3: Time series for January (*a*) and May (*b*) from 2002 to 2010 area-averaged monthly precipitation (mm/month) over Spain from observational analysis by AEMET (red) and from model results (blue).

the Center region have on average a very small water imbalance, with precipitation nearly equaling ET. The average net divergence for the whole IP is also small (-0.14 mm/day), in part due to the high positive value of 2008 (2.49 mm/day, as shown in Table 4.1).

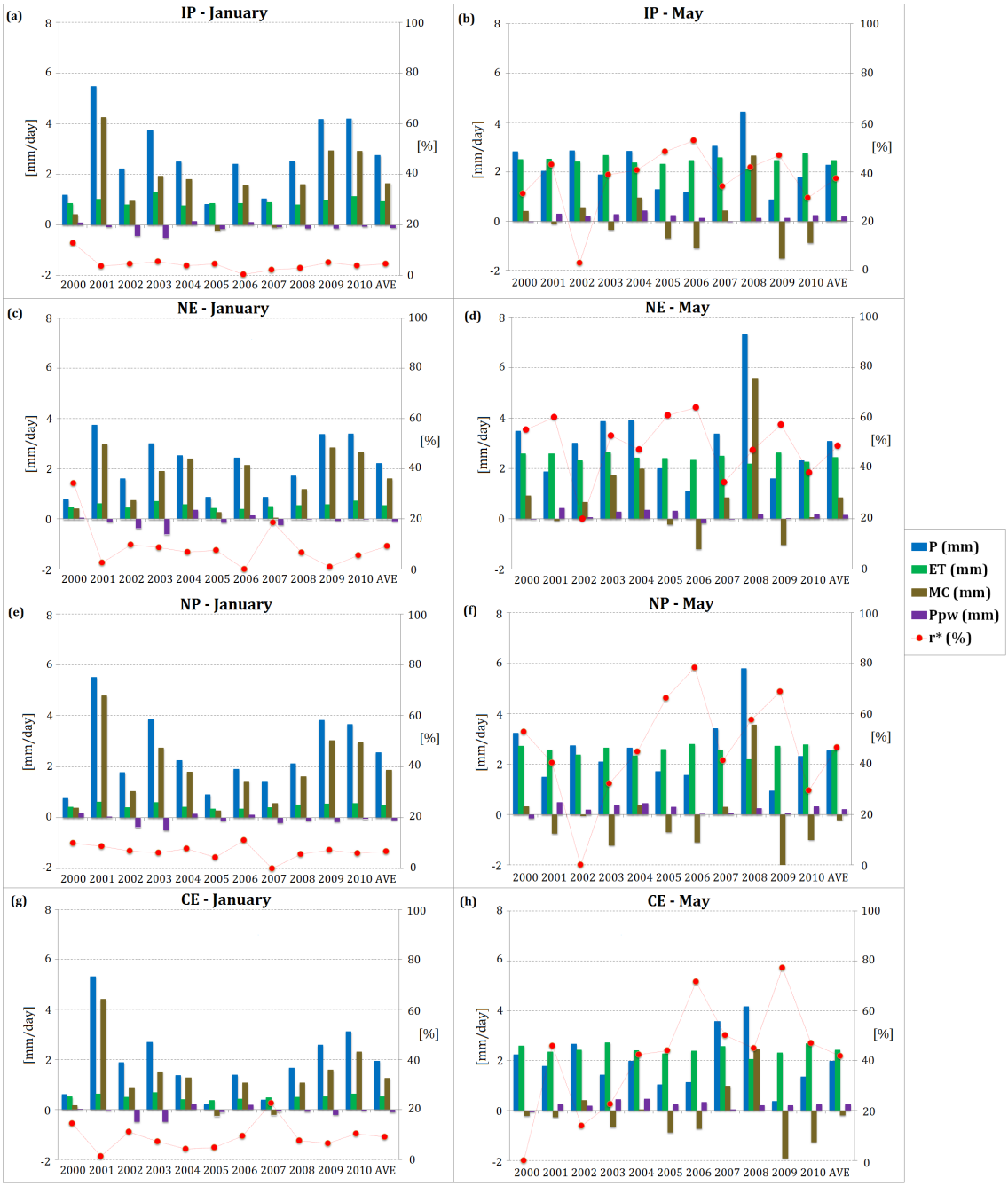

Figure 4.4: Terms of the water budget in mm/day (P in blue, ET in green, MC in brown and change in N in purple), together with the experimental relative change in precipitation (line with red dots, in %) for the whole Iberian Peninsula (pannels *a* and *b*) and for three of the selected sub-domains within: NE (*c*, *d*), NP (*e*, *f*) and CE (*g*, *h*). Pannels *a*, *c*, *e* and *g* correspond to the period January 2000 - January 2010, whereas pannels *b*, *d*, *f* and *h* correspond to May 2000 - May 2010.

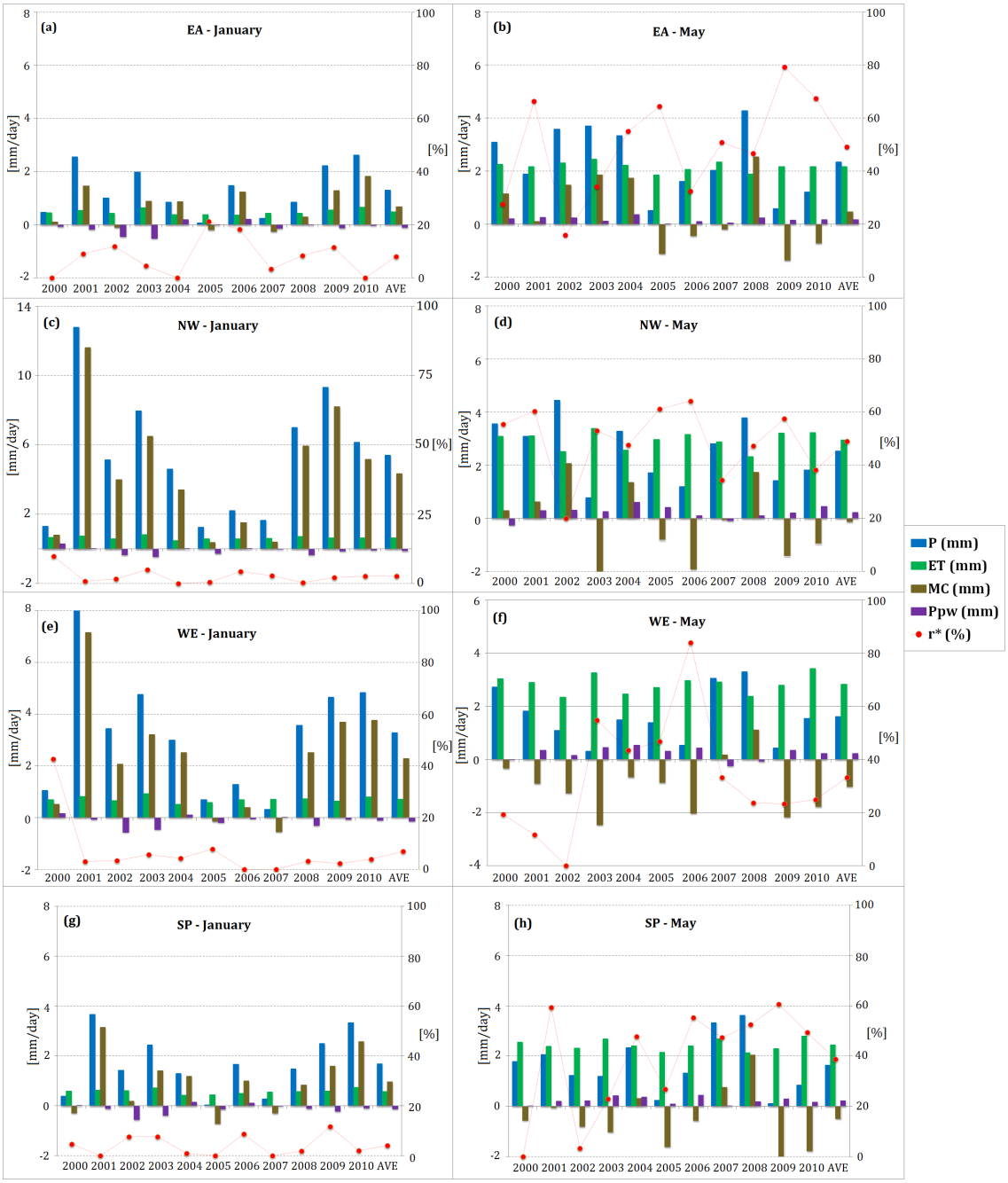

Figure 4.5: (Continuation of Fig. 4.4) Terms of the water budget in mm/day (P in blue, ET in green, MC in brown and change in N in purple), together with the experimental relative change in precipitation (line with red dots, in %) for the remaining sub-domains within the IP: EA (a,b), NW (c, d), WE (e, f) and SP (g, h). Pannels a, c, e and g correspond to the period January 2000 - January 2010, whereas pannels b, d, f and h correspond to May 2000 - May 2010.

(mm/day)	Control run				*No-ET* experiment			
	May 2008	May 2004	May 2000-10	January 2000-10	May 2008	May 2004	May 2000-10	January 2000-10
Lower atmopshere	2.06	0.57	0.81	-0.46	1.88	0.61	0.85	-0.22
Upper atmosphere	0.43	-0.18	-0.95	2.06	0.62	0.65	0.31	2.15
Total	2.49	0.39	-0.14	1.60	2.50	1.26	1.16	1.93

Table 4.1: Average moisture flux (mm/day) in the lower atmosphere (below 700 mb) and in the upper atmosphere (above 700 mb) for May of 2004, May of 2008 and also for the periods May 2000-2010 and January 2000-2010. Results are shown for both control runs and experiments with no ET.

Fig. 4.7 shows the mean moisture flux patterns at 850 hPa and 500 hPa for January and May, averaged over the 11 years of simulation. In winter, the influx of moisture is at all levels mostly determined by the prevailing westerlies that derive from the Atlantic Ocean. This oceanic moisture is discharged as precipitation on the Iberian Peninsula, particularly on the orographically favorable areas of the north and west, and the exiting fluxes off the Mediterranean coast are significantly drier. The net input of moisture in the mid and upper levels (above 700 hPa) is 2.06 mm/day, whereas there is a net small water content loss at low levels (below 700 hPa) of 0.46 mm/day along the eastern coast. These values, shown in Table 4.1, can be easily visualized in Figs. 4.6a and 4.6b (Fig. 4.6c is analogous to panel 4.6*a*, but referred to the *no-ET* experiment). The intense moisture convergence at mid and upper levels and small divergence below is consistent with convection not being the driving mechanism for precipitation, but rather large-scale forcing associated to passing fronts within the storm systems moving along in the prevailing zonal circulation.

In May, in contrast, the moisture influx from the Atlantic is considerably weaker, particularly at low levels, where it has more of a northwesterly component. Associated to easterly winds, there is a reversal of the moisture flux on the lee side of Iberia, with weak net on-shore influxes of moisture resulting along the Mediterranean coast (Fig. 4.7b). This pattern of low-level moisture flux presents a larger year-to-year variability and it is not very well organized, in general, for most areas. When averaged over the 11 simulated months of May, it does however correspond to a positive value of moisture convergence below 700 hPa of 0.81 mm/day (Table 4.1). At 500 hPa the flux is still clearly zonal (Fig. 4.7c and 4.7d), but in contrast with the situation in winter, it has considerable lower values when entering the IP than when exiting toward the Mediterranean, so that for the layers above 700 hPa, the multiyear average value of moisture convergence is -0.95 mm/day (Table 4.1). When considering the total air columns, the result for May is the aforementioned net moisture divergence or loss of water vapor to the surrounding area of -0.14mm/day (Fig. 4.6a). The similar values of moisture convergence at low levels and divergence aloft is an indication that moisture is lifted through convection from the interior of Iberia and transported elsewhere by the prevailing westerlies in the mid and upper atmosphere. This configuration,

opposite to that of January, can be observed in Fig. 4.6b. Convective precipitation associated with the low level convergence is much higher than the moisture convergence term, suggesting that local ET is an important source for rainfall.

As discussed in chapter 1, the difference in large-scale moisture transport is related to the general circulation changes with season. As the summer approaches, the prevailing zonal circulation and moisture advection is displaced northward and weakened. In addition, the main westerly flow tends to meander and form cut off lows in the vicinity or over the IP, one of the areas in the Northern Hemisphere with a higher frequency of these features forming during the spring (Bell and Bosart, 1989 [12]; Nieto et al., 2005 [187]; Nieto et al., 2007a [189]). Cut-off lows favor locally generated circulations and low level moisture convergence to the center, as reflected in Fig. 4.7b. The upper level cold core associated to these systems creates instability, which enhances convection and leads to an increase in the potential impact of land-surface fluxes on precipitation (Nieto et al., 2005 [187]), which can be measured through the analysis of the recycling ratio. Convection, related or not to cut-off lows, is most frequent in the spring in the IP, and a majority of inland and eastern stations of the Spanish Meteorological Office (AEMET) network report a peak in the monthly number of thunderstorm days in May (1971-2000 means available at *http://aemet.es/en/serviciosclimaticos/datosclimatologicos/valoresclimatologicos*). In winter, in contrast, the frequency of occurrence of cut-off lows is much lower (Nieto et al., 2007a [189]; Nieto et al., 2007b [190]) and the intensity of large-scale moisture advection and baroclinic forcing is enhanced.

4.3 Moisture recycling and spring rainfall

IMB recycling ratio

The regional recycling ratios computed for the different years and the multiannual mean are presented in Table 4.2. Schär's (IMB) formula yields an average value for January of 0.04. It is a small number, as expected, given the reduced ET and the strong large-scale forcing and external moisture advection in this winter period. For May, in contrast, with much larger ET and an enhanced convective activity, the multiannual mean value is still only 0.10 (varying from 0.08 in 2008 to 0.13 in 2010). These low values of the IMB recycling ratios are consistent with our previous discusion on the fact that this method tends to underestimate the recycling ratio if precipitation is unevenly distributed in the considered region, which is the case for the IP. Consequently, assuming that both precipitation and recycling ratio are uniformly distributed across the whole box, as it is considered in the IMB, leads to the underestimation of the latter magnitude.

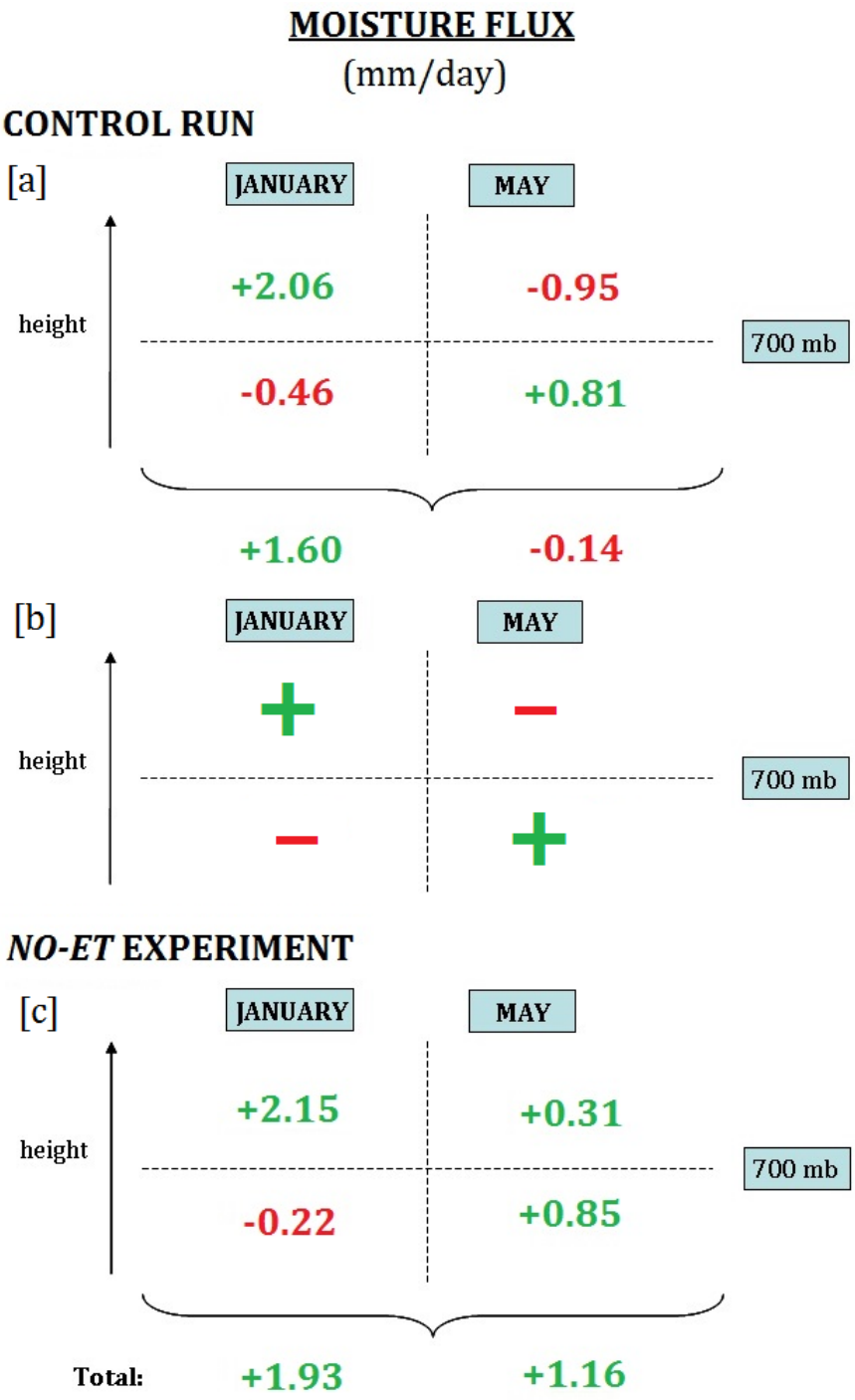

Figure 4.6: Average moisture flux (mm/day) in the lower atmosphere (below 700 mb) and in the upper atmosphere (above 700 mb) for the periods May 2000-2010 and January 2000-2010. Results are shown for both control runs and *no-ET* experiments.

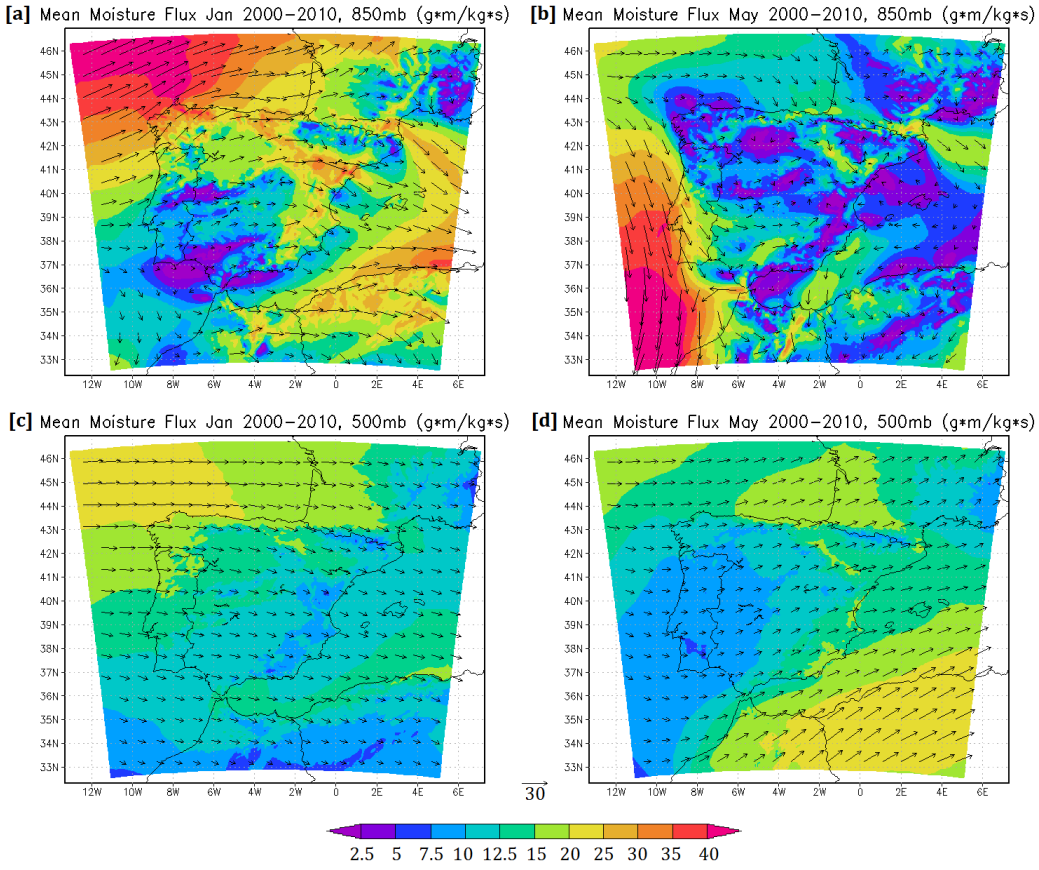

Figure 4.7: Average moisture flux patterns (g kg^{-1} m s^{-1}) at 850 hPa (*a*, *b*) and 500 hPa (*c*, *d*) for January 2000-2010 (*a*, *c*) and May 2000-2010 (*b*, *d*).

EBRM recycling ratio

The regional EBRM recycling ratios are higher than those from IMB, not so much for January as for May, when the mean value of 0.22 (varying from 0.14 in 2002 to 0.35 in 2009) is about twice the obtained via Schär's method. According to EBRM, this means that on average 22% of the total rainwater derives from local ET, and therefore that the main source of precipitation in spring is still advected moisture. This method also accounts for the spatial variability of the recycling ratio within the considered box. The pattern of the multiannual average of this "local" recycling ratio, together with the mean moisture flux integrated over the column is displayed in Fig. 4.8. Both EBRM recycling ratio and moisture flux patterns are highly related, with ρ_{EBRM} tending to have higher values on the eastern and northeastern parts of Iberia ($\rho_{\mathrm{EBRM}} > 30\%$ in large areas there), where the flow, predominantly from west to east, has been over land for a longer time and has a higher load of moisture with origin in terrestrial ET. The smoothness of the spatial patterns of the EBRM recycling ratios

Month	r_{IMB}	r_{EBRM}	r^*	Month	r_{IMB}	r_{EBRM}	r^*
Jan 2000	0.07	0.23	0.13	May 2000	0.10	0.21	0.31
Jan 2001	0.03	0.02	0.04	May 2001	0.12	0.31	0.43
Jan 2002	0.04	0.05	0.05	May 2002	0.09	0.14	0.03
Jan 2003	0.05	0.05	0.05	May 2003	0.11	0.31	0.39
Jan 2004	0.03	0.02	0.04	May 2004	0.11	0.31	0.41
Jan 2005	0.06	0.08	0.05	May 2005	0.09	0.15	0.48
Jan 2006	0.05	0.12	0.00	May 2006	0.10	0.16	0.53
Jan 2007	0.05	0.06	0.02	May 2007	0.09	0.17	0.34
Jan 2008	0.03	0.03	0.03	May 2008	0.08	0.13	0.42
Jan 2009	0.04	0.03	0.05	May 2009	0.11	0.35	0.47
Jan 2010	0.04	0.04	0.04	May 2010	0.13	0.20	0.30
Average	0.04	0.07	0.05	Average	0.10	0.22	0.37

Table 4.2: Recycling ratio [-] (computed via both EBRM and IMB), and experimental relative changes in precipitation [-] for the periods May 2000 - 2010 and January 2000 - 2010.

is related to their high correlation with the integrated mean moisture flux, since the assumption here is that the recycling ratio, even though variable in space, is constant throughout the month and the mean moisture fluxes are used in the computation (see section 2.3 and appendix C for further details on the computation method). The large spatial variability of the precipitation field in our 5 km resolution simulations (and also in reality), together with the varied genesis of precipitation (convective or not) throughout the considered months, makes it very unlikely that the recycling ratio has such smooth spatial distribution. This is explored in more detail in chapter 5 by incorporating moisture tracers to the WRF simulations.

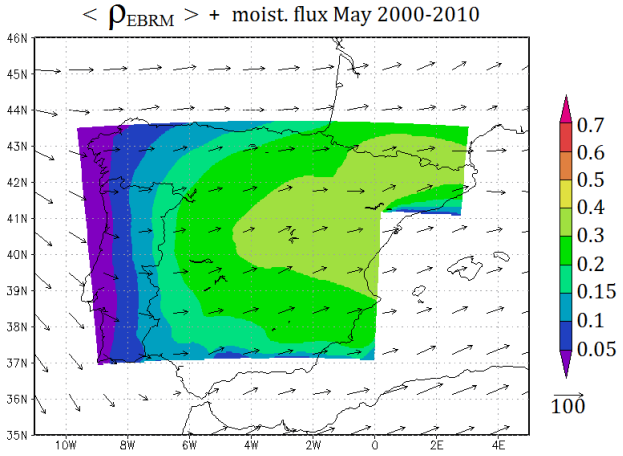

Figure 4.8: Spatial distribution of the multiannual average of EBRM recycling ratio [-] (May 2000 to May 2010), together with the average pattern of vertically integrated moisture flux ($\mathrm{kg^{vap}\ m^{-1}\ s^{-1}}$) for the same period.

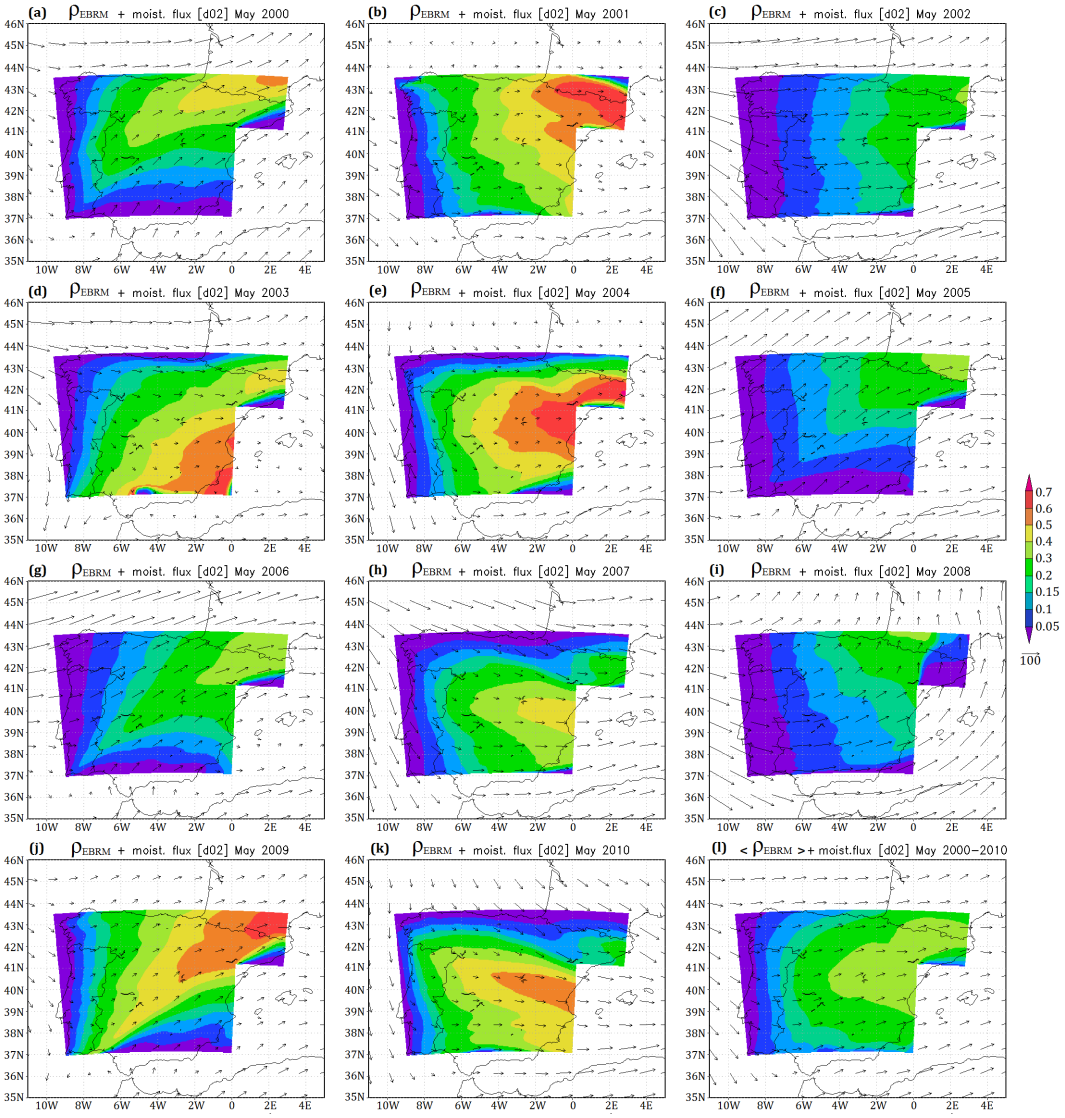

Figure 4.9: Spatial distribution of the local EBRM recycling ratio [-] during the period May 2000 (panel *a*) to May 2010 (panel *k*), together with the corresponding average pattern of vertically integrated moisture flux (kg^{vap} m^{-1} s^{-1}), computed with WRF outputs for the nested domain. The multiannual average is also included (panel *l*) for comparison with Fig. 4.10.

The above-mentioned connection between moisture fluxes and EBRM recycling ratio is also apparent in Fig. 4.9, where the spatial patterns of recycling are shown from May 2000 (panel *a*) to May 2010 (panel *k*). These maps reflect the strong variability in the spring rainfall regime of the IP, discussed in section 1.1. For instance, the recycling map observed in May of 2002 (panel *c*) is related to an intense, winter-

like zonal flow, leading to a pattern of low values that gradually increase from western to eastern Iberia. On the contrary, May of 2001 or May of 2004 (panels *b* and *e*) present higher recycling values organized in a more complex spatial pattern. The latter is directly related to the weaker zonal circulation observed, which facilitates the triggering of convective mechanisms.

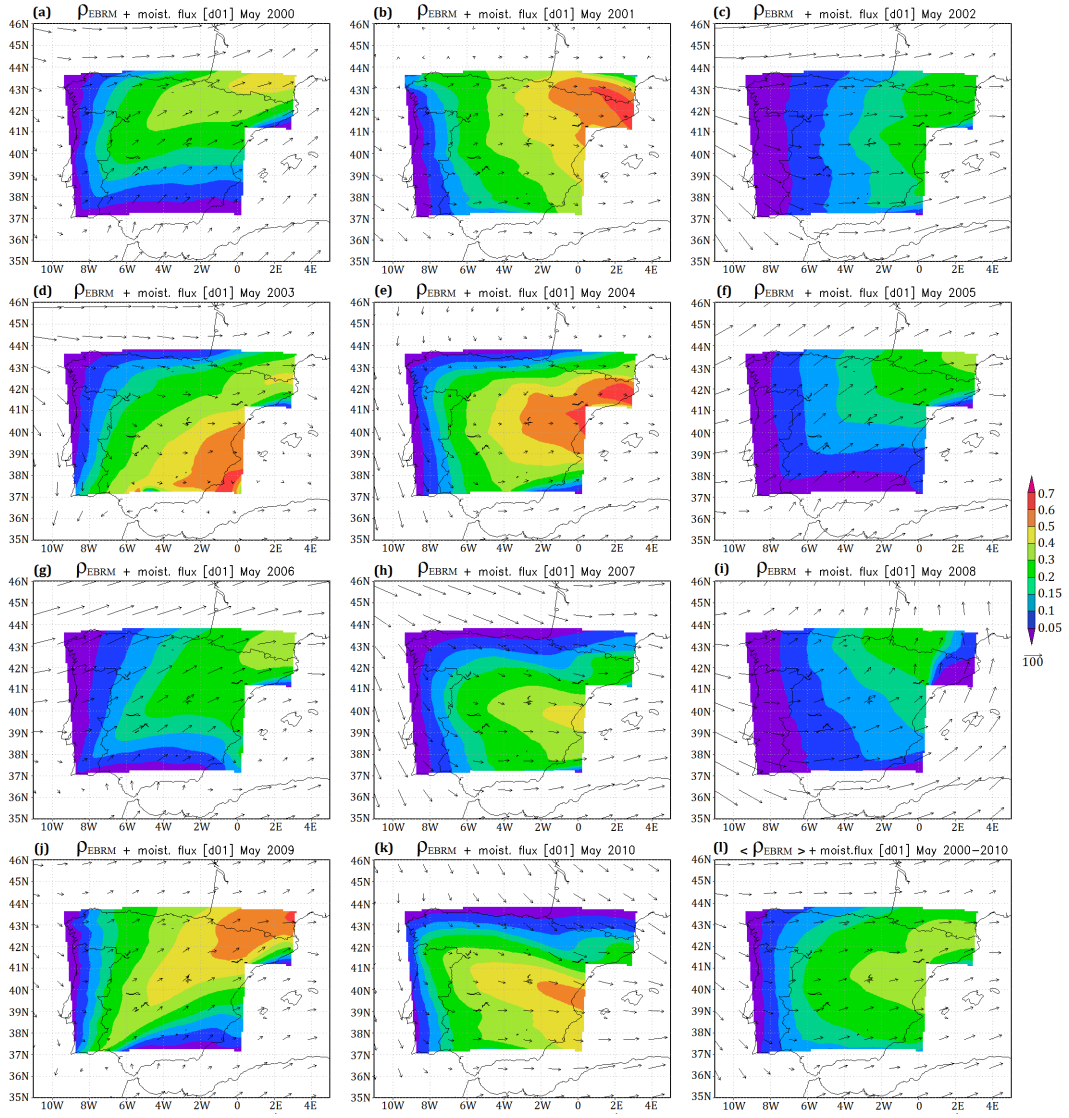

Figure 4.10: Spatial distribution of the local EBRM recycling ratio [-] during the period May 2000 (panel *a*) to May 2010 (panel *k*), together with the corresponding average pattern of vertically integrated moisture flux (kg^{vap} m^{-1} s^{-1}), computed with WRF outputs for the parent domain. The multiannual average is also included (panel *l*) for comparison with Fig. 4.9.

Recycling maps of Fig. 4.9 are computed from nested domain WRF output files. This implies that these spatial patterns are computed at 5 km horizontal resolution. Fig. 4.10 shows the corresponding maps computed from parent domain WRF output files, thus at 20 km resolution. Both figures include the average May 2000-2010 recycling patterns (panel *l* of both 4.9 and 4.10). The remarkable correspondence among the maps constitutes a first assessment of the robustness of the EBRM method and its reduced dependence on the spatial resolution of the simulation. This sensitivity of the EBRM recycling ratio to the spatial resolution is further discussed in appendix E.

Representation of the Iberian water budget

On the other hand, the average water budgets for January and May are summarized in Fig. 4.11, where the regional EBRM recycling ratios are used for the computations. The diagrams represent the hydrological cycle with arrows for fluxes and their relative importance reflected in the numbers. As in Elthair and Bras (1994) [76] the values are normalized by the total precipitation for each month, which is set to 100 units. The total moisture convergence (MC) is separated into its positive component associated with the inflow of moisture and its negative component related to the outflow of humidity from the considered box covering the IP (Fig. 2.2b). Evapotranspired moisture is also split into the component that contributes to precipitation (the recycling ratio times the total precipitation) and the component that is transported away by the flow. Subtracting the latter from the total outflow of moisture yields the portion of the total outflow that derives from moisture advected into the box from somewhere else. Precipitation minus ET gives the net flux into the soil plus surface runoff.

The differences in the hydrological cycle between winter and spring are apparent in the diagrams of Fig. 4.11. Even though precipitation totals are comparable ($\langle P \rangle_{2000-2010}^{January} = 79.5$ mm month^{-1} and $\langle P \rangle_{2000-2010}^{May} = 60.7$ mm month^{-1}), the high ET in May leads to a negative total water budget in this month, with a net loss of moisture to the surroundings and a net flux of moisture from the land surface to the atmosphere. In January, in contrast, the water balance is largely positive, with the soil gaining humidity that derives from the atmosphere. As it can be observed, ET has a much larger relative contribution to precipitated water in May than in January. As discussed earlier, this difference is related to the nature of the precipitation processes in the season. Note that, from Fig. 4.11, it follows that $IN_{May} = 9.55 \cdot P_{May}$, $IN_{Jan} = 7.70 \cdot P_{Jan}$, $ET_{May} = 1.09 \cdot P_{May}$ and $ET_{Jan} = 0.34 \cdot P_{Jan}$ and thus making use of equation (2.6) we obtain:

$$r_{\mathrm{IMB}}^{\mathrm{Jan}} = \frac{0.34 \cdot P_{\mathrm{May}}}{7.70 \cdot P_{\mathrm{May}} + 0.34 \cdot P_{\mathrm{May}}} = 0.04 \tag{4.1a}$$

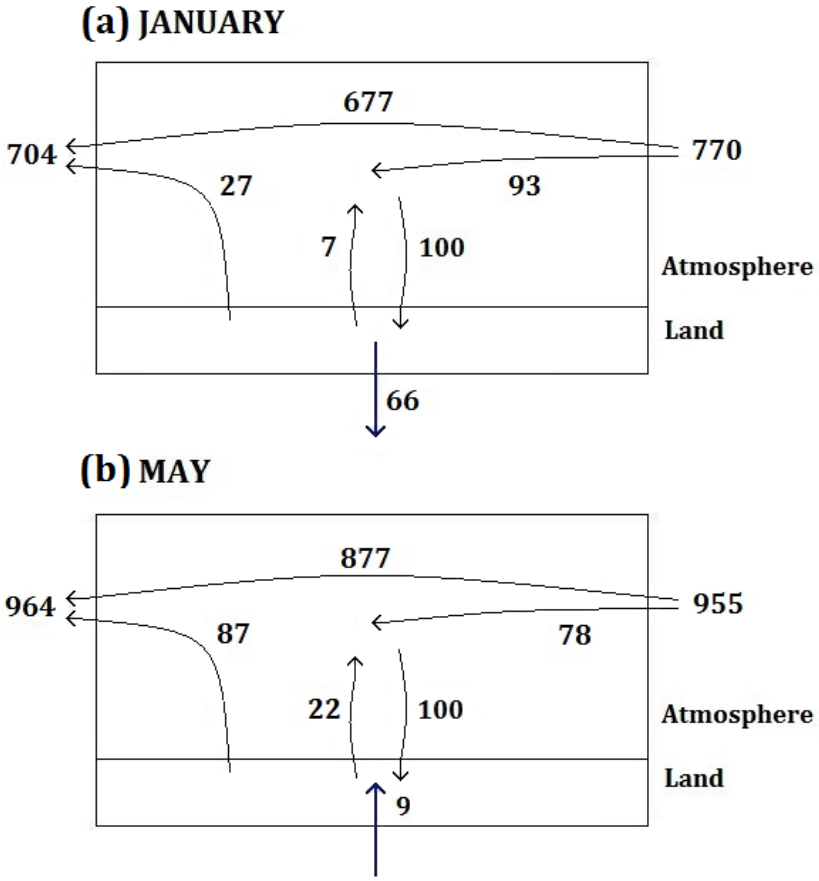

Figure 4.11: Representation of the average Iberian hydrological cycle for (a) January 2000-2010 ($\langle P \rangle_{2000-2010}^{January} = 79.5$ mm month^{-1}, taken as 100 units); and (b) May 2000-2010 ($\langle P \rangle_{2000-2010}^{May} = 60.7$ mm month^{-1}, taken as 100 units.

$$r_{\mathrm{IMB}}^{\mathrm{May}} = \frac{1.09 \cdot P_{\mathrm{May}}}{9.55 \cdot P_{\mathrm{May}} + 1.09 \cdot P_{\mathrm{May}}} = 0.10 \tag{4.1b}$$

which of course corresponds to the average 2000-2010 regional IMB values presented in the first paragraph of this section. In the next section, we investigate more on the contribution of ET to precipitation by analyzing results from the experiments where we suppress those land-air fluxes.

Comparison to recycling values obtained in chapter 3

In the present chapter, WRFS-2 model simulations carried out for the months of January 2000 - 2010 and May 2000 - 2010 are analyzed. Within this period, the months of January 2000 - 2007 and May 2000 - 2007 had been already run in the WRFS-1 simulation explored in chapter 3. In both cases, EBRM and IMB recycling ratios are computed and a thus comparison of the results is necessary. These EBRM and IMB recycling values are indeed comparable, as they are calculated over the same region (Figs. 2.1b and 2.2b), and time periods. Nevertheless, WRFS-2 simulations show some relevant differences with respect to WRFS-1, as mentioned in section 2.1. The most relevant divergence lies on the fact that the WRFS-1 simulation is continous (that is, the period 1990-2007 is simulated "without stopping"), whereas simulations for the months of January and May in this chapter (WRFS-2) are initialized at the begining of each month and last only 31 days. In addition, other important discrepancies are the use of different model parameterizations, different horizontal resolution and model domains, different initial and lateral boundary conditions and the use or not of the spectral nudging technique. As a result, relevant differences between both recycling calculations are expected to emerge.

Fig. 4.12 shows the regional recycling ratio computed through both IMB and EBRM from WRF outputs at 9 and 5 km horizontal resolution, corresponding WRFS-1 and WRFS-2 simulations, respectively. Once again, we observe higher values of recycling in May with respect to January (with the exception of the year of 2000, already discussed in section 3.1). In addition, the 5 km computation provides significantly higher recycling ratios than the 9 km one, even though the horizontal resolution of the calculations is not the only reason, as discussed above and explored in more detail in appendix E. Despite the differences observed in Fig. 4.12, it is important to mention the good correlation among the data series. This can be observed in Table 4.3, where the corresponding correlation coefficients are found to be significantly high.

Correlation coefficient	EBRM 5 km	EBRM 9 km	IMB 5 km	IMB 9 km
EBRM 5 km	-	-	-	-
EBRM 9 km	0.93	-	-	-
IMB 5 km	0.90	0.76	-	-
IMB 9 km	0.94	0.85	0.94	-

Table 4.3: Correlation coefficient among the data series represented in Fig. 4.12.

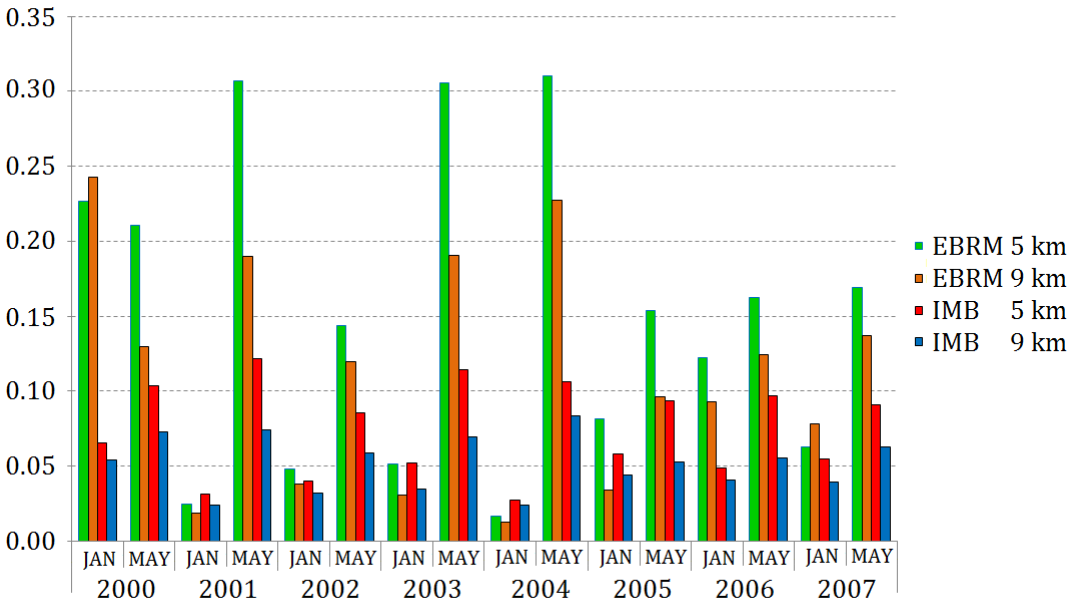

Figure 4.12: Regional EBRM and IMB recycling ratios [-] computed at 5 km (WRFS-2 simulations) and 9 km (WRFS-1 simulation) during the months of January 2000 - 2007 and May 2000 - 2007.

4.4 Precipitation amplification and spring rainfall

Experimental relative change in precipitation

In addition to the analytical recycling ratios, discussed above, the local fractional change in precipitation in the control runs with respect to the *no-ET* experiments (ρ^*), defined in section 2.5, is shown in Fig. 4.13a. On average, it presents higher values than the regional recycling ratio computed from the control simulations alone. This is expected, since according to the discussion of section 1.5, eliminating the ET flux not only reduces the amount of moisture available for rainfall, but also its capacity to increase the atmospheric instability giving rise to extra precipitation. On average for the 11 years of simulation, disabling the ET fluxes reduces rainfall by 37% in May, with this value exceeding 45% for several years. In January, the impact is only a 5% decrease, about the same as for the EBRM and IMB recycling ratios. This indicates that, in winter, ET has only a direct contribution to precipitation by supplying more moisture to the precipitation genesis mechanism and that it has a limited influence on the genesis mechanism itself. This is consistent with the previous discussion about the main source of moisture and the nature of the forcing for winter

precipitation being large-scale, baroclinic systems. In May, on the contrary, the large difference between ρ and ρ^* suggests that the input of moisture at lower levels has a significant effect on precipitation dynamics and not just in total amounts. This confirms that regional recycling ratios alone are not sufficient to assess the impact of the land-atmosphere interactions on the spring rainfall regime and therefore indirect (amplification) mechanisms must be taken into consideration.

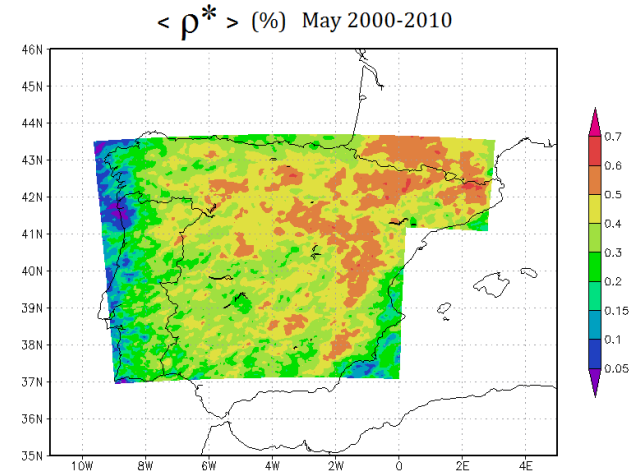

(a)

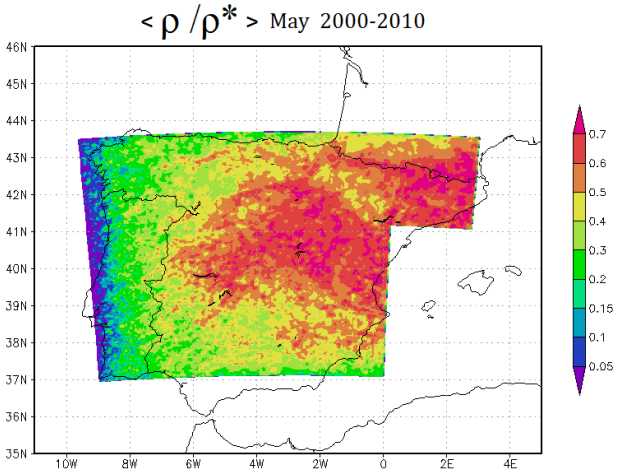

(b)

Figure 4.13: Spatial distribution of the relative change in precipitation [-], averaged over the period May 2000-2010 (a) and spatial distribution of ρ/ρ^* [-], equaling the fraction of ΔP deriving from direct recycling, for the same period (b).

As mentioned, the spatial pattern of the relative change in precipitation, ρ^*, represented in Fig. 4.13a, shows large values exceeding 60% towards the east and

northeast of the Iberian Peninsula and lesser values towards the west and southwest. It is very difficult, if not impossible, to verify with observations that the effect of ET fluxes on precipitation is as large as shown in Fig. 4.13a. Nevertheless, a comparison to the observational analyses of Figs. 1.1, 1.2, 1.3 and 1.4 supports that qualitatively this may be the case. The pattern of ρ^* (Fig. 4.13a), revealing the regions where ET fluxes have a large impact on May precipitation, is very similar to the patterns in Figs. 1.3 and 1.4 showing the areas with a maximum of precipitation in May. The latter makes the precipitation regime of those regions distinct from the rest of the IP and suggests some sort of local control on precipitation processes there.

Separation of recycling and amplification contributions

The bar diagrams in Figs. 4.14a and 4.14b show the relative change in precipitation between control and *no-ET* experiments ($\Delta P = P_{\text{control}} - P_{\text{no-ET}}$) for the years considered and for the multiannual mean. Each bar is divided in two colored sections, representing the contribution of recycling (blue) and amplification (red) calculated via the two different approaches described in chapter 2 (sections 2.6 and 2.7): Schär et al.'s (1999) Separation Method (SSM, Fig. 4.14a) and the new procedure derived here (equations 2.47 and 2.48; Fig. 4.14b), where the regional recycling ratios computed via EBRM are used. According to SSM (Fig. 4.14a), 62% of the extra precipitation (ΔP) derives on average from amplification and therefore this process is dominant over direct recycling (the remaining 38%). This behavior holds for almost all of the analyzed months of May, with the exception of years 2001 and 2010 when the recycling component is larger than the indirect term. May 2002 is not represented in Fig. 4.14 because the change in precipitation efficiency $\Delta\chi$ between control and experiment has a negative value and, as a result, equation (2.28b) is not satisfied and the SSM method cannot be applied. As it has been mentioned, the month of May of 2002 is an outlier in the set, with a strong synoptic forcing that is similar to a winter situation. This intense westerly flow (and passing fronts associated to Atlantic baroclinic systems) is responsible for the low value of the relative change in precipitation (r^* is only 3%), which corresponds to one order of magnitude less than the average for May and is similar to the January cases. $\Delta\chi$ has also an anomalous small value, one order of magnitude less than average and negative. The average precipitation efficiencies during the period May 2000 - May 2010 are $\chi_{\text{control}} = 10.7\%$ and $\chi_{\text{no-ET}} = 7.7\%$ for control and *no-ET* experiment, respectively, meaning that the system is about 40% more efficient in producing precipitation when moisture coming from ET fluxes is considered (control runs) than when it is removed (experiments).

In general, the partition between recycling and amplification contributions estimated through our method (Fig. 4.14b) shows a good agreement with that of SSM, even though relevant differences occur for some particular years, as is the case with 2000, 2003, 2004 and 2009. On average, according to our method, amplification explains 41% of the effect of ET fluxes on precipitation, while recycling is associated to

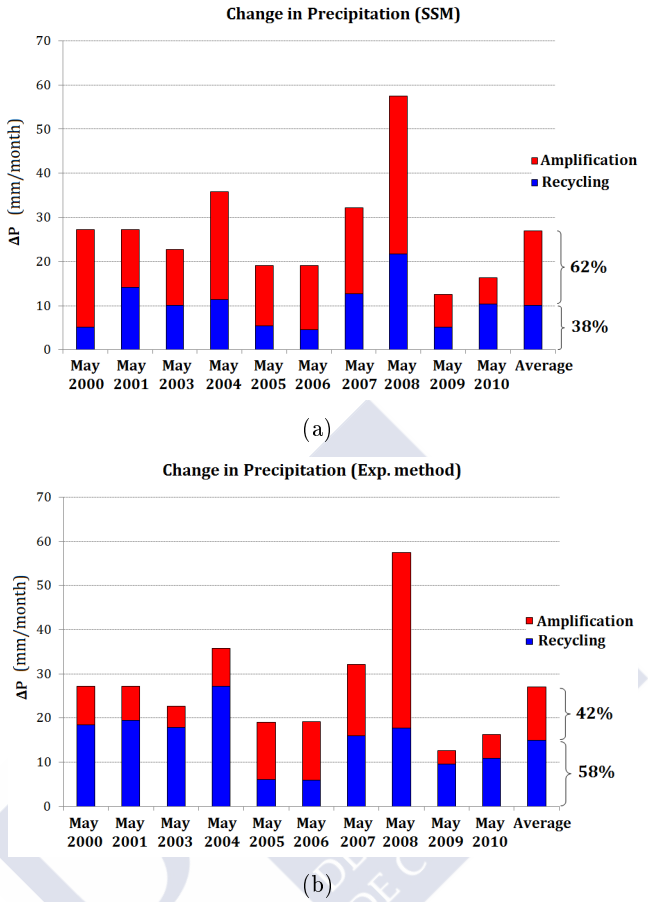

Figure 4.14: Fraction of the change in precipitation ($\Delta P = P_{\text{control}} - P_{\text{no-ET}}$, in mm month^{-1}) deriving from direct recycling (blue) and from indirect amplification (red) according to (a) SSM and (b) New experimental method, for the period May 2000 - May 2010 (with the exception of May 2002, where condition 2.28b does not hold), and average values for the complete time series.

the remaining 59%. The discrepancy between the results obtained through our procedure and via SSM is likely linked to the dependency of our estimation on the method used to calculate the recycling ratio. In Table 4.4, the results obtained via SSM are compared with those provided by our new separation method, using the two different regional recycling ratios, IMB and EBRM (new method I and II, respectively, in the Table). As discussed, recycling ratios computed via EBRM are higher than those obtained via IMB, which explains why, in general, we find:

$$\frac{r_{\text{IMB}}}{r^*} < \frac{\langle \Delta P_{rec} \rangle}{\langle \Delta P \rangle}|_{SSM} < \frac{r_{\text{EBRM}}}{r^*} \tag{4.2}$$

On average we obtain $\frac{r_{\text{IMB}}}{r^*} = 0.27$ (new method I), $\frac{r_{\text{EBRM}}}{r^*} = 0.58$ (new method

II) and $\frac{\langle \Delta P_{rec} \rangle}{\langle \Delta P \rangle}|_{SSM} = 0.38$. This analysis suggests that the rate $\frac{r}{r^*}$ might be interpreted in this case not only as an additional manner to calculate the fraction of ΔP deriving from recycling, but also as a means to estimate an uncertainty range for those values. Regardless, our results confirm that indirect amplification of precipitation generating mechanisms related to land-surface interactions plays an important role on the Iberian rainfall regime in the spring, even though computations of r via EBRM suggest that direct recycling might still be the main responsible for the increase of precipitation.

Month	$\Delta P_{\text{rec}}/\Delta P$ (SSM)	$\Delta P_{\text{rec}}/\Delta P$ (New Method, I)	$\Delta P_{\text{rec}}/\Delta P$ (New Method, II)
May 2000	0.19	0.33	0.68
May 2001	0.52	0.28	0.71
May 2003	0.45	0.29	0.79
May 2004	0.32	0.26	0.76
May 2005	0.29	0.19	0.32
May 2006	0.24	0.18	0.31
May 2007	0.39	0.27	0.50
May 2008	0.38	0.19	0.31
May 2009	0.41	0.23	0.76
May 2010	0.64	0.44	0.67
Average	0.38	0.27	0.58

Table 4.4: Fraction of the extra precipitation in May [-] coming from direct recycling (ΔP_{rec}), estimated via SSM and through our new approach based on the rate r/r^*. In the latter, the computation of r is done through both IMB method (New method I) and EBRM method (New method II). May 2002 is not represented as condition (2.28b) does not hold for this month, and thus it is not possible to compute $\Delta P_{\text{rec}}/\Delta P$ through SSM.

The average fraction of local recycling ratio ρ (computed via EBRM) to the total relative change in precipitation ρ^* is depicted in Fig. 4.13b. The impact of suppressing the water vapor fluxes, measured by ρ^* (Fig. 4.13a), is similar in pattern to the recycling ratio (Fig. 4.8) with higher values towards the east and northeast. The fraction ρ/ρ^* (Fig. 4.13b) is found to be maximized also over this area, yielding a regional value of $r_{\text{EBRM}}/r^* = 0.58$ when averaged for the whole Iberian Peninsula. The corresponding values of r_{EBRM}/r^* over the different small boxes defined in Fig. 2.2b are shown in Table 4.5. r_{EBRM}/r^* is consistently found to increase from the relative low values in the Atlantic regions (e.g. 0.23 for the northwest [NW] and 0.39 for the west [WE] boxes) to the high values toward the interior and northeast areas (0.65 for the northeast [NE], 0.66 in the east [EA] and 0.71 in the center [CE]). Notwithstanding, r^* is much larger that the recycling ratio calculated via EBRM or with any analytical method, and therefore our experiments and calculations indicate that the impact of ET fluxes on precipitation is not just related to recycling, but has a significant contribution from amplification mechanisms.

It is widely known that the impact of ET fluxes on precipitation and the recycling ratio depend strongly on the synoptic forcing (e.g. Brown and Arnold, 1998 [31]; Schär et al., 1999 [221]). The evidence comes from the case of May of 2002, when the circulating pattern, similar to a winter situation, leads to a very small r^* (3%) and recycling ratios, even though precipitation is abundant and, unlike in the winter, evaporation is as well (Fig. 4.4). When r^* is indeed high, our separation method shows that the contributions of recycling and amplification processes can vary from year to year. To investigate the mechanisms whereby ET fluxes affect precipitation and how they might diverge when there is predominantly recycling or amplification, we focus in the next section on two representative examples: May of 2004 and May of 2008. To examine each month, we use an ensemble of three control and three experimental (*no-ET*) simulations beginning at 00Z on May 1st, April 30th and April 29th, respectively. May of 2004 and May of 2008 are the two cases with the highest absolute precipitation differences between control and experiments and with a similar relative change r^* (47% and 46%), significantly above the 37% average. According to our separation method (Fig. 4.14b), both cases have a very different relative importance of recycling and amplification, with the impact of ET fluxes being mostly associated to recycling in 2004, whereas amplification dominates in 2008.

Region	May 2000-2010		
	r_{EBRM}	r^*	r_{EBRM}/r^*
NW	0.11	0.49	0.23
WE	0.13	0.33	0.39
NP	0.25	0.47	0.53
CE	0.30	0.42	0.71
SP	0.29	0.39	0.77
NE	0.32	0.49	0.65
EA	0.32	0.49	0.66

Table 4.5: Average May 2000-2010 regional EBRM recycling ratio [-], relative change in precipitation [-] and quotient of both magnitudes [-] calculated for the small boxes defined in Fig. 2.2b within the IP.

4.5 ET-Precipitation coupling mechanisms in May of 2004 and May of 2008

Synoptic configuration and precipitation

The synoptic setting for May of 2004 and 2008 is illustrated in Fig. 4.15 and briefly summarized next, highlighting the differences between both periods. Fig. 4.15a shows the average geopotential height at 850 hPa over the North Atlantic and Western Europe, obtained from ERA-Interim (Berrisford et al., 2011 [15]; Dee et al., 2011 [50]),

for May of 2004; the corresponding anomaly with respect to the average geopotential for the period May 1957 to May 2002 (from ERA-40; Uppala et al., 2005 [255]) is shown in Fig. 4.15c. During this period, the Azores high was further north than average, displacing the storm track poleward and favoring the flow with easterly or northeasterly component over Iberia. In the first half of the month, Atlantic low pressure systems still made their way south and affected the IP. In the second half of the month, with the high centered around the British Isles, only short wave disturbances in the easterly flow along the south flank of the anticyclone created conditions favorable for precipitation (of convective origin), mostly on the eastern side of Iberia. The modeled total rainfall is shown in Fig. 4.16a. As a consequence of the general circulation patterns, in May of 2004 precipitation was above the mean for the IP as a whole, however mostly concentrated on the north and eastern half, where it was frequently of convective origin, as it will be discussed below. The precipitation was anomalously high in the interior south and in the east, about average in the north, and only the northwest saw below average rainfall.

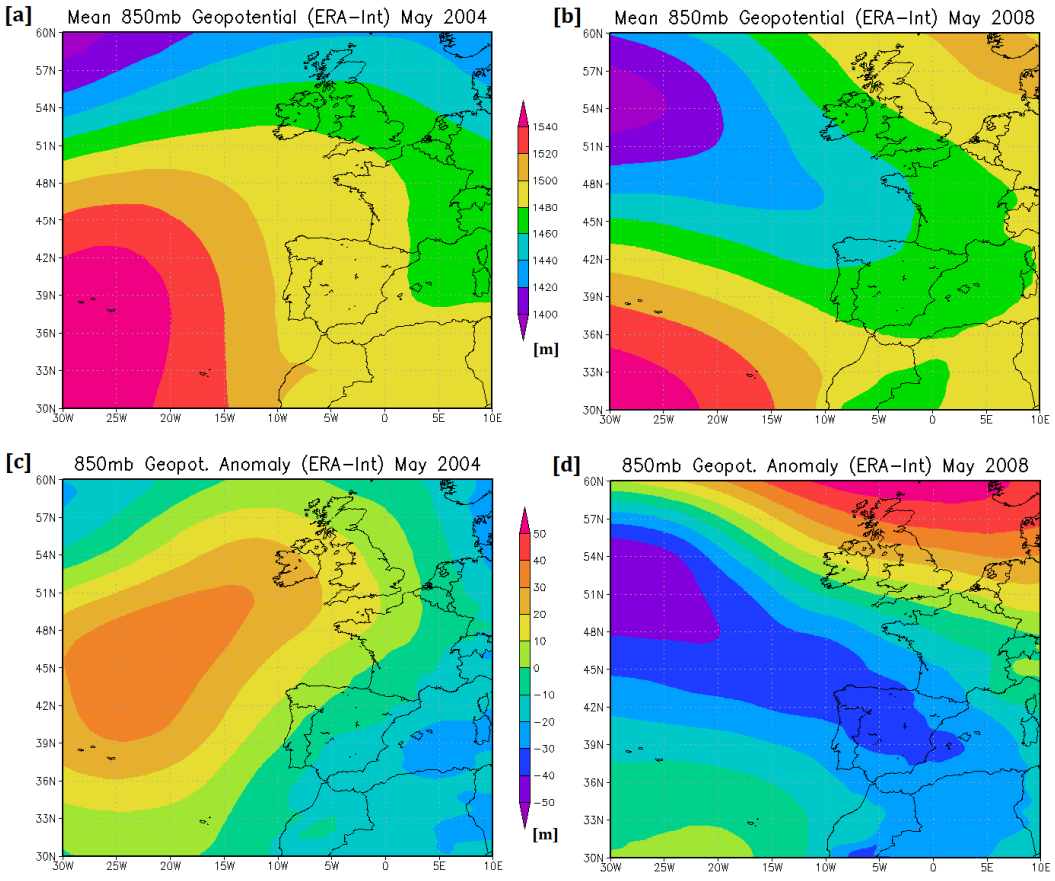

Figure 4.15: Mean geopotential height (m) at 850hPa for May of 2004 (*a*) and 2008 (*b*) from ERA-Interim dataset; geopotential anomaly (m) for May 2004 (*c*) and 2008 (*d*) with respect to the period May 1958 - May 2002 (ERA-40 dataset).

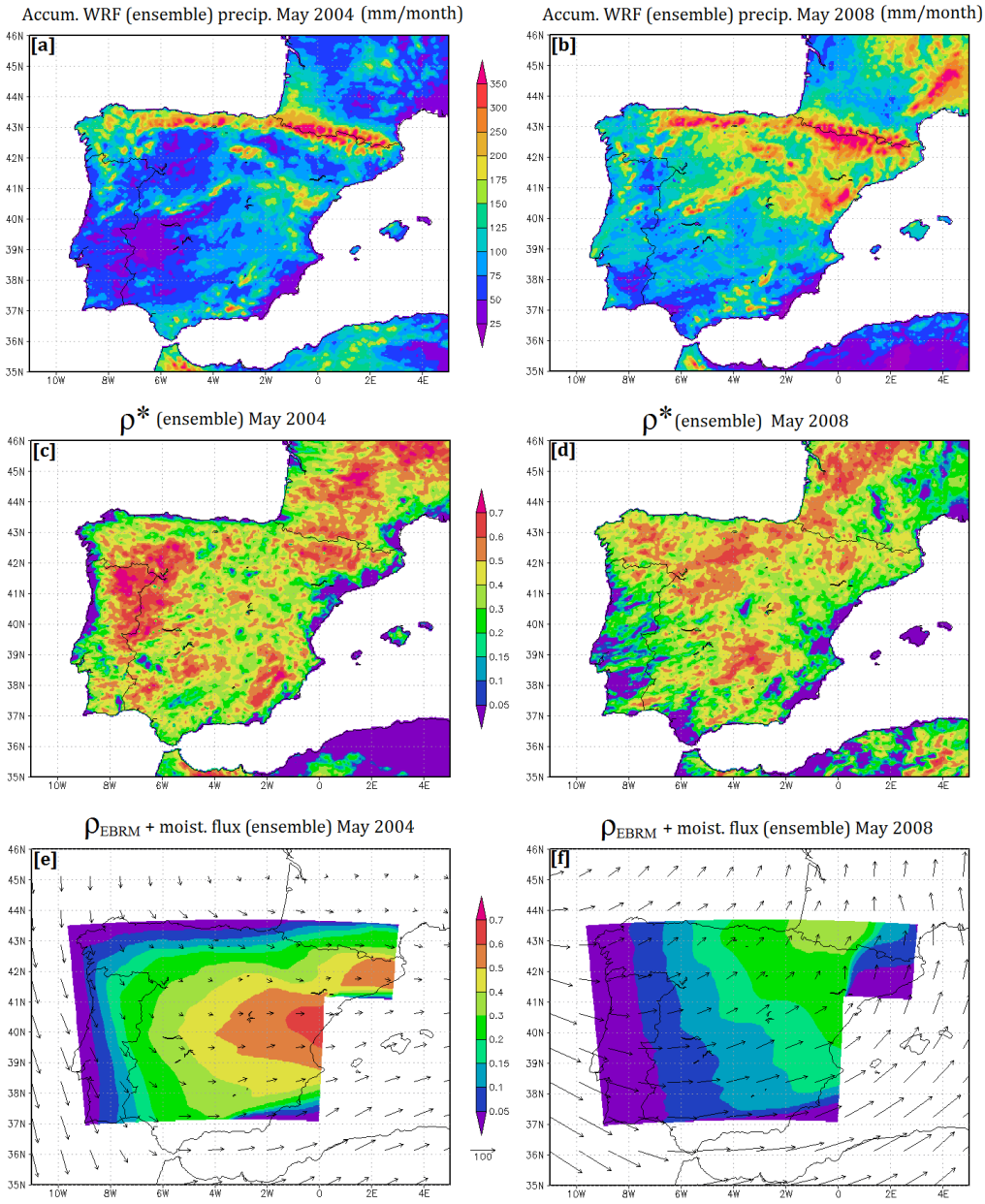

Figure 4.16: Ensemble total precipitation (mm/month) in the control simulation (*a*) and ensemble relative change in precipitation [-] for May of 2004 (*c*) and the same for May of 2008 (*b*, *d*). Ensemble recycling ratio [-] computed through the EBRM and vertically integrated moisture flux (kg^{vap} m^{-1} s^{-1}) for May of 2004 (*e*) and 2008 (*f*).

Fig. 4.15b depicts the average geopotential height at 850 hPa and Fig. 4.15d its anomaly for May of 2008. During this month, the synoptic setting was characterized by a persistent blocking high in the Norwegian Sea, with the south branch of

the split jet going right over the Iberian Peninsula. Storms followed a path across Spain and Portugal, becoming cut off from the main circulation and lingering around the IP for several days. The cold core of the cut off lows provides favorable conditions for building instability and convection over land, in particular late in the spring when solar heating is already quite significant at these mid-latitudes. The persistence of the situation is exceptional for May of 2008, but the presence of cut off low systems in the spring in the vicinity of the IP is not (Nieto et al., 2005 [187]; Nieto et al., 2007a [189]), and they were also observed in the first half of the month of May of 2004, also discussed here. May of 2008 was one of the wettest Mays on record, with largely above average or all-time-high rainfall totals in many locations in the interior, most of them in the North Plateau (León, 146.6 mm/month; Valladolid, 162.7 mm/month; Soria, 164.5 mm/month; Burgos, 194 mm/month; Segovia, 150 mm/month and Ávila, 152.5 mm/month) and northeast areas (Vitoria, 201.3 mm/month; Logroño, 199.4 mm/month; Zaragoza, 141.9 mm/month, Teruel, 125.9 mm/month) (http://www.aemet.es/documentos/es/elclima/datos_climat/resumenes_climat/mensuales/2008/res__mens_clim_2008_05.pdf). Vigorous convection and abundant moisture supply were responsible for most of these large precipitation amounts, with the instability favored by the cold air aloft associated to the cut off low systems in the area, so frequent during this particular month. The model produces realistic results, with rainfall amounts that agree well with the aforementioned station values (Fig. 4.16b).

Recycling and r^* values

Figs. 4.16c and 4.16d depict ρ^*, the ensemble average relative change in precipitation in the control runs with respect to the experiments where ET fluxes are removed over land, for May of 2004 and May of 2008, respectively. Despite the very different synoptic patterns, in both cases the relative change in precipitation is high in all regions, in areas with large and low precipitation amounts alike. The mean numbers for the whole Iberian box are almost identical, with $r^* = 0.47$ for 2004 and $r^* = 0.46$ for 2008, indicating that ET fluxes have a sizeable impact on precipitation during these periods. The key feature that in our analyses separates both cases is the value of the recycling ratio, shown for EBRM together with the mean, vertically integrated moisture flux in Figs. 4.16e and 4.16f for 2004 and 2008, respectively. For May of 2004, $r_{\mathrm{EBRM}} = 0.28$, which is significantly large, representing 27% above the 0.22 average; in contrast, for May of 2008, $r_{\mathrm{EBRM}} = 0.14$, about half of that of 2004 and considerably below average. Using the IMB to calculate r, the same reasoning applies, but there is much less spread in the values, with the multi-year average being $r_{\mathrm{IMB}} = 0.10$ and, for 2004 and 2008, $r_{\mathrm{IMB}} = 0.11$ and $r_{\mathrm{IMB}} = 0.08$, respectively. As it was discussed before, EBRM recycling ratios are strongly linked to the mean moisture flux, thus the difference in contribution of recycling and amplification processes toward the impact of ET fluxes on precipitation should be also related to it. In 2004, when recycling is

the main process whereby ET fluxes affect precipitation, the mean moisture flux with a general westward direction is much weaker than normal, indicating the large-scale moisture supply, from the Atlantic Ocean for the most part, is much diminished. The reason for this is the predominant easterly flow from the Mediterranean for part of the month (Fig. 4.16a), which is drier, particularly at upper levels. The contrary happens in May 2008: recycling has a reduced importance, and this is likely due to the stronger than normal moisture flux from the Atlantic, as a consequence of the synoptic pattern discussed earlier.

Water budget, CAPE and convective events

The daily time series of the water budget terms for the IP is shown for May of 2004 in Figs. 4.17a and 4.17c (*control* and *no-ET* experiment) and likewise for May of 2008 in Figs. 4.17b and 4.17d. ET is drawn for the *no-ET* experiment only for reference, as it is removed from the system and not incorporated into the atmosphere, following the experiment's design. The spread of the three ensemble members for each case is reflected in the error bars in each term. In addition, Figs. 4.17e (2004) and 4.17f (2008) display, for control (red dotted line) and experiment (purple dotted line), the daily area average of CAPE at 12Z (noon, 2pm local time) weighted by the total precipitation for the day n:

$$\langle CAPE \rangle_n^{12Z} = \frac{\int_A CAPE_n^{12Z}(x,y) P_n(x,y) dxdy}{\int_A P_n(x,y) dxdy} \tag{4.3}$$

The convective available potential energy, CAPE, is an indicator of the convective nature of the precipitation process, increasing with warmer and moister conditions at the low levels of the atmosphere (DeAngelis et al., 2010 [49]). Note that high values of CAPE alone might not be sufficient for intense convection to occur, since this magnitude accounts for the *potential* capability of the system to trigger convection. Therefore, as shown by DeAngelis et al. (2010) [49], a favorable synoptic configuration is also a necessary requirement.

When the ET fluxes are not considered (Figs. 4.17c and 4.17d), major rain events coincide very clearly with moisture convergence peaks, even though not always that there is convergence of moisture there is precipitation (for example the last week of May 2004 or the first week of May of 2008). Rainfall amounts also match very closely the external supply of humidity, as expected, for there cannot be recycling with ET fluxes disabled. In these *no-ET* experiments, CAPE (purple line in Figs. 4.17e and 4.17f) is in general small for both years. In 2004 only the second half of the month shows CAPE amounts indicative of significant convective activity, but precipitation totals are not very important beyond the local scale. In 2008, only the largest precipitation event, around the 22$^{\text{nd}}$ of the month, has some CAPE associated.

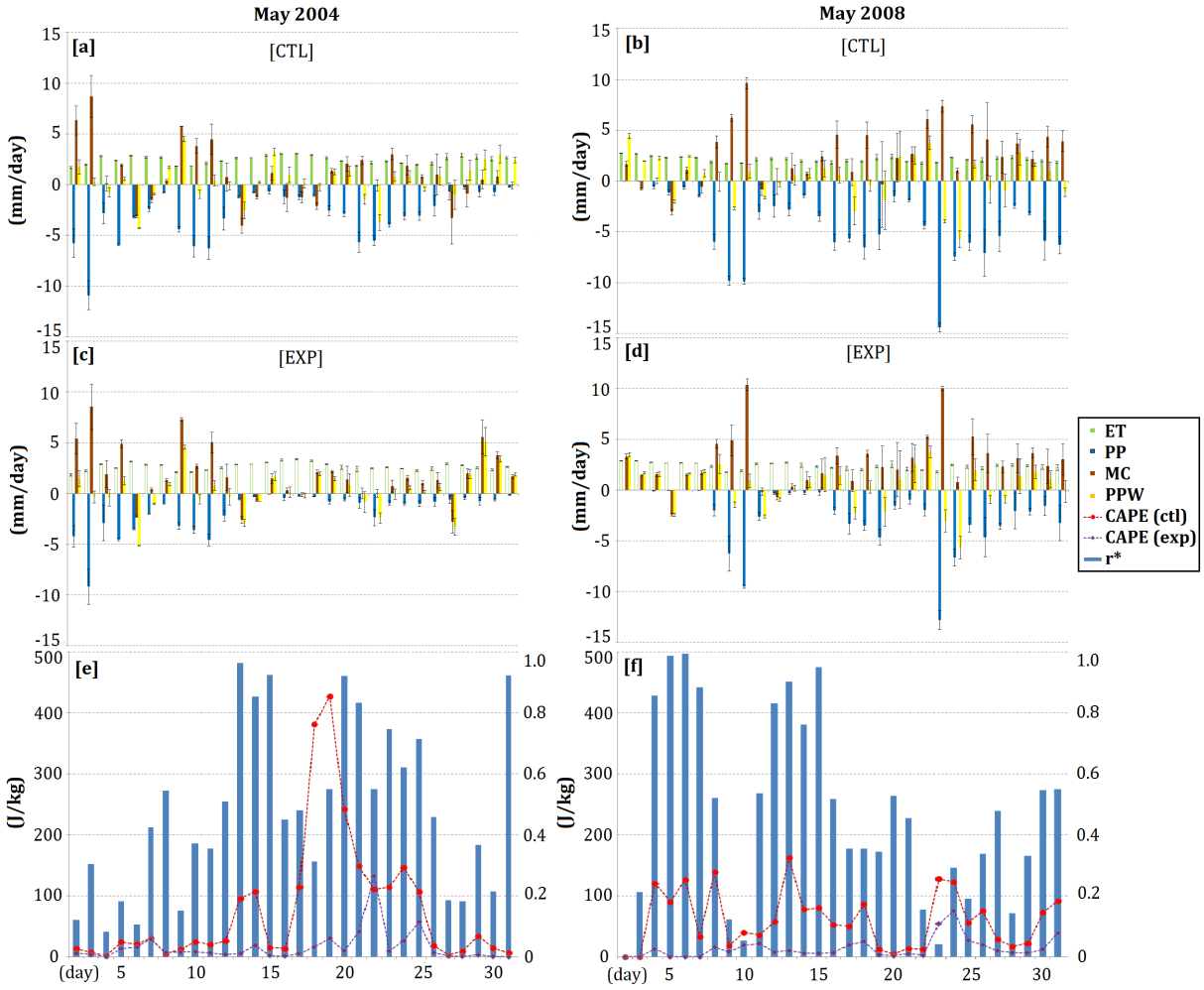

Figure 4.17: Daily time series of the ensemble mean water budget terms (mm/day) in the Iberian Peninsula for control simulation (May of 2004, *a*; May of 2008, *b*) and *no-ET* experiment (May of 2004, *c*; May of 2008, *d*) (note that precipitation values are displayed as if they were negative, only to help the eye). Daily values of ensemble mean CAPE (J/kg) in control (red line) and experiments (purple line) and r^* [-] (blue bars) for May of 2004 (*e*) and 2008 (*f*) are also shown.

The impact of the surface moisture fluxes is noticeable when comparing the *no-ET* experiments results (Figs. 4.17c and 4.17d) to the respective panels for the control simulations (Figs. 4.17a and 4.17b). The events in the *no-ET* experiments for both years, which reflect only external forcing and moisture supply, have a correspondence in each control run. In May 2004 there are two distinct periods: the first half of the month, where the impact of surface moisture fluxes on precipitation is relatively small and the second half, when there is little precipitation in the experiment with no ET over land, but a major and long-lasting rain event in the control run, with a very large

relative difference in precipitation between both runs (see the high values of r^*, bars in Fig. 4.17e). Recalling the discussion on the synoptic setting for this month, the first part of the month is a period of precipitation caused by Atlantic storm systems, while the second one has precipitation caused by short wave disturbances on easterly flow, much drier, particularly at upper levels. When the synoptic forcing and moisture supply are strong (the first half of the month), ET fluxes have a limited impact on rainfall; however when the large-scale forcing is weaker and the advection of moisture is not very large, the effect of the surface fluxes is maximized. Fig. 4.17e shows a very large increase in CAPE (purple line) and precipitation during this latter part of the month and our calculations of the recycling ratio indicate that the land surface supply of moisture is a very significant source for the precipitated water in this case.

In May of 2008 the situation is more homogeneous during the whole month. In general, ET fluxes increase the moist static energy at low levels and CAPE, as shown in Fig. 4.17f, but the increase is not as dramatic as in the second half of May of 2004. The time series of r^* (bars in Fig. 4.17f) indicate that the impact of surface moisture fluxes is small (low r^*) when the large-scale forcing and precipitation are the highest around the 10th and the 24th, and bigger (higher r^*) when the forcing is not so strong at the onset of those main rainfall episodes and as they fade out. This coincides in general with the previous discussion for May of 2004: the effect of ET fluxes is important in convective prone situations (added low level moisture can increase CAPE) and when the synoptic forcing is weaker; however, the influx of external moisture seems to be the factor determining whether recycling or amplification effects are more relevant. As it is also shown in Table 4.1, the advection term is significantly higher in May of 2008 than in May of 2004 and therefore the importance of the local source of moisture for precipitation (i.e. recycling) is enhanced in the latter month, for there is not enough external moisture supply to support any significant rainfall. The large-scale environment favors precipitation, but ET provides a final "push" by increasing CAPE and moisture to produce the rain. In contrast, the positive value of moisture convergence (principally at low levels) in May of 2008 suggests that, when the external moisture supply is significant, the role of surface moisture fluxes is less decisive in those convective favorable situations, and it is mostly directed to increase the efficiency of the precipitation mechanism, that is, the amplification term becomes predominant.

The connection between external moisture supply and the amplification or recycling role of land surface moisture fluxes is illustrated in Fig. 4.18, showing (for all the years in our experiments) the fraction of the difference in precipitation between control and *no-ET* experiment (ΔP) that our method attributes to amplification (the complimentary would be the recycling fraction) versus the monthly total influx of water in the Iberian box. The positive correlation between the monthly inward moisture flux and the fraction of ΔP related to amplification is apparent, or inversely, the more external moisture advection, the less recycling. These results depend as well on the type of precipitation (convective or not) and the strength of the large-scale

forcing, as discussed previously, but in general they show that the role of the surface moisture fluxes turns from being mostly the moisture source (recycling) to enhance the efficiency of the precipitation process as the external moisture supply increases.

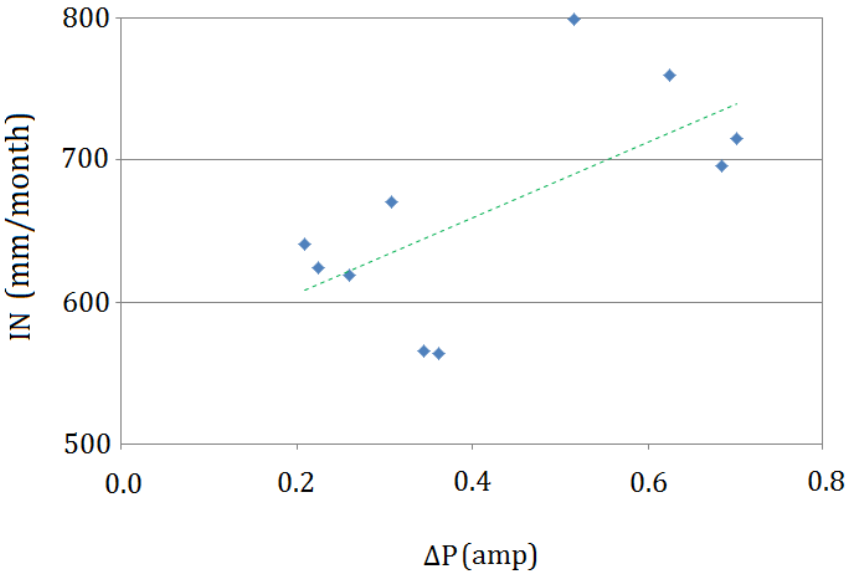

Figure 4.18: Relationship between the average inward moisture flux (IN, mm/month) and the fraction of ΔP originating from amplification [-], for the period May 2000 - May 2010 (with the exception of May 2002). The correlation coefficient is $R = 0.66$.

The effect of ET fluxes in enhancing CAPE and thus the likelihood of convection is also apparent in Fig. 4.19, which represents the monthly ensemble CAPE at 12Z for May of 2004 (panel *a*) and May of 2008 (panel *b*), as well as the corresponding ensemble CAPE difference between *control* and *no-ET* simulations (panels *c* and *d*). In general, the areas with highest CAPE tend to overlap with those regions where CAPE difference between *control* and experiment is more relevant, thus confirming the relevant role of ET in enhancing unstable atmospheric conditions.

The connection between high CAPE values and increased precipitation is further explored in Fig. 4.20, showing two selected rainfall events in May of 2008. Panels *a* and *c* show the ensemble map of CAPE difference (*control* minus *experiment*) at 12Z for two specific days (8^{th} and 31^{st} May 2008), whereas panels *b* and *d* represent the associated precipitation, accumulated during the subsequent six hours (that is, from 12Z to 18Z). These examples provide further evidence of the critical role of local ET fluxes (and land-atmosphere interactions, in general) on increasing the convective activity. This results in a surplus of precipitation which becomes essential for the sustainability of large interior, semiarid regions.

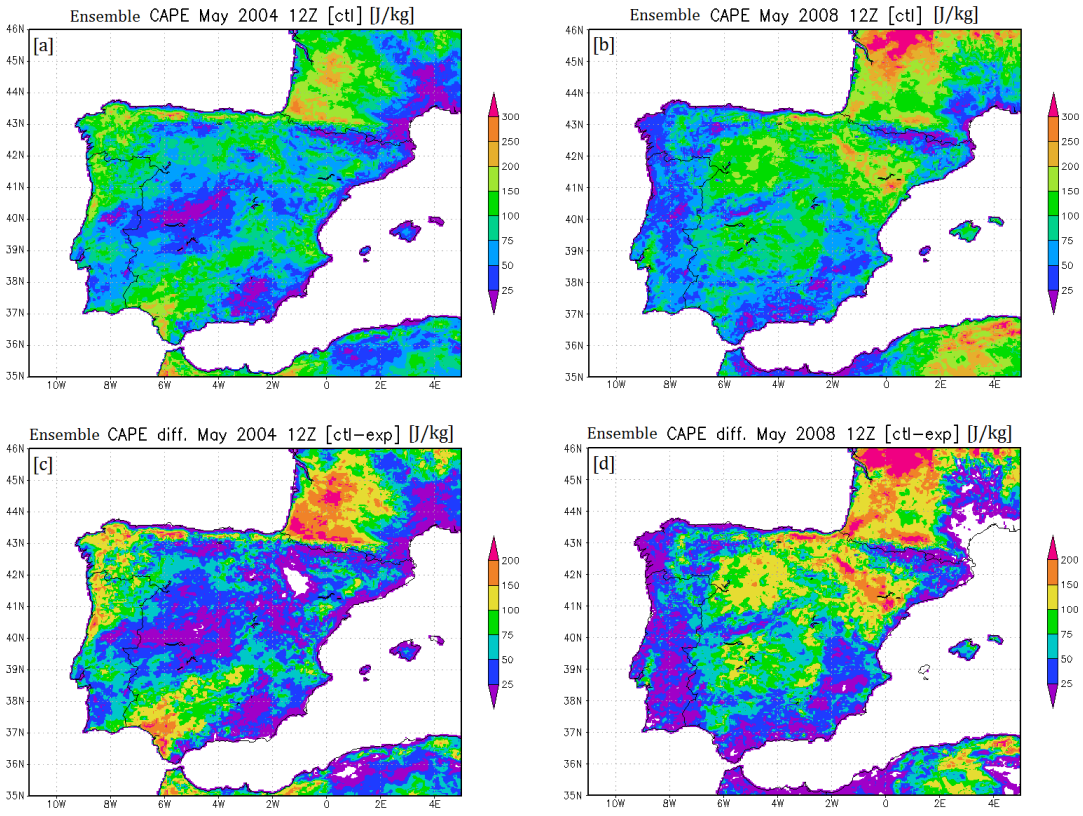

Figure 4.19: Monthly ensemble CAPE (J/kg) at 12Z for May of 2004 (*a*) and May of 2008 (*b*). Panels *c* and *d* show the corresponding CAPE differences (J/kg) between *control* and *no-ET* simulations.

4.6 Conclusions of this chapter

The objective of the study presented in this chapter is to investigate the role of ET fluxes on the precipitation regime of the interior of Iberia. Shielded from maritime influence by the configuration of the relief, the semiarid interior lands present a peak of precipitation in late spring, in contrast with the Atlantic coastal areas, with one rainfall maximum in autumn-winter, and the Mediterranean shore, with the maximum in early autumn. The coastal areas follow mostly large-scale forcing and moisture supply, whereas the interior diverges in some cases very markedly from this trend. We investigate the role of land-surface interactions in precipitation processes in the latter region.

We used data from high-resolution (5 km) simulations with the WRF-ARW model, for eleven months of May (from 2000 to 2010). To test the model response and sensitivity to seasonal differences in synoptic configuration, we also carried out model runs for the eleven months of January of the same years. For each month, we

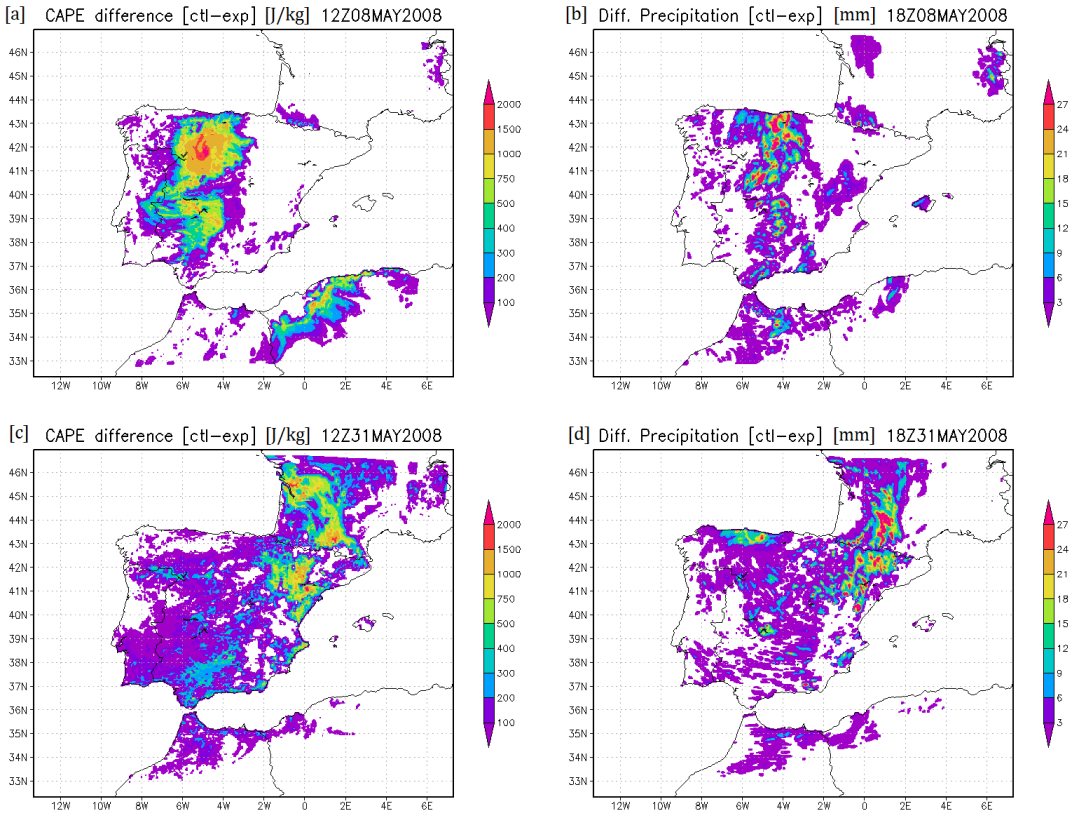

Figure 4.20: Ensemble CAPE differences (J/kg) between *control* and *no-ET* simulations, at 12Z, for two specific days (8th and 31st May 2008, panels *a* and *c*). Panels *b* and *d* represent the total precipitation (mm) accumulated in the subsequent six hours (from 12Z to 18Z of the same days).

performed two simulations: a control experiment and a *no-ET* experiment where the ET water flux to the atmosphere over land was eliminated, although the corresponding latent heat flux was still considered in the surface energy budget. The *no-ET* experiments bring out the effect of surface water fluxes on precipitation dynamics, both the direct or recycling component and the indirect or amplification contribution. From the control results we calculate the standard recycling ratio r via two different methods: the IMB (Schär et al., 1999 [221]), and the EBRM, by Eltahir and Bras (1994) [76]. In addition, we compute the relative change in precipitation r^* between control and *no-ET* runs. The comparison between both variables gives a first assessment of the impact of ET fluxes on precipitation processes. The recycling ratio is a measure of the percentage of rainfall that comes from local ET and, in the *no-ET* experiment, this local ET is eliminated. As a result, similar values of the recycling ratio and the relative change in precipitation would indicate that the role of ET fluxes is to simply provide more water for precipitation and that they have limited impact on dynamics. This is the case for the January simulations when, as

expected, the regional recycling ratio is small, as winter ET is moderate and the effect of ET fluxes is reduced since precipitation comes mostly from large-scale forcing and oceanic moisture supply associated to fronts in Atlantic baroclinic systems. On average, ET fluxes over land provide only 5% of the total moisture for precipitation in these January simulations. The situation for May is different: the multiannual average of the relative change in precipitation between control and *no-ET* experiments, r^*, reaches 0.37 for the IP as a whole, meaning that on average it rains about 37% less if ET is eliminated from the system. The pattern of r^*, with high values towards the interior north and northeast resembles the area where observations indicate an annual maximum of precipitation in May, suggesting that surface moisture fluxes do have an important effect in rainfall dynamics in spring in those regions, as we had hypothesized. The regional recycling ratio, r, is 0.23 via EBRM and 0.10 according to IMB, which are relatively high values, evidencing an important role of local ET as a water source for precipitation. The differences between the experimental change in precipitation and the recycling ratios in spring indicate that the soil moisture - precipitation coupling cannot be interpreted exclusively in terms of moisture recycling, and that ET fluxes have a significant effect on precipitation dynamics, apart from being an important water source for rainfall.

We quantified the recycling and amplification contributions to the increase in precipitation in the control with respect to the *no-ET* experiments, ΔP, via two different methods: the SSM (Schär et al., 1999 [221]), and a new approach based on parameters r and r^*, whose ratio we show to be an estimate of the recycling contribution to ΔP. In addition, using EBRM recycling ratios with the later method allows us to analyze the spatial variability of the recycling ($\langle \Delta P_{\mathrm{rec}} \rangle$) and amplification ($\langle \Delta P_{\mathrm{amp}} \rangle$) components. Average results in May for ΔP_{rec} computed with this procedure vary significantly in the general west-southwest direction of the mean circulation, as ρ and ρ^* do, increasing from relative low values in the Atlantic regions (0.39 for the west and 0.23 for the northwest) to high values toward the interior and northeast areas (0.71 in the center, 0.66 in the east and 0.65 for the northeast). This suggests that direct recycling might be the main contribution to the extra spring precipitation observed in inland Iberia, with this predominance over the amplification mechanisms becoming less clear as we consider the Peninsula as a whole, mostly because in the western areas with plenty of external maritime moisture advection, the recycling contribution is small. In those Atlantic regions, the impact of ET fluxes on precipitation is also reduced, especially when comparing to the interior and northeast. If we consider only the part of Iberia where ET fluxes really make a difference in precipitation amounts, our experiments indicate this is mostly through recycling; nevertheless the extra precipitation produced by amplification mechanisms is far from being negligible, and it is very relevant in areas with semiarid climate like these, as it incorporates external moisture to the regional water budget.

Results for individual years show that the impact of ET on precipitation depends on synoptic forcing, with precipitation associated to frontal systems with relatively

strong moisture inflow being less affected by land surface vapor fluxes. When conditions are more favorable for free convection, the impact of ET fluxes is important, and the relative contribution of amplification or recycling depends on the availability of external, advected moisture. ET fluxes moisten the boundary layer and increase the potential for convection. In general, precipitation events, always triggered by synoptic forcing, have a stronger start and ending in the control simulations than in the experiments without ET and there is a positive correlation between external moisture availability and the significance of amplification effects. It is under weak synoptic forcing that ET water vapor fluxes have a greater impact on precipitation, because the extra moist static energy at lower levels can strengthen the effect of a feeble moisture convergence and produce precipitation that otherwise would not have occurred at all or to a much less extent. While recycling of local water vapor is predominant in this case, there is also a component of total rainfall from external sources that it is included into the regional water budget because of this amplification effect on precipitation dynamics.

These conclusions are drawn from model simulations that may have some deficiencies in simulating precipitation, particularly when it is convective. Nevertheless, the fact that the most sensitive area to the suppression of ET fluxes over Iberia is the interior north and northeast agrees well with the regions observed to have a distinct precipitation cycle with a maximum in May and indicates that the role of land-surface moisture fluxes in rainfall processes there could be the explanation. Estimating to which extent this role is being the water source or to amplify rainfall dynamics depends more on the method to calculate the recycling ratio, since its values can diverge significantly when using different approaches. We make use of analytical recycling models that rely on assumptions, such as that moisture from ET mixes well through the column, which may not be very true, particularly when there is significant wind shear. Simulations including moisture tracers, as those presented in the next chapter, are thus necessary to calculate the recycling ratio precisely and give an unequivocal answer to this question.

5

Regional climate simulations with moisture tracers to investigate the spring peak of rainfall in inland Iberia

Abstract. In this chapter, eleven monthly simulations are carried out with the WRF model along the period May 2000 - May 2010. A new computational tool is used, consisting of moisture tracers implemented in the WRF model that allow tracking the trajectories of the water molecules evapotranspired within the Iberian Peninsula. The aim of this experimental investigation is twofold: on the one hand, quantifying the intensity of the recycling mechanism in May through the explicit method of moisture tracers (MMTR); on the other hand, using these MMTR recycling values to provide a definitive assessment of the relative contribution of both recycling and amplification mechanisms to the upturn of precipitation in spring observed throughout the interior of the Iberian Peninsula. As expected, the MMTR method accounts for the spatial heterogeneity of the recycling patterns with accuracy, in contrast with the smooth distribution of the local recycling ratio obtained through the EBRM method due to Eltahir and Bras (1994). The latter procedure is confirmed to depend excessively on the monthly mean moisture flux, showing a tendency to overestimate recycling. The highest MMTR recycling values are more evenly spread over the interior areas of the northern half of Iberia, with particular relevance in the North Plateau, the Iberian and Central Systems and the Pyrenees, where average recycling values in May are found to be close to 20%. On average for the Iberian Peninsula, the May mean regional MMTR recycling ratio is 0.11, very close to the 0.10 obtained through the IMB method by Schär et al. (1999) and significantly below the EBRM mean regional value (0.22). Additionally, MMTR recycling ratios are used to asses the

relative weight of both recycling and amplification contributions to the spring peak of precipitation, revealing that on average, and for the entire Iberia, 72% of the surplus of precipitation related to land-air interactions in May is due to amplification mechanisms. Nevertheless, under a weak synoptic forcing, as it is the case e.g. with the month of May of 2004, the recycling contribution is found to be predominant in large interior regions. Finally, the vertical distribution of moisture tracers is analyzed, confirming the limitations of the well-mixed atmosphere hypothesis, which is indeed one of the mainstays of traditional recycling models.

*****

In the previous chapters, we provided experimental evidences of the crucial role that evapotranspiration fluxes play in the spring precipitation regime of the Iberian Peninsula. In some interior regions, locally evapotranspired moisture was found to be responsible, directly or indirectly, for over 50% of the total precipitation. In chapter 4, a new method to separate those direct (recycling) and indirect (amplification) contributions to the spring surplus of precipitation was applied. The most relevant limitation of this procedure is linked to the high uncertainty in the recycling calculations, excessively dependent on the methods used. In this chapter, we compute the local recycling ratio during eleven months of May (from May 2000 to May 2010) through the more accurate method of moisture tracers (MMTR). For this purpose, monthly simulations with the WRF model over the Iberian Peninsula, including moisture tracers that allow tracking the trajectories described by the water molecules, are carried out. This constitutes, nowadays, the more accurate procedure to calculate the recycling ratio. The aim of the study presented in this chapter is twofold: first, we want to quantify the intensity of the recycling mechanism in May (a crucial month in terms of precipitation in the Iberian Peninsula, as it has been discussed) through a more accurate method; and second, we use these MMTR recycling values to provide a final assessment of the relative contribution of recycling and amplification mechanisms to the spring peak of rainfall.

As mentioned in section 2.1, the WRF model simulations presented and discussed in this chapter (WRFS-3 set of simulations) are carried out over the same model domains as those used in WRFS-2 runs. Moreover, the same horizontal resolution, initial and lateral boundary conditions and model options and parameterizations are selected. As a consequence, and even though WRFS-3 simulations use a more recent version of the WRF model, for this preliminary study we assume that the results obtained from WRFS-2 and WRFS-3 simulations can be comparable. Such comparison is of the greatest interest to complement the analysis presented in chapter 4.

5.1 Computation of the recycling ratio: the method of moisture tracers (MMTR)

As described in section 2.4, local and regional recycling ratios can be directly computed through the method of moisture tracers from equations (2.17a) and (2.17b). In this section, we present the results obtained through the MMTR method and compare them to those presented in chapter 4, in accordance with the previous discussion.

Local MMTR recycling ratio

In Fig. 5.1 the multiannual average of local MMTR recycling ratio over the period May 2000 - May 2010 is shown. The area where the moisture tracers are activated, and therefore the evapotranspired water molecules consequently tagged, is also represented. MMTR recycling ratios exceeding 10% are found throughout most of the interior, eastern and northeastern Iberia. Moreover, in some areas in the North Plateau, the Iberian and Central Systems and the Pyrenees, average recycling values are close to 20%. This average recycling pattern accounts more accurately for the spatial heterogeneity of the recycling mechanism, in contrast to the smooth recycling distribution produced by the EBRM method (Fig. 4.8), excessively dependent on the prevailing wind direction, as discussed in section 4.3. This feature is responsible for the most relevant difference between both average recycling patterns (MMTR, Fig. 5.1, and EBRM Fig. 4.8): whereas the EBRM distribution presents the higher values to the east and northeast, as a result of the prevailing direction of the moisture flux, the MMTR values are more spread over interior lands of the northern half of Iberia, drawing a more realistic pattern. This shows that the EBRM method tends to distort the recycling distribution because its depends too much on the predominant wind direction. In addition, the comparison between both figures shows a tendency of the EBRM method to significantly overestimate recycling, as EBRM values more than double the MMTR results in the areas to the east and northeast.

This overestimation can be examined in more detail by comparing the monthly MMTR maps from May 2000 to May 2010, represented in Fig. 5.2, with the corresponding EBRM spatial patterns, represented in Fig. 4.9. To facilitate comparison, the correponding multiannual averages are also represented (panel l in both figures). In general, for those months affected by a more intense circulation, as it is the case with 2005 or 2008, the qualitative distribution of the EBRM recycling values essentially corresponds to that obtained through the MMTR, even though the latter produces significantly lower values, as indicated, and they are more heterogeneously distributed. In May of 2002, consistently low MMTR recycling values are observed, coinciding with an intense zonal circulation, typical of the winter months, as discussed in section 4.3. In contrast, in May of 2000, 2001 or 2004, with synoptic configurations that favor, to a greater extent, the development of convective structures, we found

high MMTR recycling ratios in large areas of the interior, with values close to or even exceeding 30%. In the months of May 2002 and May 2006, the EBRM method is unable to account for the high recycling values obtained through the MMRT in the southwest and in the northeast of Portugal, respectively. This suggests that the EBRM method might be considered only as an approach to study the intensity of recycling, since the consideration of mean moisture fluxes alone is not sufficient to reproduce the real recycling patterns accurately. The procedure based on moisture tracers is much more reliable, since it is able to follow the trajectories of the water molecules and thus reproduce the spatial details of the recycling mechanism.

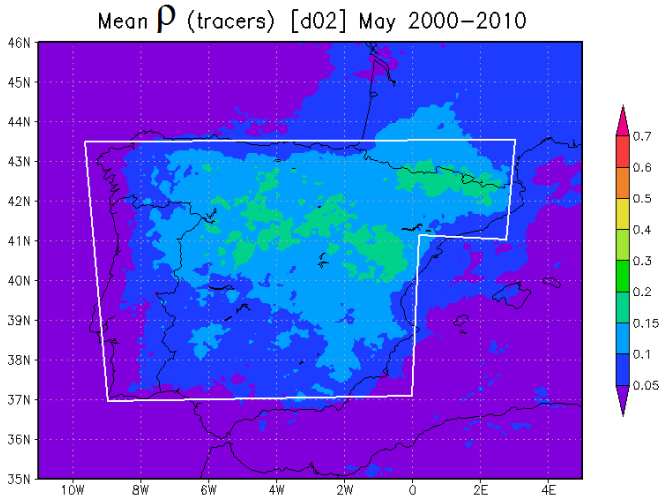

Figure 5.1: Multiannual average of the local recycling ratio [-] computed through the MMTR (May 2000 to May 2010).

Regional MMTR recycling ratio

Local MMTR recycling values are integrated over our study region to obtain the corresponding regional MMTR recycling ratios. They are presented in Table 5.1, together with the corresponding IMB and EBRM values, taken from Table 4.2. An average regional MMTR recycling value of 0.11 is obtained for the Iberian Peninsula in May along the considered period (2000-2010), ranging from 0.05 in 2002 to 0.13 in 2004. This average value is very close to that obtained through the IMB method (0.10) and exactly half of the one computed through the EBRM method (0.22). This occurs along the whole series, with IMB values tending to slightly underestimate recycling and EBRM values even doubling, in many cases, the MMTR ratios. It is interesting to note that the IMB (a much less sophisticated method than the EBRM) gives rise to regional recycling estimates that are much closer to the accurate computations by MMTR. The latter method, as discussed, constitutes the best procedure to estimate

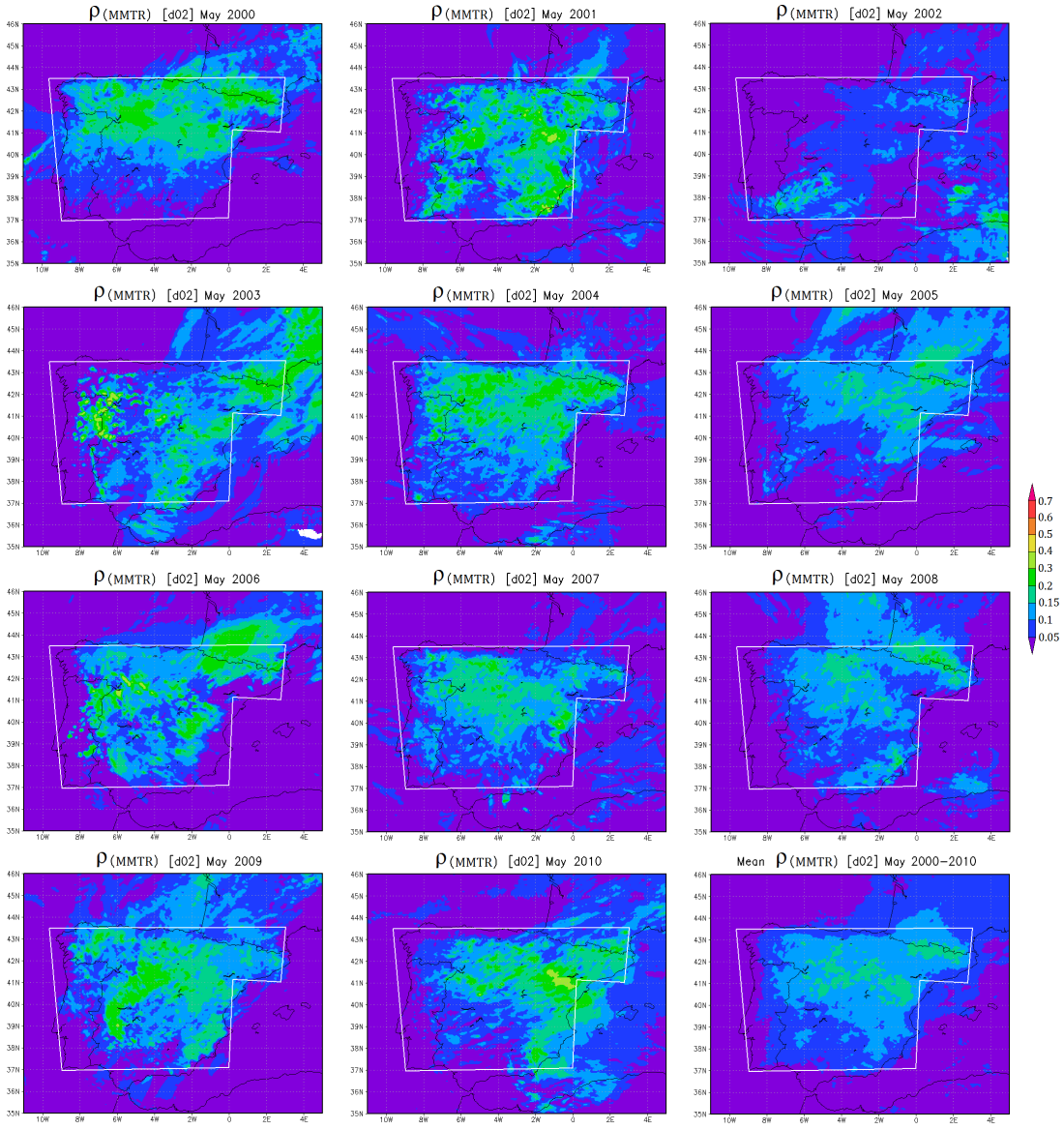

Figure 5.2: Spatial distribution of the local MMTR recycling ratio [-] during the period May 2000 (panel *a*) to May 2010 (panel *k*) and multiannual average (panel *l*).

the recycling ratio. More evidence of this fact is given by looking at the MMTR, IMB and EBRM values of May 2002 and May 2004. According to the synoptic configuration of these months (section 4.4), the intensity of recycling is expected to be very low in 2002 and significantly higher than average in 2004. Among the three methods, the MMTR is clearly the one that better reflects these variations.

Month	r_{MMTR}	r_{IMB}	r_{EBRM}	r^*	r_{MMTR}/r^*
May 2000	0.12	0.10	0.21	0.31	0.39
May 2001	0.11	0.12	0.31	0.43	0.26
May 2002	0.05	0.09	0.14	0.03	-
May 2003	0.12	0.11	0.31	0.39	0.30
May 2004	0.13	0.11	0.31	0.41	0.32
May 2005	0.10	0.09	0.15	0.48	0.21
May 2006	0.11	0.10	0.16	0.53	0.21
May 2007	0.10	0.09	0.17	0.34	0.30
May 2008	0.09	0.08	0.13	0.42	0.23
May 2009	0.12	0.11	0.35	0.47	0.26
May 2010	0.11	0.13	0.20	0.30	0.36
Average	0.11	0.10	0.22	0.37	0.28

Table 5.1: Recycling ratio [-] computed via MMTR, IMB and EBRM, regional relative changes in precipitation (r^*) [-] and rate r_{MMTR}/r^* [-] for the period May 2000-2010.

5.2 Relative contribution of recycling and amplification mechanisms: a final assessment with MMTR

As mentioned at the beginning of this chapter, WRFS-2 and WRFS-3 sets of simulations are comparable. Taking advantage of this feature, Table 5.1 includes the monthly regional relative changes in precipitation, r^*, computed in chapter 4, as well as the rates r_{MMTR}/r^*. The latter magnitude accounts for the recycling contribution to the surplus of rainfall in the control runs with respect to the *no-ET* experiments conducted in chapter 4 (see section 2.7 and, in particular, equations 2.47 and 2.48). Average results show that the direct or recycling contribution is responsible for 28% of the increase in precipitation that is observed when the ET fluxes are not eliminated (Table 5.1), with this magnitude ranging from 21% in May of 2005 and 2006 to 39% in May of 2000. On average, the remaining 72% of the increased precipitation is related to amplification processes, which are confirmed to be the predominant mechanism when the whole Iberian Peninsula is considered. The above calculated 28% value of recycling contribution is very close to the average 27% obtained when the regional recycling ratio is computed through the IMB method (r_{IMB}/r^*; Table 4.4). In contrast, the corresponding EBRM value reaches 58% (r_{EBRM}/r^*; Table 4.4). On the other hand, average r_{MMTR}/r^* does not differ significantly from SSM estimate (section 4.4), where 62% of the increased May precipitation is found to be related to amplification and the remaining 38% to recycling.

The relative weight of recycling and amplification contributions is not uniform over Iberia, as it has already been discussed in chapter 4, where the average map of $\rho_{\mathrm{EBRM}}/\rho^*$ was calculated (Fig. 4.13b). The corresponding pattern using the more

accurate MMTR recycling ratio is shown in Fig. 5.3. According to the previous discussion, the most relevant difference between the $\rho_{\mathrm{EBRM}}/\rho^*$ map (Fig. 4.13b) and the $\rho_{\mathrm{MMTR}}/\rho^*$ pattern (Fig. 5.3) is again that the highest values are more evenly distributed over the interior lands of the northern half of the Iberian Peninsula in the latter representation, in contrast with the less realistic $\rho_{\mathrm{EBRM}}/\rho^*$ pattern, where the highest values occur in the east and northeast and are related to the high EBRM recycling values obtained in these areas. All over the northern half of the IP, the average recycling contribution can be as relevant as the amplification term, with $\rho_{\mathrm{MMTR}}/\rho^*$ exceeding 50% in some concrete areas over the North Plateu, Iberian and Central Systems, Pyrennes and even the western sector of the Cantabrian Mountains (Fig. 5.3). In the interior areas of the South Plateau, as well as in the great valleys of the Guadalquivir, Guadiana, Tagus and Douro rivers, indirect or amplification processes have clearly a predominant impact on the local rainfall regime.

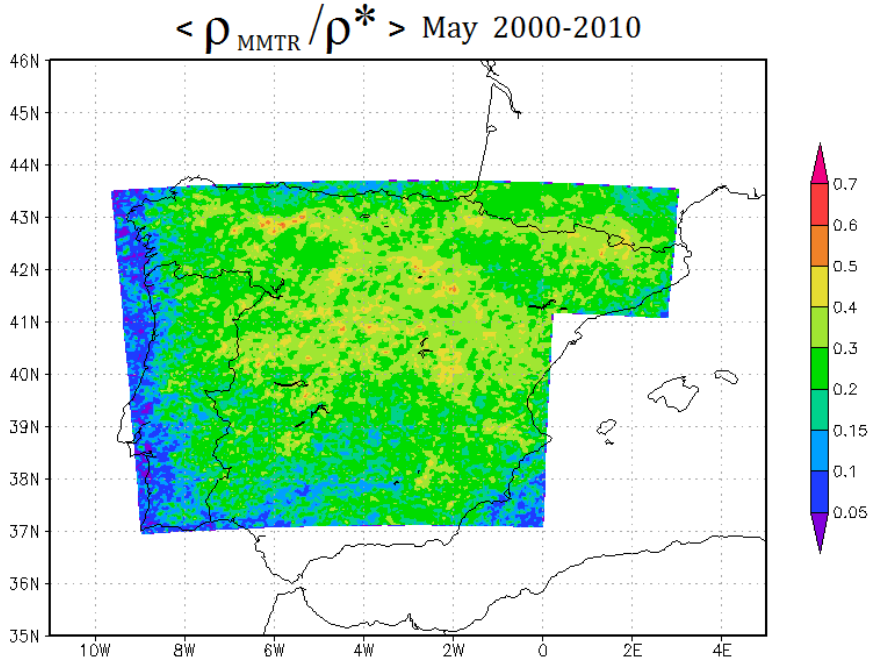

Figure 5.3: Spatial distribution of $\rho_{\mathrm{MMTR}}/\rho^*$ [-], equaling the fraction of ΔP deriving from direct recycling, averaged over the period May 2000-2010.

Two particular cases: May of 2004 and May of 2008

As it has been done in chapter 4, we complete this analysis by focusing on the months of May of 2004 and May of 2008. They correspond to the two wettest months of May along the simulated decade, presenting similar values of the regional relative change in

precipitation, r^*. In chapter 4, the increased precipitation was found to be principally associated with recycling processes in May of 2008, whereas amplification was found to predominate in May of 2004. In this section, we revise and complete these results in the light of the new MMTR results.

Fig. 5.4 shows the daily evolution of the regional MMTR recycling ratio (blue), relative change in precipitation (red), recycled contribution (green columns) and amplification contribution (light blue column) for May of 2004 (panel *a*) and May of 2008 (panel *b*). In this figure, which complements the information given in Fig. 4.17, it is apparent that the recycling contribution (r_{MMTR}/r^*) is much more relevant in May of 2004 than in May of 2008, when the amplification mechanism clearly dominates. When considering the whole month, the recycling term represents 32% of the total increased precipitation in May of 2004, whereas this value is reduced until 23% in May of 2008 (Table 5.1). This confirms that, if we consider the whole Iberian Peninsula, then the amplification contribution tends to be predominant. Regarding Fig. 5.4, we note that a relevant advantage of the MMTR recycling method with respect to the classical procedures is that the recycling ratio can be computed at the daily (or even lower) time scale, thus allowing to explore the daily cycle of the recycling mechanism.

When considering the spatial patterns of $\rho_{\mathrm{MMTR}}/\rho^*$, represented in Fig. 5.5 for May 2004 and May 2008 (panels *a* and *b*), we observe that the recycling contribution exceeds 50% in large interior areas not only in May of 2004 but also, to a much lesser extent, in May of 2008. For completeness, the local MMTR recycling ratio is also represented for both months (panels *c* and *d*). Our analysis seems to confirm the previous discussion of chapter 4, when we concluded that the recycling contribution is very relevant in inland Iberia under weak external moisture supply, as is the case May of 2004 (Fig. 4.16e). In contrast, under strong external forcing, as is the case of May of 2008 (Fig. 4.16f), the amplification mechanism predominates in general over the recycling term, retaining an important fration of the large amounts of advected moisture and incorporating this water to the regional hydrology cycle.

5.3 Distribution of moisture tracers in the atmosphere

Unlike the MMTR recycling method, both IMB and EBRM procedures are based on hypotheses that, in general, do not reproduce the reality with accuracy. This is the case of the well-mixed atmosphere assumption, analyzed in detail in section 1.4. The method of moisture tracers, which tracks the pathways of the water molecules evapotranspired inside the study region, constitutes an optimal tool to assess to what extent this locally evapotranspired water vapor effectively mix or not with the advected moisture. By setting latitude to 40°N, the vertical profile of the fraction of internal humidity, tagged with moisture tracers and averaged over the months of May of 2004 and May of 2008, is represented in Figs. 5.6a and 5.6b, respectively. In ad-

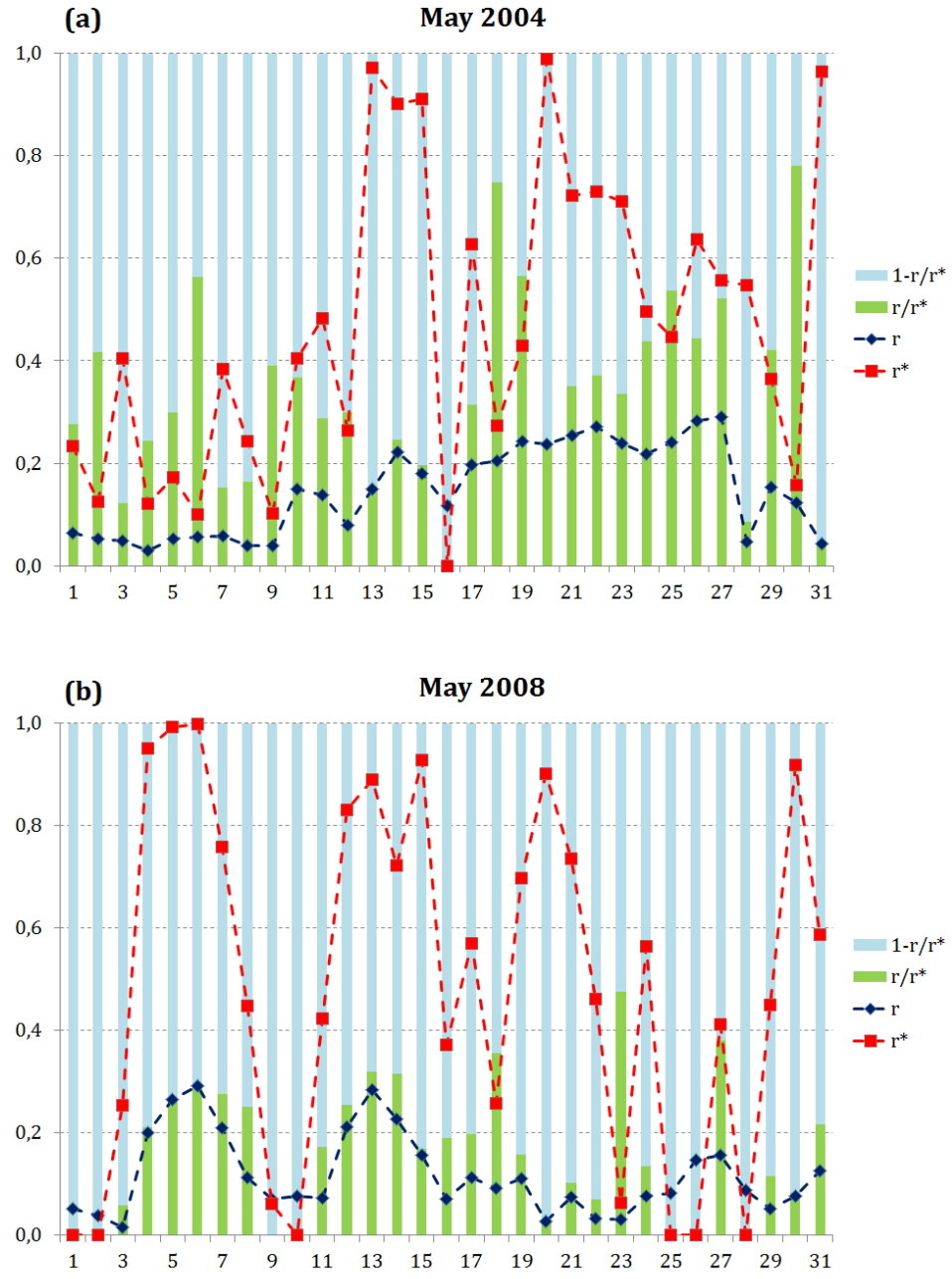

Figure 5.4: Daily values of regional MMTR recycling ratio [-] (blue), relative change in precipitation [-] (red), recycling contribution [-] (green columns) and amplification contribution [-] (light blue column) for May of 2004 (*a*) and May of 2008 (*b*).

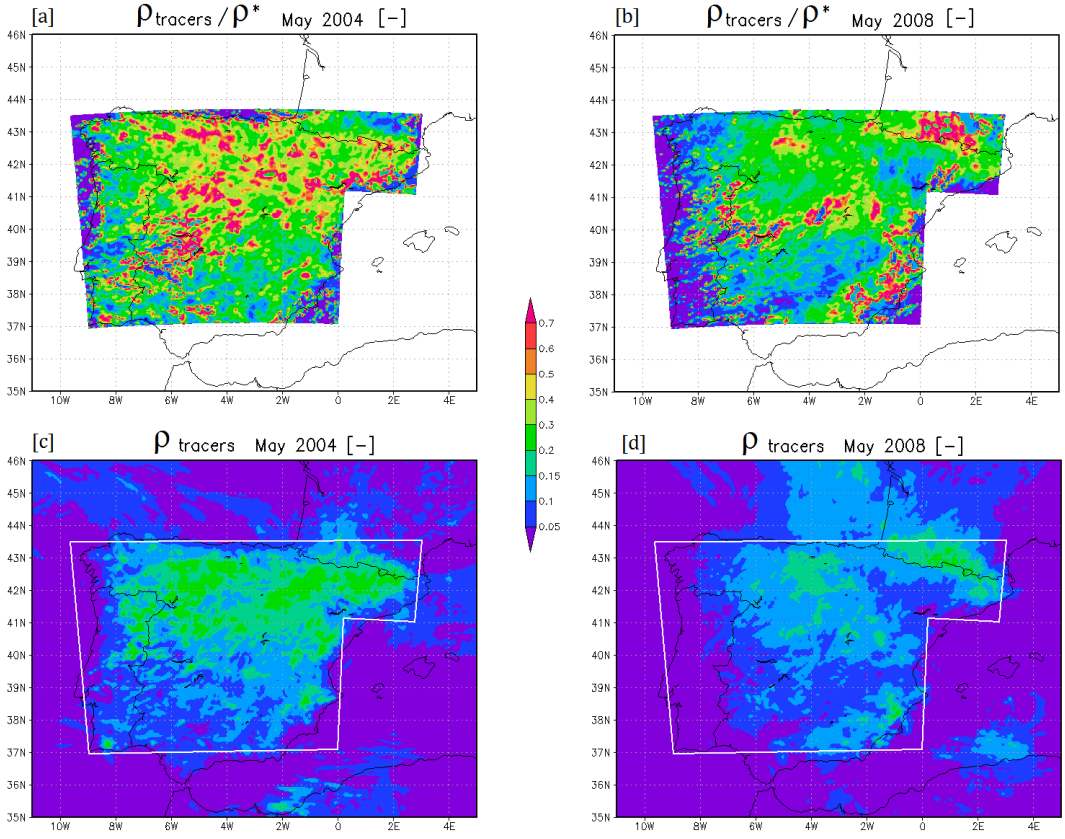

Figure 5.5: $\rho_{\mathrm{MMTR}}/\rho^*$ [-] and, for comparison, MMTR recycling ratio [-] for May of 2004 (panels *a* and *c*). Panels *b* and *d* show the corresponding maps for May of 2008.

dition, the corresponding vertical profiles for two particular episodes on the 8$^{\mathrm{th}}$ and 31$^{\mathrm{st}}$ of May 2008, previously analyzed in section 4.5 (and selected because of the high CAPE and rainfall values registered), are also shown.

In both Figs. 5.6 and 5.7, local ET tends to remain in the lower atmospheric layers, even though strong convective events facilitate its distribution towards upper atmospheric levels. The latter is clearly visible in Fig. 5.7. In accordance with the previous discussion, we can observe that whereas in May of 2008 the Iberian evapotransporation is transported, to a relevant extent, out of the IP by the strong flow (Fig. 5.6b), local humidity tends to remain in the atmosphere above and surrounding the IP in May of 2004 (Fig. 5.6b), as a result of the weakened circulation observed during the latter month. In general, this analysis confirms that the well-mixed assumption presents relevant limitations that might affect the IMB and EBRM estimates. As discussed in section 1.4, a relevant advantage of the MMTR recycling method with respect to the classical recycling models is that it does not rely on this assumption.

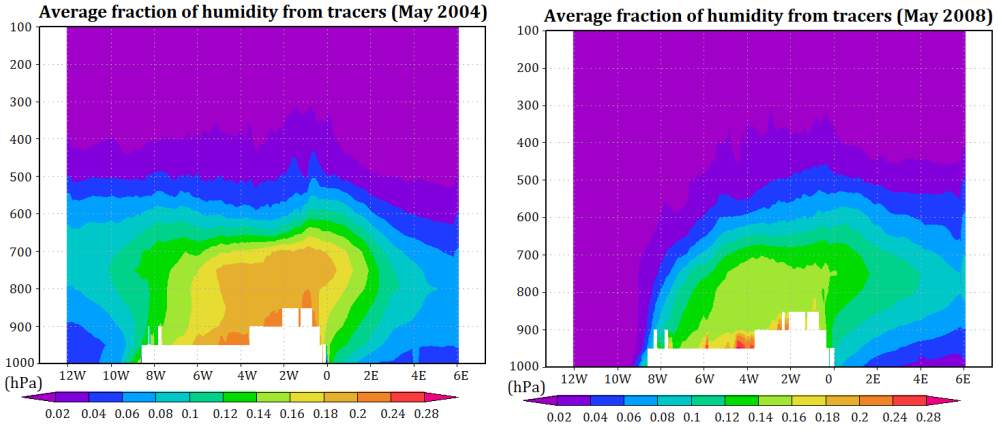

(a) (b)

Figure 5.6: Vertical profile (latitude set as 40°N) of the fraction of humidity from tracers [-] averaged over (*a*) May of 2004 and (*b*) May of 2008. The scale of the vertical axis is expressed in (hPa).

5.4 Conclusions of this chapter

In order to complete the analysis of chapters 3 and 4, we carried out eleven WRF simulations during the months of May of the period 2000-2010. These WRF simulations include a new capability of moisture tracers, allowing to track the pathways of the water molecules evapotranspired within the Iberian Peninsula. This procedure allows to compute the recycling ratio directly, presenting two major advantages with respect to classical models: 1) the method computes explicitly the fraction of water molecules evaporated within the IP contributing to the Iberian precipitation, without requiring any additional assumption; and 2) it allows to compute the recycling ratio at any time scale, and not only at monthly or larger scales as it is imposed by the limitations of the traditional recycling models. The WRFS-3 set of simulations, analyzed in this chapter, maintain the same characteristics (domains, parameterizations selected and lateral boundary conditions used) of the WRFS-2 set of runs, thus enabling comparison. In this chapter, we use the more accurate recycling ratios computed through the method of moisture tracers (MMTR) to recalculate the relative contribution of recycling and amplification contributions to the spring peak of precipitation.

The MMTR method describes the spatial heterogeneity of the recycling patterns with accuracy, in contrast to the smoother maps produced by the EBRM method, which depend excessively on the mean moisture flux and tend to overestimate recycling in general. Coherently, the highest MMTR values are more spread over the northern half of Iberia and no so concentrated to the eastern and northeastern areas as the EBRM method estimates. This spatial distribution is maintained when the MMTR recycling ratio is used to separate the recycling from the amplification contri-

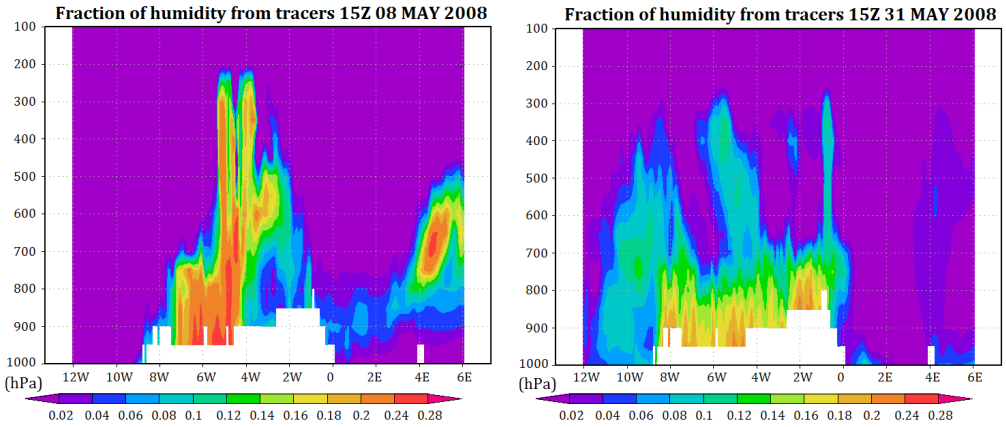

(a) (b)

Figure 5.7: Vertical profile (latitude set as 40°N) of the fraction of humidity from tracers [-] for two particular episodes in May of 2008, on the 8th (panel *a*) and 31st (panel *b*), at 15Z in both cases. The scale of the vertical axis is expressed in (hPa).

bution to the spring peak of rainfall, showing that when the whole IP is considered, amplification is confirmed to be the prevailing term, even thought in large areas of the interior and mainly under weak synoptic circulations, the recycling contribution can be the predominant.

On average for the Iberian Peninsula, the average regional MMTR recycling ratio is 0.11 for May, very close to the IMB calculation (0.10) and significantly below the EBRM value (0.22). In some specific areas in the North Plateau, the Iberian and Central Systems and the Pyrenees, average 2000-2010 May recycling ratios are found to be close to 20%. For the entire Iberia, the recycling contribution to the May extra precipitation is found to be 28%, with the remaining 72% being related to amplification. During some particular months, as is the case of May of 2004, the recycling term can be however responsible for over 50% of the surplus of precipitation in most interior regions.

The computational tool of moisture tracers, implemented in the WRF model and experimentally used in this chapter, is expected to be widely used in the future to give a precise answer to a variety of issues, as it is the case of the accurate computation of the recycling ratio at the regional scale or the analysis, at high resolution, of the distribution of evapotranspired humidity in the atmosphere, exploring its sources and sinks and allowing to complete the characterization of the regional water cycle. In this chapter, we make use of these moisture tracers to discuss the accuracy of the well-mixed atmosphere hypothesis, a critical assumption that underlies most classical recycling methods, as is the case of both IMB and EBRM.

6

General conclusions and outlook

In this thesis, we investigate the physical processes underlying the spring maximum of precipitation observed throughout the interior of the Iberian Peninsula, with a specific incidence in the inland regions to the east and northeast. This upturn in the rainfall totals occurs mostly in May, having a critical impact on human activities, and in particular on agriculture over these interior areas, most of them suffering from water scarcity. The present thesis adds valuable information to better characterize the precipitation regime of these regions. In a context of climate change, this study may be useful for hydrological planning and long-term sustainability there. We next summarize the main findings and general conclusions of this investigation.

1. The spring maximum of precipitation occurring in inland Iberia cannot be explained without considering the crucial role of land-atmosphere interactions, and in particular evapotranspiration (ET) fluxes. Our experiments show that suppressing land evapotranspiration in May would lead to an average reduction of precipitation by 37%. This value corresponds to the normalized difference (or relative change) in precipitation between control WRF simulations and experimental runs where the ET flux is not incorporated to the atmosphere. Interestingly, the average spatial pattern of this magnitude, revealing the regions where ET fluxes have a larger impact on rainfall (North Plateau, east and northeast) overlap with those areas where the spring peak of rainfall is more intense, turning to be the absolute maximum in the annual cycle. As a consequence, we state that the pluviometric upturn observed in large interior regions of the Iberian Peninsula in May is directly related to the intensification of the hydrological cycle and to the impact of ET fluxes on rainfall.

2. In the Iberian spring, the evapotranspiration flux becomes an essential source of humidity for further precipitation. This direct effect of local ET in the regional rainfall regime is quantified through the computation of the recycling

ratio through three different methods: 1) the analytical recycling model due to Schär et al. (1999); 2) the numerical procedure proposed by Eltahir and Bras (1994); and 3) a new method based on moisture tracers. The fraction of recycled precipitation is found to be the highest in spring and early summer, with a specific relevance in the interior of Iberia and coinciding with the areas where the peak of precipitation is observed. Recycling values seem to be the highest when a positive coupling of the two following conditions takes place: 1) availability of sufficient soil moisture, resulting from abundant rainfall during the previous season; and 2) occurrence of appropriate synoptic configurations that favor the development of convective regimes. This twofold mechanism might be useful to assess the relevance of the recycling contribution during any period of the year in Iberia and in other regions of the world with semi-arid types of climate. On average for May, the Iberian recycling ratio is found to be 0.10 (or 10%) according to Schär et al.'s (1999) model and 0.22 according to Eltahir and Bras's (1994), whereas the more accurate method of moisture tracers yields a recycling value of 0.11. These average values are found to be significantly higher in the interior, eastern and northeastern areas, confirming that the internal evapotranspiration is an essencial source of moisture for spring precipitation in the Iberian Peninsula.

3. Apart from being an important source of moisture, ET fluxes have also an indirect impact on spring rainfall by increasing the low level instability of the atmospheric column. This is apparent if we observe the differences between the average recycling ratio in May (0.11 according to the method of moisture tracers) and the corresponding average relative change in precipitation (0.37). Indirect or amplification mechanisms favor the retention of a fraction of the advected moisture that is added to the regional precipitation. In this thesis, we develop a new method to separate and quantify both direct (recycling) and indirect (amplification) contributions to rainfall totals, based on experimental model simulations where land evapotranspiration over the Iberian Peninsula is suppressed. For the entire Iberian Peninsula, results show that the indirect mechanism (72%) is even more relevant than the direct contribution (the remaining 28%). This result is not far from the estimation obtained through the analytical separation method due (also) to Schär et al. (1999), whereby amplification (recycling) is responsible for 62% (38%) of the extra May precipitation related to land-atmosphere interactions. Nevertheless, in the interior areas, the recycling contribution tends to be the most important. In general, the recycling term predominates under weak external forcings, as expected, as in this situation locally evapotranspired moisture is essentially the only source for further precipitation. On the contrary, under synoptic circulations favoring the advection of external moisture, the amplification mechanism is the most important, incorporating to the regional hydrology cycle a fraction of external moisture which otherwise would be simply blown across the Iberian Peninsula.

4. An innovative method of moisture tracers implemented in the WRF regional meteorological model is experimentally used to more accurately explore the Iberian peak of precipitation in spring. This technique allows to explicitly compute the recycling ratio, presenting two major advantages with respect to traditional recycling models: 1) the method of moisture tracers does not make use of any of the common hypotheses and simplifications assumed in the classical recycling models; and 2) the recycling ratio can be computed at any time scale, and not only at monthly or larger scales as it is imposed by the limitations of the traditional recycling models. In light of the results obtained from simulations with moisture tracers, we observe that both the recycling ratio and the recycling contribution to the spring surplus of precipitation are more spread throughout the northern half of inland Iberia, with the highest intensity being found in the North Plateau, Central and Iberian Systems and the Pyrenees.

5. The fraction of spring precipitation directly and indirectly related to land-atmosphere interactions is found to be of the same order as the reduction in precipitation totals expected as a consequence of climate change in the Iberian Peninsula (e.g. Giorgi and Lionello, 2008 [115]). As a result, a better understanding of land-air interactions in the large water-limited regions of the interior of Iberia is very relevant to assess the impact of future climate change scenarios in the regional hydrological cycle.

Future work

This thesis constitutes an important improvement in the description of the precipitation regime of the interior of Iberia. The main physical mechanisms underlying the intensification of rainfall amounts in spring are identified and the methods used and developed here account satisfactorily for their relative impacts. However, the development of better computational tools in the future will help assessing the impact of land-atmosphere interactions on the Iberian climate with more accuracy. In our view, two main research lines should be explored.

On the one hand, the incorporation of this tool of moisture tracers to regional numerical simulations opens a wide field for the comprehensive exploration of the water cycle at the regional scale. This capability, used here only in an experimental and preliminary way, must be more systematically explored and applied to different regions, within and outside the Iberian Peninsula. The characterization, at higher resolution, of the sources, pathways and sinks for moisture molecules is of the greatest interest, particularly in water-stressed areas as is the case of large interior regions of Iberia, and even more in a context of climate change.

On the other hand, the current numerical meteorological models still present important limitations when describing some relevant physical processes. This is pre-

cisely the case of land-atmosphere interactions, despite the remarkable improvement on land-surface schemes observed during the last decades (e.g. Pitman, 2003 [204]). Nowadays, most land-surface schemes (as it is the case of the NOAH land-surface model, used in the WRF simulations analyzed in this thesis) do not include an appropriate representation of groundwater flow and water table dynamics. Interestingly, the water table is found to be shallow in large interior areas of the Iberian Peninsula, most of them classified as arid or semiarid and thus affected by water scarcity. We strongly believe that a correct representation of soil moisture dynamics would better represent the evapotranspiration fluxes in these areas, whose impact on further precipitation might be still underestimated in this investigation. Actually, the idea of coupling a complete land-surface model with a regional meteorological model has been suggested in several papers (e.g. Bierkens and Van der Hurk, 2007 [20]) and preliminary explored for the Iberian Peninsula in a recent study by Gestal-Souto et al. (2010) [109]. In the latter investigation, the WRF model was coupled to the LEAF2-Hydro land-surface model (Fan et al., 2007 [84]; Miguez-Macho et al., 2007 [181]; Anyah et al., 2008 [5]), giving rise to the WRF-Hydro model. Similar investigations have been recently carried out by other authors, as a way to better reflect the impact of soil moisture and groundwater memory on climate and improve seasonal forecasts (Maxwell et al., 2007 [175]; Yuan et al., 2008 [269]).

In summary, WRF model simulations including moisture tracers and a fully coupled land-surface scheme, representing the groundwater and water table dynamics accurately, would probably constitute the optimal tool to improve our comprehension of the hydrology cycle and the precipitation regime at the regional scale, not only in the interior areas of the Iberian Peninsula but also in any other semiarid area all over the world.

Appendices

USC
UNIVERSIDADE DE SANTIAGO DE COMPOSTELA

USC
UNIVERSIDADE
DE SANTIAGO
DE COMPOSTELA

Appendix A

Computation of the water budget terms

The conservation of water within a certain region and during a given period of time can be expressed through the water budget equation (2.1) or, alternatively, through its discrete version:

$$\Delta N = N(\Delta t) - N_0 = IN - OUT + ET - P \tag{A.1}$$

where N represents the storage of water in the atmosphere (precipitable water), IN (OUT) stands for the average inward (outward) moisture fluxes into (from) the region, ET is the evapotranspiration and P is the precipitation accumulated over a period of time Δt (in this thesis, Δt corresponds always to one month). Usually, the difference of inward and outward vertically-integrated moisture flux is referred to as *moisture convergence*, MC:

$$MC = IN - OUT \tag{A.2}$$

This variable measures the net water flux across the lateral boundaries of the region. According to (A.2), equation (A.1) can be also expressed as:

$$\Delta N = N(\Delta t) - N_0 = MC + ET - P \tag{A.3}$$

Among these variables, ET and P are the easiest to obtain, as they can be computed simply from WRF model outputs. In this appendix, we examine the procedures to compute both the storage and the moisture convergence terms from WRF model outputs.

Storage term

The storage of water, N, also referred to as precipitable water, is formally defined as the total amount of water at time t inside an atmospheric column of base area ΔA, within the study region, and centered at (x,y):

$$N(x,y,t) = \frac{1}{\Delta A} \lim_{\Delta A \to 0} \iint_{\Delta A} dxdy \int_{z_0}^{z_{top}} \varrho(x,y,z,t) q(x,y,z,t) dz \tag{A.4}$$

where z_0 is the surface level, z_{top} represents the height of the top of the atmosphere, $\varrho(x,y,z,t)$ stands for the air density and $q(x,y,z,t)$ is the water vapor mixing ratio. By consideration of the hydrostatic equation,

$$\frac{dP}{dz} = -\varrho g_0 \tag{A.5}$$

(A.4) can be alternatively expressed as

$$N(x,y,t) = \frac{1}{g_0 \Delta A} \lim_{\Delta A \to 0} \iint_{\Delta A} dxdy \int_{P_{top}}^{P_0} q(x,y,P,t) dP \tag{A.6}$$

where g_0 is the acceleration due to gravity, P_{top} represents the pressure at the top of the atmosphere (ideally equal to zero) and P_0 stands for the surface pressure. The total amount of water per unit area inside the whole study region at time t is thus given by:

$$N(t) = \frac{1}{A} \iint_{A} N(x,y,t) dxdy \tag{A.7}$$

where A stands for the region size. In practice, N is computed via the discrete versions of equations (A.6) and (A.7), expressed as:

$$N(i,j,t) = \frac{1}{g_0} \sum_{k=1}^{n} q(i,j,k,t) \Delta P(i,j,k,t) \tag{A.8}$$

and

$$N(t) = \frac{1}{A} \sum_{i,j} N(i,j,t) \Delta A(i,j) \tag{A.9}$$

with n standing for the number of model vertical levels and $\Delta P(x, y, z, t)$ representing the discrete intervals of pressure interpolated from the model output. It is easy to check that $[N] = kg_{\text{vapor}} \cdot m^{-2}$.

Moisture Convergence term

The moisture convergence term is obtained by adding the vertically integrated moisture flux throughout all the sides of the box bounding the region:

$$MC = \frac{1}{g_0 \cdot A} \int_{\Delta t} dt \int_{boundaries} dl \int_{P_{top}}^{P_0} q(x, y, z, t) \cdot v_{\perp}(x, y, z, t) dP \tag{A.10}$$

where dl is the infinitesimal horizontal distance along the boundary line and $v_{\perp}$ stands for the perpendicular component of the horizontal wind along the borders of the region.

The discretized (practical) version of equation (A.10) is expressed as:

$$MC = \frac{1}{g_0 \cdot A} \sum_{\Delta t} \delta t \sum_{i,j \in boundaries} \Delta l(i, j) \sum_{k=1}^{n} q(i, j, k, t) \cdot v_{\perp}(i, j, k, t) \Delta P(i, j, k, t) \tag{A.11}$$

where δt corresponds to the period of time, expressed in seconds, between two consecutive WRF model outputs. In the computations performed from WRFS-1 simulation outputs, $\delta t = 3600$ s, whereas for those calculations from WRFS-2 output $\delta t = 10800$ s. Also in equation (A.11), $\Delta l(i, j)$ represents the length of the grid cell along the boundary line. We note that the moisture convergence contribution is normalized to the region size, A, and therefore $[MC] = kg_{\text{vapor}} \cdot m^{-2}$.

The practical computation of both IN and OUT does not differ significantly from equation (A.11). Nevertheless, the sign of the wind velocity must be evaluated, at every boundary, in order to decide if the water vapor flux is entering (IN) or exiting (OUT) the region. The procedure to compute these magnitudes presents some differences in the IMB with respect to the EBRM. We discuss this feature in detail in Appendices B and C.

USC
UNIVERSIDADE
DE SANTIAGO
DE COMPOSTELA

Appendix B

The Schär et al.'s (1999) Integral Moisture Budget Recycling Model. Computation details

In order to evaluate equation (2.6), we need to compute both *IN* and *ET*. As mentioned in appendix A, the latter flux can be directly read from WRF model output. In this appendix, we present the procedure to compute the total moisture input along the boundaries of our study region. As indicated, it does not differ significantly from the method to compute the moisture convergence, expressed in equation (A.11). Let us examine it in detail.

Roughly, each WRF model output represents the state of the atmospheric system at a given instant of time, t. Let δt account for the period of time, expressed in second, between two consecutive WRF model outputs. In our case, the total input of moisture is accumulated over a period of time Δt, corresponding to one month. From each WRF model output, the following magnitude must be evaluated at the boundaries of our study region:

$$in^{[+]}(t) = \frac{1}{g_0} \sum_{i,j \in boundaries} \Delta l(i,j) \sum_{k=1}^{n} q(i,j,k,t) \cdot v_{\perp}^{[+]}(i,j,k,t) \Delta P(i,j,k,t) \qquad \text{(B.1)}$$

In this equation, very similar to (A.11), g_0 is the acceleration due to gravity, $\Delta l(i,j)$ represents the length of the grid cell along the boundary line, n is the number of vertical model levels, $q(i,j,k,t)$ is the water vapor mixing ratio and $\Delta P(x,y,z,t)$ represents the discrete intervals of pressure interpolated from model output. Note that $v_{\perp}^{[+]}(i,j,k,t)$ is the component of the horizontal wind perpendicular to the con-

sidered boundary, with super-index [+] expressing the requirement that the sign of the velocity must imply that water vapor is entering the region.

The total inward moisture flux during the considered period (Δt) is obtained by adding *only* those positive contributions:

$$IN = \sum_{\Delta t} in^{[+]}(t)\delta t \tag{B.2}$$

The accumulated moisture input flux IN can be now used to compute the regional recycling ratio via equation (2.6). It is relevant to note that $[IN] = kg_{\text{vapor}}$. This value can be normalized to the area of the region, A if we desire to work with all the fluxes expressed in mm.

USC UNIVERSIDADE DE SANTIAGO DE COMPOSTELA

Appendix C

The Eltahir and Bras's (1994) Recycling Model. Computation details

In order to evaluate equation (2.15), the computation of $ET(x,y)$, $IN_m^*(x,y)$ and $IN_a^*(x,y)$ is required at every grid cell within the study region. As mentioned in appendix A, the computation of the moisture input term in the EBRM presents some differences with respect to the IMB, as it is explicit by the use of different symbols in equations (2.1) and (2.9). The essential reason is that, in the EBRM, the moisture fluxes must be computed at the boundaries of every grid cell, and not only at the boundaries of the entire region, as it is the case in the IMB. More in detail, in the EBRM, the vertically-integrated moisture flux must be accumulated at each border separating neighboring cells, regardless the sign of the wind velocity. This justifies the use a different symbol, $F(x,y)$, to account for this magnitude. As it has also been done in Appendices A and B, hereafter we change the coordinates (x,y) into (i,j), in order to better represent the discrete nature of the calculations below. As explained,

$$F(i,j) = \frac{1}{g_0} \sum_{\Delta t} \delta t \sum_{i,j \in A} \Delta l(i,j) \sum_{k=1}^{n} q(i,j,k,t) \cdot v_{\perp}(i,j,k,t) \Delta P(i,j,k,t) \qquad \text{(C.1)}$$

In equation (C.1), g_0 is the acceleration of the gravity, Δt is the whole computations period (in our case, one month), δt is the number of seconds between two consecutive WRF model outputs, $\Delta l(i,j)$ stands for the length of the grid cell along the boundary line, n is the number of vertical model levels, $q(i,j,k,t)$ is the water vapor mixing ratio, $v_{\perp}(i,j,k,t)$ is the component of the horizontal wind perpendicular to the considered boundary and $\Delta P(x,y,z,t)$ represents the discrete intervals of

pressure interpolated from model output. Note that $[F] = kg_{\text{vapor}}$.

Only in the end of the computation period (in our case, as mentioned, Δt equals one month), the sign of the accumulated vertically-integrated moisture flux, $F(i,j)$, is evaluated at each grid cell to decide if it enters or exits the corresponding cell. As a result, for each grid cell it is possible to *classify* $F(i,j)$ into $IN^*(i,j)$ or $OUT^*(i,j)$, as it is examined below. Note that in the limit case of application of the EBRM with only one grid cell, where $IN_m^* = 0$ and $IN_a^* = IN^*$, equation (2.15) is formally equal to (2.6), as expected. However, the corresponding numerical results might not converge, as the computation of the total moisture input is performed in different ways (see appendix E for the experimental results).

For computation purposes, it is useful to explicitly rewrite equation (C.1) for both x and y directions:

$$F_x(i,j) = \frac{1}{g_0} \sum_{\Delta t} \delta t \sum_{i,j \in A} \Delta y(i,j) \sum_{k=1}^{n} q(i,j,k,t) \cdot v_x(i,j,k,t) \Delta P(i,j,k,t) \tag{C.2a}$$

$$F_y(i,j) = \frac{1}{g_0} \sum_{\Delta t} \delta t \sum_{i,j \in A} \Delta x(i,j) \sum_{k=1}^{n} q(i,j,k,t) \cdot v_y(i,j,k,t) \Delta P(i,j,k,t) \tag{C.2b}$$

where Δx and Δy stand for the size of the grid cell in the x and y directions, respectively.

Iterative method to compute the EBRM Recycling Ratio

As described in the previous section, the EBRM requires the verically-integrated moisture fluxes to be computed at the borders of all the grid cells within the study region. As a result, depending on their sign, they will correspond to input, $IN^*(i,j)$, or output fluxes, $OUT^*(i,j)$. Therefore, if

$$F_x(i,j) \geq 0 \rightarrow F_x(i,j) = OUT_x^*(i,j) = IN_x^*(i+1,j) \tag{C.3a}$$

$$F_x(i,j) < 0 \rightarrow F_x(i,j) = OUT_x^*(i+1,j) = IN_x^*(i,j) \tag{C.3b}$$

$$F_y(i,j) \geq 0 \rightarrow F_y(i,j) = OUT_y^*(i,j) = IN_y^*(i,j+1) \tag{C.3c}$$

$$F_y(i,j) < 0 \rightarrow F_y(i,j) = OUT_y^*(i,j+1) = IN_y^*(i,j) \tag{C.3d}$$

As mentioned in section 2.3, a first guess for the recycling ratio is required to start the iterative process:

$$\rho(i,j) = \rho_0(i,j) \tag{C.4}$$

In addition, the initialization of the following variables to zero is also required:

$$IN^*_{m_x}(i,j) = IN^*_{m_y}(i,j) = IN^*_{a_x}(i,j) = IN^*_{a_y}(i,j) = 0 \; \forall (i,j) \in A \tag{C.5}$$

For the x component, if $F_x(i-1,j) \geq 0$ and according to equations (C.3a) and (C.3b), the new values of the inward fluxes will be given by:

$$IN^{*'}_{m_x}(i,j) = IN^*_{m_x}(i,j) + \rho_0(i-1,j)F_x(i-1,j) \tag{C.6a}$$

$$IN^{*'}_{a_x}(i,j) = IN^*_{a_x}(i,j) + [1-\rho_0(i-1,j)]F_x(i-1,j) \tag{C.6b}$$

Similarly, if $F_x(i,j) < 0$, then:

$$IN^{*'}_{m_x}(i,j) = IN^*_{m_x}(i,j) - \rho_0(i+1,j)F_x(i,j) \tag{C.7a}$$

$$IN^{*'}_{a_x}(i,j) = IN^*_{a_x}(i,j) - [1-\rho_0(i+1,j)]F_x(i,j) \tag{C.7b}$$

For the y component, if $F_y(i,j-1) \geq 0$, then according to equations (C.3c) and (C.3d):

$$IN^{*'}_{m_y}(i,j) = IN^*_{m_y}(i,j) + \rho_0(i,j-1)F_y(i,j-1) \tag{C.8a}$$

$$IN^{*'}_{a_y}(i,j) = IN^*_{a_y}(i,j) + [1-\rho_0(i,j-1)]F_y(i,j-1) \tag{C.8b}$$

Finally, if $F_y(i,j) < 0$, then:

$$IN^{*'}_{m_y}(i,j) = IN^*_{m_y}(i,j) - \rho_0(i,j+1)F_y(i,j) \tag{C.9a}$$

$$IN^{*'}_{a_y}(i,j) = IN^*_{a_y}(i,j) - [1-\rho_0(i,j+1)]F_y(i,j) \tag{C.9b}$$

By adding the x and y components from equations (C.6), (C.7), (C.8) and (C.9),

$$IN_m^{*'}(i,j) = IN_{m_x}^{*'}(i,j) + IN_{m_y}^{*'}(i,j) \tag{C.10a}$$

$$IN_a^{*'}(i,j) = IN_{a_x}^{*'}(i,j) + IN_{a_y}^{*'}(i,j) \tag{C.10b}$$

we can already evaluate equation (2.15):

$$\rho'(i,j) = \frac{IN_m^{*'}(i,j) + ET(i,j)}{IN_m^{*'}(i,j) + IN_a^{*'}(i,j) + ET(i,j)} \tag{C.11}$$

Let us define the *error* of the iteration as

$$\epsilon = \left|\rho'(i,j) - \rho_0(i,j)\right| \tag{C.12}$$

An ϵ_0 must be defined so that, whenever

$$\epsilon \leq \epsilon_0 \tag{C.13}$$

the iterative computation is stopped and $\rho(i,j) = \rho'(i,j)$ is considered the final result. On the contrary, while condition (C.13) is not satisfied, $\rho_0(i,j) = \rho'(i,j)$ must be replaced in equation (C.4) and the above-described procedure (from equation C.4 until equation C.13) must be performed again. This numerical procedure can be implemented in a code that converges quickly.

Appendix D

Removing the land ET in the WRF model. Configuration of the *No-ET* experiments

In this appendix, the procedure to remove the land ET over the nested domain from WRF model simulations is described. This modified configuration of the model allows to carry out experimental simulations (included in the WRFS-2 set of runs) which can be compared to *control* simulations where the ET fluxes are normally set up. This strategy is used in chapter 4.

These are the steps to implement the new configuration on the model.

1. Access folder *dyn_em/* and open file "*module_first_rk_step_part1.F*". Find the subroutine *surface_driver* and introduce the variable *id*, which allows identifying each of the domains [in our case, the parent ($id = 1$) and the nested ($id = 2$) domains], as follows:

```
CALL surface_driver( &
  &  id=grid%id  &
  &     ,ACSNOM=grid%acsnom  ,ACSNOW=grid%acsnow  ,AKHS=grid%akhs  &
  (...)
```

2. Access folder *phys/* and open file "*module_surface_driver.F*". Find the subroutine *surface_driver* and introduce again the variable *id* in this manner:

```
SUBROUTINE surface_driver( &
  &          id                          &
```

```
&           ,acsnom,acsnow,akhs,akms,albedo,br,canwat      &
(...)
```

3. In the same file and subroutine, declare the variable *in*:

```
INTEGER, INTENT(IN)::   id
```

4. In the same file and subroutine, find the following commented instruction:

```
!Optional urban
```

and modify the subsequent loop by adding the instruction:

```
IF((XLAND(I,J).lt.1.5).and.(id.eq.2))QFX(I,J)=0
```

The final result is:

```
DO j=j_start(ij),j_end(ij)
   DO i=i_start(ij),i_end(ij)
       SFCEVP(I,J)= SFCEVP(I,J) + QFX(I,J)*DTBL
       SFCEXC(I,J)= CHS(I,J)
             IF((XLAND(I,J).lt.1.5).and.(id.eq.2))QFX(I,J)=0
   ENDDO
ENDDO
```

This ensures that evapotransporation (QFX) is set equal to zero over land (since $xland = 1$ indicates land and $xland = 2$ indicates water) within the nested domain ($id = 2$).

5. Recompile the model by execution of command:

```
compile em_real >& compile.log
```

Now the WRF model is ready to carry out the *no-ET* experimental runs.

Appendix E

Sensitivity of the Eltahir and Bras's (1994) Recycling Model to spatial resolution

In the original paper of Eltahir and Bras (1994) [76], a very limited analysis of the sensitivity of the method to the spatial resolution is given. In this appendix, we therefore provide a more detailed assessment of this relevant issue by using WRFS-1 outputs. In chapters 3 and 4, monthly regional EBRM recycling values were computed by using as subdivisions the cells of the model themselves. As a result, the horizontal resolution was set to 9 km (chapter 3; WRFS-1 simulation) and 5 km (4; WRFS-2 simulation), respectively. However, the EBRM method can be applied to computation cells including more than one grid cell of the model's domain. The limit case corresponds to the consideration of the whole study region as only one computation cell. In that situation, the EBRM formula (2.15) is found to formally converge to the IMB formula (2.6).

A grid of 128 x 128 points at 9 km horizontal resolution (WRFS-1 data) is initially considered. We note that the study region used here does not correspond to that defined in chapters 3 or 4, even though it also includes the whole Iberian Peninsula. Represented in Fig. E.1, this region is only considered to assess the sensitivity of the EBRM recycling model to the spatial resolution. As it can be seen, it includes a relevant portion of sea, which suggests that the recycling values may not be very representative of the intensity of land-atmosphere coupling in the IP and are expected to differ from those more accurately calculated in chapters 3 and 4. The important thing here is assessing the dependence of the EBRM values with the horizontal resolution, and the consideration of a 128 x 128 points area is appropriate for this purpose.

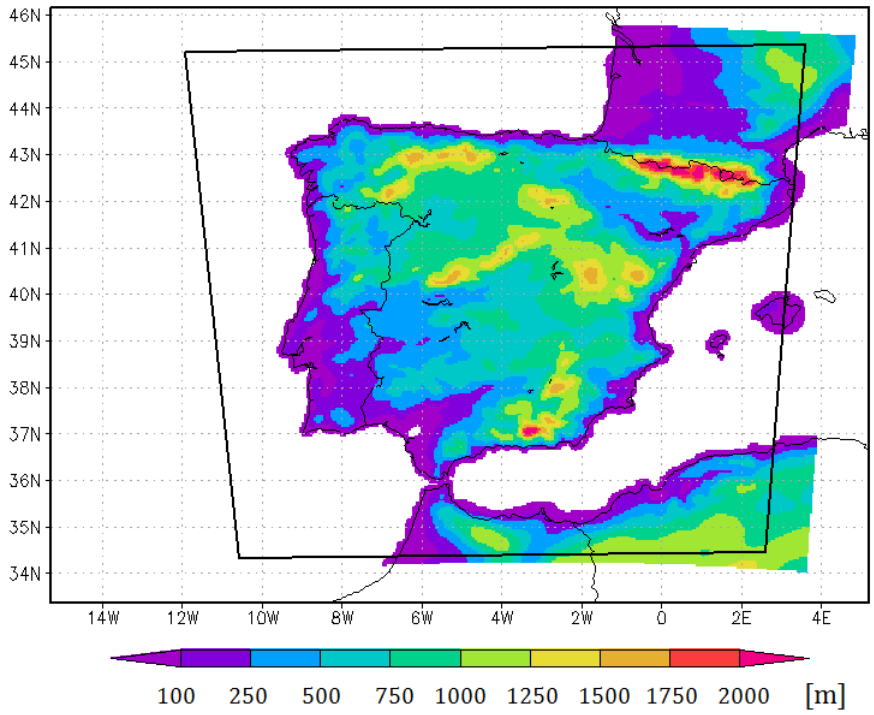

Figure E.1: 128 x 128 points region (at 9 km horizontal resolution) including the Iberian Peninsula where the sensitivity of the EBRM recycling ratio to the computation resolution is assessed. The terrain height above the sea level is expressed in (m)

An initial calculation is carried out by considering the EBRM calculation subdivisions to coincide with the model grid cells. As a result, monthly local EBRM recycling values, along the period 1990-2007, are computed over a study region constituted by 128 x 128 calculation cells. From this result, the corresponding monthly regional EBRM recycling ratios are obtained. Then, each group of 4 model cells is aggregated to form a new computation subdivision. This implies that the study region is now divided in 64 x 64 computation cells, and therefore the local recycling ratio is now calculated at lower horizontal resolution. The aggregation process is illustrated in Fig. E.2, where the black and white squares of the chessboard represent the individual model cells.

Successively, calculations of the EBRM regional recycling ratio are performed by using different grids of 128x128, 64x64, 32x32, 16x16, 8x8, 4x4, 2x2 and 1x1 subdivisions over the same study region (Fig E.1). Monthly values calculated along the period 1990-2007 (as done in chapter 3) are averaged and presented in Fig. E.3, where the corresponding mean IMB recycling ratios are calculated over the same region.

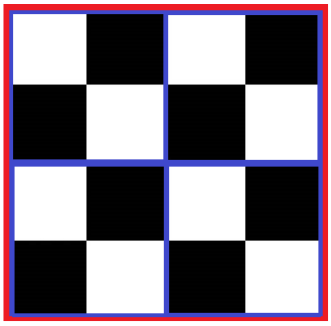

Figure E.2: Illustration of the procedure used to compute the EBRM regional recycling ratio by successively decreasing the computation resolution.

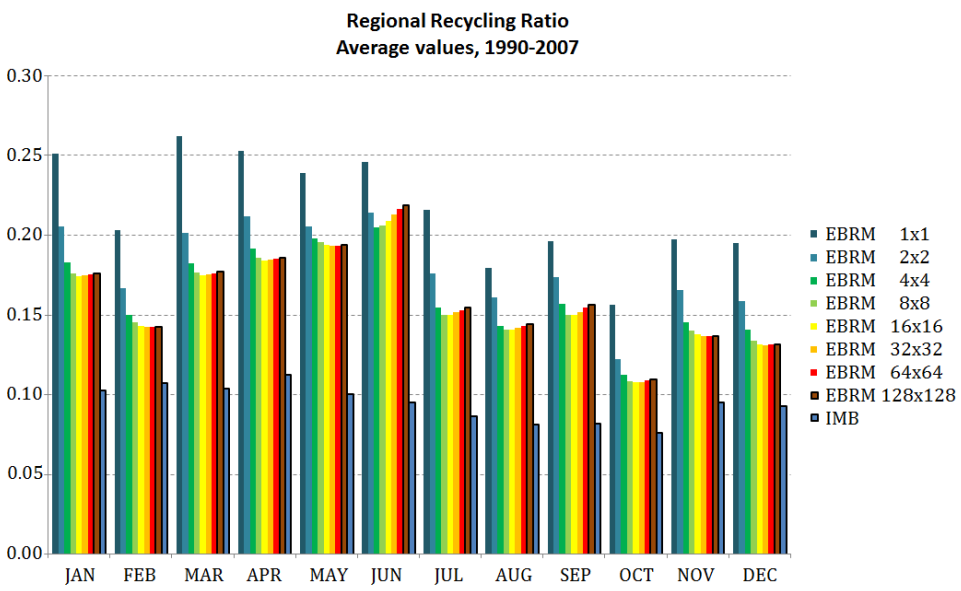

Figure E.3: EBRM regional recycling ratios [-] computed by successively decreasing the computation resolution and comparison with the IMB value.

Results show that computing the EBRM regional recycling ratio by considering the whole region as a single calculation cell introduces a significant error with respect to the more accurate 128x128 assessment, with relative deviations exceeding 40% in many cases. Nevertheless, from the 4x4 calculation onwards, results are found to be significantly close. Relative deviations of the 4x4 recycling ratios (with respect to the 128x128 ones) are generally below 5%, turning to be progressively lower for the 8x8 (usually below 1%), 16x16 (below 0.8%), 32x32 (below 0.6%) and 64x64 (below 0.3%) computations. This suggests that, to a large extent, EBRM regional recycling ratios are robust and their sensitivity to spatial resolution is reduced. Only in the extreme

cases of using 1x1 or 2x2 computation cells, the error of the method is significantly increased. In addition, the decreasing trend observed in the 1x1 calculations from March to June contrasts with the increasing trend in the more accurate recycling values during the same period. This confirms that 1x1 calculations are not able to represent recycling values properly. As mentioned, these recycling values must not be taken too literally, since the study area is not restricted to the land areas of the IP.

IMB regional recycling values are significantly lower than EBRM ones, in accordance with the results discussed in chapters 3 and 4. It is interesting to remark that, even though IMB and 1x1 EBRM computations formally converge, the divergences in the numerical calculations lead to significantly different results, as it is apparent in Fig. E.3. Interestingly, IMB computations systematically underestimate recycling, whereas 1x1 EBRM results systematically overestimate it. The main conclusion of this analysis is that, due to the use area integrated quantities, 1x1 (or bulk) recycling models are not able to represent the spatial heterogeneity of the recycling process, and thus more accurate procedures are generally required to obtain a better quantification of this crucial magnitude for the complete characterization of the terrestrial water cycle at the regional scale.

USC UNIVERSIDADE DE SANTIAGO DE COMPOSTELA

References

[1] Acero FJ, García JA, Gallego MC (2011): Peaks-over-threshold study of trends in extreme rainfall over the Iberian Peninsula. *J Climate*, 24: 1089-1105.

[2] Alfieri L, Claps P, D'Odorico P, Laio F, Over TM (2008): An analysis of the soil moisture feedback on convective and stratiform precipitation. *J Hydrometeor*, 9: 280-291.

[3] Andrés M, Tomás C, De Pablo F (2000): Spatial patterns of the daily non-convective rainfall in Castilla y León (Spain). *Int J Climatol*, 20: 1207-1224.

[4] Anthes RA (1984): Enhancement of convective precipitation by mesoscale variations in vegetative convering in semiarid regions. *J Climate Appl Meteor*, 23: 541-554.

[5] Anyah RO, Weaver CP, Miguez-Macho G, Fan Y, Robock A (2008): Incorporating water table dynamics in climate modeling: 3. Simulated groundwater influence on coupled land-atmosphere variability. *J Geophys Res-Atmospheres*, 113: D07103.

[6] Arakawa A (2004) The cumulus parameterization problem: past, present, and future. *J Climate*, 17 (13): 2493-2525

[7] Arora V (2002): Modeling vegetation as a dynamic component in soil-vegetation-atmosphere transfer schemes and hydrological models. *Rev Geophys*, 40, doi:10.1029/2001RG000103.

[8] Avissar R, Liu Y (1996): Three-dimensional numerical study of shallow convective clouds and precipitation induced by land surface forcing. *J Geophys Res*, 101 (NO. D3): 7499-7518.

[9] Balabanis P, Peter D, Ghazi A, Tsogas M (eds) (1999): Mediterranean Desertification - Research Results and Policy Implications. *European Commission.*

[10] Bastable HG, Shuttleworth WJ, Dallarosa RLG, Fisch G, Nobre CA (1993): Observations of climate, albedo and surthce radiation over cleared and undisturbed Amazonian forest. *Int J Climatol*, 13: 783-796.

[11] Beljaars ACM, Viterbo P, Miller MJ, Betts AK (1996): The anomalous rainfall over the United States during July 1993: sensitivity to land surface parameterization and soil moisture anomalies. *Mon Weather Rev*, 124: 362-383.

[12] Bell GD, Bosart LF (1989): A 15-year climatology of Northern Hemisphere 500 mb closed cyclone and anticyclone centers. *Mon Weather Rev*, 117: 2142-2163.

[13] Belo-Pereira M, Dutra E, Viterbo P (2011): Evaluation of global precipitation data sets over the Iberian Peninsula. *J Geophys Res*, 116: D20101, doi:10.1029/2010JD015481.

[14] Benton GS, Blackburn RT, Snead VO (1950): The role of the atmosphere in the hydrological cycle. *Trans Am Geophys Union*, 31: 61-73.

[15] Berrisford P et al. (2011): The ERA-Interim Archive (Second edition). *ERA Report Series*, 1.

[16] Betts AK, Ball JH, Beljaars ACM, Miller MJ, Viterbo PA (1996): The land surface-atmosphere interaction: A review based on observational and global modelling perspectives. *J Geophys Res*, 101 (NO. D3): 7209-7225.

[17] Betts AK (2004): Understanding Hydrometeorology using global models. *Bull Amer Meteorol Soc*, 85: 1673-1688.

[18] Betts AK, Viterbo P (2005): Land-surface, boundary layer and cloud-field coupling over the south-western Amazon in ERA-40. *J Geophys Res*, 110: D14108, doi:10.1029/2004JD005702.

[19] Betts AK (2007): Coupling of water vapor convergence, clouds, precipitation, and land-surface processes. *J Geophy Res*, 112: D10108, doi:10.1029/2006JD008191.

[20] Bierkens MFP, van den Hurk BJJM (2007): Groundwater convergence as a possible mechanism for multi-year persistence in rainfall. *Geophys Res Lett*, 34: L02402, doi:10.1029/2006GL028396.

[21] Bisselink B, Dolman AJ (2008): Precipitation recycling: Moisture sources over Europe using ERA-40 data. *J Hydrometeorol*, 9 (5): 1073-1083.

[22] Bisselink B, Dolman AJ (2009): Recycling of moisture in Europe: contribution to variability in very wet and dry years. *Hydrol Earth Syst Sci*, 13: 1685-1697.

[23] Bosilovich MG, Schubert SD (2001): Precipitation recycling over the central United States diagnosed from the GEOS-1 Data Assimilation System. *J Hydrometeor*, 2: 26-35.

[24] Bosilovich MG (2002): On the vertical distribution of local and remote sources of water for precipitation. *Meteor Atmos Phys*, 80: 31-41.

[25] Bosilovich MG, Schubert SD (2002): Water vapour tracers as diagnostics of the regional hydrologic cycle. *J Hydrometeor*, 3: 149-165.

[26] Bosilovich MG, Sud YC, Schubert SD, Walker GK (2003): Numerical simulation of the large-scale North American monsoon water sources. *J Geophys Res*, 108, 8614, doi:10.1029/2002JD003095.

[27] Bosilovich MG, Schubert SD, Walker GK (2005): Global changes of the water cycle intensity. *J Climate*, 18: 1591-1608.

[28] Bosilovich MG, Chern JD (2006): Simulation of water sources and precipitation recycling for the MacKenzie, Mississippi, and Amazon river basins. *J Hydrometeor*, 7: 312-329.

[29] Boucher O, Myhre G, Myhre A (2004): Direct human influence of irrigation on atmospheric water vapour and climate. *Clim Dyn*, 22: 597-603.

[30] Brolsma RJ, Karssenberg D, Bierkens MFP (2010): Vegetation competition model for water and light limitation. I: Model description, one-dimensional competition and the influence of groundwater. *Ecological Modelling*, 221: 1348-1363.

[31] Brown ME, Arnold DL (1998): Land-surface-atmosphere interactions associated with deep convection in Illinois. *Int J Climatol*, 18: 1637-1653.

[32] Brubaker KL, Entekhabi D, Eagleson PS (1993): Estimation of continental precipitation recycling. *J Climate*, 6: 1077-1089.

[33] Brubaker KL, Entekhabi D (1996): Analysis of feedback mechanisms in land-atmosphere interaction. *Water Resour Res*, 32: 1343-1357.

[34] Brubaker KL, Dirmeyer PA, Sudradjat A, Levy BS, Bernal F (2001): A 36-yr climatological description of the evaporative sources of warm-season precipitation in the Mississippi River Basin. *J Hydrometeor*, 2: 537-557.

[35] Budyko MI (1974): Climate and life. *Academic Press. International Geophysics Series*, v. 18, San Diego, CA. 508pp.

[36] Burde GI, Zangvil A, Lamb PJ (1996): Estimating the role of local evaporation in precipitation for a two-dimensional region. *J Climate*, 9: 1328-1338.

[37] Burde GI, Zangvil A (2001a): The estimation of regional precipitation recycling. Part I: review of recycling models. *J Climate*, 14: 2497-2508.

[38] Burde GI, Zangvil A (2001b): The estimation of regional precipitation recycling. Part II: a new recycling model. *J Climate*, 14: 2509-2527.

[39] Burde GI (2006): Bulk recycling models with incomplete vertical mixing. Part I: Conceptual framework and models. *J Climate*, 19: 1461-1472.

[40] Burde GI, Gandush C, Bayarjargal Y (2006): Bulk recycling models with incomplete vertical mixing. Part II: Precipitation recycling in the Amazon Basin. *J Climate*, 19: 1473-1489.

[41] Capel-Molina JJ (1981): Los climas de España. *Oikos-Tau*, Barcelona, 429 pp. ISBN: 84-281-0492-1.

[42] Capel-Molina JJ (2000): El clima de la Península Ibérica. Ariel, Barcelona, 281 pp. ISBN: 84-344-3466-0.

[43] Cardoso RM, Soares PMM, Miranda PMA, Belo-Pereira M (2012): WRF high resolution simulation of Iberian mean and extreme precipitation climate. *Int J Climatol*, doi:10.1002/joc.3616.

[44] Castro M, Martín-Vide J, Alonso S (2005): The climate of Spain: Past, present and scenarios for the 21st century - A preliminary assessment of the impacts in Spain due to the effect of climate change. *In: Moreno JM (ed), Spanish Ministry of the Environment, ECCE Project Final Rep*, pp 1-62.

[45] Chen F, Avissar R (1994): Impact of land-surface moisture variability on local shallow convective cumulus and precipitation in large-scale models. *J Appl Met*, 33: 1382-1401.

[46] Chen F, Dudhia J (2001a): Coupling an advanced land surface-hidrology model with the Penn State-NCAR MM5 modeling system. Part I: Model implementation and sensitivity. *Mon Weather Rev*, 129 (4): 569-585.

[47] Chen F, Dudhia J (2001b): Coupling an advanced land surface-hidrology model with the Penn State-NCAR MM5 modeling system. Part II: Preliminary model validation. *Mon Weather Rev*, 129 (4): 587-604.

[48] Cook BI, Bonan GB, Levis S (2006): Soil moisture feedbacks to precipitation in South Africa. *J Climate*, 19: 4198-4206.

[49] DeAngelis A, Domínguez F, Fan Y, Robock A, Kustu MD, Robinson D (2010): Evidence of enhanced precipitation due to irrigation over the Great Plains of the United States. *J Geophys Res*, 115: D15115, doi:10.1029/2010JD013892.

[50] Dee DP et al. (2011): The ERA-Interim reanalysis: configuration and performance of the data assimilation system. *Q J R Meteorol Soc*, 137 (656): 553-597.

[51] Dekker SC, Rietkerk M, Bierkens MFP (2007): Coupling microscale vegetation-soil water and macroscale vegetation-precipitation feedbacks in semiarid ecosystems. *Global Change Biology*, 13: 671-678.

[52] De Luis M, Brunetti M, Gonzalez-Hidalgo JC, Longares LA, Martin-Vide J (2010): Changes in seasonal precipitation in the Iberian Peninsula during 1946-2005. *Global Planet Change*, 74: 27-33.

[53] Delworth TL, Manabe S (1989): The influence of soil wetness on near-surface atmospheric variability. *J Climate*, 2: 1447-1462.

[54] De Ridder K (1997): Land surface processes and the potential for convective precipitation. *J Geophys Res*, 102: 30085-30090.

[55] De Ridder K, Gallée H (1998): Land Surface-Induced Regional Climate Change in Southern Israel. *J Appl Meteor*, 37: 1470-1485.

[56] Dingman, SL (2002): Physical Hydrology. Second edition. 646 pp. *Waveland Press Inc*, USA. ISBN-13: 978-1-57766-561-8, ISBN-10: 1-57766-561-9.

[57] Dirmeyer PA, Brubaker KL (1999): Contrasting evaporative moisture sources during the drought of 1988 and the flood of 1993. *J Geophys Res*, 104 (D16): 19383-19397.

[58] Dirmeyer PA (2000): Using a global soil wetness dataset to improve seasonal climate simulation. *J Climate*, 13: 2900-2922.

[59] Dirmeyer PA (2001): An evaluation of the strength of land-atmosphere coupling. *J Hydrometeor*, 2: 329-344.

[60] Dirmeyer PA (2003): The role of the land surface background state in climate predictability. *J Hydrometeor*, 4: 599-610.

[61] Dirmeyer PA (2006): The hydrologic feedback pathway for land-climate coupling. *J Hydrometeor*, 7: 857-867.

[62] Dirmeyer PA, Koster RD, Guo Z (2006): Do global models properly represent the feedback between land and atmosphere? *J Hydrometeor*, 7: 1177-1198.

[63] Dirmeyer PA, Brubaker KL (2007): Characterization of the global hydrologic cycle from a back-trajectory analysis of atmospheric water vapour. *J Hydrometeor*, 8: 20-37.

[64] Dirmeyer PA, Schlosser CA, Brubaker KL (2009a): Precipitation, recycling, and land memory: an integrated analysis. *J Hydrometeor*, 10: 278-288.

[65] Dirmeyer PA, Brubaker KL, DelSole T (2009b): Import and export of atmospheric water vapor between nations. *J Hydrol*, 365 (1-2): 11-22.

[66] D'Odorico P, Porporato A (2004): Preferential states in soil moisture and climate dynamics. *Proc Natl Acad Sci USA*, 101: 8848-8851.

[67] Domínguez F, Kumar P, Liang X, Ting M (2006): Impact of atmospheric moisture storage on precipitation recycling. *J Climate*, 19: 1513-1530.

[68] Domínguez F, Kumar P (2008): Precipitation recycling variability and ecoclimatological stability - A study using NARR data. Part I: Central U.S. Plains ecoregion. *J Climate*, 21: 5165-5186.

[69] Domínguez F, Kumar P, Vivoni ER (2008): Precipitation recycling variability and ecoclimatological stability - A study using NARR data. Part II: North American monsoon region. *J Climate*, 21: 5187-5203.

[70] Domínguez F, Villegas JC, Breshears DD (2009): Spatial extent of the North American Monsoon: increased cross-regional linkages via atmospheric pathways. *Geophys Res Lett*, 36: L07401, doi:10.1029/2008GL037012.

[71] Douville H, Chauvin F (2000): Relevance of soil moisture for seasonal climate predictions: A preliminary study. *Climate Dyn*, 16: 719-736.

[72] Drozdov OA, Grigor'eva AS (1965): The Hydrologic Cycle in the Atmosphere. *Israel Program for Scientific Translations*, 282 pp.

[73] Drumond A, Nieto R, Gimeno L, Vicente-Serrano SM, López-Moreno JI, Morán-Tejeda E (2011): Characterization of the atmospheric component of the winter hydrological cycle in the Galicia/North Portugal Euro-region: a lagrangian approach. *Clim Res*, 48: 193-201, doi:10.3354/cr00987.

[74] Dudhia J (1989): Numerical study of convection observed during the winter monsoon experiment using a mesoscale two-dimensional model. *J Atmos Sci*, 40 (20): 3077-3107.

[75] Ek M, Holtslag AAM (2004): Influence of soil moisture on boundary layer cloud development. *J Hydrometeorol*, 5: 86-99.

[76] Eltahir EAB, Bras LB (1994): Precipitation recycling in the Amazon basin. *Q J R Meteorol Soc*, 120: 861-880.

[77] Eltahir EAB, Bras LB (1996): Precipitation recycling. *Rev Geophys*, 34: 367-378.

[78] Eltahir EAB, Pal JS (1996): Relationship between surface conditions and subsequent rainfall in convective storms. *J Geophys Res*, 101: 26237-26245.

[79] Eltahir EAB (1998): A soil moisture rainfall feedback mechanism: 1. Theory and observations. *Water Resour Res*, 34: 765-776.

[80] Enthekabi D, Rodríguez-Iturbe I, Bras RL (1992): Variability in large-scale water balance with land surface-atmosphere interaction. *J Climate*, 5: 798-813.

[81] Enthekabi D, Rodríguez-Iturbe I, Castelli F (1996): Mutual interaction of soil moisture state and atmospheric processes. *J Hydrol*, 184: 3-17.

[82] Esteban-Parra MJ, Rodrigo FS, Castro-Díez Y (1998): Spatial and temporal patterns of precipitation in Spain for the period 1880-1992. *Int J Climatol*, 18: 1557-1574.

[83] Estrela MJ, Peñarrocha D, Millán M (2000): Multi-annual drought episodes in the Mediterranean (Valencia region) from 1950-1996. A spatio-temporal analysis. *Int J Climatol*, 20: 1599-1618.

[84] Fan Y, Miguez-Macho G, Weaver CP, Walko R, Robock A (2007): Incorporating water table dynamics in climate modeling: 1. Water table observations and equilibrium water table simulations. *J Geophys Res*, 112: D10125, doi:10.1029/2006JD008111.

[85] Fan Y, Miguez-Macho G (2010): Potential groundwater contribution to Amazon evapotranspiration. *Hydrol Earth Syst Sci*, 14: 2039-2056.

[86] Fennessy MJ, Shukla J (1999): Impact of initial soil wetness on seasonal atmospheric prediction. *J Climate*, 12: 3167-3180.

[87] Ferranti L, Viterbo P (2006): The European summer of 2003: sensitivity to soil water initial conditions. *J Climate*, 19: 3659-3680.

[88] Findell KL, Eltahir EAB (1997): An analysis of the soil moisture-rainfall feedbacks, based on direct observations from Illinois. *Water Resour Res*, 33: 725-735.

[89] Findell KL, Eltahir EAB (1999): Analysis of the pathways relating soil moisture and subsequent rainfall in Illinois. *J Geophys Res*, 104 (D24): 31565-31574.

[90] Findell KL, Eltahir EAB (2003a): Atmospheric controls on soil moisture-boundary layer interactions. Part I: Framework development. *J Hydrometeorol*, 4: 552-569.

[91] Findell KL, Eltahir EAB (2003b): Atmospheric controls on soil moisture-boundary layer interactions. Part II: Feedbacks within the continental United States. *J Hydrometeorol*, 4: 570-583.

[92] Fischer EM, Seneviratne SI, Luthi D, Schär C (2007a): Contribution of land-atmosphere coupling to recent European summer heat waves. *Geophys Res Lett*, 34: L06707, doi:10.1029/2006GL029068.

[93] Fischer EM, Seneviratne SI, Vidale PL, Luthi D, Schär C (2007b): Soil moisture-atmosphere interactions during the 2003 European summer heat wave. *J Climate*, 20: 5081-5099.

[94] Fitts CR (2002): Groundwater Science. 450 pp. *Academic Press*, San Diego, California (USA). ISBN-13: 978-0-12-257855-7, ISBN-10: 0-12-257855-4.

[95] Fitzmaurice JA (2007): A critical analysis of bulk precipitation recycling models. Ph.D. Thesis, Massachusetts Institute of Technology, Massachusetts.

[96] Font-Tullot I (1988): Historia del clima de España. *Instituto Nacional de Meteorología*, 297 pp. ISBN: 84-505-7178-2.

[97] Font-Tullot I (2000): Climatología de España y Portugal (Second edition). *Ediciones Universidad de Salamanca.*

[98] Froehlich K, Kralik M, Papesch W, Rank D, Scheifinger H, Stichler W (2008): Deuterium excess in precipitation of Alpine regions-Moisture recycling. *Isotopes Environ Health Stud*, 44 (1): 61-70.

[99] Galán E, Cañada R, Rasilla D, Fernández F, Cervera B (1999): Evolución de las precipitaciones anuales en la Meseta Meridional durante el siglo XX. In: *I Congreso AEC. La Climatología española en los albores del siglo XXI*, Raso Nadal JM, Martín-Vide J (eds). Publicaciones de la Asociación Española de Climatología (AEC), Serie A, nº 1. Oikos-Tau, Barcelona, 587 pp.

[100] Gallego MC, García JA, Vaquero JM (2005): The NAO signal in daily rainfall series over the Iberian Peninsula. *Clim Res*, 29: 103-109.

[101] Gallego MC, García JA, Vaquero JM, Mateos VL (2006): Changes in frequency and intensity of daily precipitation over the Iberian Peninsula. *J Geophys Res*, 111: 2156-2202, doi:10.1029/2006JD007280.

[102] García JA, Serrano A, Gallego MC (2002): A spectral analysis of Iberian Peninsula monthly rainfall. *Theor Appl Climatol*, 71: 77-95.

[103] García NO, Gimeno L, De La Torre L, Nieto R, Añel JA (2005): North Atlantic Oscillation (NAO) and precipitation in Galicia (Spain). *Atmósfera*, 18 (1): 25-32.

[104] García JA, Gallego MC, Serrano A, Vaquero JM (2007): Trends in block-seasonal extreme rainfall over the Iberian Peninsula in the second half of the Twentieth Century. *J Climate*, 20: 113-130.

[105] García-Herrera R, Gimeno L, Ribera P, Hernández E (2005): New records of Atlantic hurricanes from Spanish documentary sources. *J Geophys Res*, 110 (D3): D03109.

[106] García-Herrera R, Paredes D, Trigo RM, Trigo IF, Hernández E, Barriopedro D, Mendes MA (2007): The outstanding 2004/2005 drought in the Iberian Peninsula: Associated atmospheric circulation. *J Hydrometeor*, 8: 483-498.

[107] Georgescu M, Weaver CP, Avissar R, Walko RL, Miguez-Macho G (2003): Sensitivity of model-simulated summertime precipitation over the Mississippi River Basin to the spatial distribution of initial soil moisture. *J Geophys Res*, 108 (D22): 8855, doi:10.1029/2002JD003107.

[108] Gerard L (2007) An integrated package for subgrid convection, clouds and precipitation compatible with meso-gamma scales. *Q J R Meteorol Soc*, 133: 711-730.

[109] Gestal-Souto L, Martínez A, Rios-Entenza A (2010): O papel das augas freáticas nas interaccións terra-atmosfera, no clima e no réxime pluviométrico da Península Ibérica. *Revista Real Academia Galega de Ciencias*, vol. XXIX: 89-128.

[110] Gimeno L, Nieto R, Trigo RM, Vicente-Serrano SM, López-Moreno JI (2010a): Where does the Iberian Peninsula moisture come from? An answer based on a lagrangian approach. *J Hydrometeor*, 11: 421-436.

[111] Gimeno L, Drumond A, Nieto R, Trigo RM, Stohl A (2010b): On the origin of continental precipitation. *Geophys Res Lett*, 37: L13804, doi:10.1029/2010GL043712.

[112] Gimeno L, Trigo RM, Gómez-Gesteira M (2011): Regional climate change in the NW Iberian Peninsula. *Clim Res*, 48: 105-108.

[113] Gimeno L, Stohl A, Trigo RM, Domínguez F, Yoshimura K, Yu L, Drumond A, Durán-Quesada AM, Nieto R (2012): Oceanic and terrestrial sources of continental precipitation. *Rev Geophys*, 50: RG4003, doi:10.1029/2012RG000389.

[114] Giorgi F (2006): Climate change hot-spots. *Geophys Res Lett*, 33: L08707, doi:10.1029/2006GL025734.

[115] Giorgi F, Lionello P (2008): Climate change projections for the Mediterranean region. *Global and Planetary Change*, 63 (2-3): 90-104.

[116] Goessling HF, Reick CH (2011): What do moisture recycling estimates tell us? Exploring the extreme case of non-evaporating continents. *Hydrol Earth Syst Sci*, 15: 3217-3235.

[117] González-Hidalgo JC, De Luis M, Raventós J, Sánchez JR (2001): Spatial distribution of seasonal rainfall trends in a western Mediterranean area. *Int J Climatol*, 21: 843-860.

[118] González-Hidalgo JC, López-Bustins JA, Stepánek P, Martín-Vide J, de Luis M (2009): Monthly precipitation trends on the Mediterranean fringe of the Iberian Peninsula during the second-half of the twentieth century (1951-2000). *Int J Climatol*, 29: 1415-1429.

[119] Goodess CM, Jones PD (2002): Links between circulation and changes in the characteristics of Iberian rainfall. *Int J Climatol*, 22: 1593-1615.

[120] Gordon LJ, Steffen W, Jonsson BF, Folke C, Falkenmark M, Johannessen A (2005): Human modification of global water vapor flows from the land surface. *P Natl Acad Sci*, 102: 7612-7617.

[121] Gouveia C, Trigo RM, DaCamara CC (2009): Drought and vegetation stress monitoring in Portugal using satellite data. *Nat Hazards Earth Syst Sci*, 9: 185-195.

[122] Guo Z and coauthors (2006): GLACE: The Global Land-Atmosphere Coupling Experiment. Part II: Analysis. *J Hydrometeor*, 7: 611-625.

[123] Herrera S, Gutiérrez J, Ancell R, Pons M, Frías M, Fernández J (2010): Development and analysis of a 50-year high-resolution daily gridded precipitation dataset over Spain (Spain02). *Int J Climatol*, 32: 74-85.

[124] Hoerling M, Eischeid J, Perlwitz J, Quan X, Zhang T, Pegion P (2012): On the increased frequency of Mediterranean drought. *J Climate*, 25: 2146-2161.

[125] Hohenegger C, Brockhaus P, Bretherton CS, Schär C (2009): The soil moisture-precipitation feedback in simulations with explicit and parameterized convection. *J Climate*, 22: 5003-5020.

[126] Holton JR (1972): An Introduction to Dynamic Meteorology. *Academic Press*. San Diego, California (USA). 3rd edition (1992). ISBN: 0-12-354355-X.

[127] Holzman B (1937) Sources of moisture for precipitation in the United States. U.S. Department of Agriculture. Tech. Bull. No. 589.

[128] Hong S, Lim JJ (2006): The WRF single-moment 6-class microphysics scheme (WSM6). *J Korean Meteor Soc*, 42 (2): 129-151.

[129] Horton RE (1933): The role of infiltration in the hydrologic cycle. *Trans Am Geophys Union*, 14446-14460.

[130] Iorio JP, et al (2004): Effects of model resolution and subgrid scale physics on the simulation of precipitation in the continental United States. *Clim Dyn*, 23: 243-258.

[131] IPCC, Intergovernmental Panel on Climate Change (1990): Scientific assessment of climate change. Report of Working Group I. Houghton JT, Jenkins GJ, Ephraums JJ (eds). *Cambridge Univ Press*, Cambridge, UK.

[132] IPCC, Intergovernmental Panel on Climate Change (1996): Climate Change 1995: The Science of Climate Change. Contribution of Working Group I to the Second Assessment Report of the Intergovernmental Panel on Climate Change. Houghton JT, Meira Filho LG, Callender BA, Harris N, Kattenberg A, Maskell K (eds). *Cambridge Univ Press*, Cambridge, UK.

[133] IPCC, Intergovernmental Panel on Climate Change (2001): Climate Change 2001: The Scientific Basis. Contribution of Working Group I to the Third Assessment Report of the Intergovernmental Panel on Climate Change. *Cambridge Univ Press*, New York.

[134] IPCC, Intergovernmental Panel on Climate Change (2007): Climate Change 2007: The Physical Science Basis. Contribution of Working Group I to the Fourth Assessment Report of the Intergovernmental Panel on Climate Change. Solomon S, Qin D, Manning M, Chen Z, Marquis M, Averyt KB, Tignor M and Miller HL (eds.), 976 pp. *Cambridge Univ Press*, Cambridge, UK.

[135] Jaeger EB, Stockli R, Seneviratne SI (2009): Analysis of planetary boundary layer fluxes and land-atmosphere coupling in the regional climate model CLM. *J Geophys Res*, 114: D17106.

[136] Jiang XY, Niu GY, Yang ZL (2009): Impacts of vegetation and groundwater dynamics on warm season precipitation over the Central United States. *J Geophys Res*, 114: D06109, doi:10.1029/2008JD010756.

[137] Jiménez Muñoz PA (2010): Analysis of surface wind over complex terrain: a dynamical downscaling study with the WRF model. Ph.D. Thesis, Universidad Complutense de Madrid (Spain).

[138] Jódar J, Carrera J, Cruz A (2010): Irrigation enhances precipitation at the mountains downwind. *Hydrol Earth Syst Sci*, 14(10): 2003-2010. doi:10.5194/hess-14-2003-2010.

[139] Joussaume S, Sadourny R, Jouzel J (1984): A general circulation model of water isotope cycles in the atmosphere. *Nature*, 311: 24-29.

[140] Joussaume S, Sadourny R, Vignal C (1986): Origin of precipitating water in a numerical simulation of July climate. *Ocean-Air Interact*, 1: 43-56.

[141] Jouzel J, Merlivat L (1984): Deuterium and oxygen-18 in precipitation: Modeling of the isotopic effects during snow formation. *J Geophys Res-Atmos*, 89 (D7): 2156-2202, doi:10.1029/JD089iD07p11749.

[142] Kain HS, Fritsch JM (1990): A one-dimensional entraining/detraining plume model and its aplications in convective precipitation. *J Atmos Sci*, 47: 2784-2802.

[143] Kain HS, Fritsch JM (1993): Convective parameterization for mesoscale models: The Kain-Fritsch scheme - The representation of cumulus convection in numerical models. Emanuel KA, Raymond DJ (eds) *American Meteorological Society*, 246 pp.

[144] Kanae S, Hirabayashi Y, Yamada T, Oki T (2006): Influence of "realistic" land surface wetness on predictability of seasonal precipitation in boreal summer. *J Climate*, 19 (8): 1450-1460.

[145] Kanamitsu M, Saha S (1996): Systematic tendency error in budget calculations. *Mon Wea Rev*, 124: 1145-1160.

[146] Kochendorfer JP, Ramirez JA (2005): The impact of land-atmosphere interactions on the temporal variability of soil moisture at the regional scale. *J Hydrometeor*, 6: 53-67.

[147] Koster RD, Jouzel J, Suozzo R, Russell G, Broecker W, Read D, Eagleson PS (1986): Global sources of local precipitation as determined by the NASA/GISS GCM. *Geophys Res Lett*, 13: 121-124.

[148] Koster RD, Jouzel J, Suozzo RJ, Russell GL (1992): Origin of July Antarctic precipitation and its influence on deuterium content: a GMC analysis. *Clim Dyn*, 7: 195-203.

[149] Koster RD, de Valpine DP, Jouzel J (1993): Continental water recycling and $H_2{}^{18}O$ concentrations. *Geophys Res Lett*, 20: 2215-2218.

[150] Koster RD, Suarez MJ (1995): The relative contributions of land and ocean processes to precipitation variability. *J Geophys Res*, 100: 13775-13790.

[151] Koster RD, Suarez MJ, Heiser M (2000): Variance and predictability of precipitation at seasonal-to-interannual timescales. *J Hydrometeor*, 1: 26-46.

[152] Koster RD, Suarez MJ (2001): Soil moisture memory in climate models. *J Hydrometeor*, 2: 558-570.

[153] Koster RD, Suarez MJ (2003): Impact of land surface initialization on seasonal precipitation and temperature prediction. *J Hydrometeor*, 4: 408-423.

[154] Koster RD, Suarez MJ, Higgins RW, Van den Dool H (2003): Obervational evidence that soil moisture variations affect precipitation. *Geophys Res Lett*, 30: 1241, doi:10.1029/2002GL016571.

[155] Koster RD, Suarez MJ (2004) Suggestions in the observational record of land-atmosphere feedback operating at seasonal time scales. *J Hydrometeorol*, 5: 567-572.

[156] Koster RD and coauthors (2004): Regions of strong couplig between soil moisture and precipitation. *Science*, 305: 1138-1140.

[157] Koster RD and coauthors (2006): GLACE: The Global Land-Atmosphere Coupling Experiment. Part I: Overview. *J Hydrometeor*, 7: 590-610.

[158] Kurita N, Yoshida N, Inoue G, Chayanova EA (2004): Modern isotope climatology of Russia: A first assessment. *J Geophys Res*, 109: D03102, doi:10.1029/2003JD003404.

[159] Lam AHA, Bierkens MFP, van den Hurk BJJM (2007): Global patterns of relations between soil moisture and rainfall occurence in ERA40. *J Geophys Res*, 112: D17116, doi:10.1029/2006JD008222.

[160] Lana X, Burgueño A (2000): Some statistical characteristics of monthly and annual pluviometric irregularity for the Spanish Mediterranean Coast. *Theor Appl Climatol*, 65: 79-97.

[161] Lettau H, Lettau K, Molion LC (1979): Amazonia's hydrological cycle and the role of atmospheric recycling in assessing deforestation effects. *Mon Wea Rev*, 107 (3): 227-238.

[162] Liu Y, Avissar R (1999): A study of persistence in the land-atmosphere system using a General Circulation Model and observations. *J Climate*, 12: 2139-2153.

[163] Liu Z, Tian L, Yao T, Yu W (2008): Seasonal deuterium excess in Nagqu precipitation: Influence of moisture transport and recycling in the middle of Tibetan Plateau. *Environ Geol*, 55: 1501-1506.

[164] Llasat MC, Puigcerver M (1997): Total rainfall and convective rainfall in Catalonia, Spain. *Int J Climatol*, 17: 1683-1695.

[165] López-Moreno, JI, Beguería S, Vicente-Serrano SM, García-Ruiz JM (2007): Influence of the North Atlantic Oscillation on water resources in central Iberia: Precipitation, streamflow anomalies, and reservoir management strategies. *Water Resour Res*, 43: W09411, doi:10.1029/2007WR0095864.

[166] López-Moreno, JI, Vicente-Serrano SM, Angulo-Martínez M, Beguería S, Kenawy A (2010): Trends in daily precipitation on the northeastern Iberian Peninsula, 1955-2006. *Int J Climatol*, 30: 1026-1041.

[167] Marengo JA (2006): On the hydrological cycle of the Amazon Basin: a historical review and current state-of-the-art. *Revista Brasileira de Meteorologia*, 21 (3): 1-19.

[168] Mariotti A, Zeng N, Yoon JH, Artale V, Navarra A, Alpert P, Li L (2008): Mediterranean water cycle changes: Transition to drier 21st century conditions in observations and CMIP3 simulations. *Environ Res Lett*, 15: 674-1690.

[169] Martín A, Romero R, De Luque A, Alonso S, Rigo T, Llasat MC (2007): Sensitivities of a flash flood event over Catalonia: a numerical analysis. *Mon Wea Rev*, 135: 651-669.

[170] Martín-Vide J (1991): Fundamentos de climatología analítica. *Síntesis*, Barcelona, 157 pp. ISBN: 84-7738-113-5.

[171] Martín-Vide J, Fernández-Belmonte D (2001): El índice NAO y la precipitación mensual en la Españ peninsular. *Investigaciones Geográficas*, 26: 41-58.

[172] Martín-Vide J, Olcina-Cantos J (2001): Climas y tiempos de España. *Alianza Editorial*, ISBN: 84-206-5777-8, 258 pp.

[173] Martín-Vide J (2004): Spatial distribution of a daily precipitation concentration index in Peninsular Spain. *Int J Climatol*, 24: 959-971.

[174] Martín-Vide J, López-Bustins JA, 2006: The Western Mediterranean Oscillation and rainfall in the Iberian Peninsula. *Int J Climatol*, 26: 1455-1475.

[175] Maxwell RM, Chow FK, Kollet SJ (2007): The groundwater-land-surface-atmosphere connection: Soil moisture effects on the atmospheric boundary layer in fully-coupled simulations. *Adv Wat Resour*, 30: 2447-2466.

[176] McDonald JE (1962): The evaporation-precipitation fallacy. *Weather*, 17: 168-177.

[177] McNish AG (1936): Statistical aspects of long-range weather forecasting. *Eos Trans AGU*, 1: 124-129.

[178] Merrill JT, Bleck R, Boudra D (1986): Techniques of lagrangian trajectory analysis in isentropic coordinates. *Mon Weather Rev*, 114: 571-581.

[179] Miguez-Macho G, Stenchikov GL, Robock A (2004) Spectral nudging to eliminate the effects of domain position and geometry in regional climate model simulations. *J Geophys Res-Atmospheres*, 109: D13104.

[180] Miguez-Macho G, Stenchikov GL, Robock A (2005): Regional climate simulations over North America: Interaction of local processes with improved large-scale flow. *J Climate*, 18: 1227-1246.

[181] Miguez-Macho G, Fan Y, Weaver CP, Walko R, Robock A (2007): Incorporating water table dynamics in climate modeling: 2. Formulation, validation, and soil moisture simulation. *J Geophys Res-Atmos*, 112: D13108.

[182] Miguez-Macho G, Li H, Fan Y (2008): Simulated water table and soil moisture climatology over North America. *Bull Amer Meteor Soc*, 89: 663-672.

[183] Millán MM, Estrela MJ, Miro J (2005): Rainfall Components: Variability and Spatial Distribution in a Mediterranean Area (Valencia Region). *J Climate*, 18 (14): 2682-2705.

[184] Mlawer EJ, Taubman SJ, Brown PD, Iacono MJ, Clough SA (1997): Radiative transfer for inhomogeneous atmospheres: RRTM, a validated correlated k model for the longwave. *J Geophys Res*, 102: 16663-16682.

[185] Mosmann V, Castro A, Fraile R, Dessens J, Sánchez JL (2004): Detection of statistically significant trends in the summer precipitation of mainland Spain. *Atmos Res*, 70: 43-53.

[186] Muñoz-Díaz D, Rodrigo FS (2005): Seasonal rainfall variations in Spain (1912-2000) and their links to atmospheric circulation. *Atmos Res*, 81: 94-110.

[187] Nieto R, Gimeno L, de la Torre L, Ribera P, Gallego D, García R, García JA, Núñez M, Redaño A, Lorente J (2005): Climatological features of cut-off low systems in the Northern Hemisphere. *J Climate*, 18: 3085-3113.

[188] Nieto R, Gimeno L, Trigo RM (2006): A lagrangian identification of major sources of Sahel moisture. *Geophys Res Lett*, 33: L18707, doi:10.1029/2006GL027232.

[189] Nieto R, Gimeno L, Añel JA, de la Torre L, Gallego D, Barriopedro D, Gallego M, Gordillo A, Redaño A, Delgado G (2007a): Analysis of the precipitation and cloudiness associated with COLs occurrence in the Iberian Peninsula. *Meteorol Atmos Phys*, 96: 103-119.

[190] Nieto R, Gimeno L, de la Torre L, Ribera P, Barriopedro D, García-Herrera R, Serrano A, Gordillo A, Redaño A, Lorente J. (2007b): Interannual variability of cut-off low systems over the European sector: the role of blocking and the northern hemisphere circulation modes. *Meteorol Atmos Phys*, 96: 85-101.

[191] Nobre CA, Sellers PJ, Shukla J (1991): Amazonian deforestation and regional climatic change. *J Climate*, 4: 957-988.

[192] Numaguti A (1999): Origin and recycling process of precipitation water over the Eurasian continent: Experiments using an atmospheric general circulation model. *J Geophys Res*, 104 (NO. D2): 1957-1972.

[193] Oki T (2005): The hydrologic cycles and global circulation. In *Encyclopedia of Hydrological Sciences*, edited by MG Anderson and J McDonnell, pp 13-22, John Wiley, New York.

[194] Oki T, Kanae S (2006): Global hydrological cycles and world water resources. *Science*, 313: 1068-1072. doi:10.1126/science.1128845.

[195] Paegle J, Mo KC, Nogués-Paegle J (1996): Dependence of simulated precipitation on surface evaporation during the 1993 United States Summer Floods. *Mon Weather Rev*, 124: 345-361.

[196] Pal JS, Eltahir EAB (2001): Pathways relating soil moisture conditions to future summer rainfall within a model of the land-atmosphere system. *J Climate*, 14: 1227-1242.

[197] Pal JS, Eltahir EAB (2003): A feedback mechanism between soil-moisture distribution and storm tracks. *Q J R Meteor Soc*, 129: 2279-2297.

[198] Paredes D, Trigo RM, García-Herrera R, Trigo IF (2006): Understanding precipitation changes in Iberia in early spring: Weather typing and storm-tracking approaches. *J Hydrometeor*, 7: 101-113.

[199] Peixoto J (1973): Atmospheric vapour flux computations for hydrological purposes. *Rep.* 20, pp 1-83, World Meteorol. Organization. Geneva.

[200] Peixoto JP, Oort AH (1992): Physics of Climate. *Springer-Verlag*, New York, 520 pp, ISBN: 0-88318-712-4.

[201] Pielke RA, Avissar R, Raupach M, Dolman AJ, Zeng XB, Denning AS (1998): Interactions between the atmosphere and terrestrial ecosystems: influence on weather and climate. *Glob Chang Biol*, 4 (5): 461-475.

[202] Pielke RA (2001): Influence of the spatial distribution of vegetation and soils on the prediction of cumulus convective rainfall. *Rev Geophys*, 39: 151-177.

[203] Pielke Sr RA, Adegoke J, Beltrán-Przekurat A, Hiemstra CA, Lin J, Nair US, Niyogi D, Nobis TE (2007): An overview of regional land-use and land-cover impacts on rainfall. *Tellus Ser B-Chem Phys Meteorol*, 59: 587-601.

[204] Pitman AJ (2003): The evolution of, and revolution in, land surface schemes designed for climate models. *Int J Climatol*, 23: 479-510.

[205] Pozo-Vázquez D, Gámiz-Fortis SR, Tovar-Pescador J, Esteban-Parra MJ, Castro-Díez Y (2005): El Niño-Southern Oscillation events and associated European winter precipitation anomalies. *Int J Climatol*, 25: 17-31, doi:10.1002/joc.1097.

[206] Quante M, Matthias V (2006): Water in the Earth's atmosphere. *J Phys IV*, 139: 37-61.

[207] Quesada B, Vautard R, Yiou P, Hirschi M, Seneviratne SI (2012): Asymmetric European summer heat predictability from wet and dry southern winters and springs. *Nature Clim Change*, 2: 736-741.

[208] Raso Nadal JM (1996): Evolución secular de las precipitaciones de primavera en la Meseta Septentrional de la Península Ibérica. In: Juaristi J, Moro I (coord): Modelos y Sistemas de Información en Geografía. *Comunicaciones del VII Coloquio de Geografía Cuantitativa, SIG y Teledetección*. Vitoria, pp 147-154.

[209] Rocha A (1999): Low-frequency variability of seasonal rainfall over the Iberian Peninsula and ENSO. *Int J Climatol*, 19: 889-901.

[210] Rodríguez-Puebla C, Encinas AH, Nieto S, Garmendia J (1998): Spatial and temporal patterns of annual precipitation variability over the Iberian Peninsula. *Int J Climatol*, 18: 299-316.

[211] Rodríguez-Puebla C, Encinas AH, Sáenz J (2001): Winter precipitation over the Iberian peninsula and its relationship to circulation indices. *Hydrol Earth Syst Sci*, 5: 233-244.

[212] Romero R, Guijarro JA, Ramis C, Alonso S (1998): A 30-year (1964-1993) daily rainfall data base for the Spanish mediterranean regions: first exploratory study. *Int J Climatol*, 18: 541-560.

[213] Rozanski K, Sonntag C, Münnich KO (1982): Factors controlling stable isotope composition of European precipitation. *Tellus*, 34: 142-150.

[214] Sáenz J, Zubillaga J, Rodríguez-Puebla C (2001): Interannual variability of winter precipitation in northern Iberian Peninsula. *Int J Climatol*, 21: 1503-1513.

[215] Salati E, Olio AD, Matsui E, Gat JR (1979): Recycling of water in the Amazon Basin: An isotopic study. *Water Resour Res*, 15: 1250-1258.

[216] Salvucci GD, Saleem JA, Kaufmann R (2002): Investigating soil moisture feedbacks on precipitation with tests of Granger causality. *Advances in Water Resources*, 25: 1305-1312.

[217] Santos J, Corte-Real J, Leite S (2007): Atmospheric large-scale dynamics during the 2004/2005 winter drought in Portugal. *Int J Climatol*, 27: 571-586.

[218] Savenije HHG (1995a): New definitions for moisture recycling and the relationship with land-use changes in the Sahel. *J Hydrol*, 167: 57-78.

[219] Savenije HHG (1995b): Does moisture feedback affect rainfall significantly? *Phys Chem Earth*, 20 (5-6): 507-513.

[220] Savenije HHG (1996): The runoff coefficient as the key to moisture recycling. *J Hydrol*, 176 (1-4): 219-225.

[221] Schär C, Luthi D, Beyerle U, Heise E (1999): The Soil-Precipitation Feedback: A Process Study with a Regional Climate Model. *J Climate*, 12: 722-741.

[222] Sendiña I, Muñuzuri VP (2006): Fundamentos de Meteorología. *Universidade de Santiago de Compostela. Servizo de Publicacións e Intercambio Científico*, 194 pp, ISBN: 978-84-9750-645-8.

[223] Seneviratne SI, Luthi D, Litschi M, Schär C (2006a): Land-atmosphere coupling and climate change in Europe. *Nature*, 443 (7108): 205-209.

[224] Seneviratne SI, Koster RD, Guo Z, Dirmeyer PA, Kowalczyk E, Lawrence D, Liu P, Lu C-H, Mocko D, Oleson KW, Verseghy D (2006b): Soil moisture memory in AGCM simulations: analysis of Global Land-Atmosphere Coupling Experiment (GLACE) data. *J Hydrometeorol*, 7: 1090-1112.

[225] Seneviratne SI, Corti T, Davin EL, Hirschi M, Jaeger EB, Lehner I, Orlowsky B, Teuling AJ (2010): Investigating soil moisture-climate interactions in a changing climate: A review. *Earth Sci Rev*, 99 (3-4): 125-161.

[226] Serrano A, García JA, Mateos VL, Cancillo ML, Garrido J, 1999: Monthly modes of variation of precipitation over the Iberian Peninsula. *J Climate*, 12: 2894-2919.

[227] Shiklomanov IA (1989): Climate and water resources. *Hydrol Sci J*, 34: 495-529.

[228] Shukla J, Mintz Y (1982): Influence of land-surface evapotranspiration on the Earth's climate. *Science*, 215: 1498-1501.

[229] Skamarock WC, Klemp JB, Dudhia J, Gill D, Barker D, Wang W, Powers JG (2005): A description of the Advanced Research WRF Version 2. *NCAR Technical Note*, NCAR/TN-468-STR.

[230] Skamarock WC et al. (2008): A description of the advanced research WRF version 3. *NCAR tech. note*, NCAR/TN-475-STR (113 pp).

[231] Soares PMM, Cardoso RM, Miranda PMA, de Medeiros J, Belo-Pereira M, Espirito-Santo F (2012): WRF high resolution dynamical downscaling of ERA-Interim for Portugal. *Clim Dyn*, 39: 2497-2522.

[232] Sousa P, Trigo RM, Aizpurua P, Nieto R, Gimeno L, García-Herrera R (2011): Trends and extremes of drought indices throughout the 20th century in the Mediterranean. *Nat Hazards Earth Syst Sci*, 11: 33-51, doi:10.5194/nhess-11-33-2011.

[233] Stensrud DJ (2007): Parameterization Schemes: Keys to Understanding Numerical Weather Prediction Models. *Cambridge University Press*, 488 pp.

[234] Stidd CK (1967): Local moisture and precipitation. Preprint No. 45A [revised July 1968]. Desert Research Institute, University of Nevada, Reno, 34 pp.

[235] Stidd CK, Fowler WB, Helvey JD (1975): Irrigation increases precipitation? *Science*, 188: 279-281.

[236] Stohl A, James P (2004): A lagrangian analysis of the atmospheric branch of the global water cycle. Part I: method description, validation, and demonstration for the August 2002 flooding in Central Europe. *J Hydrometeor*, 5: 656-678.

[237] Stohl A, James P (2005): A lagrangian analysis of the atmospheric branch of the global water cycle. Part II: moisture transports between earth's ocean basins and river catchments. *J Hydrometeor*, 6: 961-984.

[238] Stull RB (1988): An introduction to boundary layer meteorology. *Kluwer Academic*, 666 pp, Dordrecht. ISBN: 90-277-2768-6.

[239] Sui C, Li X, Yang M (2007): On the definition of precipitation efficiency. *J Atmosph Sci*, 64: 4506-4513.

[240] Sumner G, Homar V, Ramis C (2001): Precipitation seasonality in eastern and southern coastal Spain. *Int J Climatol*, 21: 219-247.

[241] Sutanudjaja EH, van Beek LPH, de Jong SM, van Geer FC, Bierkens MFP (2011): Large-scale groundwater modeling using global datasets: a test case for the Rhine-Meuse basin. *Hydrol Earth Syst Sci*, 15: 2913-2935, doi:10.5194/hess-15-2913-2011.

[242] Szeto KK (2002): Moisture recycling over the Mackenzie basin. *Atmos Ocean*, 40: 181-197.

[243] Tapiador FJ, Sánchez E, Gaertner MA (2007): Regional changes in precipitation in Europe under an increased greenhouse emissions scenario. *Geophys Res Lett*, 34: L06701, doi:10.1029/2006GL029035.

[244] Thornthwaite CW (1948): An Approach toward a Rational Classification of Climate. *Geographical Review*, 38 (No. 1): 55-94.

[245] Trenberth KE, Guillemot CJ, 1996: Physical processes involved in the 1988 drought and 1993 floods in North America. *J Climate*, 9: 1288-1298.

[246] Trenberth KE (1998): Atmospheric moisture residence times and cycling: Implications for rainfall rates and climate change. *Climatic Change*, 39: 667-694.

[247] Trenberth KE (1999): Atmosphere moisture recycling: role of advective convection and local evaporation. *J Climate*, 12: 1368-1381.

[248] Trenberth KE, Dai A, Rasmussen RM, Parsons DB (2003): The changing character of precipitation. *Bull Amer Meteor Soc*, 84: 1205-1217.

[249] Trigo IF, Davies TD, Bigg GR (2000): Decline in Mediterranean rainfall caused by weakening of Mediterranean cyclones. *Geophys Res Lett*, 27: 2913-2916.

[250] Trigo RM, DaCamara CC (2000): Circulation Weather Types and their Influence on the Precipitation Regime in Portugal. *Int J Climatol*, 20 (13): 1559-1581.

[251] Trigo RM, Palutikof JP (2001): Precipitation scenarios over Iberia: a comparison between direct GCM output and different downscaling techniques. *J Climate*, 14: 4422-4446.

[252] Trigo RM, Pozo-Vázquez D, Osborn TJ, Castro-Díez Y, Gamis-Fortis S, Esteban-Parra MJ (2004): North Atlantic Oscilation influence on precipitation, river flow and water resources in the Iberian Peninsula. *Int J Climatol*, 24: 925-944.

[253] Trigo RM, García-Herrera R, Díaz J, Trigo IF, Valente A (2005): How exceptional was the early August 2003 heatwave in France? *Geophys Res Lett*, 32: L10701, doi:10.1029/2005GL022410.

[254] Trigo RM, Valente MA, Trigo IF, Miranda M, Ramos AM, Paredes D, García-Herrera R (2008): North Atlantic wind and cyclone trends and their impact in the European precipitation and Atlantic significant wave height. *Annals of the New York Academy of Sciences*, 1146: 212-234. doi:10.1196/annals.1446.014.

[255] Uppala et al. (2005): The ERA-40 re-analysis. *Q J R Meteorol Soc*, 131: 2961-3012.

[256] Van der Ent RJ, Savenije HHG, Schaefli B, Steele-Dunne SC (2010): Origin and fate of atmospheric moisture over continents. *Water Resour Res*, 46: W09525, doi:10.1029/2010WR009127.

[257] Van der Ent RJ, Savenije HHG (2011): Length and time scales of atmospheric moisture recycling. *Atmos Chem Phys*, 11: 1853-1863.

[258] Vautard R, Yiou P, D'AndreaF, de Noblet N, Viovy N, Cassou C, Polcher J, et al. (2007): Summertime European heat and drought waves induced by wintertime Mediterranean rainfall deficit. *Geophys Res Lett*, doi:10.1029/2006GL028001.

[259] Vicente-Serrano SM, Trigo RM, López-Moreno JI, Liberato MLR and coauthors (2011): Extreme winter precipitation in the Iberian Peninsula in 2010: anomalies, driving mechanisms and future projections. *Clim Res*, 46: 51-65.

[260] Wallace JM, Hobbs PV (2006): Atmospheric Science: an introductory survey. *Elsevier*, Amsterdam, 483 pp. *International Geophysics Series*, 92. ISBN: 0-12-732951-X.

[261] Wang G, Kim Y, Wang D (2007): Quantifying the strength of soil moisture-precipitation coupling and its sensitivity to changes in surface water budget. *J Hydrometeor*, 8: 551-570.

[262] Wei J, Dickinson RE, Zeng N (2006): Climate variability in a simple model of warm climate land-atmosphere interaction. *J Geophys Res*, 111: G03009, doi:10.1029/2005JG000096.

[263] Wei J, Dickinson RE, Chen H (2008): A negative soil moisture-precipitation relationship and its causes. *J Hydrometeorol*, 9: 1364-1376.

[264] Weisman ML, Skamarock WC, Klemp JB (1997) The resolution dependence of explicitly modeled convective systems. *Mon Weather Rev*, 125: 527-548.

[265] Wu W, Dickinson RE (2004): Time scales of layered soil moisture memory in the context of land-atmosphere interaction. *J Climate*, 17: 2752-2764.

[266] York JP, Person M, Gutowski MJ, Winter TC (2002): Putting aquifers into atmospheric simulation models: An example from Mill Creek Watershed, northeastern Kansas. *Adv Water Res*, 25: 221-238.

[267] Yu X, Lee TY (2010) Role of convective parameterization in simulations of a convection band at grey-zone resolutions. *Tellus*, 62A: 617-632.

[268] Yu W, Yao T, Tian L, Ma y, Kurita N, Ichiyanagi K, Wang Y, Sun W (2007): Stable isotope variations in precipitation and moisture trajectories on the western Tibetan Plateau, China. *Arctic, Antarctic, and Alpine Research*, 39 (No. 4): 688-693.

[269] Yuan X, Xie X, Zheng J, Tian X, Yang Z (2008): Effects of water table dynamics on regional climate: A case study over east Asian monsoon area. *J Geophys Res*, 113: D21112, doi:10.1029/2008JD010180.

[270] Zaitchik BF, Macaldy AK, Bonneau LR, Smith RB (2006): Europe's 2003 heat wave: a satellite view of impacts and land atmosphere feedbacks. *Int J Climatol*, 26 (6): 743-769.

[271] Zangvil A, Portis DH, Lamb PJ (2004): Investigation of the large-scale atmospheric moisture field over the midwestern United States in relation to summer precipitation. Part II: recycling of local evapotranspiration and association with soil moisture and crop yields. *J Climate*, 17: 3283-3301.

[272] Zheng X, Eltahir EAB (1998): A soil moisture-rainfall mechanism: 2: Numerical experiments. *Wat Resources Res*, 34 (NO.4): 777-785.

USC
UNIVERSIDADE
DE SANTIAGO
DE COMPOSTELA

Acknowledgements

First, I want to thank my thesis director and professor, Dr. Gonzalo Miguez Macho, for all the things I have learnt from him for the last years, for his support and for his wise advice. I also thank professor Dr. Marc F. P. Bierkens, who gave me the opportuninty to do a three-month stay at the University of Utrecht (Netherlands), which was very important for the development of this investigation. I am also grateful to professor Dr. Francina Dominguez for her patient and intelligent advice and her interest in this work. I thank the Supercomputing Center of Galicia (CESGA), where the numerical simulations were performed, for their kindness and excellent technical support. I also thank the *Instituto Português do Mar e da Atmosfera* (IPMA), the *Agencia Estatal de Meteorología (AEMET)*, the University de Cantabria (UC) and the *European Centre for Medium-Range Weather Forecasts* (ECMWF) for the data they provided us with. This investigation was financed by the FPU program of the Spanish Ministry of Education and Science.

Por outro lado, quero exprimir o meu sincero agradecimento ao professor Dr. Ricardo M. Trigo, baixo cuja supervisão realizei uma estadia de três meses no Instituto Dom Luiz da Universidade de Lisboa. O seu trabalho inesgotável e os seus valiosos conselhos foram decisivos para a realização desta tese de doutoramento. Obrigado também ao professor Dr. Pedro M. Matos Soares e à professora Dra. Rita M. Cardoso pela sua simpatia, dedicação e bons conselhos, que contribuíram de forma determinante para o sucesso deste trabalho.

Obrigado a todos os meus colegas do *Grupo de Física Não-Linear* da Universidade de Santiago de Compostela: Guillermo Fernández García, Darío M. Escala, Jacobo Guiu Souto, Alexandra von Kameke, Florian Huhn, Antonio Yáñez, Ramón Gómez Méndez, Luis Vilasa, Jorge Carballido Landeira, Jorge Eiras Barca, Daniel Cuiñas, Daniel Garaboa e muito especialmente a Carlos Otero Casal, Lucía Gestal Souto e Alberto Martínez de la Torre, pela sua amizade e ajuda constante nestes anos. Sem eles, teria sido muito mais difícil ultrapassar as pequenas dificuldades que surgem no trabalho do dia-a-dia. Obrigado igualmente aos professores Dr. Vicente Pérez Muñuzuri, Dr. Alberto Pérez Muñuzuri e Dr. Vicente Pérez Villar, pelo seu apoio e ajuda.

Obrigado a Lucía, Lorena, Lois, Menchu, Dani Garaboa, Jorge Eiras e Filipa Varino por me ajudarem na revisão e formatação do texto. Também a Olaia, Domentx, Cibrán, Menchu, Vera e Maria Àngela, que me arranjaram uma mão-cheia de ditados populares de toda a Península, nos quais se salienta a importância da chuva primaveral na Península Ibérica. Estes provérbios foram cuidadosamente selecionados e incluídos no resumo inicial deste trabalho.

Obrigado, por último, à minha família e amigos chegados, pelo seu apoio. De um jeito especial, à minha mãe, Menchu, ao meu pai, Lois, e ao meu irmão Cibrán, pelo seu carinho e alento incondicional. À minha parelha, Lorena, por me encorajar incansavelmente. Às minhas avoas, Carmen e Estrela, sempre na lembrança.

Abbreviations

Abbreviation	Description
AEMET	Agencia Estatal de Meteorología (Spanish Meteorological Office)
AGCM	Atmospheric General Circulation Model
CE	Center region of the Iberian Peninsula
EA	East Atlantic pattern
EBRM	Eltahir and Bras's (1994) Recycling Model
ECMWF	European Centre for Medium-Range Weather Forecasts
ENSO	El Niño-Southern Oscillation
GCM	Global Circulation Model
GFS	Global Forecast System
IP	Iberian Peninsula
IPMA	Instituto Português do Mar e da Atmosfera (Portuguese Meteor. Institute)
IMB	Integral Moisture Budget (Recycling Model)
MMTR	Method of Moisture Tracers
MO	Mediterranean Oscillation
NAO	North Atlantic Oscillation
NE	Northeast region of the Iberian Peninsula
NP	North Plateau region of the Iberian Peninsula
NW	Northwest region of the Iberian Peninsula
PBL	Planetary Boundary Layer
RCM	Regional Climate Model
SCAN	Scandinavian Pattern
SP	South Plateau region of the Iberian Peninsula
SRM	Schar et al.'s (1999) Recycling Model
SSM	Schar et al.'s (1999) Separation Method
UC	Universidad de Cantabria (University of Cantabria)
WE	West region of the Iberian Peninsula
WeMO	Western Mediterranean Oscillation
WRF	Weather Research and Forecasting model

USC
UNIVERSIDADE
DE SANTIAGO
DE COMPOSTELA

Symbols

Symbol	Description	Common units
$CAPE$	Convective Available Potential Energy	J kg^{-1}
ET	Evapotranspiration	kg m^{-2}
IN	Moisture Input	kg *or* kg m^{-2}
MC	Moisture Convergence	kg *or* kg m^{-2}
OUT	Moisture Output	kg *or* kg m^{-2}
P	Precipitation	kg m^{-2}
N	Precipitable Water	kg *or* kg m^{-2}
R	Correlation Coefficient	[-]
r	Regional Recycling Ratio	[-]
r^*	Regional Relative Change in Precipitation	[-]
α	Residual term in the Mass Conservation Equation	kg m^{-2}
ρ	Local Recycling Ratio	[-]
ρ^*	Local Relative Change in Precipitation	[-]

USC
UNIVERSIDADE
DE SANTIAGO
DE COMPOSTELA

List of Figures

1 Schematic representation of stocks and water fluxes (km^3) in the global hydrologic cycle. This figure is obtained from Dingman (2002) [56]. . . x

2 Representação esquemática dos reservatórios e fluxos de água (km^3) no ciclo hidrológico global. Figura obtida de Dingman (2002) [56]. xviii

3 Representación esquemática de los reservorios y flujos de agua (km^3) en el ciclo hidrológico global. Figura obtenida de Dingman (2002) [56]. xxvi

1.1 Monthly mean precipitation (1950-2007) for 28 representative Iberian locations 4

1.2 Season of highest rainfall over Iberia (1950-2007) 5

1.3 Month of highest rainfall over Iberia (1950-2007) 6

1.4 Position of May in the monthly ranking of precipitation (1950-2007) . 7

1.5 Spatial distribution of the humidity index over Iberia 8

1.6 Feedback loop in the terrestrial branch of the water cycle. 12

1.7 Simplified representation of the soil structure 15

1.8 Equilibrium water table depth (EWTD) for the Iberian Peninsula . . . 16

1.9 Illustration of the concept of local recycling ratio. 26

1.10 Impact of the area shape on recycling calculations 27

1.11 The two mechanisms for the soil-precipitation feedback: recycling and amplification 31

2.1 Parent and nested domains used in WRF simulation 1 (WRFS-1), together with the region selected to compute the recycling ratio 39

2.2 Terrain height above the sea level for the parent and nested domains used in the WRFS-2 simulations, together with the boxes considered within 42

2.3 Representation of the water budget terms: precipitation, evapotranspiration, moisture convergence and precipitable water. 44

3.1 Mean annual cycle and interannual variability of the regional recycling ratio 64

3.2 Monthly series of regional recycling ratio for the period 1990-2007 . . . 65

3.3 Monthly correlation between EBRM and IMB regional recycling ratios 66

3.4 Mean annual cycle of recycling ratio, monthly standard deviation and average precipitation (1990-2007) 69

3.5 Relative precipitation anomalies and EBRM recycling patterns for the three selected case studies (1997, 2001 and 2005) 71

4.1 Average precipitation for January 2000-2008 and May 2000-2007 according to WRF model output and UC/AEMET-IPMA analysis . . . 81

4.2 Daily, 5-days and monthly MAE and MAPE values for the periods January 2000-2008 and May 2000-2007 82

4.3 Time series of area-averaged monthly precipitation over Spain from observational analysis (AEMET) and from WRF model results (2002-2010) 83

4.4 Terms of the water budget (P, ET, MC and change in N) and experimental relative change in precipitation (2000-2010) 84

4.5 Terms of the water budget (P, ET, MC and change in N) and experimental relative change in precipitation (2000-2010; continuation of Fig. 4.4) 85

4.6 Average moisture fluxes in the lower atmosphere (below 700 mb) and in the upper atmosphere (above 700 mb) 88

4.7 Average moisture flux patterns at 850 hPa and 500 hPa for the periods January 2000-2010 and May 2000-2010 89

4.8 Spatial distribution of the multiannual average of EBRM recycling ratio (May 2000 to May 2010), together with the corresponding average pattern of vertically integrated moisture flux 90

4.9 Spatial distribution of the local EBRM recycling ratio during the period May 2000 to May 2010, together with the corresponding average pattern of vertically integrated moisture flux, computed with WRF outputs for the nested domain 91

4.10 Spatial distribution of the local EBRM recycling ratio during the period May 2000 to May 2010, together with the corresponding average pattern of vertically integrated moisture flux, computed with WRF outputs for the parent domain 92

4.11 Representation of the average Iberian hydrological cycle (January 2000-2010 and May 2000-2010) 94

4.12 Regional EBRM and IMB recycling ratios computed at 5 km (WRFS-2 simulations) and 9 km (WRFS-1 simulation) during the months of January 2000 - 2007 and May 2000 - 2007 96

4.13 Spatial distribution of the relative change in precipitation, averaged over the period May 2000-2010, and spatial distribution of ρ/ρ^* 97

4.14 Fraction of the change in precipitation deriving from direct recycling and from indirect amplification, according to SSM and the new experimental method, for the period May 2000 - May 2010 99

4.15 Mean geopotential heights from the ERA-Interim dataset, for May 2004 and 2008 (at 850 hPa), and corresponding geopotential anomalies with respect to the period May 1958-2002 (ERA-40 dataset) 102

4.16 Ensemble total precipitation, ensemble relative change in precipitation and ensemble recycling ratio for May 2004 and May 2008 103

4.17 Daily time series of the ensemble mean water budget terms over the IP (control simulation and *no-ET* experiment), daily values of ensemble mean CAPE and daily values of ensemble mean r^* (May 2004 and May 2008) 106

4.18 Correlation between the average inward moisture flux and the fraction of ΔP originating from amplification, for the period May 2000 - May 2010 108

4.19 Monthly ensemble CAPE and CAPE differences between *control* and *no-ET* simulations (12Z) for May of 2004 and May of 2008 109

4.20 Ensemble CAPE differences between *control* and *no-ET* simulations (12Z) for two specific days (8^{th} and 31^{st} May 2008) and total precipitation accumulated in the subsequent six hours 110

5.1 Multiannual average of the local recycling ratio computed through the MMTR (May 2000 to May 2010) 116

5.2 Spatial distribution of the local MMTR recycling ratio during the period May 2000 - May 2010 and multiannual average 117

5.3 Spatial distribution of $\rho_{\mathrm{MMTR}}/\rho^*$ averaged over the period May 2000-2010 119

5.4 Daily values of regional MMTR recycling ratio, relative change in precipitation, recycled contribution and amplification contribution for May of 2004 and May of 2008 121

5.5 $\rho_{\mathrm{MMTR}}/\rho^*$ and MMTR recycling ratio for May 2004 and May 2008 . . 122

5.6 Vertical profile (latitude set as 40°N) of the fraction of humidity from tracers averaged over (a) May of 2004 and (b) May of 2008 123

5.7 Vertical profile (latitude set as 40°N) of the fraction of humidity from tracers for two particular episodes in May of 2008 124

E.1 128 x 128 points region (at 9 km horizontal resolution) including the Iberian Peninsula where the sensitivity of the EBRM recycling ratio to the computation resolution is assessed 144

E.2 Illustration of the procedure used to compute the EBRM regional recycling ratio by successively decreasing the computation resolution. . . 145

E.3 EBRM regional recycling ratios computed by successively decreasing the computation resolution and comparison with the IMB value 145

List of Tables

3.1 Seasonal correlation coefficients (EBRM vs IMB) 65

3.2 Precipitation, NAO index, regional recycling ratio and relative deviation of recycling (DJF-M during the years of 1997, 2001, 2005 and 2006) 70

4.1 Average moisture fluxes in the lower atmosphere (below 700 mb) and in the upper atmosphere (above 700 mb) 86

4.2 Recycling ratio and experimental relative changes in precipitation for the periods May 2000 - 2010 and January 2000 - 2010 90

4.3 Correlation coefficient among the data series represented in Fig. 4.12. . 95

4.4 Fraction of the extra precipitation in May deriving from direct recycling, estimated via SSM and through our new approach 100

4.5 Average May 2000-2010 regional EBRM recycling ratio, relative change in precipitation and quotient of both magnitudes calculated for the small boxes considered within the IP 101

5.1 Recycling ratio computed via MMTR, IMB and EBRM, regional relative changes in precipitation (r^*) and rate r_{MMTR}/r^* for the period May 2000-2010 118

USC
UNIVERSIDADE
DE SANTIAGO
DE COMPOSTELA

List of Publications

Articles in Peer-reviewed Journals

- G. Miguez-Macho, **A. Rios-Entenza**, F. Dominguez. Regional climate simulations with moisture tracers to investigate land-atmosphere interactions in the terrestrial water cycle over the Iberian Peninsula. *In preparation.*

- **A. Rios-Entenza**, P. M. M. Soares, R. M. Trigo, R. M. Cardoso, G. Miguez-Macho. Precipitation recycling in the Iberian Peninsula: spatial patterns and temporal variability. *Submitted* (2nd August 2013) to *International Journal of Climatology.*

- **A. Rios-Entenza**, G. Miguez-Macho. Moisture recycling and the maximum of precipitation in spring in the Iberian Peninsula. *Accepted* (9th October 2013) for publication in *Climate Dynamics.* DOI : 10.1007/s00382-013-1971-x.

Other publications

- L. Gestal-Souto, A. Martínez de la Torre and **A. Rios-Entenza** (2010): O papel das augas freáticas nas interaccións terra-atmosfera, no clima e no rexime pluviométrico da Península Ibérica (The role of groundwater on the Iberian climate, precipitation regime and land-atmosphere interactions). Revista da Real Academia Galega de Ciencias, vol. XXIX, 89-128.

Selected conference abstracts

- G. Miguez-Macho, **A. Rios-Entenza**, F. Dominguez (2013): Regional climate simulations with moisture tracers to investigate land-atmosphere interactions in the terrestrial water cycle over the Iberian Peninsula. 2013 General Assembly, EGU (European Geosciences Union). Vienna (Austria), 7-12 April.

- **A. Rios-Entenza**, G. Miguez-Macho (2012): Spring precipitation in inland Iberia: land-atmosphere interactions and recycling-amplification processes. 2012 General Assembly, EGU (European Geosciences Union). Vienna (Austria), 22-27 April.

- G. Miguez-Macho, Y. Fang, **A. Rios-Entenza**, A. Martínez de la Torre and L. Gestal-Souto (2011): Implementation of water table dynamics and river routing into WRF: the LEAFHYDRO model as a new LSM option (WRFHYDRO system). 12th Annual WRF Users' Workshop. Boulder (Colorado, USA), 20-24 June.

- **A. Rios-Entenza**, G. Miguez-Macho (2010): Moisture recycling and the maximum of precipitation in the spring in the Iberian Peninsula. 2010 General Assembly, EGU (European Geosciences Union). Vienna (Austria), 2-7 May.

- **A. Rios-Entenza**, L. Gestal-Souto, G. Miguez-Macho (2009): Simulaciones del ciclo hidrológico en la Península Ibérica con WRF: importancia del reciclaje de agua en la precipitación (WRF simulations of the hydrological cycle in the Iberian Peninsula: the role of water recycling on precipitation). CLIVAR: "Clima en España: pasado, presente y futuro" ("Climate in Spain: past, present and future"). CSIC, Madrid (Spain), 11-13 February.

- **A. Rios-Entenza**, G. Miguez-Macho (2008): Regional climate simulations of the hydrological cycle in the Iberian Peninsula with WRF model. 2008 Fall Meeting, AGU (American Geophysical Union). San Francisco (California, USA), 15-19 December.